BINDING SERVICES
Tel +44 (0)29 2087 4949
Fax +44 (0)29 20371921
e-mail bindery@cardiff.ac.uk

EXACT VIBRATIONAL ANALYSIS OF PRISMATIC PLATE AND SANDWICH STRUCTURES

ABDOLREZA ZARE

BSc, MSc

This dissertation is being submitted in partial fulfilment of the requirement for the degree of Doctor of Philosophy

School of Engineering, Cardiff University

2004

ProQuest LLC
789 East Eisenhower Parkway
P.O. Box 1346
Ann Arbor, MI 48106-1346

Abstract

Transcendental stiffness matrices for vibration (or buckling) analysis have long been available for a range of structural members. Such stiffness matrices are exact in the sense that they are obtained from an analytical solution of the governing differential equations of the member. Hence, assembly of the member stiffnesses to obtain the overall stiffness matrix of the structure results in a transcendental eigenproblem that yields exact solutions and which can be solved with certainty using the Wittrick-Williams algorithm. Convergence is commonly achieved by bisection, despite the fact that the method is known to be relatively slow. Quicker methods are available, but their implementation is hampered by the highly volatile nature of the determinant of the structure's transcendental stiffness matrix, particularly in the vicinity of the poles, which may or may not correspond to eigenvalues.

However, when the exact solution exists, the member has a recently discovered property that can also be expressed analytically and is called its member stiffness determinant. The member stiffness determinant is a property of the member when fully clamped boundary conditions are imposed upon it. It is then defined as the determinant of the member stiffness matrix when the member is sub-divided into an infinite number of identical sub-members. Each sub-member is therefore of infinitely small length so that its clamped-ended natural frequencies are infinitely large. Hence the contribution from the member stiffness matrix to the J_0 count of the W-W algorithm will be zero. In general, the member stiffness determinant is normalised by dividing by its value when the eigenparameter (i.e. the frequency or buckling load factor) is zero, as otherwise it would become infinite.

Part A of this thesis develops the first two applications of member stiffness determinants to the calculation of natural frequencies or elastic buckling loads of prismatic assemblies of isotropic and orthotropic plates subject to in-plane axial and transverse loads. A major advantage of the member stiffness determinant is that, when its values for all members of a structure are multiplied together and are also multiplied by the determinant of the transcendental overall stiffness matrix of the structure, the result is a determinant which has no poles and is substantially less volatile when plotted against the eigenparameter. Such plots provide a significantly better platform for the development of efficient, computer-based routines for convergence on eigenvalues by curve prediction techniques.

On the other hand, Part B presents the development of exact dynamic stiffness matrices for three models of sandwich beams. The simplest one is only able to model the flexural vibration of asymmetric sandwich beams. Extending the first model to include axial and rotary inertia makes it possible to predict the axial and shear thickness modes of vibration in addition to those corresponding to flexure. This process culminates in a unique model for a three layer Timoshenko beam. The crucial difference of including axial inertia in the second model, enables the resulting member dynamic stiffness matrix (exact finite element) to be included in a general model of two dimensional structures for the first time. Although the developed element is straight, it can also be used to model curved structures by using an appropriate number of straight elements to model the geometry of the curve.

Finally, it has been shown that considering a homogeneous deep beam as an equivalent three-layer beam allows the beam to have additional shear modes, besides the flexural, axial and fundamental shear thickness modes. Also for every combination of layer thickness, the frequencies of the three-layer beam are less than the corresponding frequencies calculated for the equivalent beam model with only one layer, since it is equivalent to providing additional flexibility to the system. However, a suitable combination of layer thicknesses for any mode may be found that yields the minimum frequency. It is anticipated that these frequencies would probably be generated by a single layer model of the homogeneous beam if at least a third order shear deformation theory was incorporated.

Numerous examples have been given to validate the theories and to indicate their range of application. The results presented in these examples are identical to those that are available from alternative exact theories and otherwise show good correlation with a selection of comparable approximate results that are available in the literature. In the latter case, the differences in the results are attributable to many factors that vary widely from different solution techniques to differences in basic assumptions.

Dedicated to

my mother, my father,

and to my wife 'Farideh'

ACKNOWLEDGEMENTS

All praises to my almighty Lord 'Allah' for providing me the opportunity and the capability to complete this work.

My first and most earnest acknowledgement must go to my supervisor Dr Paul Howson for his continuous guidance, encouragement and support throughout. My sincere thanks should also go to Dr David Kennedy and Professor Fred Williams for their guidance in achieving a better understanding of the theoretical background of the first part of the thesis. In every sense, none of this work would have been possible without them.

The author wishes to record his gratitude to Yasuj University and the Ministry of Science, Research and Technology of the Islamic Republic of Iran who have generously supported this work.

Recognition is also due to members of staff at Shiraz University, Iran, and my colleagues who generously shared their knowledge with me to arrive at this point. I am also grateful to Mr Behzad Rafezy for many beneficial discussions and his enjoyable friendship during my period of research.

I also owe my parents a great debt of gratitude for their continuous encouragement and for being supportive when I needed them most.

My final and most heartfelt acknowledgement must go to my wife, Farideh, for her continuous love, support, encouragement and understanding throughout the duration of this research study. I also should mention my lovely children Ali, Olia and Helia for their understanding and tolerance of their father's absence on evenings and weekends that were devoted to this thesis.

CONTENTS

LIST OF SYMBOLS FOR PART A

b	Plate breadth
b_i	Breadth of member for sub-structure at level i
B,C	Dimensionless parameters defined by Eq. (2.36)
$\mathbf{D}$	Displacement vector
D	Flexural rigidity of an isotropic plate
D_{11}, D_{22}	Longitudinal and transverse flexural rigidity of an orthotropic plate
D_t	Effective torsional rigidity
$\mathbf{d}_1, \mathbf{d}_2$	Nodal displacement vectors
$\mathbf{d}_I$	Displacements vector of internal nodes of a sub-structure
$\mathbf{d}_c$	Displacements vector of connecting nodes of a sub-structure to the parent structure
E_1, E_2	Young's modulus of elasticity in the longitudinal and transverse direction of a plate, respectively
G	Shear modulus
G_{af}, G_{sf}	Constants defined by Eq. (2.12)
h	Plate thickness
H_f, H_{sf}	Constants defined by Eq. (2.17)
H_a, H_s	Constants defined by Eq. (2.38) or (2.41)
J	Number of natural frequencies of the structure exceeded by ω^*
J_0	Number of natural frequencies of the structure with $\{\mathbf{D}\} = \mathbf{0}$ exceeded by ω^*
J_0^I	J_0 for the in-plane contribution
J_0^O	J_0 for the out-of-plane contribution
J_m	Number of natural frequencies of a member exceeded by n^*
J_s	Number of natural frequencies of sub-structure exceeded by n^*
J_{r1}	Out-of-plane contribution of simply supported element to J
J_{r2}	In-plane contribution of simply supported element to J
$\mathbf{K}$	Overall dynamic stiffness matrix of a structure
$\overline{\mathbf{K}}$	Normalised overall dynamic stiffness matrix of a structure
$\mathbf{K}_\infty$	Infinite order dynamic stiffness matrix of a structure
$\overline{\mathbf{K}}_\infty$	normalised infinite order dynamic stiffness matrix of a structure
$\mathbf{K}_s$	Sub-structure stiffness matrix
$\mathbf{k}$	Element stiffness matrix
$\mathbf{k}_{si}$	Element stiffness matrix for sub-structure at level i
$\mathbf{k}_{11}^I, \mathbf{k}_{12}^I, \mathbf{k}_{21}^I, \mathbf{k}_{22}^I$	Partitioned components of the in-plane stiffness matrix of a plate
$\mathbf{k}_{11}^O, \mathbf{k}_{12}^O, \mathbf{k}_{21}^O, \mathbf{k}_{22}^O$	Partitioned components of the out-of-plane stiffness matrix of a plate
L	Dimensionless parameter defined by Eq. (2.25)

L_1, L_3	Force per unit length defined by Eq. (2.35)
l	Length of a plate
M	Number of elements in the structure
m	Member number
M_j	Amplitude of the bending moment per unit length of plate along edge j
n	Circular frequency
n^*	Trial frequency
n_{kj}	The j^{th} natural frequency for $\lambda_k = b/k$
N_L	Longitudinal force per unit length
N_T	Transverse force per unit length
N_S	Shear flow per unit length
N^*	Longitudinal Force per unit length defined by Eq. (2.2)
${}_{kj}N_L^{cr}$	The j^{th} longitudinal critical buckling load for $\lambda_k = b/k$
$p_\chi, q_\chi, \hat{p}_\chi, \hat{q}_\chi$	Real functions defined by Eqs. (2.10) and (2.24)
P_{xj}, P_{yj}, P_{zj}	Amplitude of the in-plane shear force, in-plane transverse force and out of-plane shear force per unit length of plate edge j, respectively
$\mathbf{p}_1, \mathbf{p}_2$	Nodal force vectors
$\mathbf{p}_I$	Force vector at internal nodes of a sub-structure
$\mathbf{p}_c$	Force vector at connecting nodes of a sub-structure to the parent structure
$s_{MM}, \ldots, f_{MM}, \ldots$	Components of an element stiffness matrix
$s\{\ \}$	Sign count of a matrix
$sg(\ )$	1 or −1, depending on the sign of the parameter within the bracket
T	Dimensionless parameter defined by Eq. (2.25)
u_j, v_j, w_j, ψ_j	Elements of a nodal displacement vector
x, y, z	Longitudinal, transverse and out-of-plane co-ordinates
$\alpha_{11}, \alpha_{12}, \alpha_{33}$	Dimensionless parameter defined by Eq. (2.26)
$\alpha, \gamma, \tau, \zeta$	Non-dimensional parameter
φ	Dimensionless parameter defined by Eq. (2.7)
λ	Longitudinal half-wave length
$\bar{\lambda}$	λ/π
Δ_m	Member stiffness determinant
$\bar{\Delta}_m$	Normalised member stiffness determinant
Δ	Stiffness determinant of the structure
$\bar{\Delta}$	Normalised stiffness determinant of the structure
ρ	mass density of a plate
χ	Dimensionless parameter which may take any of the values $\alpha, \gamma, \tau, \zeta$ or any combination of them or simply a constant
ν_1, ν_2	longitudinal and transverse Poisson's ratio of an orthotropic plate
ν	Poisson's ratio of an isotropic plate
ε	Dimensionless parameter defined by Eq. (2.8)
η	Dimensionless parameter defined by Eq. (2.8)

LIST OF SYMBOLS FOR PART B

a	Distance between centre lines of the bottom faceplate and the core
A_i	constants
b_i	constants
B_i	constants
c_i	constants
$C_i, \overline{C}_{ij}$	constants
d	Distance between centre lines of the faceplates
D_x, D	$\mathrm{d}/\mathrm{d}x, \mathrm{d}/\mathrm{d}\xi$
$\mathbf{D}$, $\mathbf{d}$	Structure and element displacement vector, respectively
D_i, d_i	Elements of the structure and element displacement vector, respectively
e_i	constants
e_1, e_2, e_3, e_4	Constants defined around Eqs. (6.5) and (6.82)
f_i	Natural frequency (Hz)
g_i	constants
$G_i, \quad (i = t,c,b)$	Shear modulus of layer i
H_{ij}	constants
J	Number of natural frequencies of the structure exceeded by ω^*
J_0	Number of natural frequencies of the structure with $\{\mathbf{D}\} = \mathbf{0}$ exceeded by ω^*
J_m	Number of natural frequencies of a member exceeded by ω^*
J_{rr}	Number of natural frequencies of roller-roller supported member exceeded by ω^*
J_{ss}	Number of natural frequencies of simply supported member exceeded by ω^*
$\mathbf{k}$, $\mathbf{k}^{ss}$, $\mathbf{k}^{rr}$, $\mathbf{K}$	Stiffness matrix
K_{ij}, k_{ij}	Elements of stiffness matrix $\mathbf{K}$ and $\mathbf{k}$, respectively
$K_i = E_i b t_i, (i = t,c,b)$	Axial rigidity of layer i
L	Length of a member
L	Lagrangian
$m_i, \quad (i = t,c,b)$	Bending moment at layer i
m, M	Instantaneous resultant bending moment and corresponding amplitude
$\overline{m}$, $\overline{M}$	Instantaneous couple due to axial forces in the faceplates and corresponding amplitude
$n_i, N_i \quad (i = t,c,b)$	Instantaneous axial force at layer i and corresponding amplitude
P_i	Elements of force vector
$\mathbf{P}$, $\mathbf{p}$	Structure and element force vector

$q_i, \quad (i = t,c,b)$	Shear force acting at layer i
q, Q	Instantaneous resultant shear force and corresponding amplitude
r	Constants defined around Eq. (6.82)
$s\{\ \}$	Sign count of a matrix
$S_i = G_i b t_i, (i = t,c,b)$	Shear rigidity of layer i
S	Total shear rigidity of a beam
$\hat{S}_c$	$G_c d^2 / t_c$
t	time
$t_i, \quad (i = t,c,b)$	Thickness of layer i
T	Kinetic energy
$\mathbf{T}_i, \tilde{\mathbf{T}}_i$	Transformation matrices
$u_i, U_i \quad (i = t,c,b)$	Instantaneous axial displacement and corresponding amplitude at the centre of layer i
u_1, U_1	Instantaneous axial displacement and corresponding amplitude at the external edge of the top layer
u_2, U_2	Instantaneous axial displacement and corresponding amplitude at the interface of the top layer and the core
u_3, U_3	Instantaneous axial displacement and corresponding amplitude at the interface of the bottom layer and the core
u_4, U_4	Instantaneous axial displacement and corresponding amplitude at the external edge of the bottom layer
U	Potential energy
w, W	Instantaneous transverse displacement of the beam and corresponding amplitude
x, y	Longitudinal and transverse co-ordinates
z	Transverse location co-ordinate for each layer
Z_i	constants
$\alpha, \quad \beta, \quad \lambda$	Constants defined by Eq. (5.23)
δ	$\frac{n\pi}{L}, (n = 0,1,2,3,\ldots).$
$\delta^{(1)}$	First variation
$\varepsilon_i, \quad (i = t,c,b)$	Average normal strain of layer i
$\varphi_i, \quad (i = t,c,b)$	Average rotation of the cross-section of layer i
$\varphi, \quad \Phi$	Average rotation of the beam's cross section
$\gamma_i, \quad (i = t,c,b)$	Average shear strain in layer i
η	Root of characteristic equation
κ	$1/(E_t I_t + E_b I_b)$
$\mu_i, \quad (i = t,c,b)$	Mass per unit length of layer i
μ	Mass per unit length of the beam
$\rho_i, \quad (i = t,c,b)$	Mass density of layer i
σ	Normal stress
ς	$K_t K_b / (K_t + K_b)$
$\hat{\varsigma}$	$K_t K_b / (K_t \mu_t + K_b \mu_b)$
ω	Circular frequency

ω^*	Trial frequency
ξ	Non-dimensional length
ψ, Ψ	Instantaneous total slope of beam's deflection curve and corresponding amplitude
ζ	Transverse co-ordinate for each layer
ζ_j	$e^{\eta_j \xi}$ or $e^{\eta_j x}$

CHAPTER 1

INTRODUCTION

1.1 GENERAL

Advances in technology over the last fifty years have made it possible to analyse and design complex structural system that were undreamed of by former generations. Nowhere has this been more evident than in the rapid development of digital computers and the parallel development of matrix methods of structural analysis that exploit the computer's ability to perform repetitive tasks extremely efficiently. In particular, the mathematical models used to solve practical problems in structural dynamics have been developed from simple systems having only a few degrees of freedom to highly sophisticated models containing thousands of nodes.

Moreover, it is now relatively simple to predict the dynamical behaviour of physical systems and a knowledge of their natural frequencies is often a pre-requisite to detailed design.

A popular approach is the dynamic stiffness method in which the overall structure matrix is assembled from the dynamic stiffness matrices of its individual members, which may be developed in an approximate way or a way which can be considered to be exact. This leads to a set of linear equations in the former case and transcendental equations in the latter case, with the natural frequencies being determined by solving the related eigenvalue problem.

The most popular approximate technique is the finite element method, in which either a consistent mass matrix is evaluated or the element mass is simply assumed to be concentrated at the nodes, with the dynamic stiffness matrix derived by assuming a static displaced shape for the member. The resulting dynamic stiffness matrix is then a linear combination of two individual matrices, the static stiffness matrix that defines the elastic properties of the member and the mass matrix that defines the inertial properties. In this case, the overall structure matrix is a linear function of ω^2, the square of the circular frequency, and the problem of determining the natural frequencies is known as a linear eigenvalue problem. However, the accuracy of the finite element technique can be unsatisfactory due to the fact that the method only approximates the partial differential equations describing the structure, where the quality of the approximation depends on the idealisation.

In the so called 'exact' method for deriving the member dynamic stiffness matrix, the partial differential equation of motion is solved analytically in such a way that the closed form solution satisfies inter-element compatibility as well as the boundary conditions. In contrast with the finite element approximation, the dynamic member stiffness matrix is a single matrix in which the exact and continuous mass distribution is automatically accounted for and the model therefore has an infinite number of degrees of freedom. The matrix contains transcendental functions and therefore the resulting dynamic stiffness matrix has a transcendental dependence on ω.

1.2 THE EXACT DYNAMIC STIFFNESS MATRIX METHOD

Kolousek was the first to use the concept of exact dynamic stiffnesses for the vibration analysis of Bernoulli-Euler beams (Kolousek 1941; Kolousek 1943). [This work is elegantly described in his textbook (Kolousek 1973).] Later, in the field of plate analysis, Veletsos and Newmark used this concept for the vibration analysis of continuous plates with hinged supports along two opposite edges (Veletsos and Newmark 1956). However, one of the earliest works on the formulation of a dynamic stiffness matrix was reported by Laursen *et al.* (Laursen et al. 1962) for an Euler-Bernolli beam. Soon after, Simpson and Tabarrok (Simpson and Tabarrok 1968), Armstrong (Armstrong 1969) and Williams and Wittrick (Williams and Wittrick 1970) used it for the vibration analysis of rigidly jointed plane frames. Later, Wittrick (Wittrick 1968a) developed the general sinusoidal stiffness matrices for thin flat-walled structures which have been used for determining the natural vibration of uniformly longitudinally stressed isotropic plate assemblies (Wittrick and Williams 1971b). Also Henshell and Warburton (Henshell and Warburton 1969) developed a general dynamic stiffness matrix which included the effects of longitudinal and torsional motion of an Euler-Bernoulli beam. This was followed by Cheng (Cheng 1970) and Wang and Kinsman (Wang and Kinsman 1971) who presented the dynamic stiffness matrix for a Timoshenko beam which could be used in the vibration analysis of frameworks. Howson and Williams (Howson and Williams 1973) later incorporated the effect of a compressive or tensile axial force in a member when deriving the dynamic stiffness matrix of an axially loaded Timoshenko beam, which has been used in eigensolution of plane frames (Howson 1979) and space frames (Anderson and Williams 1986). This theory was also incorporated into a framework program by Åkesson and his colleagues that provides an exact vibration analysis of linearly elastic frames (Åkesson 1976).

Since then, research on the dynamic stiffness matrix formulation of structural elements has grown enormously and has taken numerous turns, including bending-torsion coupled beams (Banerjee 1989; Banerjee and Williams 1992; Banerjee and Williams 1994a; Banerjee and Williams 1994b; Friberg 1983; Hallauer and Liu 1982; Hashemi and Richard 2000a; Hashemi and Richard 2000b; Li et al. 2003), varying cross section elements (Busool and Eisenberger 2002; Eisenberger 1990; Eisenberger 1991;

Eisenberger 1995; Eisenberger 1997; Huang et al. 1998; Jabareen and Eisenberger 2001; Leung and Zhou 1995a; Leung and Zhou 1995b; Mou et al. 1997; Yanghu et al. 1997), layered beams (Abramovich et al. 1995; Banerjee 1998; Banerjee et al. 1996; Banerjee and Williams 1995; Banerjee and Williams 1996; Eisenberger et al. 1995; Heinisuo 1988; Leung and Zhou 1996), sandwich beams (Banerjee 2003; Howson and Zare 2004), beams on elastic foundations (Capron and Williams 1988; Eisenberger 1994), tapered beams (Banerjee and Williams 1985), curved elements (Eisenberger and Efraim 2001; Howson and Jemah 1999a; Howson and Jemah 1999b; Huang et al. 2000; Huang et al. 1998), pre-twisted beams (Banerjee 2001; Banerjee 2004), helical springs (Busool and Eisenberger 2002; Lee and Thompson 2001; Pearson and Wittrick 1986), rotating shafts (Hashemi and Richard 2001; Raffa and Vatta 1996; Raffa and Vatta 2002) and beams with thin-walled cross section (Kim et al. 2003; Leung 1992; Li et al. 2003; Matsui and Hayashikawa 2001; Moon-Young et al. 2003a; Moon-Young et al. 2003b). Furthermore, Eisenberger (Eisenberger 2003) presented the derivation of the exact dynamic stiffness matrix for a high-order beam element. The dynamic stiffness matrix method has also been used for analysis and vibration of orthotropic plates by Bercin (Bercin 1995; Bercin 1997; Bercin and Langley 1996), Leung and Zhou (Leung and Zhou 1996) for composite plates, and Wittrick and Williams (Wittrick and Williams 1974) for anisotropic flat plates without coupling of in-plane and out-of-plane behaviour and with any combination of uniform in-plane stresses. Although, in most of the reported work the dynamic stiffness matrices are real, there are also a some examples of exact complex dynamic stiffness matrices for damped second-order Rayleigh-Timoshenko beam vibration (Hjelmgren et al. 1993; Lunden and Åkesson 1983; Schill 1988).

Although the procedure for the derivation of exact dynamic stiffness matrices has been long established and used by many authors, its general procedure has been described systematically by Banerjee in reference (Banerjee 1997). Since the dynamic stiffness matrix in this case contains terms that are transcendental functions of frequency, a suitable eigenvalue problem solver is needed and this is dealt with in the following section.

1.3 THE SOLUTION OF THE TRANSCENDENTAL EIGENVALUE PROBLEM

The general form of transcendental eigenvalue problems may be written as

$$\mathbf{K}(\lambda)\mathbf{D} = \mathbf{0} \tag{1.1}$$

where **K** is the system characteristic matrix in which the elements are transcendental functions of the eigenparameter λ and **D** is the corresponding eigenvector.

Transcendental eigenvalue problems arise in many different fields such as physics (Romeiras and Rowlands 1986; Shastry 1983), chemistry (Kumpinsky 1992), applied mathematics (Bateson et al. 1999) and structural engineering (Paz 1973; Qi et al. 2004; Simpson 1974; Simpson 1984; Simpson and Tabarrok 1968; Williams and Wittrick 1970; Williams et al. 2002b). Sometimes, their solution has been formulated for special cases (Kumpinsky 1992; Romeiras and Rowlands 1986; Shastry 1983), while some authors formulate the problem to various levels of precision (Fontgalland et al. 1998; Singh and Ram 2002; Sotiropoulos 1982) including general exact solutions (Williams and Wittrick 1970; Wittrick and Williams 1971a).

In the field of structural engineering the exact analysis of buckling and vibration problems leads to the transcendental eigenvalue problem of Eq. (1.1), where **K** is now the appropriate overall stiffness matrix of the structure and **D** is the corresponding nodal displacement vector. The eigenparameter λ is equivalent to ω^2 in vibration problems while in buckling problems it relate to the value of destabilising load on the structure. However, since the duality of the vibration and buckling phenomena is clear, from now on we will solely concern in vibration. As stated in Section 1.1, the exact dynamic stiffness matrix of any structural member has a transcendental dependence on ω, thus the elements of **K** are often highly complicated transcendental functions of the frequency ω. In general, the eigenvalues correspond to natural frequencies in undamped free vibration problems and the eigenvectors are the corresponding vibration modes.

However, the common procedure for finding the natural frequencies is to track the value of the determinant of **K** (Abramovich et al. 1995; Bercin and Langley 1996; Busool and Eisenberger 2002; Eisenberger 1991; Eisenberger 1994; Huang et al. 1998; Leung and Zhou 1995a; Leung and Zhou 1995b; Matsui and Hayashikawa 2001). In this case, the determinant $|\mathbf{K}(\omega)|$ is usually plotted at fine intervals of the eigenparameter, to give the natural frequencies at those values of ω at which $|\mathbf{K}(\omega)| = 0$. Despite the acceptance of the major computational expense of using small intervals of ω, still possibility of missing some close or coincident natural frequencies still exists. In addition, due to the highly irregular behaviour of the determinant, it is possible that $|\mathbf{K}|$ becomes infinite at certain values of the eigenparameter, which may or may not correspond to eigenvalues. It has been proved that the natural frequencies of any isolated member in the system are critical values for the determinantal function (Paz 1973; Simpson 1974; Wittrick and Williams 1971a). Moreover, some exceptional natural frequencies that correspond to the case of $|\mathbf{K}(\omega)| \to \infty$ with $\mathbf{D} = \mathbf{0}$ and the case of $|\mathbf{K}(\omega)| \neq 0$ with $\mathbf{D} \neq \mathbf{0}$ (Williams et al. 2002b) are bound to be missed.

These problems can be completely overcome by use of the Wittrick-Williams (W-W) algorithm (Williams and Wittrick 1970; Wittrick and Williams 1971a). The W-W algorithm was developed over thirty years ago and, when allied to some form of convergence technique, remains the only way of solving the transcendental eigenproblems of structural analysis with the certainty that any required eigenvalue will be found to any desired accuracy.

Early papers derived the W-W algorithm in four different ways. Two started from Rayleigh's theorem (Williams and Wittrick 1970; Wittrick and Williams 1971a), one started from energy arguments (Wittrick and Williams 1973a) and the final one (Simpson 1984; Wittrick and Williams 1973b) started from the Sturm sequence property of an exactly equivalent finite element model of (hypothetically) infinite order. In general, the Wittrick-Williams algorithm can be expressed in its simplest form as $J = J_0 + s\{\mathbf{K}\}$, where J is the number of eigenvalues of the complete structure exceeded by a trial frequency or load factor; $s\{\mathbf{K}\}$ is the sign count of **K**, the overall transcendental dynamic or buckling stiffness matrix of the structure evaluated at the trial value of the

eigenparameter; and J_0 denotes the value of J if clamps were to be applied at all of the degrees of freedom corresponding to **K** so as to make their displacements zero. The sign count is calculated as the number of negative leading diagonal elements of the upper triangular matrix obtained from **K** by using the usual form of Gauss elimination without pivoting.

The W-W algorithm has also been applied outside the area of structural engineering such as fluid vibration in pipes (Frid 1989; Frid 1990), heat and mass diffusion (Mikhailov and Ozisik 1984; Mikhailov et al. 1983) and Sturm-Liouville problems (Mikhailov and Vulchanov 1983; Williams et al. 2004a).

The J_0 term in the Wittrick-Williams algorithm corresponds to the poles on a plot of the determinant of **K** versus the eigenparameter. Such a plot is usually extremely volatile (Paz 1973; Simpson 1974; Simpson and Tabarrok 1968; Wittrick and Williams 1971a), particularly in the vicinity of the poles which, as mentioned earlier, may or may not correspond to eigenvalues. This makes it extremely difficult to implement computer based methods which use the value of the determinant in order to improve the rate of convergence upon the required eigenvalue (Kennedy and Williams 1991; Williams and Kennedy 1988).

The Wittrick-Williams algorithm, which is very often used to converge on the required roots by bisection, is known to be relatively slow. Dramatically more efficient convergence routines are available (Ammar et al. 1996; Kennedy et al. 1995; Kennedy and Williams 1991; Kennedy and Williams 1997; Qi et al. 2004; Simpson 1984; Williams and Kennedy 1988; Williams and Kennedy 1996), but their application is hampered by the highly volatile nature of the determinant of the structure's transcendental stiffness matrix, particularly in the vicinity of the poles, which may or may not correspond to eigenvalues.

When the closed form solution for the exact dynamic stiffness matrix of an element exists, a recently discovered member property, the member stiffness determinant (Williams and Kennedy 2003; Williams et al. 2002a; Williams et al. 2004b; Williams et al. 2002b; Zare et al. 2003a), enables the poles on a plot of the determinant of **K** versus

the eigenparameter to be eradicated and the general volatility of the plot to be substantially reduced with no loss of computational efficiency. It therefore provides a platform from which significantly more efficient eigenvalue extraction routines can be developed. However, obtaining the necessary analytical expression for the member stiffness determinant is far from straightforward. So far, such expressions have been reported for axially vibrating bars and Bernoulli-Euler beams (Williams et al. 2002a), for axially loaded Timoshenko beams (Williams et al. 2004b) and for isotropic and orthotropic prismatic plates (Zare et al. 2003a; Zare et al. 2003b; Zare et al. 2003c).

1.4 THESIS OUTLINE

Chapter 1 has so far given a brief overview of the origin and history of development of exact dynamic stiffness matrices, along with the corresponding methods of solving the transcendental eigenvalue problem. The reminder of this thesis consists of two parts, both of which have the common characteristic of using the concept of dynamic stiffness matrices. In the first part, the member stiffness determinant is derived for the first time for both isotropic and orthotropic prismatic plates. The second part considers the development of exact dynamic stiffness matrices for sandwich beams. This culminates in a unique model for a three layer Timoshenko beam.

1.4.2 Outline of Part A

In Part A, analytical expressions for the member stiffness determinant of isotropic and orthotropic prismatic plates are derived on the assumption that the plates carry in-plane compressive loads. This enables more efficient convergence routines to be used to calculate the natural frequencies or critical buckling loads, together with their corresponding mode shapes, of any prismatic plate assembly formed from such members.

In Chapter 2, the existing dynamic stiffness matrices for isotropic and orthotropic prismatic plates are introduced. Then, by using useful identities, alternative forms of the

elements of the stiffness matrices are developed that are more amenable to the derivation of the member stiffness determinant.

Chapter 3 deals with the derivation of the member stiffness determinant for both the isotropic and orthotropic plates and several examples illustrate the advantage of the theories. A method is also presented for obtaining the same advantages for plates carrying in-plane shear load or anisotropic plates by obtaining numerically an approximation to their member stiffness determinants.

1.4.3 Outline of Part B

Despite the availability of extensive literature on sandwich beams, there is very little work that utilises a dynamic stiffness formulation. More specifically, a precise and general stiffness formulation that accounts in an exact way for the uniform distribution of mass in a member can not be found. Therefore, the main aim of the work in Part B is to present an exact and concise dynamic stiffness method for the free vibration analysis of sandwich elements and the structures that can be fabricated from them. The analysis will be 'exact' in the sense that the solution, as opposed to the finite element method's solution, satisfies the governing differential equation exactly in the same way that the 'exact' solution can be obtained in conventional analytical theories.

Chapter 4 presents a general survey on the theory and application of sandwich beams.

Chapter 5 studies the flexural vibration of sandwich beams that have unequal faceplates. The resulting governing differential equation is of sixth order and the element has three degrees of freedom at each end. Therefore, the theory is only able to model the flexural vibration of sandwich beams.

In Chapter 6, the theory of Chapter 5 is extended to include the effects of longitudinal and rotary inertia. The inclusion of longitudinal inertia raises the order of the governing differential equation to eight. The resulting model provides four degrees of freedom at

each end and is able to predict the axial and shear thickness modes of vibration in addition to those corresponding to flexure.

Chapter 7 develops the most sophisticated sandwich beam theory developed herein, which includes all necessary theoretical and practical effects, including shear deformation in the faceplates and axial and bending stiffness of the core. The governing differential equation rises to tenth order and the model has five degrees of freedom at each end. Besides the flexural and axial modes of vibration, three classes of shear thickness modes can also be predicted by the theory.

Finally, Chapter 8 provides a summary of the thesis, draws conclusions and suggests those areas of thesis that could be usefully extended.

Part A

Member stiffness determinant for prismatic plates

CHAPTER 2

PRISMATIC PLATES

2.1 INTRODUCTION

Many structures consist essentially of a series of thin, flat plates rigidly connected together along their longitudinal edges, as typified by the structures of Figure 2.1. Such plate assemblies, which often take the form of flat panels with longitudinal thin-walled stiffeners attached, occur frequently in the aircraft and ship building industries. Corrugated panels are also used frequently for floor, roof and cladding systems. The basic state of stress may in general arise from loads applied at the ends, from variations of temperature over the cross-section and from the residual effects of the fabrication process.

In plate structures, the term *prismatic plate* is concerned with an individual plate which has a longitudinally invariant cross-section and is in a state of *plane stress* that is *longitudinally invariant* (Wittrick 1968a). Also to make it possible to treat each plate as a single element, it is postulated that *whatever type of mode occurs*, it is *sinusoidal* in the *longitudinal direction.* Hence, along any longitudinal line in any individual plate, the

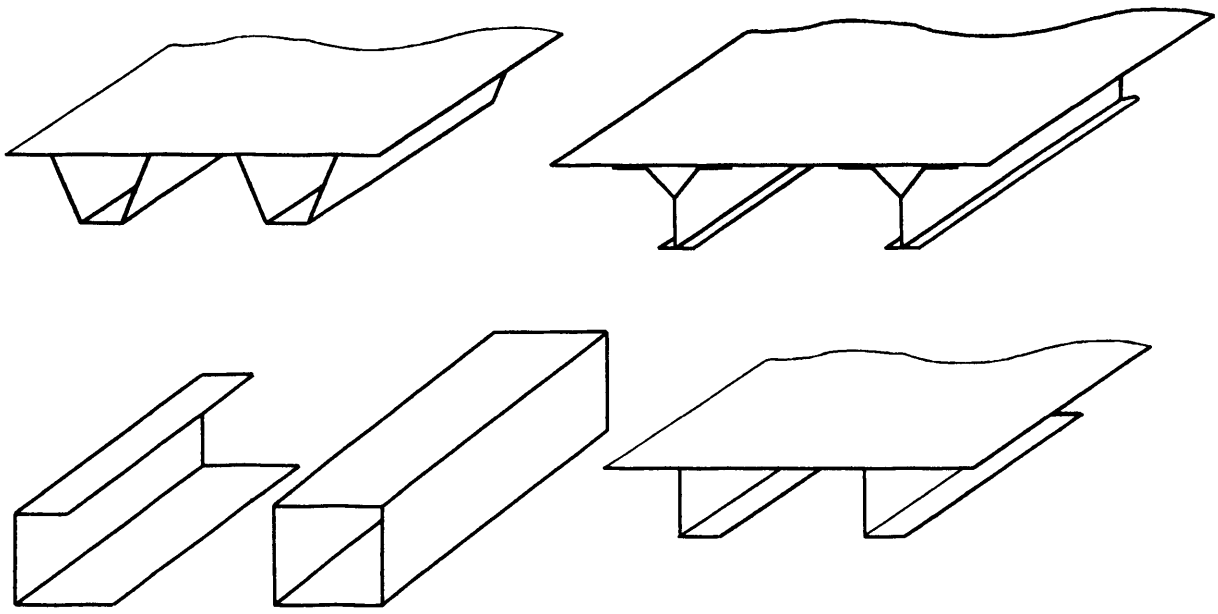

Figure 2.1: Examples of prismatic plate assemblies.

displacements vary sinusoidally. This requires either that the length of the structure is considerably greater than the half-wavelength of the mode, so that end effects are unimportant, or that the end supports permit such a mode to occur. The assumption of a sinusoidal mode implies that the perturbation edge forces at the edges of an individual plate also vary sinusoidally in the longitudinal direction. The fact that any mode is sinusoidal enables both time and the longitudinal co-ordinate to be eliminated. This enables an individual plate to be reduced from a two dimensional to a one-dimensional element, with the result that the structure can be treated as a two-dimensional skeletal structure whose topology is defined by the original cross section (Wittrick and Williams 1971b)

It has already been mentioned that for prismatic plates, the only requirement for the state of stress is that it should be uniform longitudinally. In general, the structure is assumed to be subjected to a 'dead load' system which does not cause buckling. (In buckling problems, a 'live load' system that has its magnitude defined by a single load factor may also be applied and the value of the load factor at buckling can be determined.) Figure 2.2 shows the general in-plane state of stress, consisting of a uniform longitudinal compressive force N_L per unit length, a uniform transverse compressive force N_T per

unit length and a uniform shear flow N_S per unit length. In a buckling problem these are the forces which give rise to the instability, whilst in a vibration problem they are regarded as defining the datum state of the structure about which small vibrations occur.

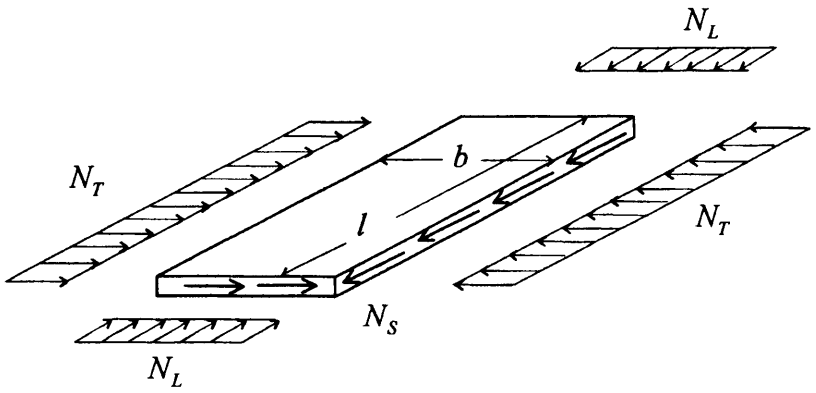

Figure 2.2: An individual plate of breadth b and length l subjected to a general in-plane force system.

During perturbations any individual prismatic plate is subjected to three components of distributed force and a distributed moment along each of its two longitudinal edges, Figure 2.3. In this figure, the positive directions of the edge forces and displacements are also shown, where P_x, P_y, P_z and M, respectively, represent the amplitude of the in-plane shear force, in-plane transverse force, out-of-plane shear force and bending moment per unit length of the plate edge. The amplitudes of these forces vary sinusoidally with time and the longitudinal co-ordinate, as do the corresponding components of edge displacement and rotation. Hence, it is possible to define stiffness matrices for an individual plate that relate the amplitudes of the force and displacement vectors at its longitudinal edges. If the material properties are isotropic and only longitudinal forces are present, the plate is identified as an *isotropic* prismatic plate. Similarly, when using orthotropic material or including transverse forces the plate is referred to as an *orthotropic* prismatic plate. In both cases the nodal lines are straight and perpendicular to the longitudinal edges. On the other hand, whenever in-plane shear stress is included or material property is anisotropic, the nodal lines in the plates will not be straight and perpendicular to the edges, Figure 2.3. Consequently, spatial phase differences occur between the perturbation edge forces and the displacements. This is accounted for by defining their magnitudes in terms of complex quantities.

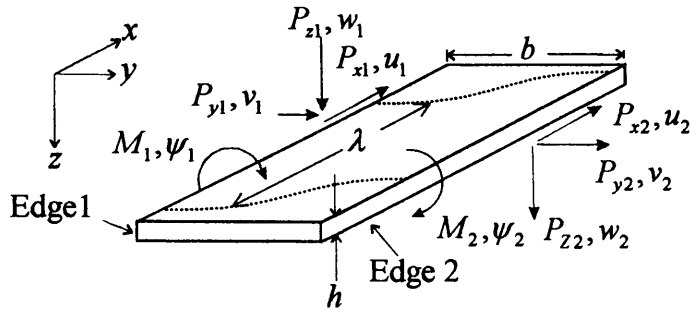

Figure 2.3: The amplitudes of the perturbation edge forces and displacements on an individual prismatic plate. Dotted lines show the nodal lines.

The complete set of sinusoidal forces and displacements at the edges of an individual plate comprise two uncoupled systems, one corresponding to out-of-plane behaviour and the other corresponding to in-plane behaviour. Therefore, the overall stiffness matrix can be split into two completely separate stiffness matrices corresponding to each plane. The in-plane stiffness matrix is always real and symmetric. However, the out-of-plane stiffness matrix is real and symmetric for orthotropic and isotropic prismatic plates, but complex and Hermitian for the anisotropic case. Throughout this study attention is mainly confined to either isotropic or orthotropic prismatic plates where the stiffness matrix is real and symmetric.

Irrespective of the classification, the elements of the stiffness matrix for all the plates considered are functions of the basic stresses and the wavelength (not the length of the plate) and also of the frequency in the case of vibration problem.

2.2 EIGENVALUE PROBLEM

In the late 1960s and early 1970s, Wittrick and Williams (Wittrick 1968a; Wittrick 1968b; Wittrick and Williams 1974) developed an exact dynamic stiffness matrix for prismatic plates that can be used very efficiently when solving both buckling and

vibration problems of structures comprising an assembly of isotropic, orthotropic or anisotropic prismatic plates. In each case, the exact solution to the member differential equations is employed to yield explicit analytical expressions of an 8×8 stiffness matrix which converts the eight amplitudes of the displacements at the edges to the corresponding amplitudes of the edge forces (including two moments), where the amplitudes are defined more precisely in Figure 2.3.

Assembling the exact element stiffness matrices, by the usual procedures of the finite element method, leads to a transcendental eigenvalue problem. Whether the problem under consideration is buckling or free vibrations, the eigenvalues are obtained from an equation of type

$$\mathbf{K}\,\mathbf{D} = \mathbf{0} \tag{2.1}$$

where $\mathbf{K}$ is the appropriate overall stiffness matrix of the structure and $\mathbf{D}$ is the corresponding nodal displacement vector.

Throughout the present theory the longitudinal direct force per unit length N_L and the frequency of vibration n always appear in association with each other through the relationship

$$N^* = N_L + 4\rho h\lambda^2 n^2 \quad \text{or} \quad \varepsilon = (N_L + 4\rho h\lambda^2 n^2)/Eh \tag{2.2}$$

in which, ρ and h are the plate density and thickness, respectively, E is Young's modulus for isotropic plates and λ is the longitudinal half-wavelength. In the vibration problem, we suppose that the structure is subjected to a specified system of dead loads which do not cause it to buckle. Hence, the eigenvalues of Eq. (2.1) correspond to the natural frequencies of vibration of the structure when acted upon by the given dead loads. On the other hand, the parameter n^2 in the vibration problem can in general be thought of as a load factor on a set of live loads in the buckling problem, which gives rise to a uniform longitudinal compressive force per unit length N_L, proportional to the value of $4\rho h\lambda^2$ in each plate. Therefore n can be regarded as an eigenparameter for both problems.

Thus, it is evident that buckling and vibration problems can be regarded as the same from a computational point of view and the equivalent critical buckling load can be determined from a knowledge of the corresponding natural frequency. Hence, hereafter, the theory that enables the eigenvalues of such structures to be determined is described in detail in the more demanding context of vibration.

However, in the vast majority of buckling problems interest is centred on the lowest eigenvalue, while in vibration problems it may be desired to calculate all natural frequencies in a specified band or to calculate the first m natural frequencies. It is necessary to note that if all the natural frequencies of the structure lying in a specified band are required, it is necessary to consider all possible wavelengths of the structure. This means that for any half-wave length λ, a family of modes and their frequencies exist. Hence, by choosing various wave numbers k the longitudinal half-wave length can be specified as $\lambda = l/k$, where $(k = 1, 2, 3, \ldots)$. This series could be terminated when a half-wave length become sufficiently short for the lowest natural frequency to lie above the upper limit of the specified frequency band. For example, Table 2 of (Wittrick and Williams 1971b) gives all the natural frequencies in the range $0 < \bar{n} < 0.1$ for a free-free panel, where $\bar{n}$ is a dimensionless frequency parameter. Those natural frequencies refer to wave numbers 1 to 6.

2.3 STIFFNESS MATRIX

The governing equations for the individual plate of Figure 2.2, in which x is the longitudinal axis, are given in (Wittrick and Williams 1974) as

$$\left.\begin{aligned} \mathbf{p}_1 &= \mathbf{k}_{11}\mathbf{d}_1 + \mathbf{k}_{12}\mathbf{d}_2 \\ \mathbf{p}_2 &= \mathbf{k}_{21}\mathbf{d}_1 + \mathbf{k}_{22}\mathbf{d}_2 \end{aligned}\right\} \qquad (2.3)$$

where

$$\mathbf{p}_j = \{M_j, P_{zj}, P_{yj}, \mathrm{i}P_{xj}\} \quad \text{and} \quad \mathbf{d}_j = \{\psi_j, w_j, v_j, \mathrm{i}u_j\} \quad (j = 1,2) \tag{2.4}$$

are four element vectors containing the amplitudes of, respectively, the sinusoidally varying force and displacement components at longitudinal edge j. The reason for associating i $(=\sqrt{-1})$ with P_{xj} and u_j is the 90° spatial phase difference between the longitudinal component of displacement and the two perpendicular components. Using Eq. (2.4) and the constitutive relations for prismatic plates (see Appendix A) yield the necessary stiffness matrix in Eq. (2.3). The $\mathbf{k}_{ij}$ $(i = 1,2\,;\, j = 1,2)$ are 4×4 stiffness matrices and may be partitioned into its uncoupled out-of-plane and in-plane components, denoted by superscripts O and I, to give

$$\mathbf{k}_{11} = \begin{bmatrix} \mathbf{k}_{11}^{O} & \mathbf{0} \\ \mathbf{0} & \mathbf{k}_{11}^{I} \end{bmatrix} \;;\; \mathbf{k}_{22} = \begin{bmatrix} \mathbf{k}_{22}^{O} & \mathbf{0} \\ \mathbf{0} & \mathbf{k}_{22}^{I} \end{bmatrix} \;;\; \mathbf{k}_{12} = \mathbf{k}_{21}^{\mathrm{T}} = \begin{bmatrix} \mathbf{k}_{12}^{O} & \mathbf{0} \\ \mathbf{0} & \mathbf{k}_{12}^{I} \end{bmatrix} \tag{2.5}$$

The out-of-plane stiffnesses correspond to the first two elements of $\mathbf{p}_j$ and $\mathbf{d}_j$ in Eq. (2.4) and the last two elements correspond to the in-plane ones. The out-of-plane and the in-plane matrices $\mathbf{k}_{11}^{O}$, $\mathbf{k}_{22}^{O}$, $\mathbf{k}_{12}^{O}$, $\mathbf{k}_{11}^{I}$, $\mathbf{k}_{22}^{I}$ and $\mathbf{k}_{12}^{I}$ are

$$\left.\begin{aligned} \mathbf{k}_{11}^{O} &= \begin{bmatrix} s_{MM} & -s_{MQ} \\ -s_{MQ} & s_{QQ} \end{bmatrix} ;\; \mathbf{k}_{22}^{O} = \begin{bmatrix} s_{MM} & s_{MQ} \\ s_{MQ} & s_{QQ} \end{bmatrix} ;\; \mathbf{k}_{12}^{O} = (\mathbf{k}_{21}^{O})^{\mathrm{T}} = \begin{bmatrix} f_{MM} & f_{MQ} \\ -f_{MQ} & -f_{QQ} \end{bmatrix} \\ \mathbf{k}_{11}^{I} &= \begin{bmatrix} s_{NN} & -s_{NT} \\ -s_{NT} & s_{TT} \end{bmatrix} ;\; \mathbf{k}_{22}^{I} = \begin{bmatrix} s_{NN} & s_{NT} \\ s_{NT} & s_{TT} \end{bmatrix} ;\; \mathbf{k}_{12}^{I} = (\mathbf{k}_{21}^{I})^{\mathrm{T}} = \begin{bmatrix} -f_{NN} & -f_{NT} \\ f_{NT} & f_{TT} \end{bmatrix} \end{aligned}\right\} \tag{2.6}$$

where expressions for their elements are given in the next sections for isotropic and orthotropic prismatic plates. The following dimensionless parameter is used for both cases

$$\varphi = b / \bar{\lambda} \tag{2.7}$$

where b is the breadth of an individual plate and $\bar{\lambda} = \lambda/\pi$ where λ is the half-wavelength of the mode.

2.4 ELEMENTS OF THE STIFFNESS MATRIX FOR ISOTROPIC PRISMATIC PLATES

Expressions for the elements of the matrices of Eq. (2.6) for the case of isotropic prismatic plates are given in reference (Wittrick and Williams 1971b; Wittrick and Wright 1978). The following dimensionless parameter are used

$$\varepsilon = (N_L + 4\rho h\lambda^2 n^2)/Eh; \qquad \eta = 2\sqrt{3(1-\nu^2)\varepsilon}\ \lambda/\pi h \tag{2.8}$$

where h is the thickness of an individual plate, λ is the half-wavelength of the mode, ν, E and ρ are Poisson's ratio, Young's modulus and density of the plate material, respectively, n is the frequency of vibration and N_L is the longitudinal force per unit breadth which is longitudinally invariant and constant across the breadth b of the plate. Hence buckling problems can be solved by setting $n = 0$ and vibration problems have $N_L = 0$ (constant) for unloaded (loaded) problems, enabling the natural frequencies to be found for unloaded or for axially compressed plate assemblies. Other definitions used are

$$\begin{aligned} &\alpha^2 = 1+\eta; && \gamma^2 = -\hat{\gamma}^2 = 1-\eta \\ &\tau^2 = -\hat{\tau}^2 = 1-(1-\nu^2)\varepsilon; && \zeta^2 = -\hat{\zeta}^2 = 1-2(1+\nu)\varepsilon \end{aligned} \tag{2.9}$$

Note that α is always real but that γ, τ and ζ can be complex. Furthermore, functions p_χ and q_χ of a parameter χ can be defined in general way such that

$$p_\chi = (1/\chi)\sinh\frac{\varphi\chi}{2} = (1/\hat{\chi})\ \sin\frac{\varphi\hat{\chi}}{2}\ ; \qquad q_\chi = \cosh\frac{\varphi\chi}{2} = \cos\frac{\varphi\hat{\chi}}{2} \tag{2.10}$$

where $\hat{\chi} = \mathrm{i}\chi$ whenever χ is imaginary. χ may take any of the values α, γ, τ, ζ, any combination of them or simply a constant.

2.4.2 Out-of-plane stiffness coefficients

In reference (Wittrick and Wright 1978) the out-of-plane stiffness coefficients of Eq. (2.6) have been given as

$$\left.\begin{aligned}
s_{MM} &= p_\alpha p_\gamma G_{af} + q_\alpha q_\gamma G_{sf} \\
f_{MM} &= p_\alpha p_\gamma G_{af} - q_\alpha q_\gamma G_{sf} \\
s_{MQ} &= [2\pi(1-\nu)D/\lambda - (\alpha^2 p_\alpha q_\gamma + \gamma^2 q_\alpha p_\gamma)G_{sf} - (q_\alpha p_\gamma + p_\alpha q_\gamma)G_{af}]\pi/2\lambda \\
f_{MQ} &= [(\alpha^2 p_\alpha q_\gamma + \gamma^2 q_\alpha p_\gamma)G_{sf} - (q_\alpha p_\gamma + p_\alpha q_\gamma)G_{af}]\pi/2\lambda \\
s_{QQ} &= (\alpha^2\gamma^2 p_\alpha p_\gamma G_{sf} + q_\alpha q_\gamma G_{af})\pi^2/\lambda^2 \\
-f_{QQ} &= (\alpha^2\gamma^2 p_\alpha p_\gamma G_{sf} - q_\alpha q_\gamma G_{af})\pi^2/\lambda^2
\end{aligned}\right\} \qquad (2.11)$$

where $D = Eh^3/12(1-\nu^2)$ is the plate flexural rigidity, and

$$\left.\begin{aligned}
G_{af} &= \pi D\eta/(q_\alpha p_\gamma - p_\alpha q_\gamma)\lambda \\
G_{sf} &= \pi D\eta/(\alpha^2 p_\alpha q_\gamma - \gamma^2 q_\alpha p_\gamma)\lambda
\end{aligned}\right\} \qquad (2.12)$$

The out-of-plane stiffness coefficients of Eq. (2.11) have been available in the literature for a number of years. However, during the development of the work reported herein, it soon become clear that considerable advantage could be gained by reformulating them so as to have a common component in the denominator of each of the stiffness coefficients. Therefore, using various trigonometric manipulations (some useful identities used are given in Appendix B) the following equations which are better suited to the subsequent development of the member stiffness determinant are obtained as

$$
\left.
\begin{aligned}
s_{MM} &= \left(q_{2\alpha} p_{2\gamma} - p_{2\alpha} q_{2\gamma} \right) \varsigma \, \bar{\lambda} / \delta \\
f_{MM} &= \left(p_{2\alpha} - p_{2\gamma} \right) \varsigma \, \bar{\lambda} / \delta \\
s_{MQ} &= D \left(1 - \nu\right) / \bar{\lambda}^2 - 2 p_{2\alpha} p_{2\gamma} \; \varsigma \, \eta / \delta \\
f_{MQ} &= \left(q_{2\gamma} - q_{2\alpha} \right) \varsigma / 2 \, \delta \\
s_{QQ} &= \left(\alpha^2 p_{2\alpha} q_{2\gamma} - \gamma^2 q_{2\alpha} p_{2\gamma} \right) \varsigma / \bar{\lambda} \delta \\
f_{QQ} &= \left(\alpha^2 p_{2\alpha} - \gamma^2 p_{2\gamma} \right) \varsigma / \bar{\lambda} \delta
\end{aligned}
\right\} \qquad (2.13a)
$$

where

$$
\varsigma = D \eta / \bar{\lambda}^2 ; \qquad \bar{\lambda} = \lambda / \pi \qquad \text{and} \qquad \delta = \tfrac{1}{2} \left(4 p_{2\alpha} p_{2\gamma} - q_{2\alpha} q_{2\gamma} + 1 \right) \qquad (2.13b)
$$

All quantities in Eq. (2.13) are real, and can be determined using real arithmetic. However, Eq. (2.13) cannot be used when the eigenparameter is zero (very close to zero) as in this case the expressions become undefined (unstable). Therefore, by using complex arithmetic an alternative set of expressions for this case are presented as

$$
\left.
\begin{aligned}
s_{MM} &= \left(\, p_{2(\alpha+\gamma)} - p_{2(\alpha-\gamma)} \, \right) D / \bar{\lambda} \, \hat{\delta} \\
f_{MM} &= \left(\, p_{(\alpha-\gamma)} q_{(\alpha+\gamma)} - p_{(\alpha+\gamma)} q_{(\alpha-\gamma)} \, \right) D / \bar{\lambda} \, \hat{\delta} \\
s_{MQ} &= \left(D \, / \bar{\lambda}^2 \right) \{ 1 - \nu - [(1 + \alpha\gamma) \, p^2_{(\alpha+\gamma)} - (1 - \alpha\gamma) \, p^2_{(\alpha-\gamma)}] / \hat{\delta} \, \} \\
f_{MQ} &= -2 \left(p_{(\alpha+\gamma)} \, p_{(\alpha-\gamma)} \right) D \alpha\gamma / \bar{\lambda}^2 \hat{\delta} \\
s_{QQ} &= \left(p_{2(\alpha+\gamma)} + p_{2(\alpha-\gamma)} \right) D \alpha\gamma / \bar{\lambda}^3 \hat{\delta} \\
f_{QQ} &= \left(\, p_{(\alpha-\gamma)} q_{(\alpha+\gamma)} + p_{(\alpha+\gamma)} q_{(\alpha-\gamma)} \, \right) D \alpha\gamma / \bar{\lambda}^3 \hat{\delta}
\end{aligned}
\right\} \qquad (2.14a)
$$

where

$$
\hat{\delta} = \frac{\eta^2}{\alpha\gamma} \delta = p^2_{(\alpha+\gamma)} - p^2_{(\alpha-\gamma)} \qquad (2.14b)
$$

Although Eq. (2.14) may contain some complex quantities, the final results of its right-hand sides are real. Also it is more convenient to set the stiffness coefficients for zero eigenparameters by taking their limit at $\varepsilon \to 0$ as

$$\left.\begin{aligned} s_{MM}\big|_{(\varepsilon=0)} &= 2(\,2p_2q_2-\varphi\,)\,D/\bar{\lambda}\,\hat{\delta}_0 \\ f_{MM}\big|_{(\varepsilon=0)} &= -2(\,2p_2-\varphi q_2\,)\,D/\bar{\lambda}\,\hat{\delta}_0 \\ s_{MQ}\big|_{(\varepsilon=0)} &= (D\,/\bar{\lambda}^{\,2})[1-\nu-8p_2^2/\hat{\delta}_0\,] \\ f_{MQ}\big|_{(\varepsilon=0)} &= -4\varphi\,p_2\,D/\bar{\lambda}^{\,2}\hat{\delta}_0 \\ s_{QQ}\big|_{(\varepsilon=0)} &= 2(\,2p_2q_2+\varphi\,)\,D/\bar{\lambda}^{\,3}\hat{\delta}_0 \\ f_{QQ}\big|_{(\varepsilon=0)} &= 2(\,2p_2+\varphi q_2\,)D/\bar{\lambda}^{\,3}\hat{\delta}_0 \end{aligned}\right\} \qquad (2.15)$$

where $\hat{\delta}_0 = 4\,\underset{\varepsilon}{\lim_0}\hat{\delta} = 4p_2^2-\varphi^2$. From definitions in Eq. (2.10), it is also clear that

$$p_2 = (\frac{1}{2})\sinh\frac{2\varphi}{2} = \tfrac{1}{2}\sinh\varphi \quad \text{and} \quad q_2 = \cosh\frac{2\varphi}{2} = \cosh\varphi \qquad (2.16)$$

2.4.3 *In-plane stiffness coefficients*

Similar to previous section, reference (Wittrick and Wright 1978) has been used for definition of the in-plane stiffness coefficients of Eq. (2.6). By introducing the coefficients

$$\left.\begin{aligned} H_f &= \pi E\,\varepsilon\,h/2(p_\tau q_\zeta-\zeta^2 q_\tau p_\zeta)\lambda \\ H_{sf} &= \pi E\,\varepsilon\,h/2(q_\tau p_\zeta-\tau^2 p_\tau q_\zeta)\lambda \end{aligned}\right\} \qquad (2.17)$$

the in-plane stiffness coefficients of Eq. (2.6) have been given as

$$
\left.
\begin{aligned}
s_{NN} &= q_\tau q_\zeta H_{sf} + \zeta^2 p_\tau p_\zeta H_f \\
f_{NN} &= q_\tau q_\zeta H_{sf} - \zeta^2 p_\tau p_\zeta H_f \\
s_{NT} &= q_\tau p_\zeta H_{sf} + p_\tau q_\zeta H_f - \pi E h/(1+\nu)\lambda \\
f_{NT} &= q_\tau p_\zeta H_{sf} - p_\tau q_\zeta H_f \\
s_{TT} &= q_\tau q_\zeta H_f + \tau^2 p_\tau p_\zeta H_{sf} \\
f_{TT} &= -q_\tau q_\zeta H_f + \tau^2 p_\tau p_\zeta H_{sf}
\end{aligned}
\right\} \qquad (2.18)
$$

In a similar fashion to the out-of-plane expressions, Eqs. (2.17) and (2.18) cannot be used to calculate the stiffness matrices for the static case or when the eigenparameter is zero. Also they are not in the most suitable form for further development of the member stiffness determinants. Thus, as for the out-of-plane case, more suitable in-plane stiffness coefficients can be developed from Eq. (2.18) as (See Appendix B)

$$
\left.
\begin{aligned}
s_{NN} &= (p_{2\tau} q_{2\zeta} - \zeta^2 p_{2\zeta} q_{2\tau})\kappa / \mu \\
f_{NN} &= (p_{2\tau} - \zeta^2 p_{2\zeta})\kappa / \mu \\
s_{NT} &= (4 p_{2\tau} p_{2\zeta} - q_{2\tau} q_{2\zeta} + 1)\kappa / 2\mu - 2\kappa / \varepsilon (1+\nu) \\
f_{NT} &= (q_{2\tau} - q_{2\zeta})\, \kappa / 2\mu \\
s_{TT} &= (p_{2\zeta} q_{2\tau} - \tau^2 p_{2\tau} q_{2\zeta})\kappa / \mu \\
f_{TT} &= (\tau^2 p_{2\tau} - p_{2\zeta})\kappa / \mu
\end{aligned}
\right\} \qquad (2.19a)
$$

where

$$
\kappa = E h \varepsilon / 2\bar{\lambda} \qquad \text{and} \qquad \mu = (1+\tau^2\zeta^2) p_{2\tau} p_{2\zeta} - \tfrac{1}{2}(q_{2\tau} q_{2\zeta} - 1) \qquad (2.19b)
$$

Although the expressions in Eq. (2.19) are real, they still cannot be used for calculating stiffness coefficients when the eigenparameter is zero. Hence, allowing for real and complex quantities, an alternative set of expression are developed as

$$
\left.
\begin{aligned}
s_{NN} &= [\beta_1 p_{2(\tau+\zeta)} + \beta_2 p_{2(\tau-\zeta)}]\zeta\,\bar{\kappa}/\hat{\mu} \\
f_{NN} &= \{\beta_1 p_{(\tau+\zeta)} q_{(\tau-\zeta)} + \beta_2 p_{(\tau-\zeta)} q_{(\tau+\zeta)}\}\zeta\,\bar{\kappa}/\hat{\mu} \\
s_{NT} &= -\bar{\kappa}\,\{1-[(\tau+\zeta)\beta_1 p^2_{(\tau+\zeta)} - (\tau-\zeta)\beta_2 p^2_{(\tau-\zeta)}]/\hat{\mu}\} \\
f_{NT} &= 2(1+\nu) p_{(\tau+\zeta)} p_{(\tau-\zeta)}\,\tau\zeta\,\bar{\kappa}/\hat{\mu} \\
s_{TT} &= [\beta_1 p_{2(\tau+\zeta)} - \beta_2 p_{2(\tau-\zeta)}]\tau\,\bar{\kappa}/\hat{\mu} \\
f_{TT} &= -[\beta_1 p_{(\tau+\zeta)} q_{(\tau-\zeta)} - \beta_2 p_{(\tau-\zeta)} q_{(\tau+\zeta)}]\tau\,\bar{\kappa}/\hat{\mu}
\end{aligned}
\right\} \qquad (2.20a)
$$

where $\beta_1 = 2\tau + \zeta(1-\nu)$, $\beta_2 = 2\tau - \zeta(1-\nu)$ and

$$
\bar{\kappa} = E\,h/(1+\nu)\bar{\lambda} \qquad \text{and} \qquad \hat{\mu} = \frac{4\tau\zeta}{(1+\nu)^2\varepsilon^2}\mu = [\,\beta_1^2\, p^2_{(\tau+\zeta)} - \beta_2^2\, p^2_{(\tau-\zeta)}\,] \qquad (2.20b)
$$

Although Eq. (2.20) may contain some complex quantities, the final results of the right-hand sides are real. Finally, the stiffness coefficients when the eigenparameter is zero can be derived from the expressions of Eq. (2.20) by taking their limit at $\varepsilon \to 0$ as

$$
\left.
\begin{aligned}
s_{NN}\big|_{(\varepsilon=0)} &= 2\,[2(3-\nu)p_2 q_2 + (1+\nu)\varphi]\bar{\kappa}/\hat{\mu}_0 \\
f_{NN}\big|_{\varepsilon=0)} &= 2\,[(1+\nu)\varphi q_2 + 2(3-\nu)p_2]\bar{\kappa}/\hat{\mu}_0 \\
s_{NT}\big|_{\varepsilon=0)} &= -\bar{\kappa}\,[1-8(3-\nu)p_2^2/\hat{\mu}_0\,] \\
f_{NT}\big|_{\varepsilon=0)} &= 4(1+\nu)\varphi\, p_2\bar{\kappa}/\hat{\mu}_0 \\
s_{TT}\big|_{\varepsilon=0)} &= 2\,[2(3-\nu)p_2 q_2 - (1+\nu)\varphi]\bar{\kappa}/\hat{\mu}_0 \\
f_{TT}\big|_{\varepsilon=0)} &= 2\,[(1+\nu)\varphi q_2 - 2(3-\nu)p_2]\bar{\kappa}/\hat{\mu}_0
\end{aligned}
\right\} \qquad (2.21)
$$

where $\hat{\mu}_0 = 4\,\underset{\varepsilon \to 0}{\lim}\hat{\mu} = 4\,(3-\nu)^2 p_2^2 - (1+\nu)^2\varphi^2$.

2.4.4 Determination of J_0

In the general form of the Wittrick-Williams algorithm, J_0 denotes the value of J if clamps were to be applied at all of the degrees of freedom corresponding to **K** so as to make their displacements zero. In this case, all the elements of the structure act as clamped-clamped elements and J_0 for the complete structure is the summation of J_0 for each element of the structure calculated separately. Now, in the case of prismatic plate assemblies

$$J_0 = \Sigma\left(J_0^O + J_0^I\right) \tag{2.22}$$

where J_0^O and J_0^I are, respectively, the number of out-of-plane and in-plane natural frequencies of a component plate exceeded by the trial frequency when all the nodal degrees of freedom of the plate are clamped and the summation is taken over all the plates comprising the assembly. Using the rules of (Wittrick and Wright 1978) and the current notation, J_0^O and J_0^I may be calculated as follows

$$\left.\begin{aligned} J_0^O &= \begin{cases} 0 & \text{if } \eta \le 1+(\lambda/b)^2 \\ l - \frac{1}{2}\left[1-(-1)^l sg\left(\delta\right)\right] & \text{if } \eta > 1+(\lambda/b)^2 \end{cases} \\ J_0^I &= \begin{cases} 0 & \text{if } \zeta^2 \ge 0 \\ 2m-1+\frac{1}{2}(-1)^m\left[sg\left(H_f\right)+sg\left(H_{sf}\right)\right] & \text{if } \zeta^2 < 0 \end{cases} \end{aligned}\right\} \tag{2.23}$$

where l is the highest integer less than $(b/\lambda)(\eta-1)^{1/2}$ and m is the highest integer less than $(0.5+0.5b\hat{\zeta}/\lambda)$ for $\tau^2 \ge 0$. When $\tau^2 < 0$, m is the sum of the highest integer less than $(0.5+0.5b\hat{\zeta}/\lambda)$ and the highest integer less than $(0.5+0.5b\hat{\tau}/\lambda)$. $sg(\ )$ is 1 or -1, depending on the sign of the parameter within the bracket.

2.5 ELEMENTS OF THE STIFFNESS MATRIX FOR ORTHOTROPIC PRISMATIC PLATES

Detailed expressions for the elements of the matrices of Eq. (2.6) for the case of orthotropic prismatic plates are given in reference (Wittrick and Williams 1974). As stated in Section (2.4), when developing the member stiffness determinant it will be very helpful if an alternative set of stiffness coefficients can be obtained from those in reference (Wittrick and Williams 1974) in such a way that a common term is present in the denominator of each of the stiffness coefficients. Therefore, by various trigonometric manipulations (some useful identities used are given in Appendix B) the coefficients given in reference (Wittrick and Williams 1974) are reworked in this section to be more suitable for the subsequent development of the member stiffness determinant.

The out-of-plane elements of the stiffness matrix of orthotropic prismatic plates are complicated transcendental functions of N_L, N_T, n and λ, while the in-plane elements depend on N_L, n and λ. Furthermore, in order to represent the elements of the stiffness matrix, real functions p_χ, q_χ, $\hat{p}_\chi$ and $\hat{q}_\chi$ are defined such that

$$\left.\begin{aligned} p_\chi &= (1/\chi)\sinh\varphi\chi = (1/\hat{\chi})\ \sin\varphi\hat{\chi}; & q_\chi &= \cosh\varphi\chi = \cos\varphi\hat{\chi} \\ \hat{p}_\chi &= (1/\chi)\sin\varphi\chi; & \hat{q}_\chi &= \cos\varphi\chi \end{aligned}\right\} \qquad (2.24)$$

where χ is a general subscript representing α, γ, τ and ζ, as defined in the following sections, or any combination of them, and $\hat{\chi} = \mathrm{i}\,\chi$ whenever χ is not real. φ is given by Eq. (2.7). Note that Eq. (2.24) is different from Eq. (2.10) and clearly, any equation related to orthotropic prismatic plates is based on Eq. (2.24).

2.5.2 Out-of-plane stiffness coefficients

The dimensionless parameters used in references (Lekhnitskii 1968; Wittrick 1968a; Wittrick and Williams 1974) for out-of-plane behaviour of orthotropic plates are given with some simplification as

$$L=\frac{\lambda^2}{\pi^2 D_{22}}N^*+T^2-\alpha_{11} \quad \text{and} \quad T=\alpha_{12}+2\alpha_{33}-\frac{\lambda^2 N_T}{2\pi^2 D_{22}} \tag{2.25}$$

where

$$\alpha_{11}=\frac{E_1}{E_2};\quad \alpha_{12}=\nu_1;\quad \alpha_{33}=\frac{G(1-\nu_1\nu_2)}{E_2}\quad D_{22}=\frac{E_2 h^3}{12(1-\nu_1\nu_2)} \tag{2.26}$$

and ν_1, ν_2, E_1, E_2 are Poisson's ratio and Young's modulus in the longitudinal and transverse in-plane directions of the plate, respectively, G is the shear modulus and N^* is defined in Eq. (2.2). Depending on the value of L, (Eq. (2.25)), the elements of the out-of-plane stiffness matrix should be defined for three different cases. Nevertheless, it is necessary to note that the three different cases may happen for various ranges of eigenparameter for the same plate element or even simultaneously for different elements of the problem. Furthermore, in contrast with the isotropic case, all relationships are well defined even for the zero eigenparameter, hence, there is no need to redefine them in alternative form or seeking limiting values.

2.5.2.1 Case 1: $L>0$

In this case the out-of-plane stiffness coefficients of Eq. (2.6) can be written as

$$\left.\begin{aligned}
s_{MM} &= D_{22}L^{1/2}(q_\alpha p_\gamma - q_\gamma p_\alpha)/\bar{\lambda}Z \\
s_{QQ} &= D_{22}L^{1/2}(\alpha^2 p_\alpha q_\gamma - \gamma^2 p_\gamma q_\alpha)/\bar{\lambda}^3 Z \\
s_{MQ} &= D_{22}\left(T-\alpha_{12}-L\,p_\alpha q_\gamma / Z\right)/\bar{\lambda}^2 \\
f_{MM} &= D_{22}L^{1/2}(p_\alpha - p_\gamma)/\bar{\lambda}Z \\
f_{QQ} &= D_{22}L^{1/2}(\alpha^2 p_\alpha - \gamma^2 p_\gamma)/\bar{\lambda}^3 Z \\
f_{MQ} &= -D_{22}L^{1/2}(q_\alpha - q_\gamma)/\bar{\lambda}^2 Z
\end{aligned}\right\} \tag{2.27}$$

where

$$Z = Tp_\alpha p_\gamma - q_\alpha q_\gamma + 1 \;; \quad \alpha^2 = -\hat{\alpha}^2 = T + L^{1/2} \;; \quad \gamma^2 = -\hat{\gamma}^2 = T - L^{1/2} \tag{2.28}$$

2.5.2.2 *Case 2:* $L < 0$

Defining the real and positive values of α and γ in the following way

$$\alpha = \sqrt{\frac{1}{2}\left(\sqrt{T^2 - L} + T\right)}; \quad \gamma = \sqrt{\frac{1}{2}\left(\sqrt{T^2 - L} - T\right)} \tag{2.29}$$

the stiffness coefficients become

$$\left.\begin{aligned} s_{MM} &= D_{22}(p_{2\alpha} - \hat{p}_{2\gamma})/\bar{\lambda} Z \\ s_{QQ} &= AD_{22}(p_{2\alpha} + \hat{p}_{2\gamma})/\bar{\lambda}^3 Z \\ s_{MQ} &= D_{22}\left(A - \alpha_{12} - A p_\alpha^2 / Z\right)/\bar{\lambda}^2 \\ f_{MM} &= D_{22}(q_\alpha \hat{p}_\gamma - \hat{q}_\gamma p_\alpha)/\bar{\lambda} Z \\ f_{QQ} &= AD_{22}(q_\alpha \hat{p}_\gamma + \hat{q}_\gamma p_\alpha)/\bar{\lambda}^3 Z \\ f_{MQ} &= -AD_{22} p_\alpha \hat{p}_\gamma / \bar{\lambda}^2 Z \end{aligned}\right\} \tag{2.30}$$

where

$$A = \alpha^2 + \gamma^2; \quad Z = \tfrac{1}{2}(p_\alpha^2 - \hat{p}_\gamma^2) \tag{2.31}$$

2.5.2.3 *Case 3:* $L = 0$

In this case the out-of-plane stiffness coefficients of Eq. (2.6) can be written as

$$\left.\begin{aligned} s_{MM} &= D_{22}(p_{2\alpha} - \varphi)/\varphi^2\bar{\lambda}Z \\ s_{QQ} &= D_{22}T(p_{2\alpha} + \varphi)/\varphi^2\bar{\lambda}^3 Z \\ s_{MQ} &= -D_{22}(T + \alpha_{12} + T/Z)/\bar{\lambda}^2 \\ f_{MM} &= D_{22}(q_\alpha - p_\alpha/\varphi)/\varphi\bar{\lambda}Z \\ f_{QQ} &= D_{22}T(q_\alpha + p_\alpha/\varphi)/\varphi\bar{\lambda}^3 Z \\ f_{MQ} &= -D_{22}Tp_\alpha/\bar{\lambda}^2 Z \end{aligned}\right\} \qquad (2.32)$$

where

$$\alpha^2 = -\hat{\alpha}^2 = T; \quad Z = (p_\alpha^2 - \varphi^2)/2\varphi^2 \qquad (2.33)$$

2.5.3 *In-plane stiffness coefficients*

Appropriate plate properties and necessary parameters for the in-plane behaviour of orthotropic prismatic plates can be obtained from those in (Wittrick and Williams 1974) and after some simplification yield

$$A_{11} = E_1 h/(1 - \nu_1\nu_2); \quad A_{12} = \nu_2 A_{11}; \quad A_{22} = \nu_2 A_{11}/\nu_1; \quad A_{33} = Gh \qquad (2.34)$$

$$A_0 = A_{12} + A_{33}; \quad L_1 = A_{11} - N^*; \quad L_3 = A_{33} - N^* \qquad (2.35)$$

$$B = \frac{A_{22}L_1 + A_{33}L_3 - A_0^2}{2A_{22}A_{33}}; \quad C = \frac{L_1 L_3}{A_{22}A_{33}} \qquad (2.36)$$

Depending on the value of B and C the elements of the in-plane stiffness matrix (Wittrick and Williams 1974) are defined for the two cases of $B^2 > C$ and $B^2 \le C$ by the following equations, which are better suited to the subsequent development of the member stiffness determinant. Nevertheless, it is necessary to note that the two different

cases may happen for various ranges of eigenparameter in the same problem and in contrast with isotropic case, all relationships are well defined, even for the zero eigenparameter.

2.5.3.1 Case 1: $B^2 > C$

In this case the in-plane stiffness coefficients of Eq. (2.6) can be written as

$$
\begin{aligned}
s_{NN} &= \left(\tau^2-\zeta^2\right)\left(A_{22}q_{\tau/2}q_{\zeta/2}/H_s + L_3 p_{\tau/2}p_{\zeta/2}/4H_a\right)/2\bar{\lambda}\\
s_{TT} &= \left(\tau^2-\zeta^2\right)\left(L_1 p_{\tau/2}p_{\zeta/2}/4H_s + A_{33}q_{\tau/2}q_{\zeta/2}/H_a\right)/2\bar{\lambda}\\
s_{NT} &= \left[A_0\left(\tau^2 p_{\tau/2}q_{\zeta/2} - \zeta^2 q_{\tau/2}p_{\zeta/2}\right)\Big/2H_s + A_0L_3\left(q_{\tau/2}p_{\zeta/2} - p_{\tau/2}q_{\zeta/2}\right)\Big/2A_{22}H_a - 2A_{33}\right]/2\bar{\lambda}\\
f_{NN} &= \left(\tau^2-\zeta^2\right)\left(A_{22}q_{\tau/2}q_{\zeta/2}/H_s - L_3 p_{\tau/2}p_{\zeta/2}/4H_a\right)/2\bar{\lambda}\\
f_{TT} &= \left(\tau^2-\zeta^2\right)\left(L_1 p_{\tau/2}p_{\zeta/2}/4H_s - A_{33}q_{\tau/2}q_{\zeta/2}/H_a\right)/2\bar{\lambda}\\
f_{NT} &= \left[A_0\left(\tau^2 p_{\tau/2}q_{\zeta/2} - \zeta^2 q_{\tau/2}p_{\zeta/2}\right)\Big/2H_s - A_0L_3\left(q_{\tau/2}p_{\zeta/2} - p_{\tau/2}q_{\zeta/2}\right)\Big/2A_{22}H_a\right]/2\bar{\lambda}
\end{aligned}
\tag{2.37}
$$

where

$$
\begin{aligned}
2H_a &= \left(L_3/A_{22}-\zeta^2\right)q_{\tau/2}p_{\zeta/2} - \left(L_3/A_{22}-\tau^2\right)p_{\tau/2}q_{\zeta/2}\\
2H_s &= \left(L_1/A_{33}-\zeta^2\right)q_{\tau/2}p_{\zeta/2} - \left(L_1/A_{33}-\tau^2\right)p_{\tau/2}q_{\zeta/2}
\end{aligned}
\tag{2.38}
$$

and

$$
\tau^2 = -\hat{\tau}^2 = B + \left(B^2-C\right)^{1/2}\ ;\quad \zeta^2 = -\hat{\zeta}^2 = B - \left(B^2-C\right)^{1/2} \tag{2.39}
$$

2.5.3.2 *Case 2:* $B^2 \le C$

Defining the real values of τ and ζ in the following way

$$\tau^2 = \tfrac{1}{2}(\sqrt{C} + B)\,; \quad \zeta^2 = \tfrac{1}{2}(\sqrt{C} - B) \tag{2.40}$$

and using the intermediate parameters of

$$\begin{aligned} H_a &= (p_\tau - \hat{p}_\zeta) + (p_\tau + \hat{p}_\zeta) L_1 / A_{33}\sqrt{C} \\ H_s &= (p_\tau + \hat{p}_\zeta) + (p_\tau - \hat{p}_\zeta) L_1 / A_{33}\sqrt{C} \end{aligned} \tag{2.41}$$

the in-plane elements of the stiffness matrix are as follows

$$\left.\begin{aligned} s_{NN} &= A_{22}\left[(q_\tau + \hat{q}_\zeta)/H_s + (q_\tau - \hat{q}_\zeta)/H_a\right]/\bar{\lambda} \\ s_{TT} &= L_1\left[(q_\tau - \hat{q}_\zeta)/H_s + (q_\tau + \hat{q}_\zeta)/H_a\right]/\bar{\lambda}\sqrt{C} \\ s_{NT} &= \left[A_0(p_\tau + \hat{p}_\zeta)/H_s + A_0(p_\tau - \hat{p}_\zeta)/H_a - 2A_{33}\right]/2\bar{\lambda} \\ f_{NN} &= A_{22}\left[(q_\tau + \hat{q}_\zeta)/H_s - (q_\tau - \hat{q}_\zeta)/H_a\right]/\bar{\lambda} \\ f_{TT} &= L_1\left[(q_\tau - \hat{q}_\zeta)/H_s - (q_\tau + \hat{q}_\zeta)/H_a\right]/\bar{\lambda}\sqrt{C} \\ f_{NT} &= \left[A_0(p_\tau + \hat{p}_\zeta)/H_s - A_0(p_\tau - \hat{p}_\zeta)/H_a\right]/2\bar{\lambda} \end{aligned}\right\} \tag{2.42}$$

2.5.4 *Determination of* J_0

For the case of prismatic orthotropic plate assemblies, by using the rules of (Wittrick and Williams 1974) and the current notation, J_0^O and J_0^I of Eq. (2.22) may be calculated as follows

$$J_0^O = J_{r1} - \tfrac{1}{2}[1 - sg(s_{MM})] - \tfrac{1}{2}[1 - sg(s_{MM} - f_{MM}^2 / s_{MM})]$$
$$J_0^I = J_{r2} - \tfrac{1}{2}[1 - sg(s_{NN})] - \tfrac{1}{2}[1 - sg(s_{NN} - f_{NN}^2 / s_{NN})] \qquad (2.43)$$

where $sg(\ )$ is 1 or -1 depending on the sign of the parameter within the bracket and

$$\left.\begin{aligned} J_{r1} &= \begin{cases} i_2 & \text{for } L > T^2 \\ i_2 - i_1 & \text{for } L < T^2 \text{ but } L > 0 \text{ and } T < 0 \\ 0 & \text{for } L < T^2 \text{ but } L > 0 \text{ and } T > 0 \\ 0 & \text{for } L \le 0 \end{cases} \\ J_{r2} &= \begin{cases} 1 + i_3 + i_4 & \text{For } N^* > A_U \\ i_4 + \tfrac{1}{2}[1 - sg(L_3)] & \text{For } A_L < N^* \le A_U \\ 0 & \text{For } N^* < A_L \text{ and } B_L \ge 0 \\ i_4 - i_3 & \text{For } A_M < N^* \le A_L \text{ and } B_L < 0 \\ 0 & \text{For } N^* \le A_M \text{ and } B_L < 0 \end{cases} \end{aligned}\right\} \qquad (2.44)$$

in which i_1, i_2, i_3 and i_4 are the largest integers less than $b\hat{\alpha}/\lambda, b\hat{\gamma}/\lambda, b\hat{\tau}/\lambda$ and $b\hat{\zeta}/\lambda$, respectively, although it must be noted that J_0^O and J_0^I only have values when at least one of the α, γ, τ or ζ are not real. A_L and A_U are the smaller and the larger value of the two quantities A_{11} and A_{33}, respectively, and

$$B_L = [A_{11}A_{22} + A_{33}^2 - A_0^2 - A_L(A_{22} + A_{33})]/2A_{22}A_{33}$$
$$A_M = \left(d_1 + \sqrt{d_2}\right)/(A_{22} - A_{33})^2 \qquad (2.45)$$

where

$$d_1 = (A_{22} - A_{33})(A_{11}A_{22} - A_{33}^2) - A_0^2(A_{22} + A_{33})$$
$$d_2 = 4A_{22}A_{33}A_0^2\left[A_0^2 - (A_{11} - A_{33})(A_{22} - A_{33})\right] \tag{2.46}$$

Finally, it should be noted that if J_{r1} or J_{r2} is zero then the remaining parts of their respective equations in Eq. (2.43) are also zero.

CHAPTER 3

MEMBER STIFFNESS DETERMINANT

3.1 INTRODUCTION

Closed form solutions of the differential equations governing the vibration or elastic critical buckling of prismatic plates have been available in the literature for many years and were briefly presented in Chapter 2. This type of solution, expressed in the form of exact member stiffness matrices, can be assembled in the usual way to model a variety of prismatic plate assemblies. Such a formulation necessitates the solution of a transcendental eigenproblem.

In both the buckling and vibration problem, the eigenvalues are obtained from an equation of type

$$\mathbf{K}\,\mathbf{D} = \mathbf{0} \tag{3.1}$$

where **K** is the appropriate overall stiffness matrix of the structure and **D** is the corresponding nodal displacement vector. The elements of **K** are highly complicated transcendental functions of the frequency or load factor, which become infinite at certain values of the eigenparameter and which may or may not correspond to eigenvalues. In general, the eigenvalues correspond to natural frequencies in undamped free vibration problems or elastic critical loads in buckling problems. The eigenvectors are the corresponding vibration or buckling modes.

The common early approach of determining eigenvalues was to plot the determinant $|\mathbf{K}|$ at fine intervals of the eigenparameter and seek the eigenvalues corresponding to $|\mathbf{K}|$ equals zero. This is often sufficient for the linear eigenvalue problem. However, the highly volatile nature of the determinant of the structure's transcendental stiffness matrix, particularly in the vicinity of the poles, which may or may not correspond to eigenvalues, can lead to some eigenvalues being missed, especially where several eigenvalues lie very close to each other or are coincident.

As mentioned earlier in Section 1.3, the Wittrick-Williams (W-W) algorithm (Wittrick and Williams 1971a) can be used to completely overcome the difficulties associated with the curve plotting method when solving transcendental eigenvalue problems. The W-W algorithm, when allied to some form of bisection technique, remains the only way of solving the transcendental eigenproblems of structural analysis with the certainty that any required eigenvalue will be found to any desired accuracy. The rate of convergence that is commonly achieved by bisection techniques is known to be relatively slow. However, implementation of those quicker methods that are available is hampered by the highly volatile nature of the determinant of the structure's transcendental stiffness matrix, particularly in the vicinity of the poles, which may or may not correspond to eigenvalues. Therefore, if this volatile nature of the determinant could be reduced, it would produce a safe platform for using quicker methods.

Derivation of the W-W algorithm using the Sturm sequence property of an exactly equivalent finite element model of (hypothetically) infinite order (Leung 1993; Simpson 1984; Wittrick and Williams 1973b), together with two more recent alternative sources

(Howson et al. 2001; Williams et al. 2002a) is central to the work that follows and is introduced below.

In general, the Wittrick-Williams algorithm can be expressed in its simplest form as $J = J_0 + s\{\mathbf{K}\}$, where J is the number of eigenvalues of the complete structure exceeded by a trial frequency or load factor; $s\{\mathbf{K}\}$ is the sign count of $\mathbf{K}$ which evaluated at the trial value of the eigenparameter that calculated as the number of negative leading diagonal elements of the upper triangular matrix obtained from $\mathbf{K}$ by using the usual form of Gauss elimination without pivoting, and J_0 denotes the value of J if clamps were to be applied at all of the degrees of freedom corresponding to $\mathbf{K}$ so as to make their displacements zero. Clearly, $J_0 = \sum J_m$ where J_m is the number of clamped ended eigenvalues of a component member passed by the trial frequency or load factor and the summation is over all the members. It is proved (Paz 1973; Simpson 1974; Wittrick and Williams 1971a) that the J_0 term corresponds to the poles on a plot of the determinant of $\mathbf{K}$ versus the eigenparameter. Such a plot is usually extremely volatile (Simpson and Tabarrok 1968; Wittrick and Williams 1971a), particularly in the vicinity of the poles which, as mentioned earlier, may or may not correspond to eigenvalues. This makes it extremely difficult to implement computer based methods for predicting the value of the determinant in order to improve the rate of convergence upon the required eigenvalue (Kennedy and Williams 1991; Williams and Kennedy 1988).

The work reported in this study shows how the poles of such a determinant can be completely eradicated and its volatility substantially reduced. This is achieved without introducing any approximation and yields all the original eigenvalues, which now correspond entirely to the zeros of a transformed determinant. The necessary transformation utilises a recently discovered member property, the member stiffness determinant (Williams and Kennedy 2003; Williams et al. 2002a; Williams et al. 2004b), which is unique to any given member type, being equal to the limit as the number of elements approaches infinity of the determinant obtained by a traditional (i.e. approximate) FEM representation of the member. The member stiffness determinant enables the poles to be eradicated from the plot of the determinant of $\mathbf{K}$ versus the eigenparameter and the general volatility to be substantially reduced and consequently more efficient convergence algorithms to be implemented. Its use does not incur any loss

of computational efficiency and yet provides a robust platform for the implementation of substantially more sophisticated convergence algorithms.

Indeed, the member stiffness determinant transforms the determinant of the structural stiffness matrix in its usual form to the determinant of the infinite order stiffness matrix of the structure. As a result of considering an infinite number of freedoms, the length of each element will be infinitely small and therefore the resulting J_0 will be zero and consequently no pole will be appear in the plot of the determinant of the stiffness matrix.

In other words, the member stiffness determinant scales the determinant of the stiffness matrix of the structure to a matrix whose determinant has no poles and where eigenvalues correspond only to the zeros of the determinant. However, obtaining the necessary analytical expression for the member stiffness determinant is far from straightforward. Such expressions have recently been given for axially vibrating bars and Bernoulli-Euler beams (Williams et al. 2002a) and for axially loaded Timoshenko beams (Williams et al. 2004b).

This study obtains, for the first time for any type of plate structure, analytical expressions for the member stiffness determinant needed to calculate the natural frequencies of vibration or the elastic buckling loads of prismatic plate assemblies. It starts by finding analytical expressions for the member stiffness determinant for a uniformly longitudinally compressed isotropic plate. Then, it extends the development to analytical expressions for the member stiffness determinant of an orthotropic plate that is assumed to carry both longitudinal and transverse compressive loads. Finally, a method is also presented for obtaining the same advantages for assemblies containing in-plane shear loaded anisotropic plates by obtaining numerically an approximation to their member stiffness determinants.

Numerical results show the good behaviour of the overall determinant plots which are scaled by using the member stiffness determinants of the plates. The zeros of these plots correspond precisely to the eigenvalues, whether these eigenvalues refers to the zeros or poles of the not so scaled plot of determinant. The examples given in this chapter cover

cases in which poles of not so scaled overall determinant coincide with eigenvalues as well as cases where they do not.

3.2 OVERVIEW

Consider a structure composed of members for which *exact finite elements* are available, i.e. the governing differential equations can be solved to give member stiffness matrices as transcendental functions of the eigenparameter, i.e. the frequency in vibration problems or the load factor in buckling problems, and which also involve the distributed mass of the member in vibration problems or its loading in buckling problems. The prismatic plate assembly shown in Figure 3.1(a) is an example. The structure could therefore be modelled in the usual way using one exact finite element per member and 'exact' solutions could be obtained. Assume however that each member is now divided into 2^r sub-members, where $r = 2$ in Figure 3.1(b). This is an undesirable action when using 'exact' elements in computation, since the size of the model would increase substantially and the solution accuracy would remain unaltered. However, it is shown later to be a helpful concept when finding the desired exact expressions for the member stiffness determinant.

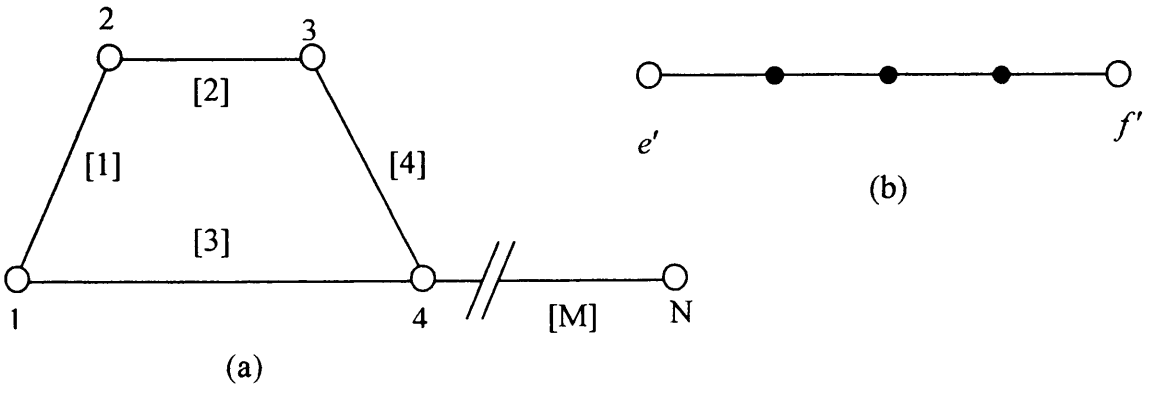

Figure 3.1: Simple prismatic plate assembly: (a) Cross section of the assembly. Open circles represent the connection nodes which run the length of the plate and are numbered 1 to N. Bracketed member numbers run from 1 to M; and (b) A typical plate connecting nodes e' and f' is divided into 2^r strips, i.e. plates of breadth $b/2^r$ ($r = 2$ in this example). The black circles represent the corresponding internal strip nodes. (Note that the sub-division into strips is not required to obtain solutions for assemblies of isotropic or orthotropic plates but is necessary whenever a plate is anisotropic).

Let us number the resulting structure so that the 'internal' freedoms associated with nodes emanating from the division of member m into 2^r sub-members, see Figure 3.1(b), are numbered first (here, the process of numbering starts from the internal freedoms of the first member and continue to the last member), followed by the equivalent freedoms from each of the M original members taken in turn. The former constitute the freedoms $\mathbf{d}_i$ of the modal vector, while the remaining freedoms $\mathbf{d}_c$, correspond to the original nodes of the parent structure. This is equivalent to solving the problem as an assemblage of sub-structures. Assume now that $r \to \infty$, so that the number of elements in $\mathbf{d}_i$ becomes infinitely greater than those in $\mathbf{d}_c$.

The resulting structure stiffness relationship can then be partitioned as

$$\begin{bmatrix} \mathbf{K}_{ii} & \mathbf{K}_{ic} \\ \mathbf{K}_{ic}^{\mathrm{T}} & \mathbf{K}_{cc} \end{bmatrix} \begin{bmatrix} \mathbf{d}_i \\ \mathbf{d}_c \end{bmatrix} = \begin{bmatrix} \mathbf{p}_i \\ \mathbf{p}_c \end{bmatrix} \tag{3.2}$$

where $\mathbf{p}_i$ and $\mathbf{p}_c$ are the perturbation forces corresponding to the freedoms $\mathbf{d}_i$ and $\mathbf{d}_c$, respectively, $\mathbf{K}_{ii}$ and $\mathbf{K}_{cc}$ are the contribution of the internal freedoms and the connecting nodes to the structure stiffness matrix, respectively, and $\mathbf{K}_{ic}$ and $\mathbf{K}_{ic}^{\mathrm{T}}$ are the cross-stiffnesses between the internal and connecting nodes of the structure. Since the internal nodes of each member are connected by the sub-members of the member and there is no connection between internal nodes of different members, it is clear that $\mathbf{K}_{ii}$ is a diagonal matrix of the form

$$\mathbf{K}_{ii} = \begin{bmatrix} \mathbf{k}_{ii}^{1} & \mathbf{0} & \cdots & \mathbf{0} \\ \mathbf{0} & \mathbf{k}_{ii}^{2} & \cdots & \mathbf{0} \\ \vdots & \vdots & \ddots & \vdots \\ \mathbf{0} & \mathbf{0} & \cdots & \mathbf{k}_{ii}^{M} \end{bmatrix} \tag{3.3}$$

where $\mathbf{k}_{ii}^{m}$ is the contribution of the internal freedoms in member m to the structure stiffness matrix. $\mathbf{k}_{ii}^{m}$ is a bounded matrix and its superscripts denote the member numbers in the original structure.

For eigenvalue problems $\mathbf{p}_i = \mathbf{p}_c = \mathbf{0}$. Gauss elimination in its usual form can then be performed on Eq. (3.2) to eliminate $\mathbf{d}_i$ by arresting the process after the rows corresponding to $\mathbf{d}_i$ have been pivotal, giving

$$\begin{bmatrix} \mathbf{K}_{ii}^{u} & \mathbf{K}^{'} \\ \mathbf{0} & \mathbf{K}_{cc}^{'} \end{bmatrix} \begin{bmatrix} \mathbf{d}_i \\ \mathbf{d}_c \end{bmatrix} = \begin{bmatrix} \mathbf{0} \\ \mathbf{0} \end{bmatrix} \tag{3.4}$$

where $\mathbf{K}_{ii}^{u}$ is the upper triangular form of $\mathbf{K}_{ii}$, $\mathbf{K}^{'}$ is of no further interest and $\mathbf{K}_{cc}^{'} = \mathbf{K}$, the global stiffness matrix governing the original structure of Figure 3.1(a), since the original problem could have been posed as $\mathbf{K}\mathbf{d}_c = \mathbf{0}$.

Now the number of elements represented by Eq. (3.4) approaches infinity when $r \to \infty$, so that the length of each element is infinitesimal and thus its clamped ended eigenvalues approach infinity. As a result, J_0 will always be zero and there will be no poles in the plot of the determinant obtained from the stiffness matrix of Eq. (3.4), which will now be called the infinite-order stiffness matrix, $\mathbf{K}_\infty$. Thus

$$|\mathbf{K}_\infty| = |\mathbf{K}_{ii}^{u}|\,|\mathbf{K}_{cc}^{'}| = |\mathbf{K}_{ii}^{u}|\,|\mathbf{K}| \tag{3.5}$$

Since $\mathbf{K}_{ii}^{u}$ is the upper triangular form of $\mathbf{K}_{ii}$, it is clear that their determinants are the same, hence

$$|\mathbf{K}_\infty| = |\mathbf{K}_{ii}|\,|\mathbf{K}| \tag{3.6}$$

From Eq. (3.3), $|\mathbf{K}_{ii}|$ may be written as

$$|\mathbf{K}_{ii}| = \prod_{m=1}^{M} |\mathbf{k}_{ii}^{m}| = \prod_{m=1}^{M} \Delta_m = \Delta \tag{3.7}$$

where

$$\Delta_m = \left| \mathbf{k}_{ii}^m \right| \tag{3.8}$$

is the determinant of the sub-structure stiffness matrix at level infinity or 'the member stiffness determinant' of member m and Δ is the product of the Δ_m taken over the members of the original structure. It is worth noting that if the structure exhibits any uncoupled behaviour, such as in-plane and out-of-plane motions in the current problem, each uncoupled component can be isolated, by separating out the corresponding rows and columns in matrix $\mathbf{k}_{ii}^m$, and its member stiffness determinant calculated separately. All individual contributions are then multiplied together to give the member stiffness determinant.

It is also important to note that Δ_m is exactly the value approached by $|\mathbf{k}_0 - \omega^2 \mathbf{m}|$ for the traditional FEM as the order of $\mathbf{k}_0$ and $\mathbf{m}$, the member static stiffness and mass matrices, approaches infinity. This is why the member stiffness determinant is a unique quantity for any given type of member, e.g. it cannot be multiplied by a constant or function and still be called the member stiffness determinant.

Now substituting Eq. (3.7) into Eq. (3.6) we may write

$$\left| \mathbf{K}_\infty \right| = \Delta \ |\mathbf{K}| \tag{3.9}$$

which will equal zero when evaluated at an eigenvalue.

However, since Δ_m is the determinant of an (approaching) infinitely large matrix because $r \to \infty$, its value is generally not finite and so it is necessary to work with normalised quantities, which yield the following relationships

$$\bar{\Delta} = \frac{\Delta}{\Delta_0}; \qquad \bar{\Delta}_m = \frac{\Delta_m}{\Delta_{m0}} \tag{3.10}$$

where the subscript zero denotes the value of the quantity when the eigenparameter is zero. If the determinant of $\mathbf{K}$, the global stiffness matrix governing the original structure, is normalised to give

$$\left|\overline{\mathbf{K}}\right| = \frac{\left|\mathbf{K}\right|}{\left|\mathbf{K}_0\right|} \tag{3.11}$$

then the final required result is

$$\left|\overline{\mathbf{K}}_{\infty}\right| = \overline{\Delta}\ \left|\overline{\mathbf{K}}\right| \tag{3.12}$$

3.3 MULTI-LEVEL SUB-STRUCTURING

In the previous section, the member stiffness determinant of element m has been defined in Eq. (3.7) where $\mathbf{k}_{ii}^{m}$ represents the contribution of the infinite number of internal freedoms in member m to the structure stiffness matrix. However, the derivation of the required member stiffness determinant is more desirable through multi-level sub-structuring, rather than working with $\mathbf{k}_{ii}^{m}$, in which the numbering was in sequence. The process is best described in the context of Figure 3.1(a), which shows the original plate assembly where each of the members can be considered to be a sub-structure with, initially, its points of attachment to the original structure treated as clamped. A typical member, of breadth b, is then divided into 2^r identical sub-members of breadth $b/2^r$ that are connected along their longitudinal edges, where $r = 2$ in Figure 3.1(b).

However, Figure 3.2 shows probably the simplest possible form of such multi-level sub-structuring with the nodes numbered in an appropriate order. In this method of numbering, the only internal node of the substructure in each level of substructuring is numbered first and the two end nodes numbered last. Such a process is very useful when developing the concept of the member stiffness determinant. Figure 3.2(a) shows a

doubling procedure with $r = 2$ levels i.e. there are two sub-structures at levels $i = 1$ and $i = 2$.

The equivalent assembly without using the concept of sub-structuring is shown in Figure 3.2(b). In this way, the node at the right-hand end of the full member is the highest numbered node i.e. $(2^r + 1)$ and the node at the left-hand end is numbered immediately below i.e. 2^r. The node at the middle of the member is then numbered immediately below them etc. and this successive halving is continued with the middle of the generated sub-members numbered from the right-hand side in descending order.

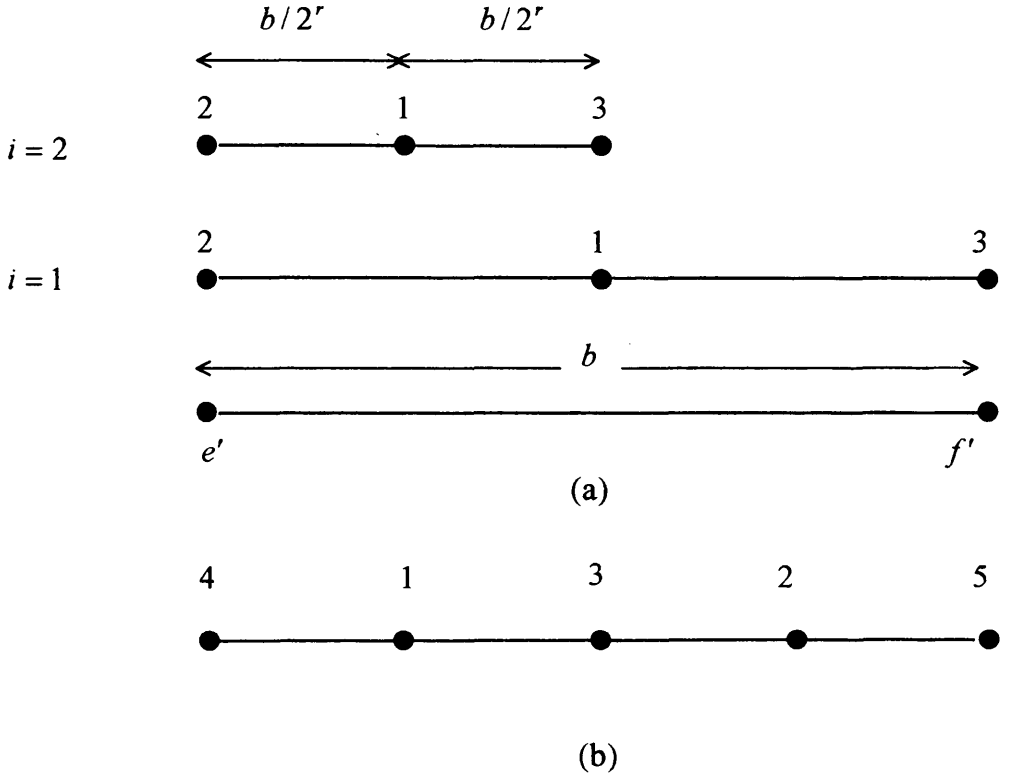

Figure 3.2: Alternative ways of assembling a typical prismatic plate of breadth b connecting nodes e' and f' from 2^r identical strips of breadth $b/2^r$, for $r = 2$. a) assembly by multi-level sub-structuring using progressive doubling, b) equivalent assembly without sub-structuring. A black circle denotes a node.

A doubling procedure is now invoked. This starts by combining two strips together and proceeds by eliminating the central node to form a sub-structure of breadth $b/2^{r-1}$ by arrested Gauss elimination in exactly the form used to obtain Eq. (3.4). The process is

then repeated, each time combining two sub-structures of the previous level, until all the internal nodes of the original plate have been eliminated.

As part of the doubling procedure, the W-W algorithm is applied at each sub-structure level to track the number of roots exceeded. The way this is achieved in such cases is described in one of the original proofs of the algorithm (Wittrick and Williams 1971a) and in the current context, but related to skeletal frames, in reference (Williams et al. 2002a). Briefly, the W-W algorithm is applied to the innermost sub-structure first, with its points of attachment to the next level of sub-structure treated as clamped. Hence Eq. (3.13) gives its J as

$$J_s = \sum J_m + s\{\mathbf{K}_{sr}\} \tag{3.13}$$

where the summation extends over the strips contained by the sub-structure, i.e. those used when assembling the sub-structure stiffness matrix $\mathbf{K}_{sr}$. Then Eq. (3.13) is executed for the next level of sub-structure, for which $\sum J_m$ is supplemented by J_s for the innermost sub-structure and the summation is over all members contributing to $\mathbf{K}_{sr}$ and so excludes members which were included in $\sum J_m$ when Eq. (3.13) was applied to the innermost sub-structure. Recursive application of Eq. (3.13) in this manner permits multi-level sub-structuring to be applied at any required level, i.e. if level r is the innermost level there is no restriction on r.

It will be shown that computation using multi-level sub-structuring is quicker because it is only necessary to perform calculations for one of each set of identical substructures. To verify this, we will examine the process for level 1 and 2 using the equivalent alternative way of assembling to show the characteristics of the substructuring and then we infer the necessary relationship for $r \to \infty$.

3.3.2 Sub-structuring with only one level

Consider a typical plate that is divided into $2^1 = 2$ identical sub-members that are connected along their edges, Figure 3.3. The resulting structure stiffness relationship can then be written as

$$\begin{bmatrix} \mathbf{k}_{22}^{a} + \mathbf{k}_{11}^{b} & \mathbf{k}_{12}^{aT} & \mathbf{k}_{12}^{b} \\ \mathbf{k}_{12}^{a} & \mathbf{k}_{11}^{a} & \mathbf{0} \\ \mathbf{k}_{12}^{bT} & \mathbf{0} & \mathbf{k}_{22}^{b} \end{bmatrix} \begin{bmatrix} \mathbf{D}_1 \\ \mathbf{D}_2 \\ \mathbf{D}_3 \end{bmatrix} = \mathbf{0} \tag{3.14}$$

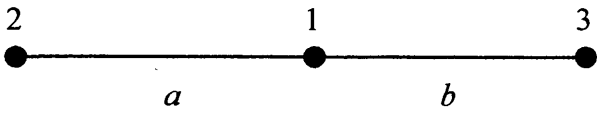

Figure 3.3: A typical plate is divided into $2^1 = 2$ identical sub-members (strips). A black circle denotes a node, numbered as shown and the strips between the nodes are named alphabetically.

Now, performing arrested gauss elimination to eliminate the internal freedoms of node 1 gives

$$\begin{bmatrix} \mathbf{k}_{s1} & \mathbf{k}_{12}^{aT} & \mathbf{k}_{12}^{b} \\ \mathbf{0} & \mathbf{k}_{11}^{ab} & \mathbf{k}_{12}^{ab} \\ \mathbf{0} & \mathbf{k}_{12}^{abT} & \mathbf{k}_{22}^{ab} \end{bmatrix} \begin{bmatrix} \mathbf{D}_1 \\ \mathbf{D}_2 \\ \mathbf{D}_3 \end{bmatrix} = \mathbf{0} \tag{3.15}$$

where $\mathbf{k}_{s1} = \mathbf{K}_{s1}$ is the only substructure stiffness matrix for internal freedoms $\mathbf{D}_1$ and may be written as

$$\mathbf{k}_{s1} = \mathbf{k}_{22}^{a} + \mathbf{k}_{11}^{b} = \mathbf{k}_{11i} + \mathbf{k}_{22i} \tag{3.16}$$

where $i = 1$ is the only level of sub-structuring for $r = 1$ and

$$\begin{bmatrix} \mathbf{k}_{11}^{ab} & \mathbf{k}_{12}^{ab} \\ \mathbf{k}_{12}^{abT} & \mathbf{k}_{22}^{ab} \end{bmatrix} \begin{Bmatrix} \mathbf{D}_2 \\ \mathbf{D}_3 \end{Bmatrix} = \mathbf{KD} = \mathbf{0} \tag{3.17}$$

represents the full member stiffness relation. $\mathbf{k}_{s1}$ is a diagonal matrix for all straight prismatic members. (To the writer's knowledge, it is not quite diagonal for curved members, tapered members or sandwich beams.) From Eq.(2.6) it can easily be seen that for prismatic plate members, isotropic or orthotropic, $\mathbf{k}_{s1}$ is diagonal.

Therefore, the determinant of the stiffness matrix, including the effects of sub-structuring with one level of sub-structuring, $\mathbf{K}_1$, can be written as

$$|\mathbf{K}_1| = |\mathbf{K}_{s1}||\mathbf{K}| \tag{3.18}$$

3.3.3 Substructuring with two levels

Now consider a typical member that is divided into $2^2 = 4$ identical sub-members that are connected along their edges, Figure 3.4. The resulting structure stiffness relationship can then be written as

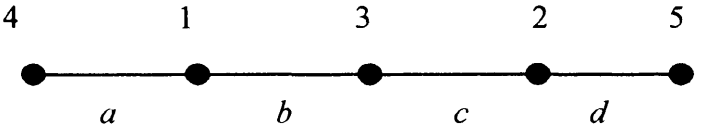

Figure 3.4: A typical plate is divided into $2^2 = 4$ identical sub-members (strips). A black circle denotes a node, numbered as shown and the strips between the nodes are named alphabetically.

$$\begin{bmatrix} \mathbf{k}_{22}^{a}+\mathbf{k}_{11}^{b} & \mathbf{0} & \mathbf{k}_{12}^{b} & \mathbf{k}_{12}^{aT} & \mathbf{0} \\ \mathbf{0} & \mathbf{k}_{22}^{c}+\mathbf{k}_{11}^{d} & \mathbf{k}_{12}^{cT} & \mathbf{0} & \mathbf{k}_{12}^{d} \\ \mathbf{k}_{12}^{bT} & \mathbf{k}_{12}^{c} & \mathbf{k}_{22}^{b}+\mathbf{k}_{11}^{c} & \mathbf{0} & \mathbf{0} \\ \mathbf{k}_{12}^{a} & \mathbf{0} & \mathbf{0} & \mathbf{k}_{11}^{a} & \mathbf{0} \\ \mathbf{0} & \mathbf{k}_{12}^{dT} & \mathbf{0} & \mathbf{0} & \mathbf{k}_{22}^{d} \end{bmatrix} \begin{bmatrix} \mathbf{D}_1 \\ \mathbf{D}_2 \\ \mathbf{D}_3 \\ \mathbf{D}_4 \\ \mathbf{D}_5 \end{bmatrix} = \mathbf{0} \tag{3.19}$$

Now, performing arrested gauss elimination to eliminate the internal freedoms of nodes 1, 2 and 3 (with the knowledge that the sub-members and their stiffness matrices are identical) gives

$$\begin{bmatrix} \mathbf{k}_{s2} & \mathbf{0} & \mathbf{k}_{12}^{b} & \mathbf{k}_{12}^{aT} & \mathbf{0} \\ \mathbf{0} & \mathbf{k}_{s2} & \mathbf{k}_{12}^{c} & \mathbf{0} & \mathbf{k}_{12}^{d} \\ \mathbf{0} & \mathbf{0} & \mathbf{k}_{s1} & \mathbf{C}_1 & \mathbf{C}_2 \\ \mathbf{0} & \mathbf{0} & \mathbf{0} & \mathbf{k}_{11}^{abcd} & \mathbf{k}_{12}^{abcd} \\ \mathbf{0} & \mathbf{0} & \mathbf{0} & \mathbf{k}_{12}^{abcdT} & \mathbf{k}_{22}^{abcd} \end{bmatrix} \begin{bmatrix} \mathbf{D}_1 \\ \mathbf{D}_2 \\ \mathbf{D}_3 \\ \mathbf{D}_4 \\ \mathbf{D}_5 \end{bmatrix} = \mathbf{0} \tag{3.20}$$

where $\mathbf{C}_1$ and $\mathbf{C}_2$ are matrices of no further interest, and the top-left 3×3 partition given by

$$\mathbf{K}_{s2} = \begin{bmatrix} \mathbf{k}_{s2} & \mathbf{0} & \mathbf{k}_{12}^{b} \\ \mathbf{0} & \mathbf{k}_{s2} & \mathbf{k}_{12}^{c} \\ \mathbf{0} & \mathbf{0} & \mathbf{k}_{s1} \end{bmatrix} \tag{3.21}$$

is the substructure stiffness matrix for internal freedoms corresponding to $\mathbf{D}_1$, $\mathbf{D}_2$ and $\mathbf{D}_3$. From the arguments of the previous section, it is clear that $\mathbf{k}_{s2}$, which has the effects of the highest level of sub-structuring, is diagonal for exactly the same reasons that $\mathbf{k}_{s1}$ of the previous section was. Now, it is necessary to verify the

characteristics of $\mathbf{k}_{s1}$ of this section. The process of gauss elimination is equivalent to substituting the following symbolic expression

$$\mathbf{k}_{s1} = (\mathbf{k}_{22}^{b} + \mathbf{k}_{11}^{c}) - \mathbf{k}_{12}^{b\mathrm{T}}(\mathbf{k}_{22}^{a} + \mathbf{k}_{11}^{b})^{-1}\mathbf{k}_{12}^{b} - \mathbf{k}_{12}^{c}(\mathbf{k}_{22}^{c} + \mathbf{k}_{11}^{d})^{-1}\mathbf{k}_{12}^{c\mathrm{T}} \tag{3.22}$$

or

$$\mathbf{k}_{s1} = (\mathbf{k}_{11}^{a} + \mathbf{k}_{22}^{a}) - \mathbf{k}_{12}^{a\mathrm{T}}(\mathbf{k}_{11}^{a} + \mathbf{k}_{22}^{a})^{-1}\mathbf{k}_{12}^{a} - \mathbf{k}_{12}^{a}(\mathbf{k}_{11}^{a} + \mathbf{k}_{22}^{a})^{-1}\mathbf{k}_{12}^{a\mathrm{T}} \tag{3.23}$$

Now, as an example, the elements of the out-of-plane stiffness matrix of Eq. (2.6) are substituted into Eq. (3.23) to show the characteristics of $\mathbf{k}_{s1}$. Thus

$$\begin{aligned}\mathbf{k}_{s1} = &\begin{bmatrix} 2s_{MM} & 0 \\ 0 & 2s_{QQ} \end{bmatrix} - \begin{bmatrix} f_{MM} & -f_{MQ} \\ f_{MQ} & -f_{QQ} \end{bmatrix}\begin{bmatrix} 1/2s_{MM} & 0 \\ 0 & 1/2s_{QQ} \end{bmatrix}\begin{bmatrix} f_{MM} & f_{MQ} \\ -f_{MQ} & -f_{QQ} \end{bmatrix} \\ &- \begin{bmatrix} f_{MM} & f_{MQ} \\ -f_{MQ} & -f_{QQ} \end{bmatrix}\begin{bmatrix} 1/2s_{MM} & 0 \\ 0 & 1/2s_{QQ} \end{bmatrix}\begin{bmatrix} f_{MM} & -f_{MQ} \\ f_{MQ} & -f_{QQ} \end{bmatrix}\end{aligned} \tag{3.24}$$

or

$$\begin{aligned}\mathbf{k}_{s1} = &\begin{bmatrix} 2s_{MM} & 0 \\ 0 & 2s_{QQ} \end{bmatrix} - \begin{bmatrix} \dfrac{f_{MM}^2}{s_{MM}} + \dfrac{f_{MQ}^2}{s_{QQ}} & \dfrac{f_{MQ}f_{MM}}{s_{MM}} + \dfrac{f_{QQ}f_{MQ}}{s_{QQ}} \\ \dfrac{f_{MQ}f_{MM}}{s_{MM}} + \dfrac{f_{QQ}f_{MQ}}{s_{QQ}} & \dfrac{f_{MQ}^2}{s_{MM}} + \dfrac{f_{QQ}^2}{s_{QQ}} \end{bmatrix} \\ &- \begin{bmatrix} \dfrac{f_{MM}^2}{s_{MM}} + \dfrac{f_{MQ}^2}{s_{QQ}} & -\dfrac{f_{MQ}f_{MM}}{s_{MM}} - \dfrac{f_{QQ}f_{MQ}}{s_{QQ}} \\ -\dfrac{f_{MQ}f_{MM}}{s_{MM}} - \dfrac{f_{QQ}f_{MQ}}{s_{QQ}} & \dfrac{f_{MQ}^2}{s_{MM}} + \dfrac{f_{QQ}^2}{s_{QQ}} \end{bmatrix}\end{aligned} \tag{3.25}$$

then

$$\mathbf{k}_{s1} = 2\begin{bmatrix} s_{MM} - \dfrac{f_{MM}^2}{s_{MM}} - \dfrac{f_{MQ}^2}{s_{QQ}} & 0 \\ 0 & s_{QQ} - \dfrac{f_{MQ}^2}{s_{MM}} - \dfrac{f_{QQ}^2}{s_{QQ}} \end{bmatrix} \tag{3.26}$$

Eq. (3.26) shows that $\mathbf{k}_{s1}$ is a diagonal matrix. The elements of stiffness matrices which are used in Eq. (3.26) are the same as those that has been used in derivation of Eq. (3.22), i.e. the elements of a substructure at the highest level of sub-structuring which in the current section is 2. Therefore, the breadth of the plate for calculating s_{MM}, s_{QQ}, ... in Eq. (3.26) is $b/2^2$. Now as the second characteristic of $\mathbf{k}_{si}$ we need to show $\mathbf{k}_{s1}$ can also be evaluated using the stiffness elements at level one, i.e. we need to show that

$$\left(s_{MM} - \frac{f_{MM}^2}{s_{MM}} - \frac{f_{MQ}^2}{s_{QQ}}\right)_{Level=2} = s_{MM}\Big|_{Level=1}$$

$$\left(s_{QQ} - \frac{f_{MQ}^2}{s_{MM}} - \frac{f_{QQ}^2}{s_{QQ}}\right)_{Level=2} = s_{QQ}\Big|_{Level=1} \tag{3.27a,b}$$

Note that the breadth of the plate for calculating s_{MM}, s_{QQ}, ... of the left-hand side of Eq. (3.27) is $b/2^2$ while it is $b/2^1$ for the right-hand side. Again, as an example, the out-of-plane stiffness coefficients of Eq.(2.25) are used and therefore, the right-hand side of Eq. (3.27a) gives

$$\left(s_{MM} - \frac{f_{MM}^2}{s_{MM}} - \frac{f_{MQ}^2}{s_{QQ}}\right)_{Level=2} = \left(D_{22}L^{1/2}/\bar{\lambda}Z\right)\left((q_\alpha p_\gamma - q_\gamma p_\alpha) - \frac{(p_\alpha - p_\gamma)^2}{(q_\alpha p_\gamma - q_\gamma p_\alpha)} - \frac{(q_\alpha - q_\gamma)^2}{(\alpha^2 p_\alpha q_\gamma - \gamma^2 p_\gamma q_\alpha)}\right) \tag{3.28}$$

and by various trigonometric manipulations (some useful identities that are used are given in Appendix B) we have

$$\left(s_{MM} - \frac{f_{MM}^2}{s_{MM}} - \frac{f_{MQ}^2}{s_{QQ}}\right)_{Level=2} = \left(D_{22}L^{1/2}/\bar{\lambda}\right)\left(\frac{(q_\alpha p_\gamma - q_\gamma p_\alpha)}{Z}\right)\Bigg|_{Level=1} = s_{MM}\Big|_{Level=1} \tag{3.29}$$

In similar fashion, the correctness of Eq. (3.27b) is verified. Hence, we can again write

$$\mathbf{k}_{si} = \mathbf{k}_{11i} + \mathbf{k}_{22i} \tag{3.30}$$

which is valid for any level of sub-structuring.

Therefore, the determinant of the stiffness matrix, including the effects of sub-structuring at level 2, i.e. $\mathbf{K}_2$ can be written as

$$|\mathbf{K}_2| = |\mathbf{K}_{s2}||\mathbf{K}| = |\mathbf{k}_{s2}|\,|\mathbf{k}_{s2}|\,|\mathbf{k}_{s1}||\mathbf{K}| \tag{3.31}$$

3.3.4 *Substructuring for level* $r \rightarrow \infty$

It can be seen from the arguments above that for the substructure of level 3, $2^3 - 1 = 7$ internal nodes have to be eliminated. The first four steps eliminate nodes 1 to 4 by repeating four times the calculations needed to eliminate the central node for $i = 3$, while the next two steps repeat two times the calculations needed for $i = 2$ and finally the last step is the calculations for $i = 1$.

$$|\mathbf{K}_3| = |\mathbf{K}_{s3}||\mathbf{K}| = |\mathbf{k}_{s3}||\mathbf{k}_{s3}||\mathbf{k}_{s3}||\mathbf{k}_{s3}|\,|\mathbf{k}_{s2}||\mathbf{k}_{s2}|\,|\mathbf{k}_{s1}||\mathbf{K}| \tag{3.32}$$

Now we can infer the expression for $\mathbf{K}_{sr}$, which corresponds to the displacement vector for the $2^r - 1$ internal nodes of substructure at level r, and its determinant can be written as

$$|\mathbf{K}_{sr}| = \prod_{i=1}^{r} \left[|\mathbf{k}_{si}|^{\left[2^{(i-1)}\right]} \right] \tag{3.33}$$

where $\mathbf{k}_{si}$ is the sub-structure formed at level i (= 1, 2, 3, ... ,r). This sub-structure has a single internal node which is replicated 2^{i-1} times during the doubling procedure. In

the limit as $r \to \infty$, we obtain the recently discovered member stiffness determinant, Δ_m, which is given by

$$\Delta_m = \prod_{i=1}^{\infty} \left[|\mathbf{k}_{si}|^{[2^{(i-1)}]} \right] \tag{3.34}$$

However the stiffness determinant for the member at level i is

$$\Delta_{m(i)}(n) = \prod_{i'=i+1}^{\infty} \left\{ \left[|\mathbf{k}_{si'}(n)| \right]^{[2^{(i'-i-1)}]} \right\} \tag{3.35}$$

The equivalent relationship for level $i-1$ is readily obtained and comparing Δ_{mi} with $\Delta_{m(i-1)}$ yields the necessary recurrence relationship for determining the member stiffness determinant as

$$\Delta_{m(i-1)}(n) = |\mathbf{k}_{si}(n)| \left[\Delta_{m(i)}(n) \right]^2 \tag{3.36}$$

The highest level of sub-structure, i.e. $i = 0$, corresponds to the original member so that

$$\Delta_m(n) = \Delta_{m(0)}(n) \tag{3.37}$$

It is worth noting that applying Eq. (3.37) to every member of a structure in the limit as $r \to \infty$ produces exact values of their member stiffness determinants Δ_m. As stated previously in Eq. (3.10), because Eq. (3.37) does not generally yield a finite value for Δ_m, it is appropriate to normalise it by dividing it by the value that it gives when the eigenparameter has the value zero, i.e. for buckling problems when the load components are zero and for vibration problems when the frequency n is zero and the load components are unaltered. This yields the normalised form as

$$\bar{\Delta}_m(n) = \frac{\Delta_m(n)}{\Delta_m(0)} \tag{3.38}$$

Also, since the in-plane and out-of-plane behaviours are uncoupled in the work that follows, the member stiffness determinant is the product of separate in-plane and out-of-plane determinants, each of which must be normalised separately by the procedure just described. These may then be combined to give the total normalised stiffness determinant for the structure as

$$\overline{\Delta} = \prod_{m} \overline{\Delta}_m \tag{3.39}$$

3.4 DERIVATION OF THE MEMBER STIFFNESS DETERMINANT FOR PRISMATIC PLATES

As mentioned earlier, the out-of-plane and in-plane behaviours of prismatic plates are uncoupled and can therefore be considered separately. Hence $\overline{\Delta}_m$ can be written as

$$\overline{\Delta}_m = \overline{\Delta}_m^O \ \overline{\Delta}_m^I \tag{3.40}$$

where $\overline{\Delta}_m^O$ and $\overline{\Delta}_m^I$ are the out-of-plane and in-plane member stiffness determinant, respectively. They can both be found by exactly the same procedure. For convenience in the development that follows, the O and I superscripts are not used when describing those parts that are identical and otherwise only when necessary to indicate the plane under consideration.

Consider the doubling sequence described previously. If the subscript i denotes one of the two members of breadth $b/2^i$, which are connected together at level i, then the stiffness equation for the two member sub-structure formed at level i is

$$\begin{bmatrix} \mathbf{k}_{22i} + \mathbf{k}_{11i} & \mathbf{k}_{12i}^T & \mathbf{k}_{12i} \\ \mathbf{k}_{12i} & \mathbf{k}_{11i} & 0 \\ \mathbf{k}_{12i}^T & 0 & \mathbf{k}_{22i} \end{bmatrix} \begin{bmatrix} \mathbf{D}_1 \\ \mathbf{D}_2 \\ \mathbf{D}_3 \end{bmatrix} = \begin{bmatrix} \mathbf{P}_1 \\ \mathbf{P}_2 \\ \mathbf{P}_3 \end{bmatrix} \tag{3.41}$$

where $\mathbf{D}_j$ are the displacement amplitudes at node j (j =1,2,3), number 1 being the central node to be eliminated, and $\mathbf{P}_j$ are the corresponding force amplitudes. Note that $\mathbf{P}_1 = \mathbf{0}$ because the vibrations are free, whereas $\mathbf{P}_2$ and $\mathbf{P}_3$ are the reaction forces exerted on the sub-structure by its parent. Using the arrested Gauss elimination procedure to eliminate $\mathbf{D}_1$ from Eq. (3.41), gives

$$\begin{bmatrix} (\mathbf{k}_{22i} + \mathbf{k}_{11i})^{\Delta} & \mathbf{k}_{12i}^{T*} & \mathbf{k}_{12i}^{*} \\ 0 & \mathbf{k}_{11(i-1)} & \mathbf{k}_{12(i-1)} \\ 0 & \mathbf{k}_{12(i-1)}^{T} & \mathbf{k}_{22(i-1)} \end{bmatrix} \begin{bmatrix} \mathbf{D}_1 \\ \mathbf{D}_2 \\ \mathbf{D}_3 \end{bmatrix} = \begin{bmatrix} \mathbf{0} \\ \mathbf{P}_2 \\ \mathbf{P}_3 \end{bmatrix} \tag{3.42}$$

where the superscript Δ denotes a transformation to upper triangular form and the superscripts * denote the consequent transformations to other matrices.

Clearly $\mathbf{D}_2$, $\mathbf{D}_3$, $\mathbf{P}_2$ and $\mathbf{P}_3$ are the $\mathbf{d}_{1(i-1)}$, $\mathbf{d}_{2(i-1)}$, $\mathbf{p}_{1(i-1)}$ and $\mathbf{p}_{2(i-1)}$ of the member of breadth $b/2^{i-1}$ at level $(i-1)$ and its stiffness matrix is the untriangulated portion $\begin{bmatrix} \mathbf{k}_{11(i-1)} & \mathbf{k}_{12(i-1)} \\ \mathbf{k}_{12(i-1)}^{T} & \mathbf{k}_{22(i-1)} \end{bmatrix}$ of the matrix of Eq. (3.42). Also from Eq. (3.41) the sub-structure stiffness matrix at level i is given by

$$\mathbf{k}_{si} = \mathbf{k}_{22i} + \mathbf{k}_{11i} \tag{3.43}$$

and can be constructed by substitution of the relevant part of Eq. (2.6) for out-of-plane or in-plane behaviour, with the member breadth b replaced by $b_i = b/2^i$, so that φ of Eq. (2.7) is replaced by $\varphi_i = \varphi/2^i$. Hereafter, this rule should be applied to all quantities with subscript i or any combination of it.

3.4.2 The normalised member stiffness determinant for isotropic plates

3.4.2.1 Detailed theory for out-of-plane normalised member stiffness determinants

For out-of-plane behaviour, the sub-structure stiffness matrix at level i is

$$\mathbf{k}_{si}^{O}(\varepsilon)=\begin{bmatrix} 2s_{iMM} & 0 \\ 0 & 2s_{iQQ} \end{bmatrix} \tag{3.44}$$

where, by using the arguments about Eq. (3.43), s_{iMM} and s_{iQQ} are the appropriate elements of Eq. (2.13a) with the member breadth of $b/2^i$. The determinant of Eq. (3.44) can then be written as

$$\left|\mathbf{k}_{si}^{O}\right| = 4\,s_{iMM}\,s_{iQQ} = \frac{4\varsigma^2}{\delta_i^2}[(q_{i,2\alpha}p_{i,2\gamma} - p_{i,2\alpha}q_{i,2\gamma})(\alpha^2 p_{i,2\alpha}q_{i,2\gamma} - \gamma^2 q_{i,2\alpha}p_{i,2\gamma})] \tag{3.45}$$

where, by using Eqs. (2.13b) and (2.10) and the arguments of Section 3.4 $\delta_i = ½\,(4p_{i,2\alpha}p_{i,2\gamma} - q_{i,2\alpha}q_{i,2\gamma} + 1)$, $p_{i,2\alpha} = (\frac{1}{2\alpha})\sinh\frac{\varphi_i(2\alpha)}{2} = (\frac{1}{2\hat{\alpha}})\sin\frac{\varphi_i(2\hat{\alpha})}{2}$, $q_{i,2\alpha} = \cosh\frac{\varphi_i(2\alpha)}{2} = \cos\frac{\varphi_i(2\hat{\alpha})}{2}$,... and $\varphi_i = \varphi/2^i$. Hence, Eq. (3.45) can be rearranged as

$$\left|\mathbf{k}_{si}^{O}\right| = \frac{4\varsigma^2}{\delta_i^2}[(\alpha^2+\gamma^2)p_{i,4\alpha}p_{i,4\gamma} - (\alpha^2 p_{i,2\alpha}^2 q_{i,2\gamma}^2 + \gamma^2 p_{i,2\gamma}^2 q_{i,2\alpha}^2)] \tag{3.46}$$

From Eq. (2.9) it is clear that $\alpha^2+\gamma^2 = 2$. Now utilising Eq. (B.12) in Eq. (3.46) gives

$$\left|\mathbf{k}_{si}^{O}\right| = \frac{4\varsigma^2}{\delta_i^2}[2p_{i,4\alpha}p_{i,4\gamma} - \frac{1}{8}(q_{i,4\alpha}q_{i,4\gamma} - 1)] \tag{3.47}$$

Now Substituting the identities of Eq.(B.15) and (B.16) into Eq. (3.47) gives

$$\left|\mathbf{k}_{si}^{O}\right| = \frac{4\varsigma^2}{\delta_i^2}[2(\tfrac{1}{2}p_{i-1,2\alpha})(\tfrac{1}{2}p_{i-1,2\gamma}) - \frac{1}{8}(q_{i-1,2\alpha}q_{i-1,2\gamma} - 1)] \tag{3.48}$$

or

$$\left|\mathbf{k}_{si}^{O}\right| = \frac{\varsigma^2}{\delta_i^2}[2p_{i-1,2\alpha}p_{i-1,2\gamma} - \frac{1}{2}(q_{i-1,2\alpha}q_{i-1,2\gamma} - 1)] \tag{3.49}$$

where the bracket on the right hand side of Eq. (3.49) is exactly δ_{i-1} and therefore

$$\left|\mathbf{k}_{si}^{O}(\varepsilon)\right| = \varsigma^2 \frac{\delta_{i-1}}{\delta_i^2} \tag{3.50}$$

Eq. (3.50) cannot be used for the evaluation of its determinant when the eigenparameter is zero. Therefore, it is necessary to represent Eq. (3.50) in an alternative suitable form in which the zero eigenparameter yields a finite value. Then substituting Eq. (2.14a) in Eq. (3.44) yields the determinant of Eq. (3.44) as

$$\left|\mathbf{k}_{si}^{O}(\varepsilon)\right| = \frac{\alpha\gamma D^2}{\bar{\lambda}^4}\frac{\hat{\delta}_{i-1}}{\hat{\delta}_i^2} \tag{3.51}$$

where $\hat{\delta}_i = p_{i,(\alpha+\gamma)}^2 - p_{i,(\alpha-\gamma)}^2 = \frac{\eta^2}{\alpha\gamma}\delta_i$. Although Eq. (3.51) contains some complex quantities, it value is real. Also Eq. (3.51) could be achieved just by substituting Eq. (2.14b) into Eq. (3.50). Eq. (3.51) can now be used to calculate the determinant of Eq. (3.44) for the case of the zero eigenparameter, i.e. for $\varepsilon = 0$, as

$$\left|\mathbf{k}_{si}^{O}(0)\right| = \frac{4D^2\left(4p_{i-1,2}^2 - \varphi_{i-1}^2\right)}{\bar{\lambda}^4\left(4p_{i,2}^2 - \varphi_i^2\right)^2} \tag{3.52}$$

Substituting Eqs. (3.50) and (3.52) in the recurrence relationship of Eq. (3.36) , gives

$$\overline{\Delta}^{O}_{m(i-1)}(\varepsilon)=\frac{\bar{\lambda}^4 \varsigma^2 \left(4p_{i,2}^2-\varphi_i^2\right)^2 \delta_{i-1}}{4D^2\left(4p_{i-1,2}^2-\varphi_{i-1}^2\right)\delta_i^2}\left[\overline{\Delta}^{O}{}_{m(i)}(\varepsilon)\right]^2 \tag{3.53}$$

i.e.

$$\frac{\eta^2\left(4p_{i-1,2}^2-\varphi_{i-1}^2\right)}{4\delta_{i-1}}\overline{\Delta}^{O}_{m(i-1)}(\varepsilon)=\left[\frac{\eta^2\left(4p_{i,2}^2-\varphi_i^2\right)}{4\,\delta_i}\overline{\Delta}^{O}_{m(i)}(\varepsilon)\right]^2 \tag{3.54}$$

which has the solution

$$\overline{\Delta}^{O}_{mi}(\varepsilon)=\frac{4\delta_i}{\eta^2\,(4p_{i,2}^2-\varphi_i^2)} \tag{3.55}$$

Now using Eq. (3.37), the full breadth out-of-plane normalised member stiffness determinant is

$$\overline{\Delta}^{O}_{m}(\varepsilon)=\frac{4\,\delta}{\eta^2(4p_2^2-\varphi^2)} \tag{3.56}$$

where η, δ and p_2 are defined in Eqs. (2.8), (2.13b) and (2.16), respectively.

3.4.2.2 Detailed theory for in-plane normalised member stiffness determinants

In similar fashion to the previous section, the sub-structure stiffness matrix for in-plane behaviour at level i is

$$\mathbf{k}^{I}_{si}(\varepsilon)=\begin{bmatrix} 2s_{iNN} & 0 \\ 0 & 2s_{iTT} \end{bmatrix} \tag{3.57}$$

where, by using the arguments about Eq. (3.43), s_{iNN} and s_{iTT} are the appropriate elements of Eq. (2.19a) with the breadth of $b/2^i$. The determinant of Eq. (3.44) can then be written as

$$\left|\mathbf{k}_{si}^{I}\right| = 4 s_{iNN}\, s_{iTT} = \frac{4\kappa^2}{\mu_i^2}[(p_{i,2\tau}q_{i,2\zeta} - \zeta^2 p_{i,2\zeta}q_{i,2\tau})(p_{i,2\zeta}q_{i,2\tau} - \tau^2 p_{i,2\tau}q_{i,2\zeta})] \tag{3.58}$$

where $\mu_i = (1+\tau^2\zeta^2)p_{i,2\tau}p_{i,2\zeta} - \tfrac{1}{2}(q_{i,2\tau}q_{i,2\zeta} - 1)$, $q_{i,2\tau} = \cosh\dfrac{\varphi_i(2\tau)}{2} = \cos\dfrac{\varphi_i(2\hat{\tau})}{2}$

$p_{i,2\tau} = (\dfrac{1}{2\tau})\sinh\dfrac{\varphi_i(2\tau)}{2} = (\dfrac{1}{2\hat{\tau}})\ \sin\dfrac{\varphi_i(2\hat{\tau})}{2}$, ... Now, Eq. (3.58) can be rearranged as

$$\left|\mathbf{k}_{si}^{I}\right| = \frac{4\kappa^2}{\mu_i^2}[(1+\tau^2\zeta^2)p_{i,4\tau}p_{i,4\zeta} - (\tau^2 p_{i,2\tau}^2 q_{i,2\zeta}^2 + \zeta^2 p_{i,2\zeta}^2 q_{i,2\tau}^2)] \tag{3.59}$$

Thus using Eqs. (B.12) ,(B.15) and (B.16) in Eq. (3.59) gives

$$\left|\mathbf{k}_{si}^{I}\right| = \frac{4\kappa^2}{\mu_i^2}[\tfrac{1}{4}(1+\tau^2\zeta^2)p_{i-1,2\tau}p_{i-1,2\zeta} - \frac{1}{8}(q_{i-1,2\tau}q_{i-1,2\zeta} - 1)] \tag{3.60}$$

where the bracket on the right hand side of Eq. (3.60) is exactly $\tfrac{1}{4}(\mu_{i-1})$ and therefore

$$\left|\mathbf{k}_{si}^{I}(\varepsilon)\right| = \kappa^2\frac{\mu_{i-1}}{\mu_i^2} \tag{3.60}$$

In a similar way to Section 3.4.1.1, an alternative form of Eq. (3.60) should be used when the eigenparameter is zero, i.e.

$$\left|\mathbf{k}_{si}^{I}(\varepsilon)\right| = \frac{E^2 h^2 \tau\zeta}{\bar{\lambda}^2(1+\nu)^2}\frac{\hat{\mu}_{i-1}}{\hat{\mu}_i^2} \tag{3.61}$$

where $\hat{\mu}_i = \left\{ [2\tau + \zeta(1-\nu)]^2 p^2_{i,(\tau+\zeta)} - [2\tau - \zeta(1-\nu)]^2 p^2_{i,(\tau-\zeta)} \right\} = \dfrac{4\tau\zeta}{(1+\nu)^2 \varepsilon^2} \mu_i$. Hence the determinant for the static case, i.e. for $\varepsilon = 0$, can easily be obtained as

$$\left| \mathbf{k}^I_{si}(0) \right| = \frac{4E^2 h^2 \, [4(3-\nu)^2 p^2_{i-1,2} - (1+\nu)^2 \varphi^2_{i-1}]}{\bar{\lambda}^2 \, (1+\nu)^2 \left[\, 4(3-\nu)^2 p^2_{i,2} - (1+\nu)^2 \varphi^2_i \, \right]^2} \tag{3.62}$$

Using Eqs. (3.60) and (3.62) in the recurrence relationship of Eq. (3.36), gives

$$\bar{\Delta}^I_{m(i-1)}(\varepsilon) = \frac{\bar{\lambda}^2 (1+\nu)^2 \kappa^2 \left[4(3-\nu)^2 p^2_{i,2} - (1+\nu)^2 \varphi^2_i \right]^2 \mu_{i-1}}{4E^2 h^2 [\, 4(3-\nu)^2 p^2_{i-1,2} - (1+\nu)^2 \varphi^2_{i-1} \,] \mu^2_i} \left[\bar{\Delta}^I_{m(i)}(\varepsilon) \right]^2 \tag{3.63}$$

or

$$\begin{aligned} \frac{(1+\nu)^2 \varepsilon^2 \, [4(3-\nu)^2 p^2_{i-1,2} - (1+\nu)^2 \varphi^2_{i-1}]}{16 \, \mu_{i-1}} \bar{\Delta}^I_{m(i-1)}(\varepsilon) = \\ \left[\frac{(1+\nu)^2 \varepsilon^2 \left[4(3-\nu)^2 p^2_{i,2} - (1+\nu)^2 \varphi^2_i \right]}{16 \, \mu_i} \bar{\Delta}^I_{m(i)}(\varepsilon) \right]^2 \end{aligned} \tag{3.64}$$

which has the solution

$$\bar{\Delta}^I_{mi}(\varepsilon) = \frac{16 \mu_i}{(1+\nu)^2 \varepsilon^2 [\, 4(3-\nu)^2 p^2_{i,2} - (1+\nu)^2 \varphi^2_i \,]} \tag{3.65}$$

and therefore using Eq. (3.37), the full breadth in-plane normalised member stiffness determinant is

$$\bar{\Delta}^I_m(\varepsilon) = \frac{16 \mu}{(1+\nu)^2 \varepsilon^2 [4(3-\nu)^2 p^2_2 - (1+\nu)^2 \varphi^2]} \tag{3.66}$$

where μ and p_2 have been defined in Eqs. (2.19b) and (2.16), respectively.

3.4.3 The member stiffness determinants for orthotropic plates

In contrast to isotropic plates, where the stiffness matrix has one form for out-of-plane and one form for in-plane behaviour, it is clear from Section 2.5 that there are three different categories for out-of-plane and two different categories for in-plane behaviour of orthotropic plates. Therefore, there is no explicit analytical definition for the normalised member stiffness determinant and the process of normalisation for orthotropic plates is slightly different.

Also, it should be noted that throughout this section Eq.(2.24) has been used to derive the member stiffness determinant for orthotropic prismatic plates.

3.4.3.1 Detailed theory for out-of-plane member stiffness determinants

For out-of-plane behaviour, the sub-structure stiffness matrix at level i is

$$\mathbf{k}_{si}^{O} = \begin{bmatrix} 2s_{iMM} & 0 \\ 0 & 2s_{iQQ} \end{bmatrix} \tag{3.67}$$

where, by using the arguments about Eq. (3.43), s_{iMM} and s_{iQQ} are the appropriate elements of Eqs. (2.27), (2.30) or (2.32) with the breadth of $b/2^i$. However, calculation of this determinant may be achieved using the value of L in Eq.(2.25) and the three different cases for the element stiffness matrix defined in Section 2.5, therefore this determinant should be established as follows.

3.4.3.1.1 $L > 0$

By using Eq. (B.19) and the definition in Eq. (2.27), the determinant of the sub-structure matrix, Eq. (3.67), is

$$\left|\mathbf{k}_{si}^{o}(n)\right| = 4 s_{iMM}\, s_{iQQ} = \frac{4L\,D_{22}^{2}}{\bar{\lambda}^{4}\,Z_i^{\,2}}[(q_{i,\alpha}p_{i,\gamma} - p_{i,\alpha}q_{i,\gamma})(\alpha^2 p_{i,\alpha}q_{i,\gamma} - \gamma^2 q_{i,\alpha}p_{i,\gamma})] \tag{3.68}$$

where $Z_i = Tp_{i,\alpha}p_{i,\gamma} - q_{i,\alpha}q_{i,\gamma} + 1$, α, γ and T are defined in Eqs.(2.28) and (2.25), respectively. Now, Eq. (3.68) can be rearranged as

$$\left|\mathbf{k}_{si}^{o}\right| = \frac{4L\,D_{22}^{2}}{\bar{\lambda}^{4}\,Z_i^{\,2}}[(\alpha^2+\gamma^2)p_{i,2\alpha}p_{i,2\gamma} - (\alpha^2 p_{i,\alpha}^2 q_{i,\gamma}^2 + \gamma^2 p_{i,\gamma}^2 q_{i,\alpha}^2)] \tag{3.69}$$

From Eq. (2.28) it is clear that $\alpha^2 + \gamma^2 = 2T$. Thus using Eq. (B.12) in Eq. (3.69) gives

$$\left|\mathbf{k}_{si}^{o}\right| = \frac{4L\,D_{22}^{2}}{\bar{\lambda}^{4}\,Z_i^{\,2}}[2Tp_{i,2\alpha}p_{i,2\gamma} - \frac{1}{2}(q_{i,4\alpha}q_{i,4\gamma} - 1)] \tag{3.70}$$

Substituting the identities of Eq.(B.15) and (B.16) into Eq. (3.70) gives

$$\left|\mathbf{k}_{si}^{o}\right| = \frac{4L\,D_{22}^{2}}{\bar{\lambda}^{4}\,Z_i^{\,2}}[2T(\tfrac{1}{2}p_{i-1,\alpha})(\tfrac{1}{2}p_{i-1,\gamma}) - \frac{1}{2}(q_{i-1,2\alpha}q_{i-1,2\gamma} - 1)] \tag{3.71}$$

or

$$\left|\mathbf{k}_{si}^{o}(n)\right| = \frac{2L\,D_{22}^{2}(Tp_{i-1,\alpha}p_{i-1,\gamma} - q_{i-1,\alpha}q_{i-1,\gamma} - 1)}{\bar{\lambda}^{4}\,Z_i^{\,2}} \tag{3.72}$$

where the bracket in right hand side of Eq. (3.72) is exactly Z_{i-1} and therefore

$$\left|\mathbf{k}_{si}^{o}(n)\right| = \frac{2L\,D_{22}^{2}Z_{i-1}}{\bar{\lambda}^{4}\,Z_i^{\,2}} \tag{3.73}$$

Substituting Eqs. (3.73) in the recurrence relationship of Eq. (3.36) , gives

$$\Delta^{O}_{m(i-1)}(n) = \frac{2L\, D_{22}^2 Z_{i-1}}{\bar{\lambda}^4 Z_i^2}\left[\Delta^{O}_{m(i)}(n)\right]^2 \tag{3.74}$$

i.e.

$$\frac{2L\, D_{22}^2\, \Delta^{O}_{m(i-1)}(n)}{\bar{\lambda}^4 Z_{i-1}} = \left[\frac{2L\, D_{22}^2\, \Delta^{O}_{m(i)}(n)}{\bar{\lambda}^4 Z_i}\right]^2 \tag{3.75}$$

which has the solution

$$\Delta^{O}_{mi}(n) = \frac{\bar{\lambda}^4 Z_i}{2L\, D_{22}^2} \tag{3.76}$$

Finally using Eq. (3.37), the full breadth out-of-plane member stiffness determinant is

$$\Delta^{O}_{m}(n) = \frac{\bar{\lambda}^4 Z}{2L\, D_{22}^2} \tag{3.77}$$

Using Eq. (B.21), Eq. (3.77) may now be rewritten in the alternative form

$$\Delta^{O}_{m}(n) = \frac{\bar{\lambda}^4 \left(p^2_{\frac{1}{2}(\alpha+\gamma)} - p^2_{\frac{1}{2}(\alpha-\gamma)}\right)}{4\alpha\,\gamma\, D_{22}^2} \tag{3.78}$$

which can easily be used to give the static member stiffness determinant

$$\Delta^{O}_{m}(0) = \frac{\bar{\lambda}^4 \left(p^2_{\sqrt{\frac{\alpha_{12}+2\alpha_{33}+\sqrt{\alpha_{11}}}{2}}} - p^2_{\sqrt{\frac{\alpha_{12}+2\alpha_{33}-\sqrt{\alpha_{11}}}{2}}} \right)}{4\sqrt{\alpha_{11}}\, D_{22}^2} \tag{3.79}$$

where $\sqrt{\frac{\alpha_{12}+2\alpha_{33}+\sqrt{\alpha_{11}}}{2}}$ and $\sqrt{\frac{\alpha_{12}+2\alpha_{33}-\sqrt{\alpha_{11}}}{2}}$ are subscripts for p in Eq.(2.24).

Hence the normalised member stiffness determinant Eq. (3.38) is

$$\bar{\Delta}^{O} = \frac{2\sqrt{\alpha_{11}}}{L} \frac{Z}{p^{2}_{\sqrt{\frac{\alpha_{12}+2\alpha_{33}+\sqrt{\alpha_{11}}}{2}}} - p^{2}_{\sqrt{\frac{\alpha_{12}+2\alpha_{33}-\sqrt{\alpha_{11}}}{2}}}} \tag{3.80}$$

3.4.3.1.2 $L < 0$

By using Eqs.(2.30) and (B.19) the determinant of the sub-structure matrix, Eq. (3.67), is

$$\left| \mathbf{k}^{O}_{si}(n) \right| = 4 s_{iMM}\, s_{iQQ} = \frac{4A\, D_{22}^{2}}{\bar{\lambda}^{4} Z_i^{2}} [(p_{i,2\alpha} - \hat{p}_{i,2\gamma})(p_{i,2\alpha} + \hat{p}_{i,2\gamma})] \tag{3.81}$$

where $Z_i = \frac{1}{2}(p^{2}_{i,\alpha} - \hat{p}^{2}_{i,\gamma})$, α, γ and A are defined in Eqs.(2.29) and (2.31), respectively. Now, rearranging Eq. (3.81) and then using Eq. (B.15) gives

$$\left|\mathbf{k}^{O}_{si}\right| = \frac{4A\, D_{22}^{2}}{\bar{\lambda}^{4} Z_i^{2}} (p^{2}_{i,2\alpha} - \hat{p}^{2}_{i,2\gamma}) = \frac{4A\, D_{22}^{2}}{\bar{\lambda}^{4} Z_i^{2}} (\tfrac{1}{4} p^{2}_{i-1,\alpha} - \tfrac{1}{4} \hat{p}^{2}_{i-1,\gamma}) = \frac{2A\, D_{22}^{2}}{\bar{\lambda}^{4} Z_i^{2}} Z_{i-1} \tag{3.82}$$

Substituting Eqs. (3.82) in the recurrence relationship of Eq. (3.36), gives

$$\Delta^{O}_{m(i-1)}(n) = \frac{2A\, D_{22}^{2} Z_{i-1}}{\bar{\lambda}^{4} Z_i^{2}} \left[\Delta^{O}{}_{m(i)}(n)\right]^{2} \tag{3.83}$$

i.e.

$$\frac{2A\, D_{22}^{2}\, \Delta^{O}_{m(i-1)}(n)}{\bar{\lambda}^{4} Z_{i-1}} = \left[\frac{2A\, D_{22}^{2}\, \Delta^{O}_{m(i)}(n)}{\bar{\lambda}^{4} Z_i} \right]^{2} \tag{3.84}$$

which has the solution

$$\Delta^{O}_{mi}(n) = \frac{\bar{\lambda}^{4} Z_i}{2A\, D_{22}^{2}} \tag{3.85}$$

Finally, using Eq. (3.37), the full breadth out-of-plane member stiffness determinant is

$$\Delta_m^o(n) = \frac{\bar{\lambda}^4 \, Z}{2A \, D_{22}^2} \tag{3.86}$$

Using Eqs. (2.25) and (2.29), the static member stiffness determinant can easily be deduced from Eq. (3.86) as

$$\Delta_m^o(0) = \frac{\bar{\lambda}^4 \left(p^2 \sqrt{\frac{\sqrt{\alpha_{11}}+\alpha_{12}+2\alpha_{33}}{2}} - \hat{p}^2 \sqrt{\frac{\sqrt{\alpha_{11}}-\alpha_{12}-2\alpha_{33}}{2}} \right)}{4\sqrt{\alpha_{11}} \, D_{22}^2} \tag{3.87}$$

Hence the normalised member stiffness determinant Eq. (3.38) is

$$\bar{\Delta}_m^o = \frac{2Z\sqrt{\alpha_{11}}}{A\left(p^2 \sqrt{\frac{\sqrt{\alpha_{11}}+\alpha_{12}+2\alpha_{33}}{2}} - \hat{p}^2 \sqrt{\frac{\sqrt{\alpha_{11}}-\alpha_{12}-2\alpha_{33}}{2}} \right)} \tag{3.88}$$

3.4.3.1.3 $L = 0$

By using the definition in Eqs. (2.32) and (2.33), the determinant of the sub-structure matrix, Eq. (3.67), is

$$\left| \mathbf{k}_{si}^o(n) \right| = 4 s_{iMM} \, s_{iQQ} = \frac{4T \, D_{22}^2}{\bar{\lambda}^4 \varphi_i^4 \, Z_i^2} [(p_{i,2\alpha} - \varphi_i)(p_{i,2\alpha} + \varphi_i)] \tag{3.89}$$

where $Z_i = (p_{i,\alpha}^2 - \varphi_i^2)/2\varphi_i^2$, α and T are defined in Eqs.(2.33) and (2.25), respectively. Now, rearranging Eq. (3.89) and then using Eq. (B.15) gives

$$\left| \mathbf{k}_{si}^o \right| = \frac{4T \, D_{22}^2}{\bar{\lambda}^4 \varphi_i^4 Z_i^2} (p_{i,2\alpha}^2 - \varphi_i^2) = \frac{4T \, D_{22}^2}{\bar{\lambda}^4 \varphi_i^4 Z_i^2} (¼ p_{i-1,\alpha}^2 - ¼ \varphi_{i-1}^2) \tag{3.90}$$

or

$$\left|\mathbf{k}_{si}^{O}\right| = \frac{2T D_{22}^2}{\bar{\lambda}^4 \varphi_i^4 Z_i^2} Z_{i-1} \varphi_{i-1}^2 \tag{3.91}$$

Substituting Eqs. (3.91) in the recurrence relationship of Eq. (3.36) , gives

$$\Delta_{m(i-1)}^{O}(n) = \frac{2T D_{22}^2 Z_{i-1} \varphi_{i-1}^2}{\bar{\lambda}^4 Z_i^2 \varphi_i^4} \left[\Delta_{m(i)}^{O}(n)\right]^2 \tag{3.92}$$

i.e.

$$\frac{2T D_{22}^2 \Delta_{m(i-1)}^{O}(n)}{\bar{\lambda}^4 \varphi_{i-1}^2 Z_{i-1}} = \left[\frac{2T D_{22}^2 \Delta_{m(i)}^{O}(n)}{\bar{\lambda}^4 \varphi_i^2 Z_i}\right]^2 \tag{3.93}$$

which has the solution

$$\Delta_{mi}^{O}(n) = \frac{\bar{\lambda}^4 Z_i \varphi_i^2}{2T D_{22}^2} \tag{3.94}$$

Finally, using Eq. (3.37), the full breadth out-of-plane member stiffness determinant is

$$\Delta_{m}^{O}(n) = \frac{\bar{\lambda}^4 \varphi^2 Z}{2T D_{22}^2} = \frac{\bar{\lambda}^4 (p_a^2 - \varphi^2)}{4T D_{22}^2} \tag{3.95}$$

Using Eqs. (2.25) and (2.33), the static member stiffness determinant can easily be deduced from Eq. (3.95) as

$$\Delta_{m}^{O}(0) = \frac{\bar{\lambda}^4 \left(p_{\sqrt{\alpha_{12}+2\alpha_{33}}}^2 - \varphi^2\right)}{4(\alpha_{12}+2\alpha_{33}) D_{22}^2} \tag{3.96}$$

Hence the normalised member stiffness determinant Eq. (3.38) is

$$\overline{\Delta}_m^o = \frac{(\alpha_{12}+2\alpha_{33})(p_\alpha^2-\varphi^2)}{\alpha^2(p^2_{\sqrt{\alpha_{12}+2\alpha_{33}}}-\varphi^2)} \tag{3.97}$$

It should be noted that Eqs. (3.80), (3.88) and (3.97) are valid when the dead load components of N_L and N_T are both zero. Otherwise, Eqs. (3.77), (3.86) and (3.95), respectively, should be used to evaluate the member stiffness determinant for the case of $n = 0$ and then the process of normalisation is continued numerically.

3.4.3.2 Detailed theory for in-plane member stiffness determinant

In similar fashion to the previous section, the sub-structure stiffness matrix for the in-plane behaviour at level i is

$$\mathbf{k}_{si}^{I}(\varepsilon)=\begin{bmatrix} 2s_{iNN} & 0 \\ 0 & 2s_{iTT} \end{bmatrix} \tag{3.98}$$

Depending on the value of B and C, the elements of the in-plane stiffness matrix of Section 2.5.2 are defined for the two cases of $B^2 > C$ and $B^2 \leq C$. Hence, the determinant of Eq. (3.98) needs to be established for these two different cases. Nevertheless, it should be noted that these two different cases may occur in various ranges of the eigenparameter for any plate element of the structure in the same problem. Therefore, in contrast with the out-of-plane behaviour of Section 3.4.2.1, in which the normalising factor and the member stiffness determinant are always calculated in the same range, here $B^2 - C$ will have different values when calculating the normalising factor than when calculating the member stiffness determinant. Thus the appropriate equation must be selected for normalisation and therefore no explicit expression for the *normalised* member stiffness determinant for in-plane behaviour can be established.

3.4.3.2.1 $B^2 > C$

By using Eqs. (2.37), the determinant of the sub-structure matrix of Eq. (3.98) is

$$\left|\mathbf{k}_{si}^{I}(n)\right| = 4s_{iNN}s_{iTT} = \frac{(\tau^2-\zeta^2)^2}{\bar{\lambda}^2}\times \left[\frac{L_3}{4H_{i,a}}p_{i,\tau/2}p_{i,\zeta/2}+\frac{A_{22}}{H_{si}}q_{i,\tau/2}q_{i,\zeta/2}\right]\left[\frac{L_1}{4H_{i,s}}p_{i,\tau/2}p_{i,\zeta/2}+\frac{A_{33}}{H_{ai}}q_{i,\tau/2}q_{i,\zeta/2}\right] \tag{3.99}$$

or

$$\left|\mathbf{k}_{si}^{I}(n)\right| = \frac{(\tau^2-\zeta^2)^2}{16\bar{\lambda}^2(H_{ai}H_{si})^2}\times \left[L_3H_{si}p_{i,\tau/2}p_{i,\zeta/2}+A_{22}H_{ai}q_{i,\tau/2}q_{i,\zeta/2}\right]\left[L_1H_{ai}p_{i,\tau/2}p_{i,\zeta/2}+A_{33}H_{si}q_{i,\tau/2}q_{i,\zeta/2}\right] \tag{3.100}$$

which may be written as

$$\left|\mathbf{k}_{si}^{I}(n)\right| = \frac{(\tau^2-\zeta^2)^2}{16\bar{\lambda}^2(H_{i,a}H_{i,s})^2}\times \begin{bmatrix} H_{ai}H_{si}(L_1L_3p_{i,\tau/2}^2p_{i,\zeta/2}^2+A_{22}A_{33}q_{i,\tau/2}^2q_{i,\zeta/2}^2) \\ +(L_1A_{22}H_{ai}^2+L_3A_{33}H_{si}^2)p_{i,\tau/2}p_{i,\zeta/2}q_{i,\tau/2}q_{i,\zeta/2}\end{bmatrix} \tag{3.101}$$

After extensive manipulations, Eq. (3.101) can be written as

$$\left|\mathbf{k}_{si}^{I}(n)\right| = \frac{16\tau\zeta A_{22}^2A_{33}^2}{\bar{\lambda}^2}\times \frac{(L_1A_{22}+L_3A_{33}+2A_{22}A_{33}\tau\zeta)p_{i,(\tau+\zeta)}^2-(L_1A_{22}+L_3A_{33}-2A_{22}A_{33}\tau\zeta)p_{i,(\tau-\zeta)}^2}{\left\{(L_1A_{22}+L_3A_{33}+2A_{22}A_{33}\tau\zeta)p_{i,\frac{1}{2}(\tau+\zeta)}^2-(L_1A_{22}+L_3A_{33}-2A_{22}A_{33}\tau\zeta)p_{i,\frac{1}{2}(\tau-\zeta)}^2\right\}^2} \tag{3.102}$$

Now by using Eq. (B.15), Eq. (3.102) can be rewritten in an appropriate form to use in the recurrence relationship of Eq.(3.36) as

$$\left|\mathbf{k}_{si}^{I}(n)\right| = \frac{4\tau\zeta A_{22}^2 A_{33}^2}{\bar{\lambda}^2} \times$$
$$\frac{(L_1A_{22}+L_3A_{33}+2A_{22}A_{33}\tau\zeta)p_{i-1,\frac{1}{2}(\tau+\zeta)}^2-(L_1A_{22}+L_3A_{33}-2A_{22}A_{33}\tau\zeta)p_{i-1,\frac{1}{2}(\tau-\zeta)}^2}{\left\{(L_1A_{22}+L_3A_{33}+2A_{22}A_{33}\tau\zeta)p_{i,\frac{1}{2}(\tau+\zeta)}^2-(L_1A_{22}+L_3A_{33}-2A_{22}A_{33}\tau\zeta)p_{i,\frac{1}{2}(\tau-\zeta)}^2\right\}^2} \tag{3.103}$$

Hence, after solving the recurrence relationship of Eq. (3.36) and using Eq. (3.37), the full breadth out-of-plane member stiffness determinant is

$$\Delta_m^I(n) = \frac{\bar{\lambda}^2}{4\tau\zeta A_{22}^2 A_{33}^2} \times$$
$$\left[(L_1A_{22}+L_3A_{33}+2A_{22}A_{33}\tau\zeta)p_{\frac{1}{2}(\tau+\zeta)}^2-(L_1A_{22}+L_3A_{33}-2A_{22}A_{33}\tau\zeta)p_{\frac{1}{2}(\tau-\zeta)}^2\right] \tag{3.104}$$

Eq. (3.104) may contain some complex quantities, but it can be presented in an alternative form in which all quantities are real i.e.

$$\Delta_m^I(n) = \frac{\bar{\lambda}^2}{4(B^2-C)A_{22}^2A_{33}^2}\left[\left(B\frac{L_1A_{22}+L_3A_{33}}{2A_{22}A_{33}}-C\right)p_\tau p_\zeta - \frac{A_0^2}{2A_{22}A_{33}}(q_\tau q_\zeta - 1)\right] \tag{3.105}$$

3.4.3.2.2 $B^2 \le C$

By using Eq. (2.42) and following extensive manipulation, the determinant of the sub-structure matrix of Eq. (3.98), is

$$\left|\mathbf{K}_{si}^{I}(n)\right| = \frac{4A_{22}L_1}{\bar{\lambda}^2\sqrt{C}} \times \frac{\left\{\left(1+L_1/A_{33}\sqrt{C}\right)^2 p_{i-1,\tau}^2 - \left(1-L_1/A_{33}\sqrt{C}\right)^2 \hat{p}_{i-1,\zeta}^2\right\}}{\left\{\left(1+L_1/A_{33}\sqrt{C}\right)^2 p_{i,\tau}^2 - \left(1-L_1/A_{33}\sqrt{C}\right)^2 \hat{p}_{i,\zeta}^2\right\}^2} \tag{3.106}$$

In a similar way to the previous section, after solving the recurrence relationship of Eq. (3.36) and using Eq. (3.37), the full breadth out-of-plane member stiffness determinant is

$$\Delta_m^I(n) = \frac{\lambda^2\sqrt{C}}{4\pi^2 A_{22}L_1}\left[\left(1+L_1/A_{33}\sqrt{C}\right)^2 p_\tau^2 - \left(1-L_1/A_{33}\sqrt{C}\right)^2 \hat{p}_\zeta^2\right] \tag{3.107}$$

where all quantities in Eq. (3.107) are real. It should be noted that Eqs. (3.105) and (3.107) should be used directly to evaluate the normalisation factor and then the process of normalisation is continued numerically.

3.5 NUMERICAL RESULTS

In this section four examples are presented to illustrate the theory. In the first two examples attention is confined to isotropic plates and the material properties used are Young's modulus $E = 70\,\text{GPa}$, Poisson's ratio $\nu = 0.3$ and mass density $\rho = 2700\ \text{kg/m}^3$. In these examples the first three natural frequencies of vibration are calculated by plotting the normalised determinant of the infinite order stiffness matrix, $\left|\overline{\mathbf{K}}_{\infty}\right|$, and the determinant of the dynamic stiffness matrix, $|\mathbf{K}|$, (see Eq. (3.12)) against vibration frequency.

Example 3.1: Consider a square plate of breadth b = 0.5m and thickness h =1.0mm, which is simply supported on all four edges. The classical solution for this plate can be found in reference (Gorman 1982) and with some simplification may be written as

$$n_j = \frac{\pi\,(1+j^2)}{2b^2}\sqrt{\frac{Eh^2}{12\rho\,(1-\nu^2)}} \tag{3.108}$$

where n_j is the j^{th} natural frequency for a longitudinal half-wavelength $\lambda = b$. The results are shown in Table 3.1.

Table 3.1: First three natural frequencies of a simply supported plate.

Mode, j	n_j, frequency of vibration (Hz) Eq. (3.108) and Current theory
1	19.362690
2	48.406724
3	96.813448

Figure 3.5(a) shows the variation of the determinant of the dynamic stiffness matrix against frequency of vibration. There are two poles at approximately 28 and 68 Hz which correspond to the first two natural frequencies of the plate if the longitudinal edges had been clamped, but do not correspond to natural frequencies of the present system. Figure 3.5(b) is the equivalent plot using the theory presented herein. The zeros of both graphs correspond identically to the natural frequency value of Table 3.1. However, the graph of Figure 3.5(b) has no poles and is clearly much less volatile than that of Figure 3.5(a).

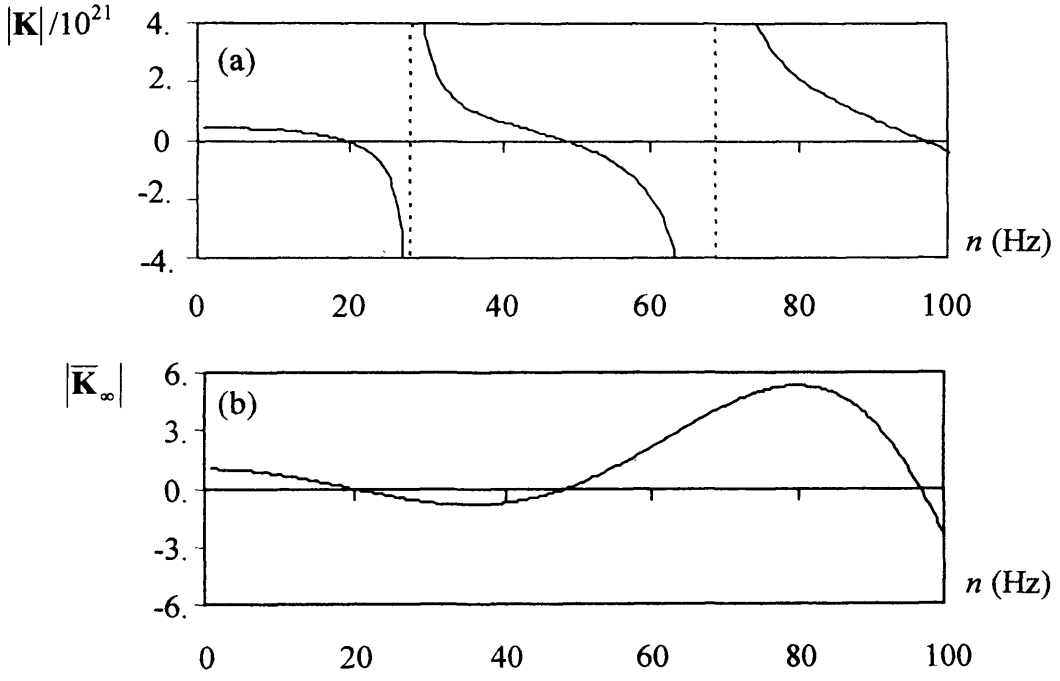

Figure 3.5: Comparison of determinant plots (Example 3.1), a) Determinant of the dynamic stiffness matrix versus frequency, b) Determinant of the normalised infinite order dynamic stiffness matrix versus frequency.

Example 3.2: For the second example, consider a continuous isotropic plate of length 0.5m, breadth 1.0m and thickness 1.0mm, Figure 3.6. The longitudinal edges are clamped, the ends are simply supported and there is a simple support at mid-span, running parallel to the longitudinal edges, so that the plate has two equal transverse spans of 0.5m.

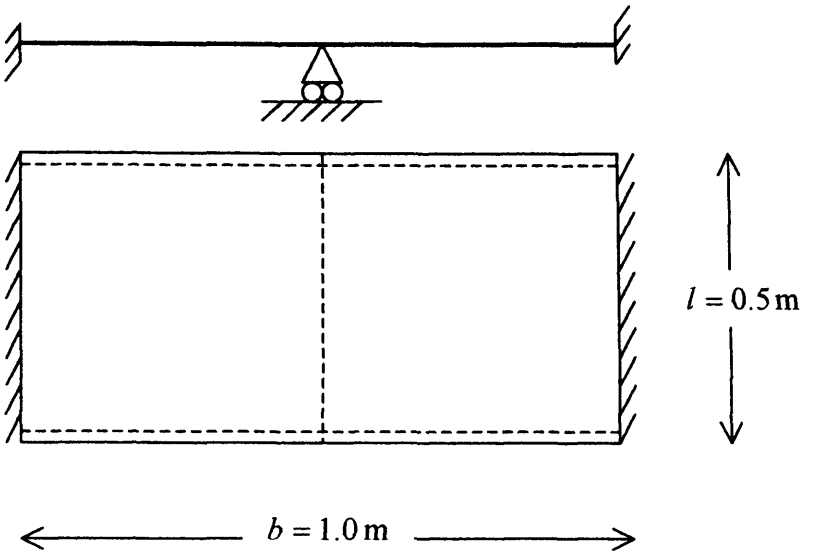

Figure 3.6: The continuous isotropic plate of Example 3.2. Plate thickness is 1.0mm.

As in Example 3.1, the longitudinal half-wavelength λ is chosen to be equal to the length of the plate in order to be compatible with prismatic plate theory i.e. $\lambda = 0.5\,\mathrm{m}$. Figure 3.7(a) shows the plot of the determinant of the dynamic stiffness matrix $|\mathbf{K}|$ versus frequency of vibration, whilst Figure 3.7(b) is the plot of $|\overline{\mathbf{K}}_\infty|$ versus frequency. The plot of $|\mathbf{K}|$ has two poles corresponding to the first two clamped natural frequencies of vibration of each component plate. Since there are two identical spans, J_0 in the W-W algorithm is ganged by two when the eigenparameter passed the poles. Also the W-W algorithm shows that these frequencies are also single fold natural frequencies of the structure, and they can clearly be identified as zeros of $|\overline{\mathbf{K}}_\infty|$ in Figure 3.7(b). Thus the plot of $|\overline{\mathbf{K}}_\infty|$ has the significant advantage that it has no poles and its zeros give all the natural frequencies of the structure. In addition, the smoothness of the plot of $|\overline{\mathbf{K}}_\infty|$ makes it more suitable for curve following and interpolation than the plot of $|\mathbf{K}|$.

Examples 3.3 and 3.4 consider orthotropic plates and in each case the first three natural frequencies of vibration are calculated in a similar way to Examples 3.1 and 3.2. The

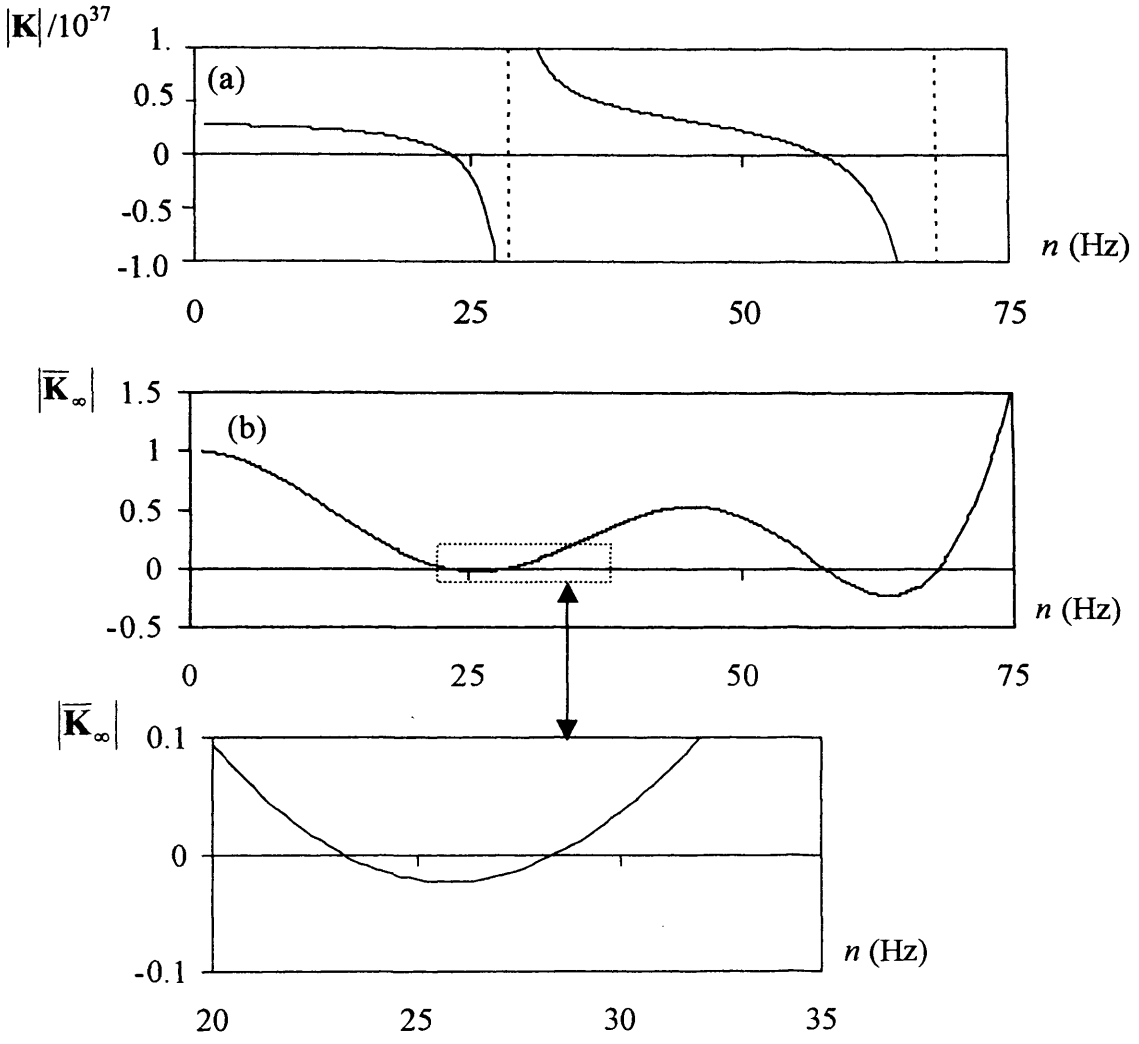

Figure 3.7: Comparison of determinant plots of Example 3.2, a) Determinant of the dynamic stiffness matrix versus frequency, b) Determinant of the normalised infinite order dynamic stiffness matrix versus frequency.

normalised determinant of the infinite order stiffness matrix, $\left|\overline{\mathbf{K}}_{\infty}\right|$, is plotted against vibration frequency and is compared to the plot of the normalised determinant of the dynamic stiffness matrix, $\left|\overline{\mathbf{K}}\right|$, (see Eqs. (3.11) and (3.12)). The material properties for orthotropic plates are as follows: Young's modulii $E_1 = 2E_2 = 70\,\text{GPa}$, Poisson's ratios $\nu_1 = 2\nu_2 = 0.3$, shear modulus $G = 20\,\text{GPa}$ and mass density $\rho = 2700\ \text{kg/m}^3$, where the subscripts denote values for the longitudinal and transverse direction, respectively.

Example 3.3: Consider a square orthotropic plate of breadth $b = 0.5\,\text{m}$ and thickness $h = 1.0\,\text{mm}$, which is simply supported on all four edges. The classical solution for orthotropic rectangular plates can be found in references (Lekhnitskii 1968; Szilard 1974) and with some simplification may be written as

$$n_{kj} = \frac{\pi}{2b^2}\left[\left(D_{11}\left(kb/l\right)^4 + 2D_t j^2\left(kb/l\right)^2 + D_{22} j^4\right)/\rho h\right]^{1/2} \tag{3.109}$$

$${}_{kj}N_L^{cr} = \frac{\pi^2\sqrt{D_{11}D_{22}}}{b^2}\left(\sqrt{\frac{D_{11}}{D_{22}}}\left(kb/l\right)^2 + \frac{2D_t j^2}{\sqrt{D_{11}D_{22}}} + \sqrt{\frac{D_{22}}{D_{11}}}\left(l/kb\right)^2 j^4\right) \tag{3.110}$$

where n_{kj} and ${}_{kj}N_L^{cr}$ are the j^{th} natural frequency and longitudinal critical buckling load for a longitudinal half-wavelength $\lambda_k = b/k$; $D_{11} = E_1 h^3/12(1-\nu_1\nu_2)$ and $D_{22} = E_2 h^3/12(1-\nu_1\nu_2)$ are the longitudinal and transverse plate flexural rigidities, respectively; $D_t = \nu_1 D_{11} + Gh^3/6$ is the effective torsional rigidity and l is the length of the plate. The results are shown in Table 3.1 for the case when $k = 1$.

Table 3.2: First three natural frequencies and critical buckling loads of the simply supported orthotropic plate of Example 3.3.

Mode, j	n_j, frequency of vibration (Hz) Eq. (3.109) **and** current theory	${}_jN_L^{cr}$, Longitudinal critical buckling load (N/m) Eq. (3.110) **and** current theory
1	16.06972	697.2454
2	36.06788	3512.408
3	69.46139	13027.19

Figure 3.8(a) shows the variation of the normalised determinant of the dynamic stiffness matrix against frequency of vibration. There are two poles at approximately 21.71 and 49.09 Hz which correspond to the first two natural frequencies of the plate if the longitudinal edges had been clamped, but do not correspond to natural frequencies of the

present system. Figure 3.8(b) is the equivalent plot using the current theory. The zeros of both graphs correspond identically to the first three natural frequency values of Table 3.2. However, the graph of Figure 3.8(b) has no poles and is clearly much less volatile than that of Figure 3.8(a).

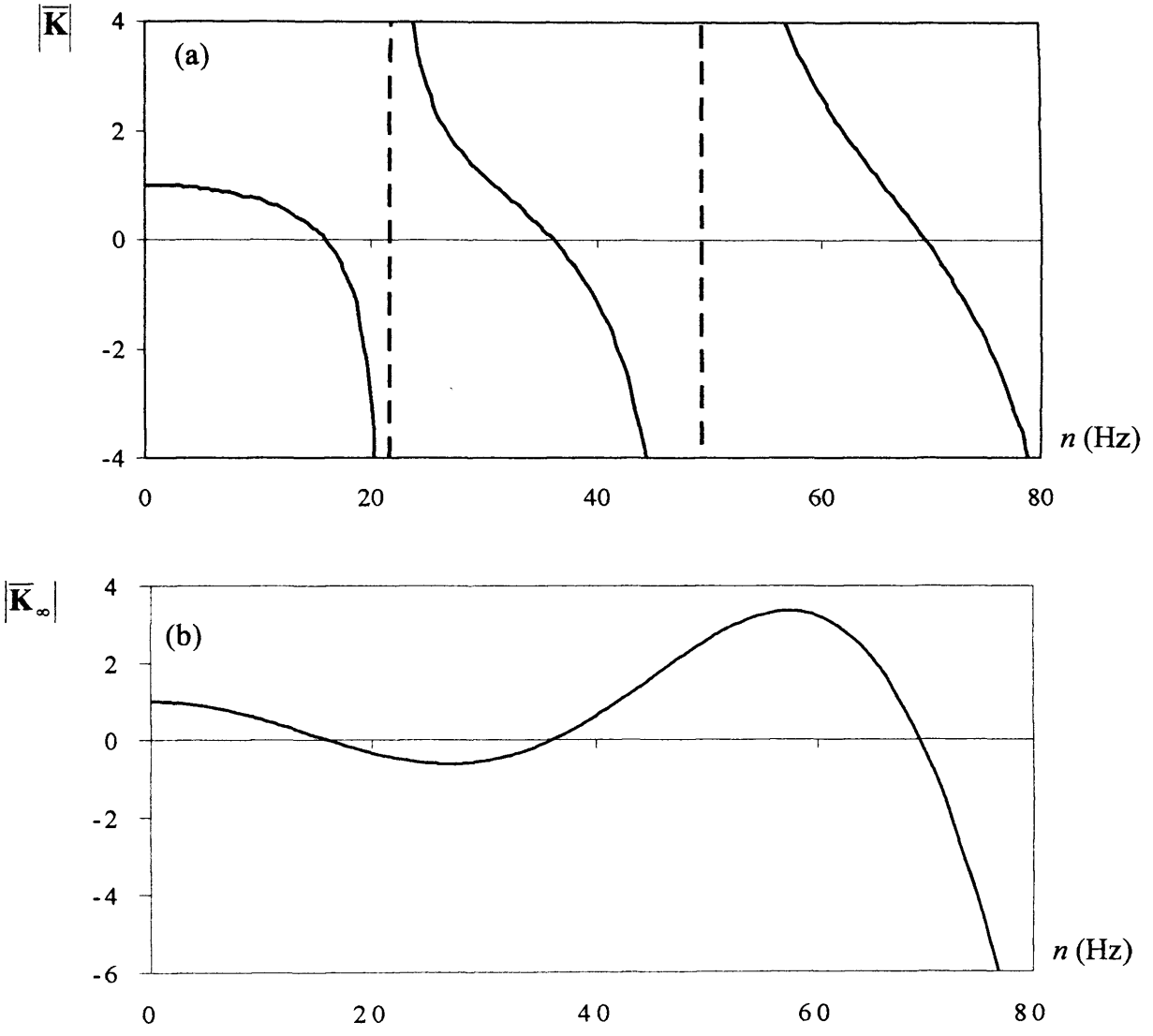

Figure 3.8: Comparison of determinant plots for Example 3.3. The zero's of both plots correspond precisely, a) Normalised determinant of the dynamic stiffness matrix versus frequency, the dashed lines are poles; and b) Determinant of the normalised infinite order dynamic stiffness matrix versus frequency.

***Example 3.4*:** For the second orthotropic example, consider a stiffened square plate of side length 0.5m and thickness 1.0mm, with three equally spaced, longitudinal stiffeners

of depth 50mm and thickness 0.8mm, see Figure 3.9. The plate is simply supported along its two longitudinal edges and is free along the remaining edges. The longitudinal half-wavelength λ is chosen to be equal to the length of the plate, l, i.e. $\lambda = 0.5\,\mathrm{m}$, while $N_L = 140\,\mathrm{N/m} \approx 0.2N_L^{cr}$ and $N_T = 70\,\mathrm{N/m} \approx 0.1N_L^{cr}$, where N_L^{cr} is the first critical buckling load of the simple plate of Example 3.3, (see Table 3.2). It should be noted that while the main plate is subjected to both N_L and N_T, the stiffeners only carry N_L.

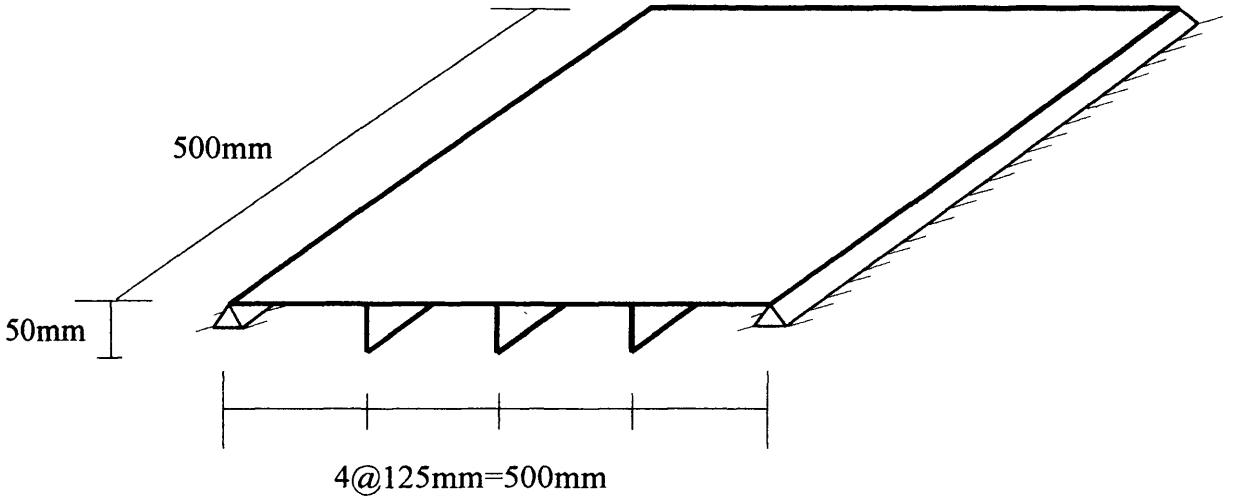

Figure 3.9: The stiffened square orthotropic plate on simple supports of Example 3.4 (the plate thickness is 1.0mm and the thickness of stiffeners is 0.8mm).

Figure 3.10(a) shows the plot of the determinant of the normalised dynamic stiffness matrix $|\overline{\mathbf{K}}|$ versus frequency of vibration, whilst Figure 3.10(b) is the corresponding plot of $|\overline{\mathbf{K}}_\infty|$. The plot of $|\overline{\mathbf{K}}|$ has a pole of multiplicity four, corresponding to the first fully clamped natural frequency of vibration of each of the four identical components of the span. It is physically evident that this frequency cannot be a natural frequency of the structure and this is confirmed by the plot of $|\overline{\mathbf{K}}_\infty|$ in Figure 3.10(b). Thus the plot of $|\overline{\mathbf{K}}_\infty|$ has the significant advantage that it has no poles and all the natural frequencies of the structure now correspond to its zero values. In addition, the smoothness of the plot of $|\overline{\mathbf{K}}_\infty|$ makes it much more suitable for curve following and interpolation than the plot of $|\mathbf{K}|$.

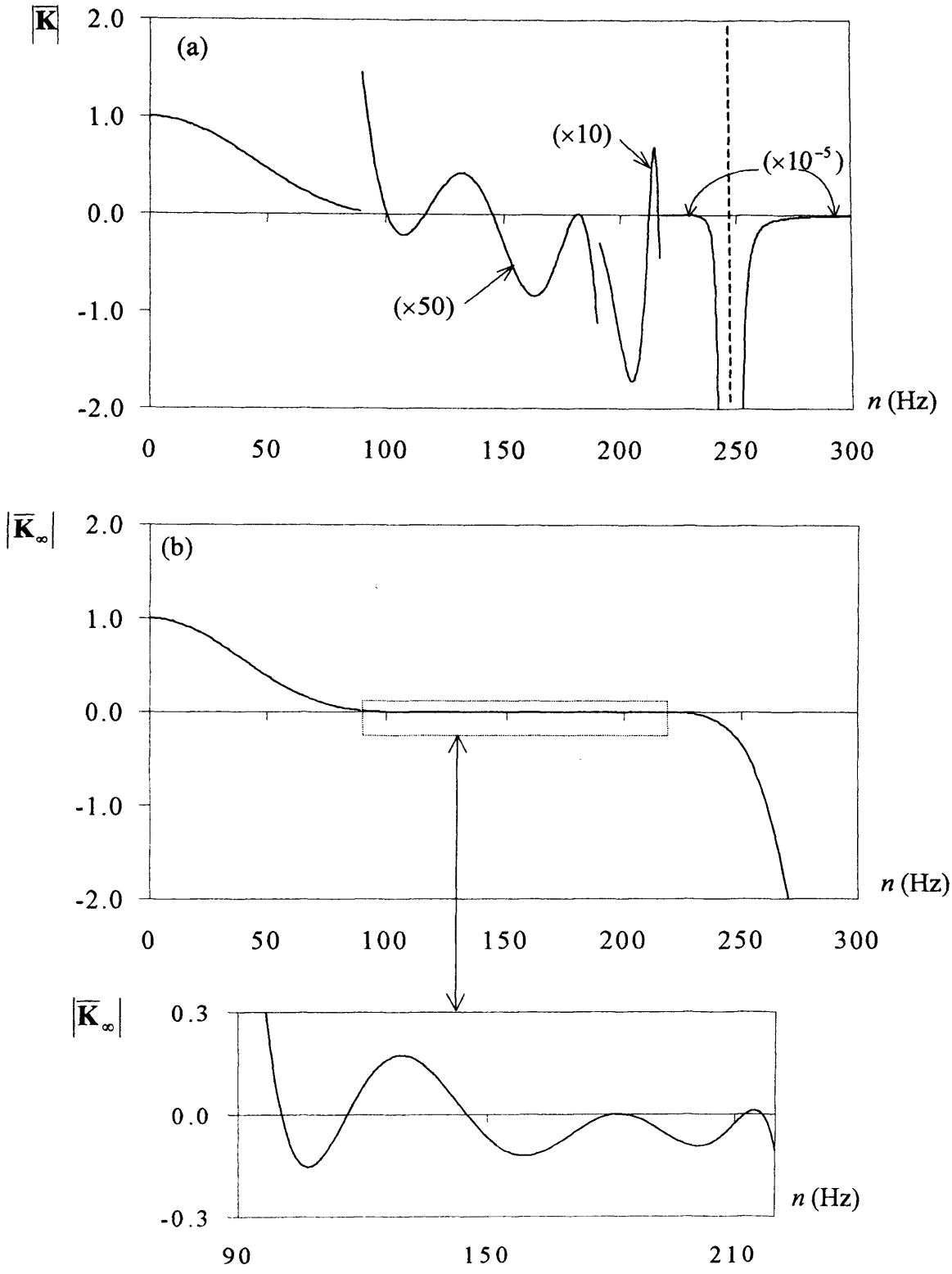

Figure 3.10: Comparison of determinant plots for Example 3.4, a) Determinant of the normalised dynamic stiffness matrix versus frequency. The dashed line is a pole of order 4 and the numbers against the various segments of the plot denote the scaling factor necessary to highlight the important features of the plot; and (b) Determinant of the normalised infinite order dynamic stiffness matrix versus frequency. The zero's of both plots correspond precisely.

3.6 SUGGESTED METHOD FOR ANISOTROPIC PLATES WITH IN-PLANE SHEAR LOADING

The paper (Wittrick and Williams 1974) used as a source for the orthotropic plate stiffnesses used in the present study also gave member stiffness matrices for anisotropic plates with in-plane shear stresses as well as in-plane longitudinal and transverse stresses. However whereas it gave exact expressions for J_0^O and J_0^I (see Eq.(2.43)) for orthotropic plates with in-plane longitudinal and transverse stresses, it was found to be impossible to provide such expressions for J_0^O when either anisotropy or in-plane shear stress were present. It is therefore not surprising that in the present study it has proved impossible to obtain an analytical expression for the out-of-plane member stiffness determinant when the plate is anisotropic and/or carries in-plane shear stress.

Because analytical expressions could not be found for J_0^O when the plate was anisotropic and/or carried in-plane shear, an alternative procedure was developed, as described in pages 229-231 of reference (Wittrick and Williams 1974). This involved halving the breadth of the plate progressively in the manner described earlier until an (exact) strip was obtained for which a logical argument showed that its J_0^O must be zero. The stiffness matrix and J_0^O of the plate were then obtained by obtaining the numerical value of the stiffnesses of the strip from the exact analytical expressions and then doubling progressively until the original plate was regenerated. However, such doubling has already been described in Section 3.3.3, around Eqs (3.33)-(3.38), and clearly Eq. (3.38) gives an approximation to the normalised member stiffness determinant, with almost no additional work above that required to find J_0^O. It will be noticed that the approximation leads to Eq. (3.33) neglecting the member stiffness determinant of the strip. Therefore the consequences of this type of approximation were evaluated for the most advanced plate for which an exact analytical expression for the member stiffness determinant is available to act as a comparator, i.e. the axially and transversely in-plane loaded plate dealt with in Section 3.4.2.

As an example, the orthotropic plate chosen has identical properties to the plate of Example 3.3. Results were then obtained for $\lambda = l$ and for $\lambda = l/5$ and are given in

Tables 3.3 and 3.4, respectively, which show the frequency ranges used. It can be seen that the frequency range in each case spans the first few natural frequencies when the longitudinal edges of the plate are clamped, because the determinant changes sign several times.

Columns two to five of Tables 3.3 and 3.4 contain the results of the normalised determinant of stiffness matrix of the clamped-clamped plate which is modelled with two, four, eight and sixteen identical strips while the last column presents the exact normalised member stiffness determinant of the plate. Since Eq. (3.33) with low value of r gives only approximate value of the exact member stiffness determinant of Eq. (3.34), columns

Table 3.3: Approximate and exact member stiffness determinants for the orthotropic plate of Example 3.3 with $\lambda = l$.

Frequency (Hz)	Suggested approximate normalised member stiffness determinant formed from				$\overline{\Delta}_m$
	2 elements	4 elements	8 elements	16 elements	
0	1.00000	1.00000	1.00000	1.00000	1.00000
4	0.96467	0.94118	0.95629	0.95604	0.95614
8	0.85918	0.82353	0.82957	0.82917	0.82903
12	0.68506	0.64706	0.63268	0.63187	0.63176
16	0.44529	0.38621	0.38594	0.38511	0.38495
20	0.14502	0.11681	0.11559	0.11513	0.11512
24	-0.20702	-0.15178	-0.14838	-0.14760	-0.14752
28	-0.59591	-0.38873	-0.37463	-0.37213	-0.37168
32	-0.99519	-0.56257	-0.53326	-0.52847	-0.52777
36	-1.35596	-0.64706	-0.59858	-0.59166	-0.59080
40	-1.58213	-0.58824	-0.55191	-0.54421	-0.54307
44	-1.46926	-0.43168	-0.38398	-0.37737	-0.37655
48	-0.53240	-0.11189	-0.09699	-0.09515	-0.09476
52	2.57295	0.34904	0.29407	0.28721	0.28615
56	12.84992	0.94118	0.76074	0.74001	0.73702
60	55.51164	1.58824	1.26142	1.22203	1.21636
64	614.22606	2.29412	1.74264	1.68082	1.67197
68	1046.49729	2.94118	2.14139	2.05569	2.04359
72	115.13526	3.41176	2.38850	2.28172	2.26651
76	41.11974	3.58824	2.41297	2.29296	2.27602
80	18.50388	3.35294	2.14725	2.02922	2.01261
84	8.22395	2.52941	1.53320	1.44056	1.42752
88	1.91928	0.94118	0.52853	0.49351	0.48867
92	-2.37039	-1.64706	-0.88650	-0.82268	-0.81367
96	-5.65396	-5.23529	-2.70254	-2.49101	-2.46163
100	-8.22395	-10.05882	-4.87510	-4.46204	-4.40524

two to five gives the approximation to the exact normalised member stiffness determinant of the last column.

Table 3.4: Approximate and exact member stiffness determinants for the orthotropic plate of Example 3.3 with $\lambda = l / 5$.

Frequency (Hz)	Suggested approximate normalised member stiffness determinant formed from				$\overline{\Delta}_m$
	2 elements	4 elements	8 elements	16 elements	
0	1.00000	1.00000	1.00000	1.00000	1.00000
10	0.99865	0.99611	0.99375	0.99308	0.99296
20	0.99459	0.98450	0.97520	0.97258	0.97211
30	0.98782	0.96534	0.94491	0.93920	0.93817
40	0.97834	0.93890	0.90379	0.89411	0.89237
50	0.96616	0.90557	0.85309	0.83884	0.8363
60	0.95117	0.86583	0.79429	0.77526	0.77188
70	0.93347	0.82028	0.72911	0.70542	0.70124
80	0.91286	0.76958	0.65938	0.63152	0.62663
90	0.88943	0.71452	0.58701	0.55577	0.55034
100	0.86309	0.65592	0.51389	0.48032	0.47453
110	0.83373	0.59471	0.44183	0.40713	0.40119
120	0.80125	0.53184	0.37251	0.33793	0.33207
130	0.76554	0.46833	0.30739	0.27414	0.26857
140	0.72660	0.40522	0.24765	0.21683	0.21173
150	0.68412	0.34356	0.19421	0.16670	0.16221
160	0.63790	0.28439	0.14766	0.12408	0.12028
170	0.58771	0.22873	0.10828	0.08894	0.08588
180	0.53316	0.17754	0.07603	0.06096	0.05861
190	0.47371	0.13171	0.05059	0.03954	0.03785
200	0.40854	0.09198	0.03141	0.02389	0.02276
210	0.33649	0.05897	0.01773	0.01311	0.01242
220	0.25560	0.03306	0.00866	0.00621	0.00586
230	0.16273	0.01440	0.00325	0.00226	0.00212
240	0.05154	0.00277	0.00053	0.00036	0.00033
250	-0.09058	-0.00242	-0.00039	-0.00025	-0.00023
260	-0.27340	-0.00230	-0.00031	-0.00019	-0.00018
270	4.95065	0.00140	0.00015	0.00009	0.00008
280	1.68100	0.00621	0.00053	0.00031	0.00028
290	0.44654	0.00884	0.00059	0.00033	0.0003
300	0.10515	0.00519	0.00026	0.00014	0.00013
310	-0.10193	-0.00938	-0.00035	-0.00018	-0.00016
320	-0.26705	-0.03887	-0.00104	-0.00051	-0.00045
330	-0.40895	-0.08338	-0.00152	-0.00071	-0.00062
340	-0.51057	-0.12951	-0.00153	-0.00068	-0.00059

From these results it can be seen that as few as 4 strips (i.e. two halvings and doublings) usually give reasonable accuracy. It should also be noted that as the number of natural frequencies of the plate with clamped longitudinal edges that have been exceeded increases, i.e. as the number of sign changes in the final column of Tables 3.3 and 3.4 increases, the computation of J_0^O will require an increasing number of strips to be present and so will result in closer approximations to the member stiffness determinant being obtained.

3.7 GENERAL REMARKS

Transcendental stiffness matrices for vibration (or buckling) have long been available for a range of structural members. Such stiffness matrices are exact in the sense that they are obtained from an analytical solution of the governing differential equations of the member. Hence, assembly of the member stiffnesses to obtain the overall stiffness matrix of the structure results in a transcendental eigenproblem that yields exact solutions and which can be solved with certainty using the Wittrick-Williams algorithm.

When such an exact solution exists, the members have a recently discovered property that can also be expressed analytically and is called its member stiffness determinant. The member stiffness determinant is a property of the member when fully clamped boundary conditions are imposed upon it. It is then defined as the determinant of the member stiffness matrix when the member is sub-divided into an infinite number of identical sub-members. Each sub-member is therefore of infinitely small length so that its clamped-ended natural frequencies are infinitely large. Hence the contribution from the member stiffness matrix to the J_0 count of the W-W algorithm will be zero. In general, the member stiffness determinant is normalised by dividing by its value when the eigenparameter (i.e. the frequency or buckling load factor) is zero, as otherwise it would become infinite. A major advantage of the member stiffness determinant is that, when its values for all members of a structure are multiplied together and are also multiplied by the determinant of the transcendental overall stiffness matrix of the structure, the result is a

determinant which has no poles and is substantially less volatile when plotted against the eigenparameter.

It should be noted that curve plotting methods of finding eigenvalues may miss roots when using the plot of either, the determinant of the dynamic stiffness matrix or the determinant of the normalised infinite order dynamic stiffness matrix versus frequency. On the other hand, the W-W algorithm in conjunction with the bisection method can find the required roots with the certain knowledge that non have been missed, despite the fact that the method is known to be relatively slow. Furthermore, the W-W algorithm in conjunction with curve plotting techniques which, for example, uses parabolic interpolation (Williams and Kennedy 1988) is relatively faster, however, the existence of the poles in the plot of determinant of the dynamic stiffness matrix hampers the method. In contrast, the W-W algorithm when used in conjunction with the determinant of the normalised infinite order dynamic stiffness matrix, provides a significantly better platform for the development of efficient, computer based routines for convergence on eigenvalues by curve prediction techniques.

Finally, a favourable preliminary investigation of a method for adequately approximating member stiffness determinants has been undertaken. The motivation for this was that it proved to be impossible to obtain an exact solution for the anisotropic case, but approximate solutions to good accuracy could be achieved straightforwardly. It also become evident that such approximate solutions could equally well be achieved for the isotropic and orthotropic cases if required.

Part B

Exact free vibration analysis of sandwich structures

CHAPTER 4

AN INTRODUCTION TO SANDWICH BEAMS

4.1 BACKGROUND

Optimisation of the strength to weight ratio in structural members has been a necessary goal in the aeronautics and space environment for many years and to a lesser extent in many other areas of structural design. Such a philosophy is epitomised by sandwich construction which, in its most usual form, is characterised by a thick lightweight core that is bonded between two external high strength layers called faceplates.

The core of a sandwich element can be almost any material or architecture, but in general, cores fall into four types, (a) foam or solid core, (b) honeycomb core, (c) web core, and (d) a corrugated or truss core (Vinson 2001). However, from a structural standpoint the function of the core of a sandwich element is twofold. First, the core must keep the faceplates apart and stabilise them against local buckling and therefore must possess a certain rigidity against deformations perpendicular to the plane of the faceplates. Secondly, the core must enable the faceplates to act more or less as the outer layers of a

beam or plate, hence it must possess a certain shearing rigidity in planes perpendicular to the faceplates. Otherwise, the faceplates behave as two independent beams or panels and the sandwich effect is lost. The outstanding strength and stiffness characteristics of sandwich construction come off from this second property (Plantema 1966).

On the other hand, almost any structural material which is available in the form of thin sheet may be used to form the faceplates of a sandwich panel (Allen 1969). However, the commonly used faceplate materials can be divided into two main groups, metallic and non-metallic materials. The former group contain steel, stainless steel and aluminium alloys and the latter include materials such as plywood, cement, veneer, reinforced plastic and fibre composites (Zenkert 1997). The importance of fibre composites lies mainly in their ability to contribute high strength properties despite their low stiffness; easier fabrication during sandwich construction and finally, their anisotropic behaviour. The latter characteristic makes it possible to ensure not only that the components are stressed to their ultimate limit, but that the component itself may be utilised in a more optimised way (Zenkert 1997).

Most often the two faceplates of a sandwich element are identical in material and thickness, but in special cases the faceplates may differ in thickness, material or fibre orientation, or any combination of these three. This may be due to the fact that one faceplate is the primary load carrying, low temperature portion of the structure, while the other faceplate may have to withstand an elevated temperature, corrosive environment etc (Vinson 2001).

Sandwich construction is frequently used wherever high strength or high structural efficiency, low-weight, low thermal conductivity through the thickness, high resistance to fatigue failure under acoustic excitation along with low noise, long life and increased reliability are important design objectives. In addition, sandwich construction, with its elegant form, can be used for dissipating the energy in structures and mechanical systems when the reduction of the transmission of vibratory energy is desired. Employing viscoelastic materials is particularly useful over a wide range of frequencies for increasing the structural damping or removing some of the vibration energy during structural vibration. Besides controlling the amplitude of resonant vibration, damping also modifies wave attenuation and sound transmission properties through structures. It

also reduces the structural fatigue and consequently increases the structural life. Nevertheless, the two main reasons for using sandwich construction are the high ratio of strength to weight and the vibration-damping characteristics.

Sandwich construction is mostly used in the aerospace, aircraft, marine, automobile and building industries. For example, over 46 percent of wetted surface of the Boeing 757 and 767 comprise sandwich construction and the floors, side panels, overhead bins and ceiling of the Boeing 747 are also of sandwich construction (Bitzer 1992). In addition, the Royal Swedish Navy has been using fibreglass- and graphite-composite sandwich construction for their naval vessels for more than 25 years (Vinson 1999). Due to necessity of carrying relatively small loads over fairly long spans in the building industry, its uses have been mainly semi-structural in character (Allen 1969). Recently, sandwich construction is being used increasingly in civil engineering infrastructure rehabilitation projects, such as bridge decks and also in low cost or emergency housing.

Honeycomb sandwich construction is excellent for absorbing mechanical and sound energy. It can also be used to transmit heat or to be an insulative barrier. In the former, a metallic honeycomb is used with natural convection; for the latter, a non-metallic core is used, with the cells filled with foam. For sound barriers, the core can be filled with a fibreglass batting and a thin porous Tedlar skin used for the interior surface (Vinson 2001).

The remaining applications are mostly related to vibrations and a knowledge of their dynamic properties, such as the natural frequencies and damping factors, are essential in the design process. However, due to the use of a relatively soft core, shear deformations in sandwich elements have such importance that the necessity for more precise theory, rather than the ordinary Euler-Bernoulli theory seems to be clear. For this reason, during the past decades, sandwich structures have been the subject of many valuable investigations. Hence, the lack of attention to an exact dynamic stiffness method in vibrational analysis of sandwich structures is surprising and demands redress.

4.2 REVIEW OF EXISTING LITERATURE

The literature on the analysis of sandwich beams is enormous and especially over the last few years, the science and technology of sandwich structures and materials has gained an impressive momentum. Early theoretical works were all restricted to a consideration of static uniform lateral loads, stability and buckling loads, and most assumed simply supported boundary conditions. However, by the 1960s, interest in sandwich structures had increased significantly. In 1966 Plantema published the first book on sandwich structures (Plantema 1966), which contained a thorough bibliography of over 350 publications on sandwich structures and related topics that had appeared before 1965. This was followed in 1969 by another book on sandwich construction by Allen (Allen 1969). Two more textbooks by Zenkert (Zenkert 1997) and Vinson (Vinson 1999) followed, which collected together the more recent works on theory and application of sandwich construction. (Davies 2001) are the most recent handbooks that record the latest technologies and standards in manufacturing and construction of sandwich elements.

In addition, there have been six international conferences devoted specifically to the theme of sandwich construction. These were held in 1989, 1992, 1995, 1998, 2000 and 2003 in Stockholm, Gainesville, Southampton, Stockholm, Zurich and Boca Raton, respectively, and have provided forums for the presentation and discussion of the latest research and technology on all aspects of sandwich structures and materials. The seventh international conference will be held in August 2005 in Aalborg, Denmark, with the aim of promoting and endorsing sandwich structures technology to the international community.

The first research paper concerning sandwich construction was written by Marguerre in 1944 (Marguerre 1944) and dealt with sandwich panels subject to in-plane compressive loads. However, the first formulation of the vibration problem was set out by Kerwin in 1959 (Kerwin 1959). In this paper he analysed three-layer sandwich beams consisting of a damping layer between two faceplates. Since then, the theory of the flexural vibration of sandwich beams has been considered by various authors. These have had two principal applications: (a) to sandwich elements that have thin, soft central layers and are used for

their high damping capacity, and (b) to sandwich elements with thick, stiff cores that are used for their lightness and high flexural stiffness.

Kerwin (Kerwin 1959) considered simply supported beams or beams with an infinitely long span so that the end effects could be neglected. Later, DiTaranto (DiTaranto 1965) derived a sixth-order, complex, homogeneous differential equation for a freely vibrating, finite-length unsymmetrical sandwich beam in terms of longitudinal displacements. In 1966 Mead and Sivakumuran (Mead and Sivakumuran 1966) adopted the Stodola method for the calculation of the natural frequencies and modes of sandwich beams in free flexural vibration. The differential equation of motion in terms of transverse displacement for a forced vibration problem was derived by Mead and Markus (Mead and Markus 1969). They showed that the solution of the differential equation developed by DiTaranto is a special class of complex, forced modes of vibration, which are completely uncoupled. Subsequently, Mead and Markus (Mead and Markus 1970a; Mead and Markus 1970b) considered both a cantilever sandwich beam and a clamped ended sandwich beam when evaluating loss factors and resonant frequencies. In 1982, Mead (Mead 1982) compared the theories of flexural vibration of damped, three-layer sandwich beams as presented by DiTaranto (DiTaranto 1965) and Mead and Markus (Mead and Markus 1969) with that of Yan and Dowell (Yan and Dowell 1974) and concluded that the former yields reliable values if the flexural wavelength is greater then about four faceplate thicknesses, whilst the latter is reliable only at much greater wavelengths or when the core is very thick.

Later, Mead (Mead and Markus 1985) examined the influence of the inertia coupling between different wave types caused by a non-structural mass that vibrates with the beam, called a ceramic layer, and concluded that if the damping layers are applied asymmetrically to the beam section, the flexural and longitudinal wave types become coupled. Using an energy approach, Rao (Rao 1978) derived the same equation as (DiTaranto 1965) and (Mead and Markus 1969) and introduced eight basic end conditions for the problem.

By using Green's function, i.e. a discrete solution to the governing differential equation for the flexural behaviour of a three-layered sandwich beam under the action of a concentrated load, Fotiu (Fotiu 1987) and Sakiyama *et al.* (Sakiyama et al. 1996a;

Sakiyama et al. 1997) reported methods of analysing the free vibration of sandwich beams.

By using Hamilton's principle, Nilsson and Nilsson (Nilsson and Nilsson 2002) derived the differential equation governing the apparent bending of sandwich beams including the effects of rotary inertia of the layers and the rigidity of the core. It is interesting that in this case the order of the differential equation is still six. Some dynamic properties of sandwich structures with honeycomb and foam cores were predicted and compared with measured results.

The vibration characteristics of undamped sandwich beams whose ends are loaded and elastically constrained was considered by Farghaly (Farghaly and Shebl 1992). Elastic bonding between the core and the two symmetrical faceplates has been the main difference between the work of Chonan (Chonan 1982) and the others.

The reduction of vibration response and the transmission of vibratory energy in structures have received wide attention for many years. Two books in this area (Nashif et al. 1985) (Sun and Lu 1995), provide practical and detailed information on the research and development of vibration damping. The damping effect of viscoelestic materials is easily introduced by utilising a complex shear modulus that has the form $G^* = G(1+i\eta)$, where G and η are the real shear modulus and the loss factor of the viscoelastic material, respectively. However, in most of the reported work, the solution for undamped vibrations can be achieved by setting the loss factor equal zero (Mead and Markus 1969; Nilsson and Nilsson 2002; Rao 1978; Sakiyama et al. 1996a).

On the other hand, the effects of longitudinal and rotary inertia, in addition to the transverse inertia, have also been considered by various authors (Chonan 1982; Mead 1982; Rao and Nakra 1970; Rao and Nakra 1973) who showed that there will be three families of modes of vibration comprising bending, extension and thickness shear.

Rao, in a further study (Rao 1977), used Hamilton's principle to formulate the equations of motion and the associated boundary conditions for flexural vibration of short, unsymmetric sandwich beams. His equations included the second order effects of rotary inertia, extension and shear of all layers. Each layer is therefore treated as a Timoshenko

beam. Maheri (Maheri and Adams 1998) verified the viability of adapting the Timoshenko beam equations to a sandwich configuration. In addition, Dugundji (Dugundji 2002) presented a sixth-order, extended set of Timoshenko beam equations that allow the necessary boundary conditions of a cantilever sandwich beam to be satisfied and the closed-form solutions are given. Cabanska-Placzkiewicz (Cabanska-Placzkiewicz 2000) also proposed a model in which the faceplates of a three-layer sandwich beam are modelled as Timoshenko beams, while the internal layer possesses the characteristics of Winkler's viscoelastic one-directional base.

Experimental observations and analytical predictions suggest that classical sandwich theory, which assumes a laterally incompressible core, is not capable of accurately predicting the free vibration response of soft-core sandwich beams. Therefore, sandwich beams with transversely flexible cores need to be modelled using a higher order sandwich theory. Frostig and several of his colleagues (Frostig 1992; Frostig 1993; Frostig and Baruch 1994; Frostig and Thomsen 2004; Sokolinsky et al. 2001) have studied the influence of compressible cores and have developed a consistent, rigorous, closed-form, higher order theory for sandwich plates and panels. On the other hand, an analytical model for the vibration of multi-span sandwich beams, which considers a damped flexible core with linear change in shear and normal deformation has been reported by He (He and Rao 1993). In this model the faceplates do not deform in shear and the longitudinal and transverse inertia have been included, but the rotary effects are neglected. Recently, the free vibration of a cantilever sandwich beam with a soft core was analysed using three different models (Sokolinsky et al. 2004): a higher-order theory for sandwich panels, a two-dimensional finite element analysis and classical sandwich theory. The inadequacy of classical sandwich theory for the free vibration response of soft-core sandwich beams was clearly demonstrated.

Free vibrations of curved sandwich beams have been studied by only a few authors (Ahmed 1971; Ahmed 1972; Sakiyama et al. 1997). Recently Bozhevolnaya and Sun (Bozhevolnaya and Sun 2004) have developed a curved sandwich beam model which takes into consideration both radial and circumferential displacements of the core with the assumption of linear variation of displacements across its thickness. The model predicts that there exists four types of natural modes, namely flexural bending, extension, shear

thickness modes and anti-phase lateral waves. The existence of anti-phase modes is due to considering the linear variation of radial displacements through the core thickness.

While the exact or closed form analytical solutions can only be obtained for problems with simple geometry and boundary conditions, numerical solution techniques like the finite element method are suitable for practical problems with complex geometries and boundaries. Ahmed (Ahmed 1971; Ahmed 1972) seems to be a pioneer in using finite element methods in the analysis of sandwich beams. Mace (Mace 1994) developed a finite element model for sandwich beams containing very thin viscoelastic layers. Silverman (Silverman 1995; Silverman 1997) used a Galerkin type solution to obtain approximate eigenvalues, while Baber (Baber et al. 1998) presented a model with a thin or moderately thick viscoelastic core with a nonlinear variation of displacements through its thickness. In the latter model by using a simple approximation, all core variables have been expressed in terms of the faceplate displacements.

Using the finite element method, Vuo-Quoc and his colleagues (Deng and Vu-Quoc 1998; Vuo-Quoc and Ebcioglu 1995; Vu-Quoc and Deng 1995; VuQuoc et al. 1996) have focused on the dynamics of geometrically exact sandwich structures. Sainsbury and Zhang (Sainsbury and Zhang 1999; Zhang and Sainsbury 2000) have combined the polynomial shape functions of conventional finite element analysis with Galerkin orthogonal functions to develop a finite element that can deal with damped sandwich beam structures. A Rayleigh-Ritz analysis of sandwich beams with a capability to include damping in any layer is presented by Fasana (Fasana and Marchesiello 2001).

Higher order theories for shear deformation have been used by Kant and several of his colleagues (Kant and Gupta 1988; Kant et al. 1998; Marur and Kant 1998). Mixed higher order theory has also been used by Rao *et al.* (Rao et al. 2001) to develop an analytical method for evaluating the natural frequencies of laminated composite and sandwich beams, while Ramtekkar *et al.* (Ramtekkar et al. 2002) used a similar approach to adapt mixed finite element modelling. In similar vein, a 18-node, three-dimensional mixed FE model has been developed by using Hamilton's principle by Desai *et al.* (Desai et al. 2003) where continuity of the transverse stress and displacement fields has been enforced through the thickness of the laminated composite plate. A semi-analytical method has also been reported by Rao and Desai (Rao and Desai 2004) in which they evaluates the

natural frequencies, as well as the displacement and stress eigenvectors, for simply supported, cross-ply laminated and sandwich plates by using a higher order mixed theory, where models based on equivalent single layer, as well as layer-wise theories, have been formulated.

Most of the literature on the torsion of sandwich beams has been reported since 1990 (Dewa 1990; Ganapathi et al. 1999a; Ganapathi et al. 1999b; Patel and Ganapathi 2001; Tanghe-Carrier and Gay 2000). A three-noded beam finite element which includes transverse shear and warping due to torsion has been derived by Ganapathi (Ganapathi et al. 1999b).

Despite the extensive literature on sandwich beams, there is very little work that utilises a stiffness formulation and also accounts in an exact way for the uniform distribution of mass. Banerjee (Banerjee 2003) developed a dynamic stiffness matrix for a three layered symmetric sandwich beam, but ignored the density of the core. Howson and Zare (Howson and Zare 2004) extended Banerjee's work by accounting for the total lateral inertia and developed a dynamic member stiffness matrix for the flexural motion of a sandwich beam with unsymmetrical cross-section.

4.3 THE CURRENT APPROACH

A precise and general stiffness formulation that accounts in an exact way for the uniform distribution of mass in a member can not be found in the literature. This is surprising since such a course offers two considerable advantages. The first of these is the opportunity to exploit the powerful modelling features of the stiffness method of analysis. For example, continuous beams with varying member properties are easily analysed and it is straightforward to incorporate translational and rotational inertia of nodal masses, spring stiffness and non-classical boundary conditions. The second advantage is that the formulation results in an idealisation containing the minimum number of elements, while leaving invariant the accuracy to which any particular natural frequency can be found. This can be important for higher natural frequencies and should be contrasted with

traditional finite elements in which the accuracy is sensitive to the idealisation. However, such a formulation is intractable and necessitates the solution of a transcendental eigenvalue problem which usually is resolved by adopting the Wittrick-Williams algorithm (Wittrick and Williams 1971a) that enables any required natural frequency to be converged upon to any required accuracy with the certain knowledge that none have been missed.

Therefore, the main aim of the work in Part B is to present an exact and concise dynamic stiffness method for the frequency analysis of sandwich beams that can be used to model framed structures. The analysis will be 'exact' in the sense that the solution satisfies the governing differential equation exactly in the same way that the 'exact' solution can be obtained in conventional analytic theories.

The flexural vibration of sandwich beams with two unequal faceplates is the subject of studies in Chapter 5. The faceplates are treated as Euler-Bernoulli beams and the core deforms only in shear. The longitudinal and rotary inertias are neglected. The resulting governing differential equation is of sixth order and the element has three degree of freedom at each end; the transverse deflection, the general slope of the member and the average rotation of the cross-section.

In Chapter 6, the theory of Chapter 5 is extended to include the effects of longitudinal and rotary inertia. This crucial difference enables the resulting member dynamic stiffness matrix (exact finite element) to be included in general two-dimensional structures for the first time. Inclusion of longitudinal inertia raises the order of the governing differential equation to eight. Although the inclusion of rotary inertia does not change the order of the problem, it increases the accuracy of the model. The resulting model provides four degrees of freedom at each end, which are the transverse deflection, the general slope of the member and the longitudinal translation of the two faceplates. In an alternative form, the two longitudinal translations of the faceplates can be replaced by the so-called average translation of the element and average rotation of the cross-section.

In Chapter 7 improvements have been made to the theory so as to include the additional effects of shear deformation in the faceplates, as well as the effects of axial and bending stiffness of the core. Inclusion of these effects causes the governing differential equation

to be of tenth order and five degrees of freedom at each end of the member are introduced. Hence, the theory can now be used for slender beams and also deep beams for which Timoshenko theory would normally be used.

In each chapter, for better understanding of the problem, the governing differential equations of motion are derived separately using both an Energy approach and an Equilibrium approach and the results are shown to be identical. Several examples are given in each chapter to validate related theories and to indicate their range of application.

CHAPTER 5

FREE FLEXURAL VIBRATIONS OF THREE-LAYER SANDWICH BEAMS

5.1 INTRODUCTION

The sandwich beam considered in this chapter comprises two unequal faceplates that are separated by a weaker core layer. All layers are isotropic and homogeneous. The following assumptions are then made. (i) The core is laterally incompressible and transverse direct strains in the faceplates and core are negligible so that small transverse displacements are the same for all points in a normal section; (ii) there is perfect bonding at the core/faceplate interfaces, so there is no slippage between the faceplates and the core layer; (iii) the faceplates are elastic and do not deform in shear, therefore the faceplates are treated as Euler-Bernoulli beams and the bending and axial forces in any section of the sandwich beam are carried by the faceplates ; (iv) the linearly elastic core deforms mainly through shear strain and carries only shear forces. In-plane normal stresses are assumed to be negligible; (v) the transverse flexural inertia is assumed to be predominant, so that the longitudinal and rotary inertia of the beam may be ignored.

5.2 EQUATIONS OF MOTION

5.2.2 *Equilibrium equations*

Figure 5.1 shows the positive sense of the forces experienced by a typical elemental length of a member at some instant during the motion. The beam has unit width. The generic quantities m, q and μ relate to bending moment, shear force and mass/unit length, respectively. When they are un-subscripted, they are resultant or total values and when subscripted with t, b, or c they relate to the top faceplate, bottom faceplate and the core, respectively. The prime and dot notations refer to partial differentiation with respect to x and time in the usual way.

Since the whole sandwich beam is assumed to be in pure bending, the overall longitudinal force on the beam section is zero. This implies that the equation of horizontal equilibrium can be written as

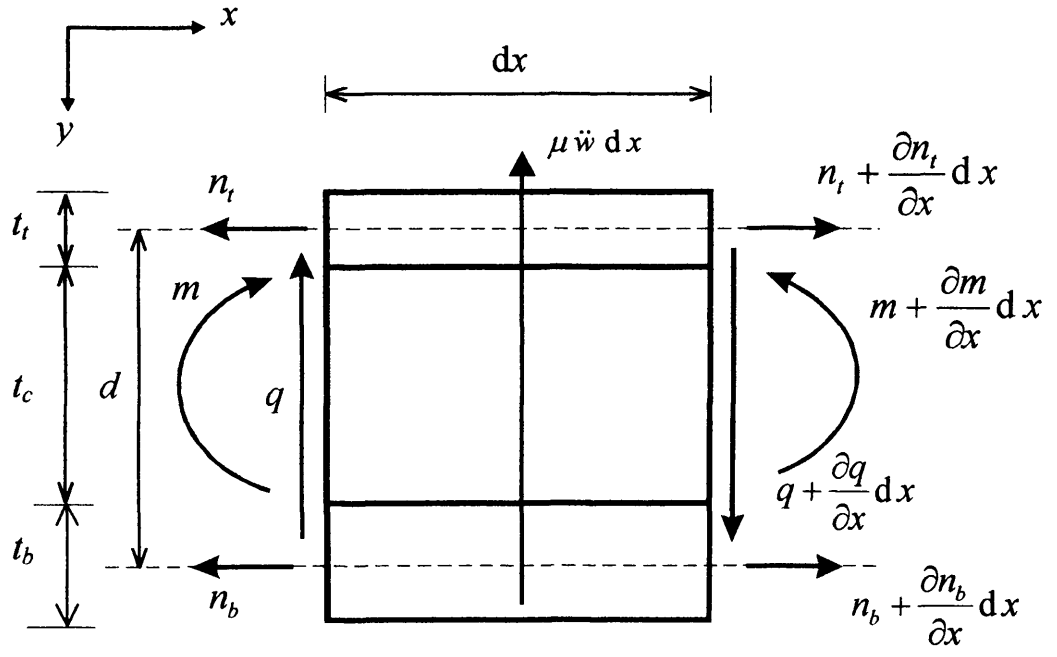

Figure 5.1: Positive resultant forces and moments and reverse inertia acting on a typical elemental length of a sandwich beam of unit width with the layer dimensions shown.

$$n_t + n_b = 0 \quad \text{or} \quad -n_t = n_b = n \tag{5.1a,b}$$

where n_t and n_b are the axial forces in top and bottom faceplates, respectively. Eq. (5.1b) shows that longitudinal forces in the faceplates are equal in magnitude but opposite in direction.

Taking moments about the centre line at the right hand side of the bottom faceplate in Figure 5.1 yields the moment equilibrium as

$$q\,\mathrm{d}x - n_t\,d + m + (n_t + \frac{\partial n_t}{\partial x}\mathrm{d}x)d - (m + \frac{\partial m}{\partial x}\mathrm{d}x) + (\mu\ddot{w}\,\mathrm{d}x)\frac{\mathrm{d}x}{2} = 0 \tag{5.2}$$

where m and q are the resultant moment and shear force on the section, respectively, w and μ are the transverse deflection and the uniform mass per unit length of the beam, respectively, and $d = t_c + \frac{1}{2}(t_t + t_b)$ is the distance between centre lines of the faceplates. Figure 5.2 shows the inter-element forces and component member stresses that act on an elemental length of the member. By comparing Figures 5.1 and 5.2 it is clear that

$$q = q_t + q_b + q_c \;; \quad m = m_t + m_b \;; \quad \mu = \mu_t + \mu_b + \mu_c \tag{5.3a,b,c}$$

where subscripted quantities with t, b, or c relate to the top faceplate, bottom faceplate and the core, respectively. Ignoring terms of second order in Eq. (5.2), the equation of moment equilibrium is

$$q = (m - \overline{m})' \tag{5.4}$$

where $\overline{m}$ denotes the couple due to the axial forces that are developed in the top and bottom faceplates during bending. From Eq. (5.1), $\overline{m}$ may be written as

$$\overline{m} = n_t d = -nd \tag{5.5}$$

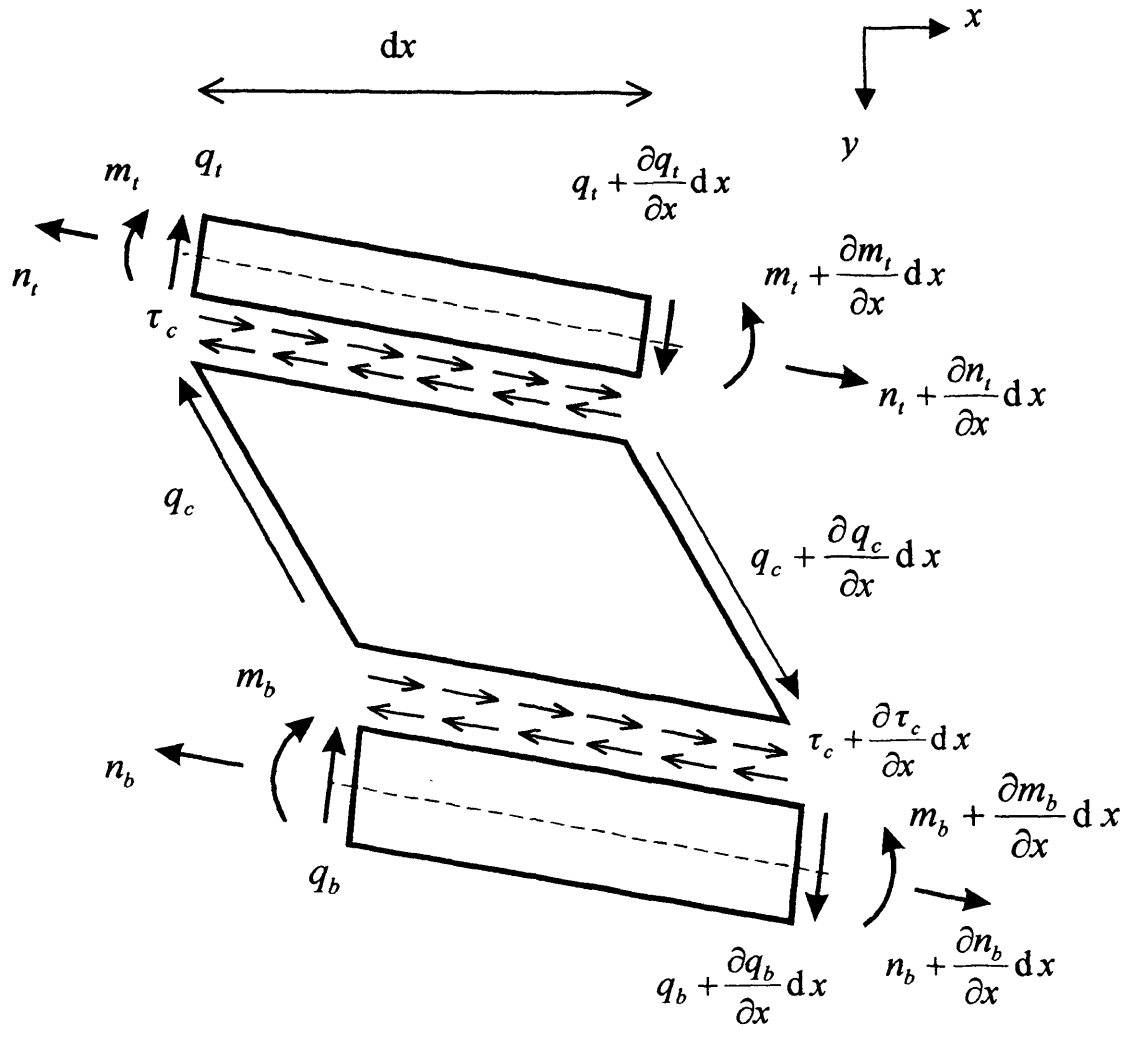

Figure 5.2: Inter-element forces and moments and component member stresses on a typical elemental length of a sandwich beam.

As it is assumed that the transverse flexural inertia is predominant and in the free vibrational analysis it is the only external vertical force, the equation of vertical equilibrium is

$$q' = \mu \ddot{w} \tag{5.6}$$

5.2.3 Force-displacement relations

Figure 5.3 shows the positive sense of the displacements experienced by a typical elemental length of a member at some instant during the motion. $w' = \psi$ is the slope of

the beam's neutral axis and u_t and u_b are the mid-layer longitudinal displacements of the top and bottom faceplates, respectively. γ_c is the shearing strain of the core and φ is the average rotation of the beam's cross-section.

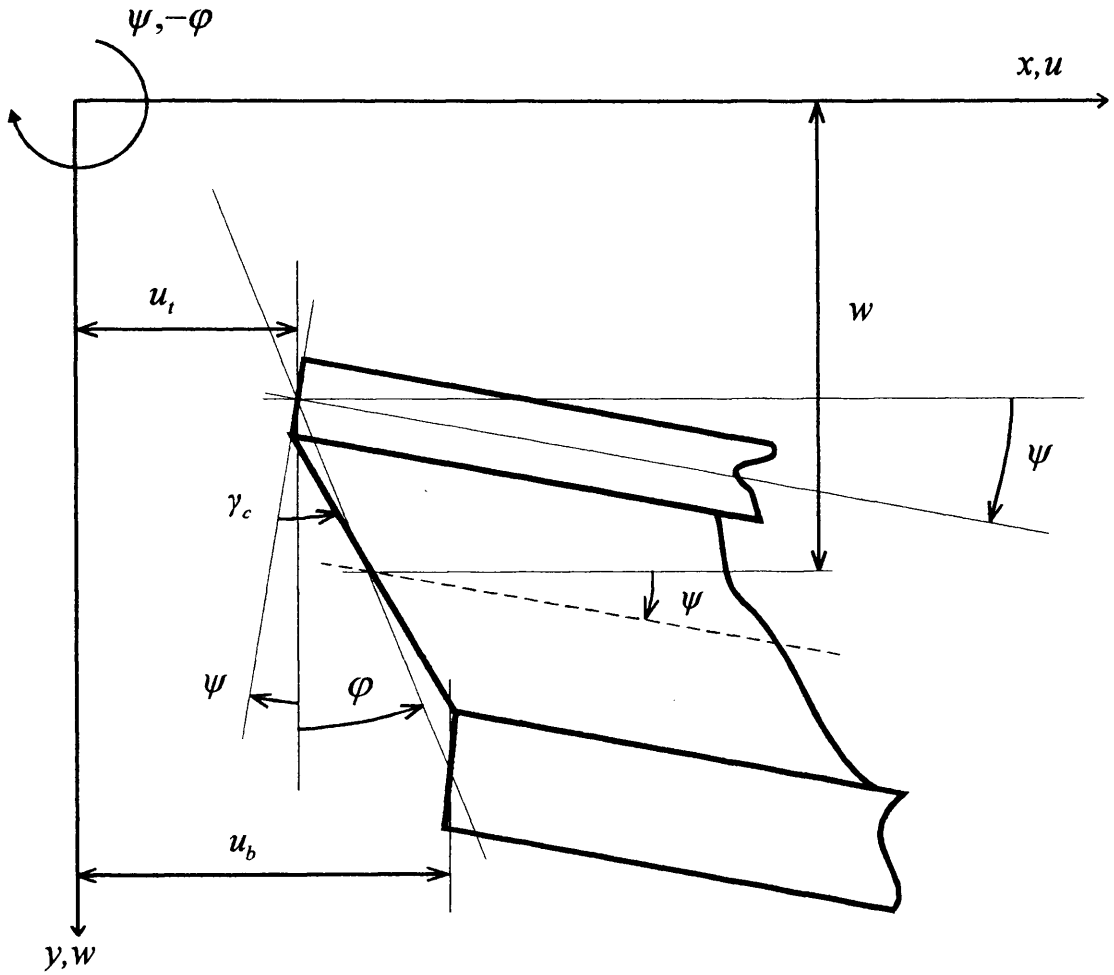

Figure 5.3: Positive displacements on a typical elemental length of a sandwich beam of unit width.

The necessary force displacement relationships for axial extension and bending of the faceplates are

$$n_i = E_i t_i u_i' = K_i u_i' \quad \text{and} \quad m_i = -E_i I_i w'' = -E_i I_i \psi' \qquad (i = t, b) \tag{5.7a,b}$$

respectively, where $K_i = E_i t_i$ and $E_i I_i$ are the axial and flexural rigidities per unit width of faceplate i, respectively, and u_i' is the average normal strain of the faceplate i. Eqs. (5.7a) and (5.1b) can be combined to give the relationship between normal strain in the two faceplates as

$$u_b' = -\frac{K_t}{K_b} u_t' \tag{5.8}$$

Also from Figure 5.3 it is clear that the shearing strain in the core may be written as

$$\gamma_c = \frac{\partial w}{\partial x} + \frac{\partial u}{\partial y} = \frac{\partial w}{\partial x} + \frac{u_3 - u_2}{t_c} \tag{5.9}$$

where u is the longitudinal displacement of any point in the core of thickness t_c and u_2 and u_3 are the longitudinal displacements of the interface between the core and the top and bottom faceplates of thickness t_t and t_b, respectively, and can be given as

$$u_2 = u_t - \frac{\partial w}{\partial x}(\frac{t_t}{2}) \quad \text{and} \quad u_3 = u_b + \frac{\partial w}{\partial x}(\frac{t_b}{2}) \tag{5.10}$$

Hence, substituting Eq. (5.10) in Eq. (5.9) gives

$$\gamma_c = \frac{\partial w}{\partial x} + \frac{u_b - u_t}{t_c} + \frac{\partial w}{\partial x}(\frac{t_b + t_t}{2t_c}) = \frac{1}{t_c}[t_c \frac{\partial w}{\partial x} + \frac{\partial w}{\partial x}(\frac{t_b + t_t}{2}) + (u_b - u_t)] \tag{5.11a}$$

or

$$\gamma_c = \frac{1}{t_c}[\frac{\partial w}{\partial x}(t_c + \frac{t_b + t_t}{2}) + (u_b - u_t)] = \frac{d}{t_c}(\frac{\partial w}{\partial x} + \frac{u_b - u_t}{d}) \tag{5.11b}$$

Now, the core shear stress/strain relationship is given by

$$\tau_c = G_c \gamma_c = G_c d(w' + \varphi)/t_c \tag{5.12}$$

where

$$\varphi = (u_b - u_t)/d \tag{5.13}$$

is the average rotation of the beam's cross-section and τ_c and G_c are the shear stress and shear modulus related to the core material, respectively. As the shear coefficient of the core, which is usually defined as the ratio of average shear stress on a section to shear stress at the neutral axis, in most of the cases is nearly 1 (Rao and Nakra 1970), its effect can be ignored. Alternatively it can be included in G_c which then becomes an effective core shear modulus. Now, substituting Eq. (5.8) into the first differential of Eq. (5.13) gives

$$\varphi' = -\frac{K_t u_t'}{\varsigma d} = -\frac{n_t}{\varsigma d} \tag{5.14}$$

where

$$\varsigma = K_t K_b / (K_t + K_b) \tag{5.15}$$

Finally, horizontal equilibrium of each faceplate along with stress compatibility at the core face/plate interface (Figure 5.2) gives

$$n_t' = -n_b' = -n' = -\tau_c \tag{5.16a}$$

Substituting Eq. (5.14) into Eq. (5.16a) gives the core shear stress in terms of the average rotation of the beam's cross-section as

$$\tau_c = \varsigma \varphi'' d \tag{5.16b}$$

5.3 DERIVATION OF THE GOVERNING DIFFERENTIAL EQUATIONS OF MOTION

5.3.2 Equilibrium method

The first differential equation of motion can be obtained by combining Eqs. (5.4) and (5.6) and using Eqs. (5.5) and (5.14) as

$$\mu \ddot{w} + \frac{w''''}{\kappa} - \varsigma \varphi''' d^2 = 0 \tag{5.17}$$

where

$$\kappa = 1/\left(E_t I_t + E_b I_b\right) \tag{5.18}$$

Substituting Eqs (5.12) into (5.16b) gives the second equation as

$$\frac{G_c d}{t_c} w' + \frac{G_c d}{t_c} \varphi - \varsigma \, \varphi'' d = 0 \tag{5.19}$$

Attention is now confined to harmonic motion in which the time dependent terms are related to ω, the circular frequency, by

$$f(x,t) = F(x)\, e^{i\omega t} \tag{5.20}$$

and the upper case characters refer to the amplitude of the equivalent time dependent quantity.

Hence, using Eq. (5.20), the partial differential equations of Eqs. (5.17) and (5.19) can be presented as a system of linear differential equations in the following way

$$\begin{bmatrix} \frac{D_x^4}{\kappa} - \mu\omega^2 & -\varsigma d^2 D_x^3 \\ \frac{G_c d}{t_c} D_x & \frac{G_c d}{t_c} - \varsigma\, d\, D_x^2 \end{bmatrix} \begin{Bmatrix} W \\ \Phi \end{Bmatrix} = 0 \tag{5.21}$$

where D_x is the operator $\mathrm{d}/\mathrm{d}x$. The determinant of the matrix operator yields the linear, sixth order, governing differential equation as

$$[D_x^6 - \frac{G_c}{\varsigma\, t_c}\left(1+\kappa\,\varsigma\, d^2\right) D_x^4 - \mu\,\omega^2\kappa\,(D_x^2 - \frac{G_c}{\varsigma\, t_c})]V = 0 \tag{5.22a}$$

and V can be either of the variables W or Φ. Finally, writing Eq. (5.22a) in terms of the non-dimensional parameter ξ gives

$$[D^6 - \alpha(1+\beta)\, D^4 - \lambda\,(D^2 - \alpha)\,]\, V = 0 \tag{5.22b}$$

where

$$\alpha = G_c L^2 / \varsigma\, t_c \;\; ; \;\; \beta = \kappa\,\varsigma\, d^2 \;\; ; \;\; \lambda = \mu\,\omega^2\kappa\, L^4 \;\; ; \;\; \xi = x/L \tag{5.23}$$

and D is the operator $\mathrm{d}/\mathrm{d}\xi$ and L is the member length.

5.3.3 *Energy approach*

In the preceding section, the free vibration of a sandwich beam has been represented by a differential equation (5.22) derived from the equilibrium of internal and inertial forces via Newton's second law of motion. This method is usually referred to as the Newtonian approach. An alternative approach, which avoids the vectorial equations of equilibrium, is to make use of scalar quantities in the variational form of Hamilton's principle. In this approach, the internal and inertial forces are not explicitly involved. Instead, variations of their potential and kinetic energy terms are utilised. The potential energy of the internal forces is the strain energy and is equal to the negative work of the internal forces. Kinetic

energy is due to the inertial forces. For a conservative system, Hamilton's principle states that the first time-variation of the difference in kinetic and potential energies over any time interval t_1 to t_2 equals zero.

5.3.3.1 Potential energy

Potential energy of a three-layer sandwich beam of length L consists of three parts.

5.3.3.1.1 Strain energy of the two faces in axial deformation

The strain energy of the top and bottom faces in axial deformation is given by

$$U_1 = \int_0^L \left(\frac{1}{2} n_t \varepsilon_t + \frac{1}{2} n_b \varepsilon_b \right) \mathrm{d}x \tag{5.24}$$

where $\varepsilon_i = u_i'$ and n_i is defined in Eq. (5.7a). Using Eqs. (5.8) and (5.14), Eq. (5.24) can be rewritten as

$$U_1 = \int_0^L \left(\frac{\varsigma d^2}{2} \varphi'^2 \right) \mathrm{d}x \tag{5.25}$$

5.3.3.1.2 Strain energy of the two faces in bending deformation

The bending strain energy of the top and bottom faces may be determined from Eqs (5.3b), (5.7b) and (5.18) as

$$U_2 = \int_0^L \left(-\frac{1}{2} m w'' \right) \mathrm{d}x \tag{5.26}$$

where

$$m = -\frac{w''}{\kappa} \tag{5.27}$$

Eq. (5.26) can therefore be written as

$$U_2 = \int_0^L \frac{w''^2}{2\kappa} \mathrm{d}x \tag{5.28}$$

5.3.3.1.3 Strain energy of the core in shear deformation

The strain energy of the core due to shear is

$$U_3 = \int_0^L \left(\frac{1}{2} q_c \gamma_c\right) \mathrm{d}x \tag{5.29}$$

where

$$q_c = \tau_c t_c = G_c t_c \gamma_c = S_c \gamma_c \tag{5.30}$$

where $S_c = G_c t_c$ is the shear rigidity of the core. Using Eq. (5.12), we have

$$\begin{aligned} q_c \gamma_c = S_c \gamma_c^2 &= S_c [\frac{d}{t_c}(w' + \varphi)]^2 \\ &= \hat{S}_c \ (w'^2 + \varphi^2 + 2w'\varphi) \end{aligned} \tag{5.31}$$

where $\hat{S}_c = \frac{G_c d^2}{t_c}$. Now Eq. (5.29) can be rewritten as

$$U_3 = \int_0^L [\frac{\hat{S}_c}{2}(w'^2 + \varphi^2 + 2w'\varphi)] \mathrm{d}x \tag{5.32}$$

Thus the total potential energy will be the sum of Eqs. (5.25), (5.28) and (5.32) which may be written as

$$U = \int_0^L [\frac{\hat{S}_c}{2}(w'^2 + \varphi^2 + 2w'\varphi) + \frac{\varsigma d^2}{2}\varphi'^2 + \frac{w''^2}{2\kappa}]\mathrm{d}x \tag{5.33}$$

5.3.3.2 *Kinetic energy*

The full transverse inertia of a beam of length L is

$$T = \int_0^L \left(\frac{1}{2}\mu\dot{w}^2\right)\mathrm{d}x \tag{5.34}$$

5.3.3.3 *Application of Hamilton's principle*

Hamilton's principle states that " *of all the paths of admissible configurations that the body can take as it goes from configuration 1 at time* t_1 *to configuration 2 at time* t_2, *the path that satisfies Newton's second law at each instant during the interval is the path that extremizes the time integral of the Lagrangian during the interval.*" Hence, for a conservative system, the first time-variation of the Lagrangian (i.e. the difference in kinetic and potential energies) over any time interval t_1 to t_2, with respect to all independent variables of the system, gives the governing differential equations of motion, i.e.

$$\delta^{(1)}\phi = \delta^{(1)}\int_{t_1}^{t_2} L\mathrm{d}t = \delta^{(1)}\int_{t_1}^{t_2}(T-U)\mathrm{d}t = \delta^{(1)}\int_{t_1}^{t_2}\int_0^L F\,\mathrm{d}x\,\mathrm{d}t = 0 \tag{5.35}$$

in which the Lagrangian, $L = T - U$, has bean replaced by the functional $\int_0^L F dx$, where the function F can be identified from Eqs. (5.33) and (5.34) as

$$F = \frac{1}{2}\mu\dot{w}^2 - \frac{\hat{S}_c}{2}(w'^2 + \varphi^2 + 2w'\varphi) - \frac{\varsigma d^2}{2}\varphi'^2 - \frac{w''^2}{2\kappa} \tag{5.36}$$

Eq.(5.35) leads to the following Euler-Lagrange equations as

$$\left.\begin{aligned} &\frac{\partial F}{\partial w} - \frac{\partial}{\partial x}\frac{\partial F}{\partial w'} - \frac{\partial}{\partial t}\frac{\partial F}{\partial \dot{w}} + \frac{\partial^2}{\partial x^2}\frac{\partial F}{\partial w''} = 0 \\ &\frac{\partial F}{\partial \varphi} - \frac{\partial}{\partial x}\frac{\partial F}{\partial \varphi'} = 0 \end{aligned}\right\} \tag{5.37}$$

and the possible boundary conditions at the ends of the member as

$$\frac{\partial F}{\partial w''} = 0 \qquad \text{or} \qquad w' = 0 \tag{5.38a,b}$$

$$\frac{\partial}{\partial x}\frac{\partial F}{\partial w''} - \frac{\partial F}{\partial w'} = 0 \qquad \text{or} \qquad w = 0 \tag{5.39a,b}$$

$$\frac{\partial F}{\partial \varphi'} = 0 \qquad \text{or} \qquad \varphi = 0 \tag{5.40a,b}$$

Eqs. (5.38a), (5.39a) and (5.40a) are the natural boundary conditions while Eqs. (5.38b), (5.39b) and (5.40b) give the kinematic boundary conditions at any end of the element.

Now, imposing Eqs. (5.37) on Eq. (5.36) gives us the required partial differential equations of motion as

$$\left.\begin{aligned} &0 - \frac{\partial}{\partial x}(-\hat{S}_c w' - \hat{S}_c\varphi) - \frac{\partial}{\partial t}(\mu\dot{w}) + \frac{\partial^2}{\partial x^2}(-\frac{w''}{\kappa}) = 0 \\ &(-\hat{S}_c w' - \hat{S}_c\varphi) - \frac{\partial}{\partial x}(-\varsigma d^2\varphi') = 0 \end{aligned}\right\} \tag{5.41}$$

The natural boundary conditions are also exactly the expressions for bending moment, shear force and couple due to the axial forces in faceplates. Thus

$$-\frac{w''}{\kappa} = m = 0 \tag{5.42}$$

$$\frac{\partial}{\partial x}(-\frac{w''}{\kappa}) + \hat{S}_c(w' + \varphi) = q = 0 \tag{5.43}$$

$$-\varsigma d^2 \varphi' = \overline{m} = 0 \tag{5.44}$$

If attention is now confined to harmonic motion as defined by Eq. (5.20), Eqs. (5.41) can be written as the following ordinary differential equations

$$\left.\begin{aligned} -\frac{W''''}{\kappa} + \hat{S}_c W'' + \mu\omega^2 W + \hat{S}_c \Phi' = 0 \\ -\hat{S}_c W' - \hat{S}_c \Phi + \varsigma d^2 \Phi'' = 0 \end{aligned}\right\} \tag{5.45}$$

Eqs. (5.45) can be presented in matrix form as

$$\begin{bmatrix} \frac{D_x^4}{\kappa} - \hat{S}_c D_x^2 - \mu\omega^2 & -\hat{S}_c D_x \\ -\hat{S}_c D_x & -\hat{S}_c + d^2 \varsigma D_x^2 \end{bmatrix} \begin{Bmatrix} W \\ \Phi \end{Bmatrix} = 0 \tag{5.46}$$

where $D_x = \mathrm{d}/\mathrm{d}x$ is the differential operator.

The determinant of the matrix operator yields the linear, sixth order, governing differential equation in terms of the non-dimensional parameter ξ (Eq. (5.23)) as

$$[D^6 - \alpha(1+\beta)D^4 - \lambda(D^2 - \alpha)]V = 0 \tag{5.47}$$

where D is the operator $\mathrm{d}/\mathrm{d}\xi$ and L is the member length. The other coefficients are defined in Eq. (5.23) and V can be either of the independent variables W or Φ. It should be noted that Eq. (5.46) differs from Eq. (5.21) but that Eq. (5.47) is the same as Eq. (5.22b). The reason for this is that the matrix operator of Eq. (5.21) can be determined from the matrix operator of Eq. (5.41) using matrix operations that don't change its determinant, as follows:

i) Multiply the second row of Eq. (5.46) by (- d) to give the second row of Eq. (5.21)

ii) Differentiate the second row of Eq. (5.46) once, and then subtract it from the first row of Eq. (5.46) to give the first row of Eq. (5.21).

5.4 DYNAMIC STIFFNESS FORMULATION

The dynamic stiffness formulation that accounts in an exact way for the uniform distribution of mass in a member offers two considerable advantages. The first of these is the opportunity to exploit the powerful modelling features of the stiffness method of analysis. For example, continuous beams with step changes in member properties are easily analysed and it is straightforward to incorporate translational and rotational inertia of nodal masses, spring support stiffness and non-classical boundary conditions. The second advantage is that the formulation is exact and results in an idealisation containing the minimum number of elements, while leaving invariant the accuracy to which any particular natural frequency can be calculated. This can be important for higher natural frequencies and should be contrasted with traditional finite elements in which the accuracy is sensitive to the idealisation. However, such a formulation is intractable and necessitates the solution of a transcendental eigenvalue problem, which is resolved herein by adopting the Wittrick-Williams algorithm (Wittrick and Williams 1971a) that enables any required natural frequency to be converged upon to any required accuracy with the certain knowledge that none have been missed.

The dynamic stiffness matrix is exact, since it is a closed form solution of the governing differential equations and therefore satisfies inter-element compatibility and all the boundary conditions. This is in contrast to the traditional finite element technique that requires the assumption of an element shape function that is invariably approximate. The dynamic stiffness method relates the harmonically varying forces to the harmonically varying displacements. Hence, after deriving the governing differential equations of motion Eq. (5.47), the next step is to solve for the harmonically varying displacement field.

5.4.2 Solution of the governing differential equation of motion

Eq. (5.47) is a linear differential equation with constant coefficients and its solution can be sought in the following form

$$V = \sum_{j=1}^{6} \overline{C}_{ij}\zeta_j \quad \text{where} \qquad \zeta_j = e^{\eta_j \xi} \tag{5.48a,b}$$

η_j are the roots of the characteristic equation stemming from Eq. (5.47) and the $\overline{C}_{ij}$ are arbitrary constants where, for convenience in developing the work that follows, i is an assigned integer that defines a set of j arbitrary constants, e.g. $\overline{C}_{1j} = \overline{A}_j$, $\overline{C}_{2j} = \overline{B}_j$ etc., where $\overline{A}_j$, $\overline{B}_j$ are independent sets of arbitrary constants.

The η_j can now be determined as the roots of

$$\eta^6 - \alpha(1+\beta)\eta^4 - \lambda\,(\eta^2 - \alpha) = 0 \tag{5.49}$$

Eq. (5.49) is a cubic equation in

$$z = \eta^2 \tag{5.50}$$

as

$$z^3 - \alpha(1+\beta)z^2 - \lambda z - \lambda\alpha = 0 \tag{5.51}$$

Eq. (5.51) can be solved by any appropriate method such as that described in Appendix C, where its three roots could be real, imaginary or complex. The six roots of Eq. (5.49) then follow automatically. These six roots η_j, which can also be real, imaginary or complex, define V (W or Φ) and the other necessary quantities for the stiffness formulation of the problem i.e. the displacements W, Ψ and Φ and the corresponding forces Q, M and $\overline{M}$ which provide the unique one-to-one relationship between displacements and forces.

To express all required quantities in terms of W only, it is necessary to identify the relationship between the independent variables W and Φ. Thus Eq.(5.40), by considering Eq (5.20) and the non-dimensional parameter ξ, gives

$$\Phi = [\, D^5 - \alpha\beta\, D^3 - (\alpha^2\beta + \lambda)D]\, W / \alpha^2\beta L \tag{5.52}$$

Furthermore, substituting Eqs. (5.20) and (5.52) into Eqs. (5.42)–(5.44) and considering once more the non-dimensional parameter ξ, gives the other necessary quantities to formulate the required stiffness relationship as

$$M = -D^2 W / \kappa L^2 \tag{5.53}$$

$$Q = [D^5 - \alpha(1+\beta)D^3 - \lambda D\,]W / \alpha\,\kappa L^3 \tag{5.54}$$

$$\overline{M} = -\,[D^4 - \alpha\beta\, D^2 - \lambda\,]W / \alpha\,\kappa L^2 \tag{5.55}$$

It is also clear that

$$\Psi = DW / L \tag{5.56}$$

Now, the η_j define W, which may be substituted into Eqs. (5.48) to (5.52) to yield the following results

$$\left.\begin{aligned} W &= \sum_{j=1}^{6} H_{1j} C_j \zeta_j \qquad & Q &= \sum_{j=1}^{6} H_{4j} C_j \zeta_j \\ \Psi &= \sum_{j=1}^{6} H_{2j} C_j \zeta_j \qquad & M &= \sum_{j=1}^{6} H_{5j} C_j \zeta_j \\ \Phi &= \sum_{j=1}^{6} H_{3j} C_j \zeta_j \qquad & \overline{M} &= \sum_{j=1}^{6} H_{6j} C_j \zeta_j \end{aligned}\right\} \tag{5.57}$$

where $H_{ij} C_j = \overline{C}_{ij}$, such that C_j is common to all the equations and H_{ij} is the relational constant.

Noting that one of the H_{ij} is arbitrary, it is convenient to set $H_{1j} = 1$, which yields the following relationships between the H_{ij} of Eqs. (5.57)

$$\left.\begin{aligned} H_{1j} &= 1 & H_{4j} &= H_{2j}(H_{5j} - H_{6j}) \\ H_{2j} &= \eta_j / L & H_{5j} &= -H_{2j}^2 / \kappa \\ H_{3j} &= -H_{2j}(1 + H_{6j}\kappa L^2 / \alpha\beta) & H_{6j} &= -(\eta_j^4 - \alpha\beta\eta_j^2 - \lambda)/\alpha\kappa L^2 \end{aligned}\right\} \quad (5.58)$$

5.4.3 Transformation between local and member co-ordinate systems

All the equations developed so far have been based on the forces and displacements in the local co-ordinate system shown in Figure 5.4(a). The stiffness formulation requires all nodal forces and displacements to be represented in the member co-ordinate system. Hence, the nodal forces and displacements in the local co-ordinate system are now transformed to the member co-ordinate system of Figure 5.4(b).

The relationship between the forces and displacements in these two co-ordinate systems can be obtained by comparing on Figures 5.4(a) and (b). This is equivalent to imposing the conditions of Eq. (5.59) onto Eqs. (5.52) to (5.56).

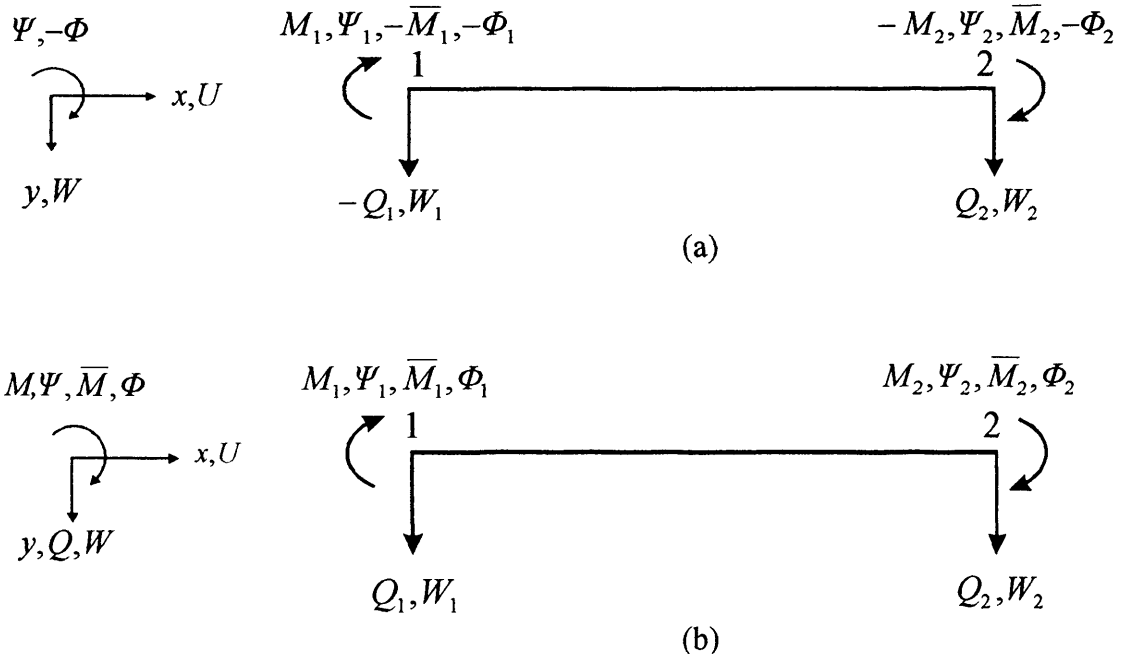

Figure 5.4: Nodal forces and displacements a) in local coordinates, b) in member coordinates.

$$\begin{aligned} &\text{At } \xi = 0 \ : W = W_1,\ \Psi = \Psi_1,\ \Phi = -\Phi_1,\ Q = -Q_1,\ M = M_1,\ \overline{M} = -\overline{M}_1 \\ &\text{At } \xi = 1 \ : W = W_2,\ \Psi = \Psi_2,\ \Phi = -\Phi_2,\ Q = Q_2,\ M = -M_2,\ \overline{M} = \overline{M}_2 \end{aligned} \tag{5.59}$$

5.4.4 Dynamic stiffness matrix formulation

The dynamic stiffness matrix relates the forces to the displacements at the two end nodes of a member as

$$\mathbf{p} = \mathbf{k}\mathbf{d} \tag{5.60}$$

where

$$\mathbf{d} = \begin{bmatrix} W_1 \\ \Psi_1 \\ \Phi_1 \\ W_2 \\ \Psi_2 \\ \Phi_2 \end{bmatrix}, \qquad \mathbf{p} = \begin{bmatrix} Q_1 \\ M_1 \\ \overline{M}_1 \\ Q_2 \\ M_2 \\ \overline{M}_2 \end{bmatrix} \tag{5.61}$$

and $\mathbf{k}$ is the six by six dynamic stiffness matrix. As a result of Eq. (5.57), all of the elements of $\mathbf{d}$ and $\mathbf{p}$ are related to the coefficient vector $\mathbf{C}$ through the matrices $\mathbf{S}$ and $\mathbf{S}^*$ by

$$\mathbf{d} = \mathbf{S}\mathbf{C} \qquad \text{and} \qquad \mathbf{p} = \mathbf{S}^*\mathbf{C} \tag{5.62a,b}$$

where

$$\mathbf{C} = \begin{bmatrix} C_1 \\ C_2 \\ C_3 \\ C_4 \\ C_5 \\ C_6 \end{bmatrix} \tag{5.63}$$

and s_{ij} and s_{ij}^*, the elements of $\mathbf{S}$ and $\mathbf{S}^*$, respectively, are as follows

$$
\begin{aligned}
&s_{1j}=H_{1j} \quad ; \quad s_{2j}=H_{2j} \quad ; \quad s_{3j}=-H_{3j} \\
&s_{4j}=H_{1j}\chi_j \; ; \quad s_{5j}=H_{2j}\chi_j \; ; \quad s_{6j}=-H_{3j}\chi_j \\
&s^*_{1j}=-H_{4j} \quad ; \quad s^*_{2j}=H_{5j} \quad ; \quad s^*_{3j}=-H_{6j} \\
&s^*_{4j}=H_{4j}\chi_j \quad ; \quad s^*_{5j}=-H_{5j}\chi_j \; ; \quad s^*_{6j}=H_{6j}\chi_j \qquad (j=1,2,\ldots 6)
\end{aligned} \tag{5.64}
$$

$$\chi_j = e^{\eta_j}$$

where their subscripts correspond to row and column co-ordinates in the usual way.

To set up the required dynamic stiffness matrix, **k**, it is necessary to eliminate the coefficient vector **C** through the following steps

$$\mathbf{C}=\mathbf{S}^{-1}\mathbf{d} \tag{5.65}$$

therefore

$$\mathbf{p}=\mathbf{S}^{*}\mathbf{S}^{-1}\mathbf{d} \tag{5.66}$$

and finally

$$\mathbf{k}=\mathbf{S}^{*}\mathbf{S}^{-1} \tag{5.67}$$

The dynamic stiffness matrix for the overall structure can now be assembled from the element matrices in the usual way. The use of 'exact' finite elements leads to an idealisation containing the minimum number of elements, while leaving invariant the accuracy to which any particular natural frequency can be converged upon. This can be important for higher natural frequencies and should be contrasted with traditional finite elements in which the accuracy is sensitive to the idealisation. Once the required natural frequencies have been determined, the corresponding mode shapes can be retrieved by any reliable method, such as described in reference (Howson 1979). In the next section, the method for converging with certainty on the required natural frequencies is described.

5.5 CONVERGING ON THE NATURAL FREQUENCIES

The dynamic structure stiffness matrix, **K**, when assembled from the element matrices, yields the required natural frequencies as solutions of the equation

$$\mathbf{K}\,\mathbf{D} = \mathbf{0} \tag{5.68}$$

where **D** is the vector of amplitudes of the harmonically varying nodal displacements and **K** is a function of ω, the circular frequency. In most cases the required natural frequencies correspond to $|\mathbf{K}|$, the determinant of **K**, being equal to zero. Traditionally the required values have been ascertained by merely tracking the value of $|\mathbf{K}|$ and noting the value of ω corresponding to $|\mathbf{K}| = \mathbf{0}$. However, when **K** is developed from exact member theory the determinant is a highly irregular, transcendental function of ω. Additionally, several natural frequencies may be close together or coincident, while others may exceptionally correspond to $\mathbf{D} = \mathbf{0}$. Thus any trial and error method which involves computing $|\mathbf{K}|$ and noting when it changes sign through zero, can miss roots. This danger can be completely overcome by use of the Wittrick-Williams algorithm (Wittrick and Williams 1971a) which indeed determines how many natural frequencies lie below a specified trial frequency. The algorithm states that

$$J = J_0 + s\{\mathbf{K}\} \tag{5.69}$$

where J is the number of natural frequencies of the structure exceeded by some trial frequency, ω^*, J_0 is the number of natural frequencies which would still be exceeded if all the elements were clamped at their ends so as to make $\mathbf{D} = \mathbf{0}$, and $s\{\mathbf{K}\}$ is the sign count of the matrix **K**. $s\{\mathbf{K}\}$ is defined in reference (Wittrick and Williams 1971a) and is equal to the number of negative elements on the leading diagonal of the upper triangular matrix obtained from **K**, when $\omega = \omega^*$, by the standard form of Gauss elimination without row interchanges.

The knowledge of J corresponding to any trial frequency makes it possible to develop a method for converging upon any required natural frequency to any desired accuracy. However, while $s\{\mathbf{K}\}$ is easily computed, the value of J_0 is more difficult to determine and is dealt with in next section.

5.5.2 Determination of J_0

From the definition of J_0 it can be seen that

$$J_0 = \sum J_m \tag{5.70}$$

where J_m is the number of natural frequencies of a component element, with its ends clamped, which have been exceeded by ω^*, and the summation extends over all such elements. In some cases it is possible to determine the value of J_m for the element type symbolically, using a direct approach (Howson 1979). However, this is impractical in the present case due to the algebraic complexity of the expressions. Instead, the same result is achieved by an argument based on Eq. (5.69) which was originally put forward by Howson and Williams (Howson and Williams 1973).

Consider an element, which has been isolated from the remainder of the structure by clamping its ends. Unfortunately, this structure cannot be solved easily. We therefore seek to establish a different set of boundary conditions that admit a simple symbolic solution and which enable solutions to the clamped ended case to be deduced. This is often most easily achieved by imposing simple supports which, in this case, permit rotation and relative motion of the faceplates, i.e. Ψ and Φ respectively, but prevent lateral displacement W.

Let the stiffness matrix for this structure be $\mathbf{k}^{ss}$, then the number of roots exceeded by ω^* is given by equation (5.69) and the arguments above as

$$J_{ss} = J_m + s\{\mathbf{k}^{ss}\} \tag{5.71}$$

where J_{ss} is the number of natural frequencies that lie below the trial frequency for the element with simple supports. It then follows directly that

$$J_m = J_{ss} - s\{\mathbf{k}^{ss}\} \tag{5.72}$$

Once more $\mathbf{k}^{ss}$, and hence $s\{\mathbf{k}^{ss}\}$, is readily obtained, this time from Eq. (5.67). J_{ss} is slightly more difficult, but relates to the element with boundary conditions that yield a simple exact solution, as shown below.

For the simply supported case, the boundary conditions are defined by

$$M = \overline{M} = W = 0 \tag{5.73}$$

These conditions are satisfied by assuming solutions of the form

$$W = B\sin\ n\pi\xi \qquad (n = 1,2,3,\ldots) \tag{5.74}$$

and B is a constant. Substituting Eq. (5.74) and its derivatives into Eq. (5.47) yields the equation of motion as

$$[n^6\pi^6 + \alpha(1+\beta)\, n^4\pi^4 - \lambda\,(n^2\pi^2 + \alpha)]B = 0 \tag{5.75}$$

which, for non-trivial solutions yields

$$\omega_n = n^2\pi^2\left\{[n^2\pi^2 + \alpha(1+\beta)]/\mu\kappa L^4(n^2\pi^2 + \alpha)\right\}^{\frac{1}{2}} \tag{5.76}$$

Hence J_{ss} is given by the number of positive values of ω_n that lie below the trial frequency, ω^*.

Thus, substituting Eq. (5.72) in to Eq. (5.70) gives

$$J_0 = \Sigma\left(J_{ss} - s\left\{\mathbf{k}^{ss}\right\}\right) \tag{5.77}$$

The required value of J then follows from Eq. (5.69).

5.6 NUMERICAL RESULTS AND COMPARISON WITH PREVIOUS WORK

Four examples are now given to validate the theory and indicate its range of application. The first three examples compare results obtained by a number of authors for a simply supported, cantilevered and fixed ended beam, respectively, which have been widely used as test examples. The final example gives only the results of this study for a simple three span continuous beam with various combinations of parameters and support conditions. It can also be used to demonstrate how the conventional method of determinant tracking to find natural frequencies can miss roots.

Example 5.1: A simply supported sandwich beam with identical faceplates is analysed. The material and geometric properties of the beam are

$E_t = E_b = 68.9\,\text{GPa}$, $G = 82.68\,\text{MPa}$, $\mu_i = \rho_i t_i$ where $i = t, b$ and c and ρ denotes material density, $\rho_t = \rho_b = 2680\,\text{kg/m}^3$, $\rho_c = 32.8\,\text{kg/m}^3$, $t_t = t_b = 0.4572\,\text{mm}$, $t_c = 12.7\,\text{mm}$, $L = 0.9144\,\text{m}$.

The results obtained by a number of authors together with the current theory are given in Table 5.1. Also the first five mode shapes of the beam are illustrated in Figure 5.5. The difference between the graph of beam slope Ψ and that of average rotation of the beam's cross-section Φ relates to the shearing strain γ, which according to Figure 5.5 is negligible for the first mode, but becomes substantial for higher modes. This figure also shows that the two graphs are in-phase and therefore the shearing strain can be regarded as a constant fraction of the beam's slope.

This beam is widely used by numerous authors to compare their results with those originally presented by Mead and Sivakumuran (Mead and Sivakumuran 1966). Unfortunately, Mead (Mead and Sivakumuran 1966) provided insufficient data to calculate the mass density of the beam. However, Table I of reference (Mead and Sivakumuran 1966) notes that the natural frequencies are calculated from equation (32) of reference (Mead and Sivakumuran 1966) which can be expressed as follows

$$f_n = \frac{\pi}{2}\frac{n^2}{L^2}\sqrt{\frac{(EI)_t}{\mu}}\frac{1}{\sqrt{1+(EI)_t n^2\pi^2 d/G(d+t)L^2}} \tag{5.78}$$

Table 5.1: Comparative results for the first ten natural frequencies (Hz) of the simply supported sandwich beam of Example 5.1.

Freq. No.	Current theory	Allen, 1969; Rao, 1978*	Mead, 1966**		Ahmed, 1972	Ahmed, 1971	Sakiyama, 1996b	Rao, 2001	Marur, 1996
			Eq. (32)	Table I					
1	57.1358	57.1358	57.1352	56.028	55.5	57.5	56.159	57.068	57.041
2	219.585	219.585	219.575	-	-	-	215.82	218.569	218.361
3	465.172	465.172	465.129	457.12	451	467	457.22	460.925	460.754
4	768.177	768.177	768.058	-	-	-	755.05	757.642	758.692
5	1106.68	1106.68	1106.43	1090.26	1073	1111	1087.9	1086.955	1097.055
6	1465.10	1465.10	1464.65	-	-	-	1440.3	1433.920	1457.064
7	1833.55	1833.55	1832.82	1809.8	1779	1842	1802.7	1789.345	1849.380
8	2206.19	2206.19	2205.09	-	-	-	2169.8	2147.969	2275.916
9	2579.79	2579.79	2578.22	2549.5	2510	2594	2538.2	-	2562
10	2952.65	2952.65	2950.52	-	-	-	2906.2	-	-

*Results in column three are generated using Eq. (5.82) or Eq. (5.76) that are equivalents to formulas in cited references

**Column five contains the results that were presented by Mead in Table I of reference (Mead and Sivakumuran 1966) and which were calculated using Eq. (32) of the same paper. Unfortunately, Mead provided insufficient data to confirm these results. Thus Eq. (32) (equivalent to Eq. (5.78) in the current notation) was used to calculate the results presented in column four from the data used to determine the results in columns two and three.

where f_n(Hz) is the n^{th} natural frequency of the simply supported sandwich beam with identical faceplates of thickness t and span length L. E, G and μ are the faceplates' elastic modulus, the core's shear modulus and the beam's mass/unit length, respectively. $(EI)_t$ denotes the total bending stiffness and for a symmetric sandwich beam of unit width I_t is given by

$$I_t = \frac{t^3}{6} + \frac{t(d+t)^2}{2} \tag{5.79}$$

Eq. (5.78) was then used to determine the results given in column 4 of Table 1 using the ρ values given above.

The theory behind the Eq. (5.78) has not been given in reference (Mead and Sivakumuran 1966), but an almost identical frequency equation can be constructed from Eq. (4.18) of reference (Allen 1969), which is based on an energy approach. Allen (Allen 1969) considers a simply supported sandwich beam with an axial end-load and a sinusoidally

distributed transverse load for which the amplitude of the transverse displacements, w, is defined. Now if we use the same approach, but assuming no axial load and that the transverse load is replaced by a transverse inertia of intensity

$$q(x,t) = -\mu \ddot{w}(x,t) = \mu \omega^2 w(x,t) \tag{5.80}$$

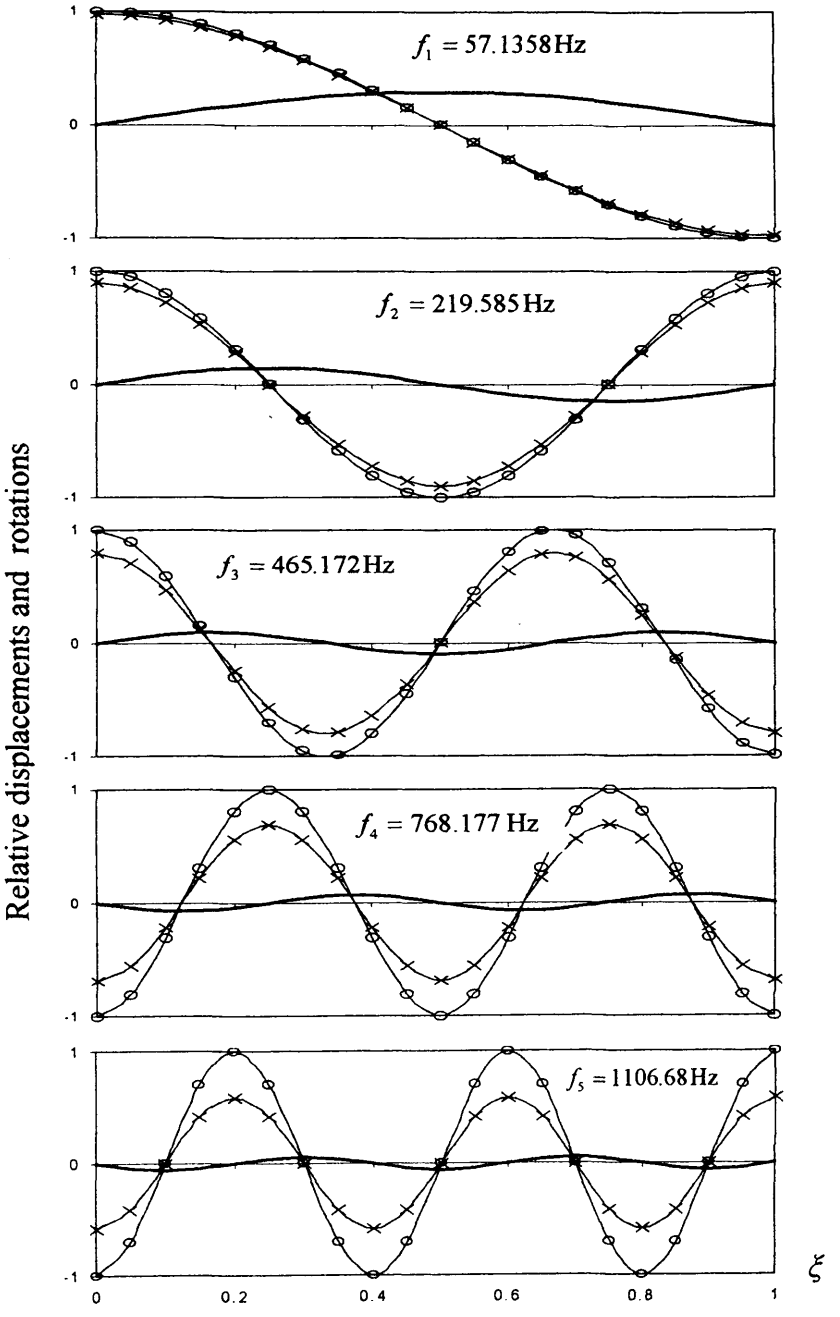

Figure 5.5: The first five natural frequencies and mode shapes of the simply supported beam of Example 5.1. The graphs show (—) the modal transverse deflection W, (-o-) beam slope Ψ and (-x-) average rotation of the beam's cross-section Φ.

where

$$w(x,t) = a_n \sin\frac{n\pi x}{L}\sin\omega t \tag{5.81}$$

Eq. (4.18) of reference (Allen 1969) then becomes an almost identical frequency equation to Eq. (5.78), i.e.

$$f_n = \frac{\pi}{2}\frac{n^2}{L^2}\sqrt{\frac{Ed^2t}{2\mu}}\sqrt{\frac{1}{1+Et_c tn^2\pi^2/2GL^2}+\frac{t^2}{3d^2}} \tag{5.82}$$

In the derivation of Eq. (5.82), it is assumed that the ratio of the core's shear strain to the slope of the beam's neutral axis throughout the length of the sandwich is uniform. The ratio depends only on the beam's material and geometric characteristics and the effects of shear deformation are ignored. Although this assumption is not generally correct, but it holds for the simply supported symmetric sandwich beam considered and therefore Eq.(5.82) is an exact frequency equation. Finally, it can easily be shown that Eq. (5.78) is an approximation to Eq. (5.82).

On the other hand, Rao (Rao 1978) derived the sixth order governing differential equation and solved it exactly for the case of simple supports. The resulting formula for the natural frequencies of a pin-pin sandwich beam is exactly the same as Eq. (5.76) when the loss factor is zero.

The difference between the results of the present study and those in references (Ahmed 1971; Ahmed 1972; Marur and Kant 1996; Mead 1982; Rao et al. 2001) are largely due to the approximations made during the formulation of the model. For example, Ahmed (Ahmed 1971; Ahmed 1972) used traditional finite elements, in which the accuracy of the results depend on the number of elements, the number of freedoms at each node and the shape functions which are used. Reference (Ahmed 1971) used six degrees of freedom per node while (Ahmed 1972) used four. Therefore, the latter theory gives more stiffness to the beam and the required natural frequencies are higher than those of the former. Reference (Sakiyama et al. 1996b) uses the discrete Green function which firstly has the

error of discreteisation and secondly the error of numerical integration. References (Marur and Kant 1996; Rao et al. 2001) use mixed higher order beam theory in which the axial and transverse displacements of any point lying in the beam's plane are expressed using the first few terms of a Taylor's series expansion. Hence, the higher order mixed theories introduce some approximation to the exact field displacements. They also generate an approximation by using only the displacements at top and bottom of the beam as degrees of freedom, which are not dependent on the number of layers.

***Example 5.2*:** The beam of Example 5.1 is now constrained to act as a cantilever and its length is reduced to 0.7112m. Results for the first eight natural frequencies are presented in Table 5.2 and compared with those from other references. Also Figure 5.6 illustrates the first five mode shapes of the beam. In contrast with the case of the simply supported beam, the graph of Ψ and Φ are not completely in-phase.

Table 5.2: Comparative results for the first eight natural frequencies (Hz) of the cantilevered sandwich beam of Example 5.2.

Freq. No.	Present theory	Ahmed, 1972	Ahmed, 1971	Sakiyama, 1996b	Marur, 1996	Banerjee, 2003
1	33.7513	32.79	33.97	33.146	33.7	31.46
2	198.992	193.5	200.5	195.96	197.5	193.7
3	512.307	499	517	503.43	505.5	529.2
4	907.299	886	918	893.28	890.5	1006
5	1349.65	1320	1368	1328.5	1321	-
6	1815.82	1779	1844	1790.7	1786	-
7	2292.45	2249	2331	2260.2	2271	-
8	2772.23	2723	2824	2738.9	2792	-

Discussion about the accuracy of the theories used by most of the authors has been given in Example 5.1. Therefore, only the results in the last column of Table 5.2 are discussed here. Banerjee (Banerjee 2003) uses an exact dynamic stiffness technique for a symmetric sandwich beam and includes the effects of the axial inertia of the faceplates, but neglects the inertia effects of the core material. Furthermore, he assumes that the motion of the two faceplates is symmetric. This results in a sixth order differential equation being derived which, overall, could yield a more accurate model for the flexural

vibration of sandwich beams. However, as will be shown in Chapter 6, the inclusion of axial inertia, but without constraining the faceplates to move symmetrically, yields a more general equation of motion. The resulting eighth order governing differential equation can then be solved exactly to yield the flexural, axial and shear thickness frequencies of the beam.

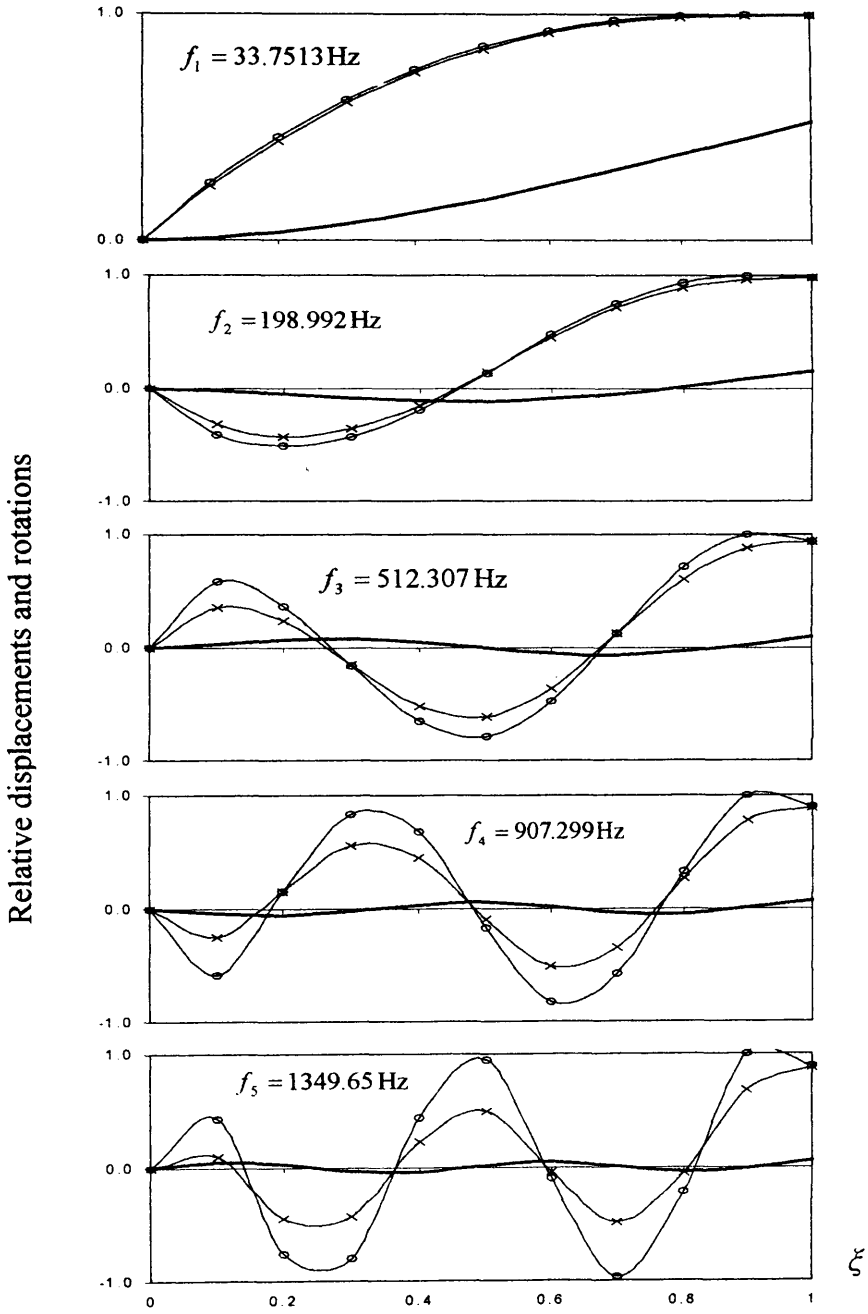

Figure 5.6: The first five natural frequencies and mode shapes of the cantilever beam of Example 5.2. The graphs show (—) the modal transverse deflection W, (-o-) beam slope Ψ and (-x-) average rotation of the beam's cross-section Φ.

Example 5.3: A fixed ended sandwich beam with the following material and geometrical properties is now considered.

$E_t = E_b = 68.9\,\text{GPa}$, $G = 68.9\,\text{MPa}$, $\rho_t = \rho_b = 2687.3\,\text{kg/m}^3$, $\rho_c = 119.69\,\text{kg/m}^3$, $t_t = t_b = 0.40624\,\text{mm}$, $t_c = 6.3475\,\text{mm}$, $L = 1.21872\,\text{m}$

Table 5.3 gives a comparison of the results from the present study and other authors (Raville et al. 1961; Sakiyama et al. 1996b). It should be noted that the results presented by Raville (Raville et al. 1961) are experimental. The results presented in Table 5.3 show good correlation between those of the current theory and others available in the literature. The results of the present study compare well with the experimental results of reference (Raville et al. 1961).

Table 5.3: Comparative results for the first ten natural frequencies (Hz) of the fixed ended sandwich beam of Example 5.3.

Freq. No.	Current theory	Sakiyama, 1996b	Raville, 1961
1	34.5965	33.563	-
2	93.1000	90.364	-
3	177.155	172.07	185.5
4	282.784	274.91	280.3
5	406.325	395.42	399.4
6	544.331	530.34	535.2
7	693.787	676.85	680.7
8	852.153	832.43	867.2
9	1017.35	995.36	1020
10	1187.70	1163.9	1201

Example 5.4: Attention is now given to the three span continuous sandwich beam of Figure 5.7, for which two sets of results are shown in Table 5.4. Type A results, in which the basic material and geometric properties of each span are identical to the beam of Example 5.3 and Type B results, which use the same data, except that the top faceplate in

the middle span has the following properties: $E_t = 207\,\text{GPa}$, $\rho_t = 7850\,\text{kg/m}^3$, $t_t = 0.4572\,\text{mm}$. In addition, various combinations of nodal mass and spring support stiffness are imposed as indicated. The rotational inertia $I_{M_1^*}$ of mass M_1^* is assumed to be significant and dependent upon Ψ alone whenever it is included. In similar fashion, K_3 is applied to Φ alone when determining the results in the last three columns of Table 5.4, but applied to both Ψ and Φ when modelling the fixed end condition for the results in the second column. Table 5.4 provides a range of 'exact' solutions, which may be helpful for future comparisons. It can also be used in conjunction with Table 5.3 to illustrate a possible pitfall that exists if the natural frequencies of a transcendental eigenvalue problem are acquired using a determinant search technique, as follows.

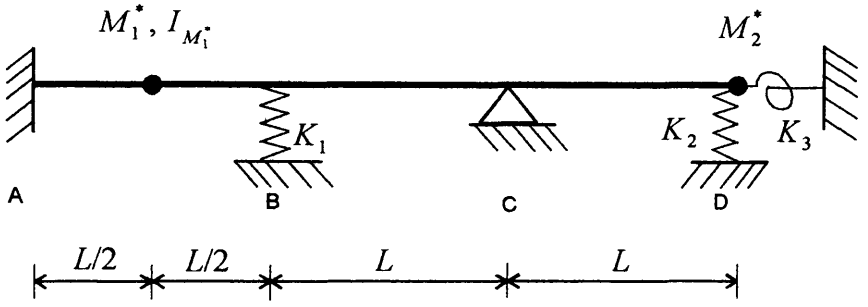

Figure 5.7: Three-span continuous sandwich beam of Example 5.4.

Consider the structure of Figure 5.7 with $M_1^* = M_2^* = I_{M_1^*} = 0$, $K_1 = K_2 = K_3 = \infty$ and beams with identical material and geometric properties in each span that correspond to the beam of Example 5.3. The resulting structure is a uniform beam that is continuous across the simple supports at B and C, clamped at A and D and symmetric about its mid point. The structure could therefore be modelled using one element per member and two nodes, namely B and C.

Since the structure is symmetric, the modes of vibration must be either symmetric or antisymmetric about the midpoint. Considering only the symmetric modes, it is clear that they fall into one of two categories. Either there is rotation at B and C or there is not. For the former category and all the antisymmetric modes, the requirement for a natural frequency, described previously by Eq. (5.68) as $\mathbf{K}\,\mathbf{D} = \mathbf{0}$, is satisfied in the usual way by

$|\mathbf{K}| = 0$. However, frequencies in the latter category satisfy $\mathbf{K}\,\mathbf{D} = \mathbf{0}$ by virtue of the fact that $\mathbf{D} = \mathbf{0}$ rather than the more usual $|\mathbf{K}| = 0$. In fact, $|\mathbf{K}|$ becomes infinite at such natural frequencies, with the consequence that they could be missed by traditional methods of determinant tracking which seek only $|\mathbf{K}| = 0$. Moreover, even if an analyst were to intervene in what is likely to be an automated process, the occurrence of $|\mathbf{K}|$ becoming infinite would not necessarily alert him to the danger that natural frequencies were being missed, since it is quite common for $|\mathbf{K}|$ to change sign through infinity at frequencies which do not correspond to natural frequencies of the structure. The fact that such a condition can arise in simple, practical structures can be seen by comparing the second columns of Tables 5.3 and 5.4. This shows that the third, sixth and ninth natural frequencies of the continuous beam of Example 5.4 correspond to the first three natural frequencies of the fixed ended beam of Example 5.3, i.e. the clamped ended frequencies of each span member.

Table 5.4: The first ten natural frequencies (Hz) of the sandwich beam described in Example 5.4 for various combinations of nodal mass and stiffness.

M_1^* (kg)	0	0	100	100	0	0	0	100	100
$I_{M_1^*}$ (kgm^2)	0	0	0	0.125	0	0	0	0.125	0.125
M_2^* (kg)	0	0	0	0	100	0	0	100	100
K_1 (N/m)	$10^{15}(\infty)$	0	0	0	0	10^7	0	10^7	10^7
K_2 (N/m)	$10^{15}(\infty)$	0	0	0	0	0	0	0	0
K_3 (Nm/rad)	$10^{15}(\infty)$	0	0	0	0	0	10^3	10^3	10^3
Freq. No.	Type A								Type B
1	19.8054	3.00131	1.85738	1.85371	0.32539	3.74241	4.16833	0.56236	0.59843
2	28.7227	7.96371	3.50043	3.50043	7.26939	19.9638	8.30131	3.41381	3.50667
3	34.5965	20.6721	11.9666	11.6151	17.6836	28.6269	21.1525	14.6566	14.6478
4	69.3442	29.6883	27.2172	14.9767	24.0821	34.4362	32.7291	18.8644	17.7480
5	84.0878	44.4183	37.1729	27.4011	43.3984	69.4403	44.9051	28.0860	26.2132
6	93.1000	70.7205	67.8202	37.6919	65.3014	84.3735	71.3082	64.1907	59.8352
7	146.067	86.6974	86.5853	68.7177	76.5946	93.0524	90.0769	76.9603	75.9475
8	165.676	109.605	106.291	86.9280	108.088	146.292	110.080	91.9690	90.7136
9	177.155	148.162	127.721	108.227	140.616	165.929	148.736	122.119	121.222
10	246.735	170.175	165.225	127.741	155.802	176.709	173.713	141.782	133.962

5.7 GENERAL REMARKS

The results presented in Tables 5.1 to 5.3 show good correlation between those of the current theory and a selection of comparable results available in the literature. The differences in the results are attributable to many factors that vary widely from approximate solution techniques to differences in basic assumptions. Table 5.4 provides a range of 'exact' solutions, which may be helpful for future comparisons.

5.7.2 Effects of nodal mass or spring constraint

In conjunction with Example 5.4 and Table 5.4, it is worth noting that imposing springs or masses at nodes may change the sequence of modes by stimulating the occurrence of additional modes and changing the frequencies of others. (Figures 5-8 to 5-10 illustrate the first six mode shapes of the continuous beam of Example 5.4 that correspond to the data in columns 3 to 5 of Table 5.4.) Comparison of the mode shapes in Figures 5.9 and 5.10 shows that imposing the mass moment of inertia on Ψ causes small changes to the mode shapes of corresponding graphs, but induces a completely new mode shape at a frequency of 14.9767Hz in Figure 5.10. This can also be seen by comparing columns 4 and 5 of Table 5.4. In addition, the frequencies of modes with frequencies higher than the induced mode (frequency numbers four to nine in column four of Table 5.4) increased and, in contrast, the frequencies of modes with lower frequency (frequency numbers one to three in column four of Table 5.4) decreased. Table 5.5 highlights the effects of gradual changes of the value of the mass moment of inertia on stimulating the new mode. It also shows how the frequency of the modes lower than the stimulated mode decreased and vice versa.

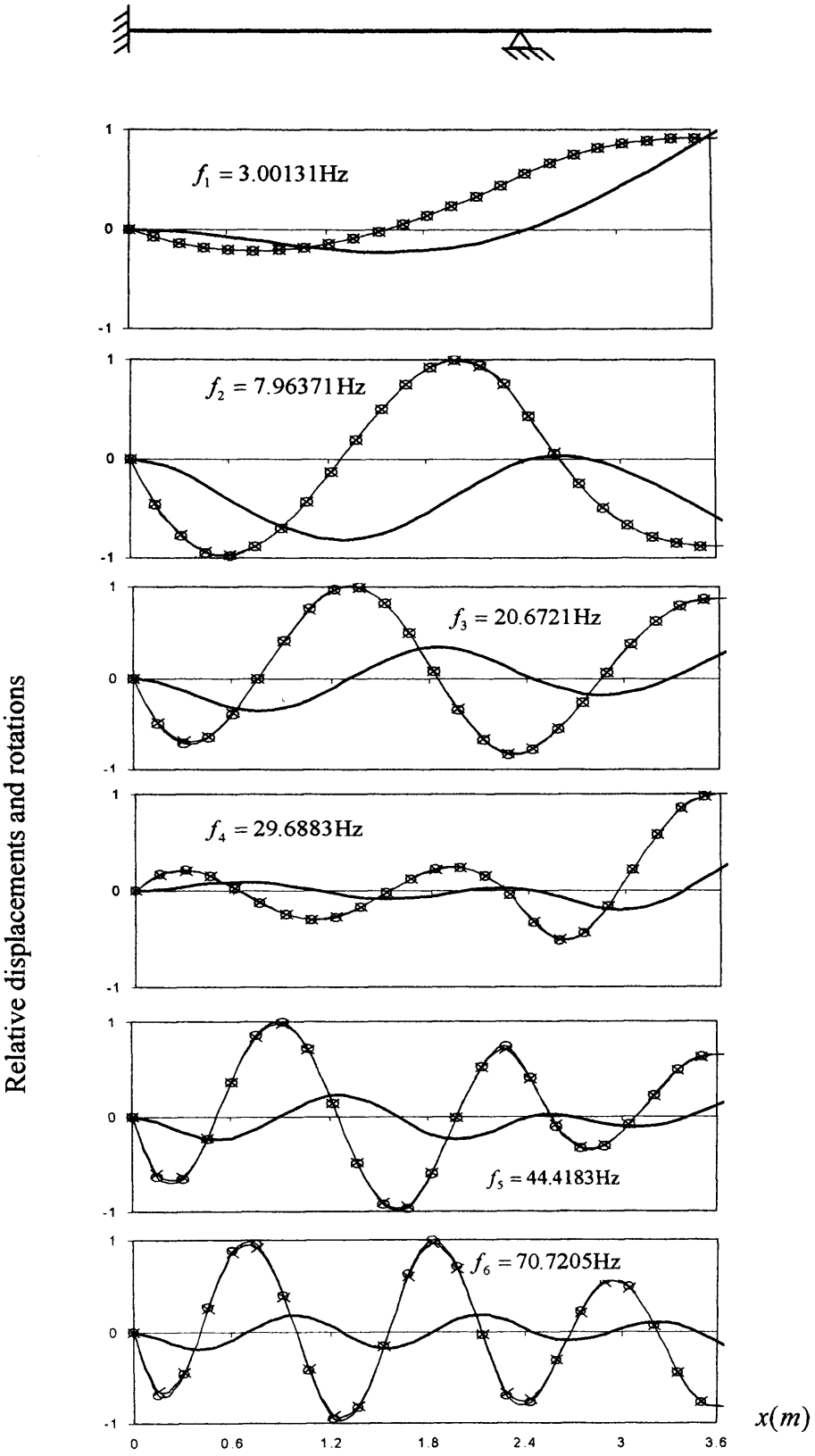

Figure 5.8: The first six natural frequencies and mode shapes of the continuous beam of Example 5.4 where the data and results are referred to column 3 of Table 5.4. The graphs show (—) the modal transverse deflection W, (-o-) beam slope Ψ and (-x-) average rotation of the beam's cross-section Φ.

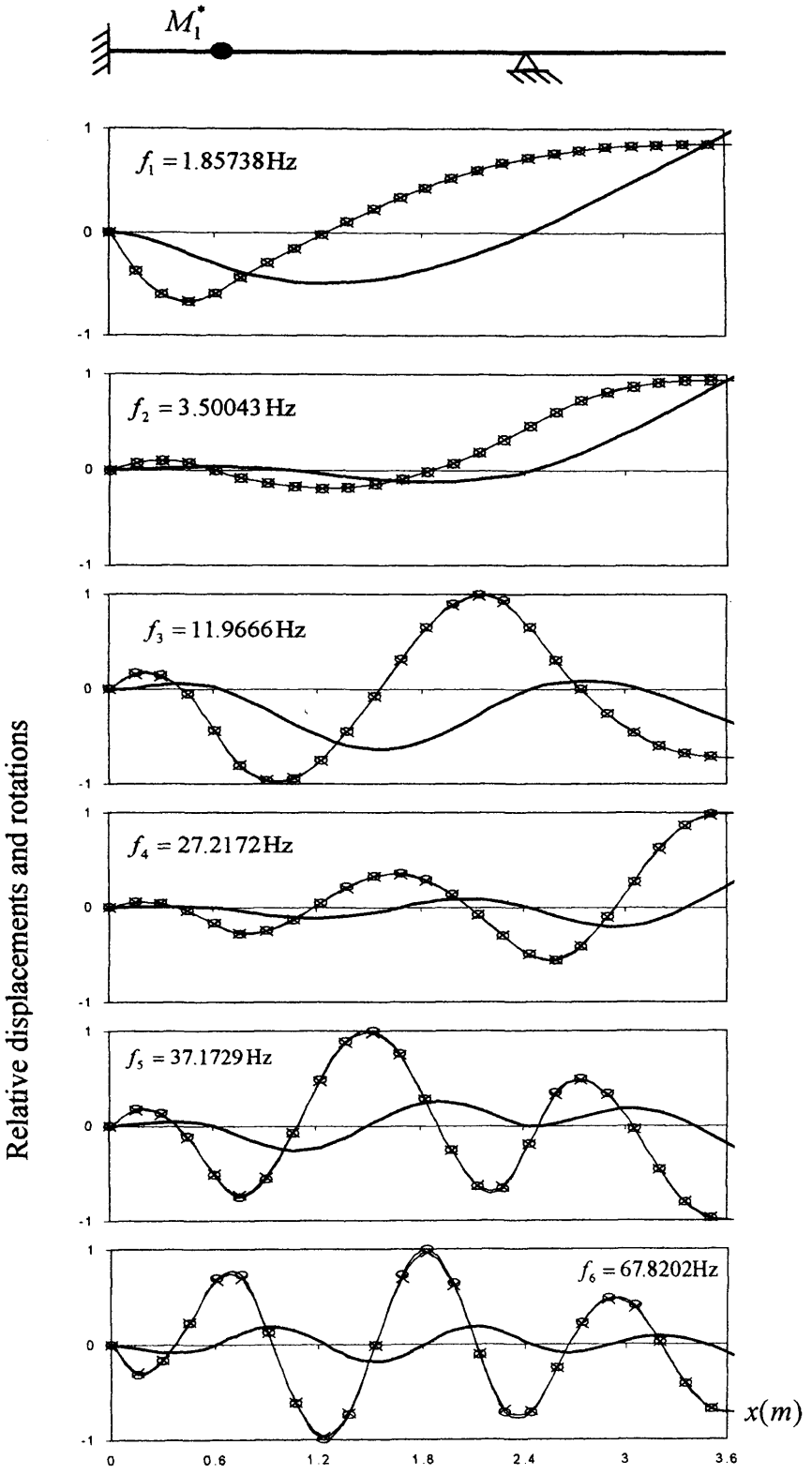

Figure 5.9: The first six natural frequencies and mode shapes of the continuous beam of Example 5.4 where the data and results are referred to column 4 of Table 5.4. The graphs show (—) the modal transverse deflection W, (-o-) beam slope Ψ and (-x-) average rotation of the beam's cross-section Φ.

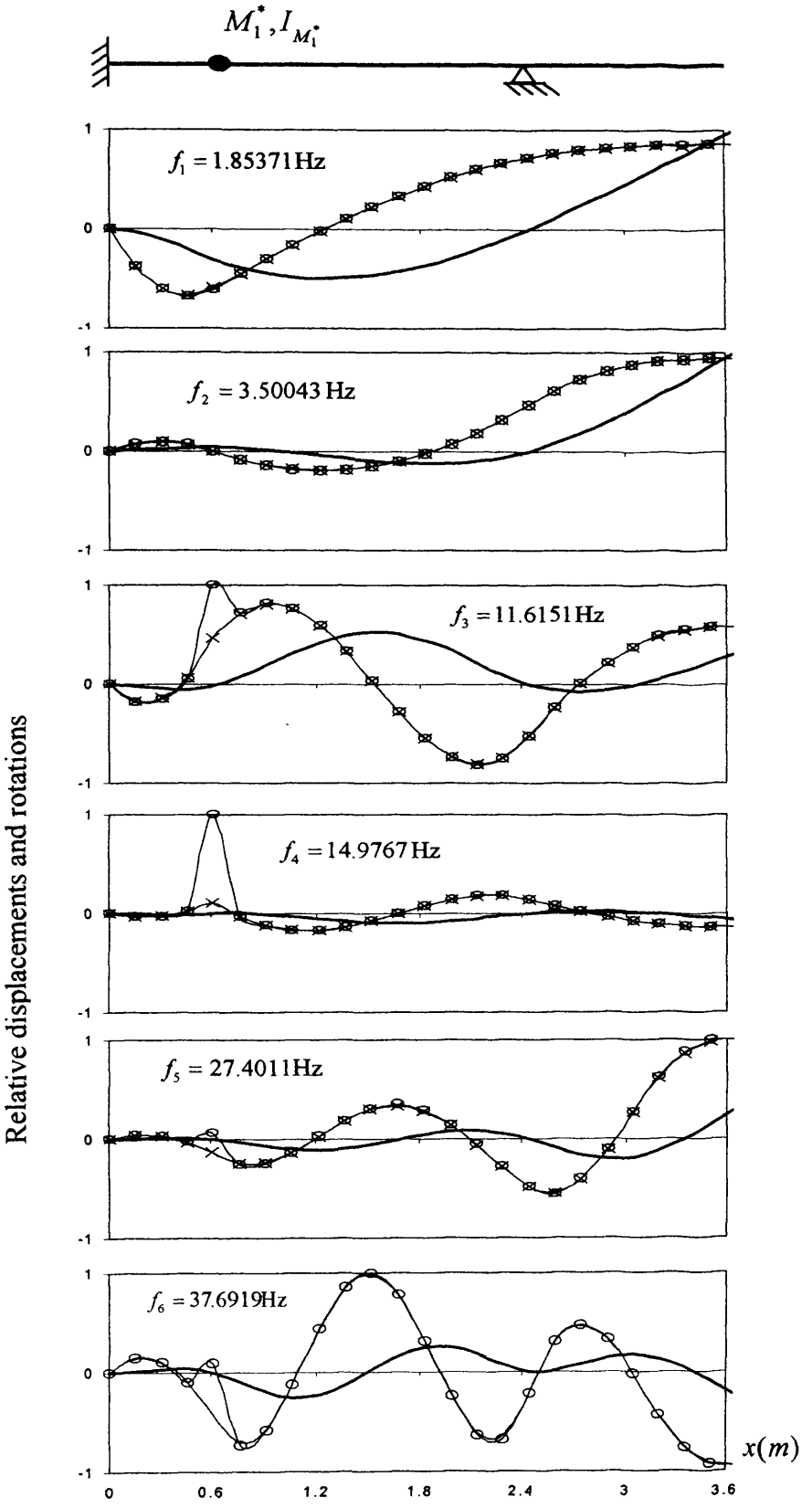

Figure 5.10: The first six natural frequencies and mode shapes of the continuous beam of Example 5.4 where the data and results are referred to column 5 of Table 5.4. The graphs show (—) the modal transverse deflection W, (-o-) beam slope Ψ and (-x-) average rotation of the beam's cross-section Φ.

Table 5.5: Effects of the rotational inertia $I_{M_1^*}$ of mass M_1^* on stimulating new modes, (Example 5.4). Bold type indicates the additional modes.

	$I_{M_1^*}$ (kgm^2)				
Freq. No	0	0.00125	0.00625	0.0125	0.125
1	1.85738	1.85734	1.85720	1.85702	1.85371
2	3.50043	3.50043	3.50043	3.50043	3.50043
3	11.9666	11.9652	11.9596	11.9522	11.6151
4	27.2172	27.2123	27.1886	27.1447	**14.9767**
5	37.1729	37.1432	36.9725	36.4877	27.4011
6	67.8202	67.5940	62.0837	**47.1559**	37.6919
7	86.5853	86.4164	**72.5350**	69.3819	68.7177
8	106.291	104.705	87.3721	87.0548	86.9280
9	127.721	127.688	109.445	108.669	108.227
10	165.225	154.461	127.749	127.744	127.741

5.7.3 Advantages of a stiffness formulation

The use of the stiffness method offers great flexibility to impose 'constraints' on any selected node. These will typically take the form of mass inertia, spring support stiffnesses or relationships that constrain one or more displacements to move in a predefined way relative to another set of displacements. Imposing such constraints follows the normal rules that would apply to a traditional beam element, except more care is required in order to associate the constraint with the appropriate degree(s) of freedom. Table 5.6 amplifies this by listing the possible rotational displacement constraints and how they are achieved, primarily as an aid to establishing boundary conditions.

In Table 5.6, a riveted node is a node in which the faceplate displacements u_t and u_b at that node are restrained by a rigid rivet through the whole sandwich beam and therefore the shear strain in the core is prevented. Hence, by setting $\gamma = 0$ in Eq. (5.12), this type

Table 5.6: Rotational displacement constraints. A(B) implies an infinitely stiff rotational spring imposed on Φ (Ψ).

Degree of freedom		Constraint	Description
$\Psi \neq 0$	$\Phi \neq 0$	$\Psi = \Phi$	Riveted
$\Psi \neq 0$	$\Phi \neq 0$	None	Free / Free
$\Psi \neq 0$	$\Phi = 0$	A	Free / Fixed
$\Psi = 0$	$\Phi \neq 0$	B	Fixed / Free
$\Psi = 0$	$\Phi = 0$	A + B	Fixed / Fixed

of constraint is easily achieved. Therefore, the special case of a riveted end in references (Mead and Markus 1969; Mead and Markus 1970a; Mead 1971) can be treated in a more general sense i.e. for any node using the stiffness formulation. The procedure is as follows. After imposing boundary conditions on the dynamic stiffness matrix we may have

$$\begin{Bmatrix} \vdots \\ P_i \\ P_{i+1} \\ \vdots \end{Bmatrix} = \begin{bmatrix} \ddots & \vdots & \vdots & \vdots \\ \cdots & K_{i,i} & K_{i,i+1} & \cdots \\ \cdots & K_{i+1,i} & K_{i+1,i+1} & \cdots \\ \vdots & \vdots & \vdots & \ddots \end{bmatrix} \begin{Bmatrix} \vdots \\ D_i \\ D_{i+1} \\ \vdots \end{Bmatrix} \tag{5.83}$$

where P_i, P_{i+1}, D_i and D_{i+1} are M_j, $\overline{M}_j$, Ψ_j and Φ_j at any riveted node j, respectively, and i is a dummy. If the node j is a riveted node, the constraint condition at this node is

$$\Psi_j = \Phi_j \qquad \text{or} \quad D_i = D_{i+1} \tag{5.84}$$

and therefore all the elements of the stiffness matrix in column $i+1$ can be added to their counterparts in column i, with the former changed to zero as follows

$$\begin{Bmatrix} \vdots \\ P_i \\ P_{i+1} \\ \vdots \end{Bmatrix} = \begin{bmatrix} \ddots & \vdots & 0 & \vdots \\ \cdots & K_{i,i} + K_{i,i+1} & 0 & \cdots \\ \cdots & K_{i+1,i} + K_{i+1,i+1} & 0 & \cdots \\ \vdots & \vdots & 0 & \ddots \end{bmatrix} \begin{Bmatrix} \vdots \\ D_i \\ D_{i+1} \\ \vdots \end{Bmatrix} \tag{5.85}$$

In this situation, it is clear that the loads P_i and P_{i+1} are applied at the identical freedom D_i or D_{i+1}, say D_i. Therefore, it is necessary to impose P_i and P_{i+1} together at the same freedom and consequently, the elements in the row $i+1$ of the dynamic stiffness matrix should be added to their counterparts in row i and then the former vanish as follows

$$\begin{Bmatrix} \vdots \\ P_i + P_{i+1} \\ 0 \\ \vdots \end{Bmatrix} = \begin{bmatrix} \ddots & \vdots & 0 & \vdots \\ \cdots & K_{i,i} + K_{i,i+1} + K_{i+1,i} + K_{i+1,i+1} & 0 & \cdots \\ \cdots & 0 & 0 & \cdots \\ \vdots & \vdots & 0 & \ddots \end{bmatrix} \begin{Bmatrix} \vdots \\ D_i \\ D_{i+1} \\ \vdots \end{Bmatrix} \tag{5.86}$$

The matrix equation (5.86) is now singular. To eliminate the singularity, row $i+1$ and column $i+1$ can be deleted from the dynamic stiffness matrix, which subsequently reduces the size of matrix by one, or the same effect can be achieved by changing the appropriate leading diagonal element to unity. The latter is easier to do as there is no need to change the previously stored addresses of freedoms and so on.

5.7.4 Numerical overflow

Finally, it is worth noting that while generating the results above, it became apparent that it is relatively easy to generate an example in which the value of α, defined in Eq. (5.23), is sufficiently large that the value of ζ in Eq. (5.48b) overflows, even when using double precision arithmetic. However, it is easy to show that the dominant term in the expression for α is the length of the member (element). Thus if difficulty is experienced a simple method is to subdivide the member into a greater number of elements until the problem is resolved.

CHAPTER 6

GENERAL VIBRATION OF A THREE-LAYER SANDWICH BEAM INCLUDING AXIAL AND ROTARY INERTIA

6.1 INTRODUCTION

In this chapter, the previous theory of Chapter 5 is extended to include the effects of axial and rotary inertia of the core and faceplates. The faceplates are therefore modelled as Rayleigh beams. This crucial difference enables the resulting dynamic member stiffness matrix (exact finite element) to be used to analyse general two-dimensional structures for the first time. The model can then be solved for any required natural frequency to any desired accuracy for both slender and deep beams using the Wittrick-Williams algorithm. In the case of single beams, it will also be confirmed that the modes of vibration are largely coupled, especially for unsymmetrical boundary conditions, and that the predominant component of the mode can be classified into one of three families of modes; flexural, extensional and thickness shear and that coupling between them may occur at frequencies of practical interest.

The dynamic stiffness matrix of a three-layer sandwich beam is now developed from first principles. It accounts exactly for the uniform distribution of mass and stiffness in the member, subject to the following assumptions:

(i) transverse direct strains in the faceplates and core are negligible so that small transverse displacements are the same for all points in a normal section;

(ii) there is perfect bonding at the core/faceplate interfaces;

(iii) the faceplates are elastic, isotropic and do not deform in shear;

(iv) the linearly elastic core carries only shear and the in-plane normal stresses are assumed to be negligible.

When dealing with general two-dimensional structures constructed from sandwich beams, it is necessary to include the effects of flexural and longitudinal inertia. In addition, the effects of rotary inertia become important when dealing with deep beams. The theory of this chapter is therefore developed in a two-stage process. Initially, longitudinal inertia is accounted for and this is subsequently enhanced by the addition of rotary inertia, which in this case, it can be say that in contrast with Chapter 5, the faceplates of the sandwich beam element are Rayleigh beams which their longitudinal inertia are also included.

6.2 FORCE-DISPLACEMENT RELATIONS

Figure 6.1 shows the positive sense of the displacements experienced at a typical section of the beam at some instant during the motion. The beam has unit width and t_t, t_c and t_b are the thickness of the top faceplate, core and bottom faceplate, respectively, u_t, u_c and u_b are the mid-layer longitudinal displacement of the top faceplate, core and bottom faceplate, respectively, γ_c and φ_c are the shear strain and the average rotation of the core, respectively, w is the transverse displacement which due to neglecting transverse direct strains in the faceplates and core remains constant throughout the section at all layers, and

$$\psi = w' \tag{6.1}$$

is the bending slope, where the prime notation refers to partial differentiation with respect to x in the usual way. The necessary force displacement relationships for axial extension and bending of the faceplates are

$$n_i = E_i t_i u_i' = K_i u_i' \quad \text{and} \quad m_i = -E_i I_i w'' = -E_i I_i \psi' \quad (i = t, b) \tag{6.2a,b}$$

respectively, where $K_i = E_i t_i$ and $E_i I_i$ are the axial and flexural rigidities per unit width of faceplate i and u_i' is the average normal strain of faceplate i.

It is assumed that plane sections of both the faceplates and core remain plane as the beam bends. However, in the former they will remain perpendicular to the beam axis, but not in the latter. Hence, in a similar way to Eq. (5.11b) the shear strain in the core layer is given by

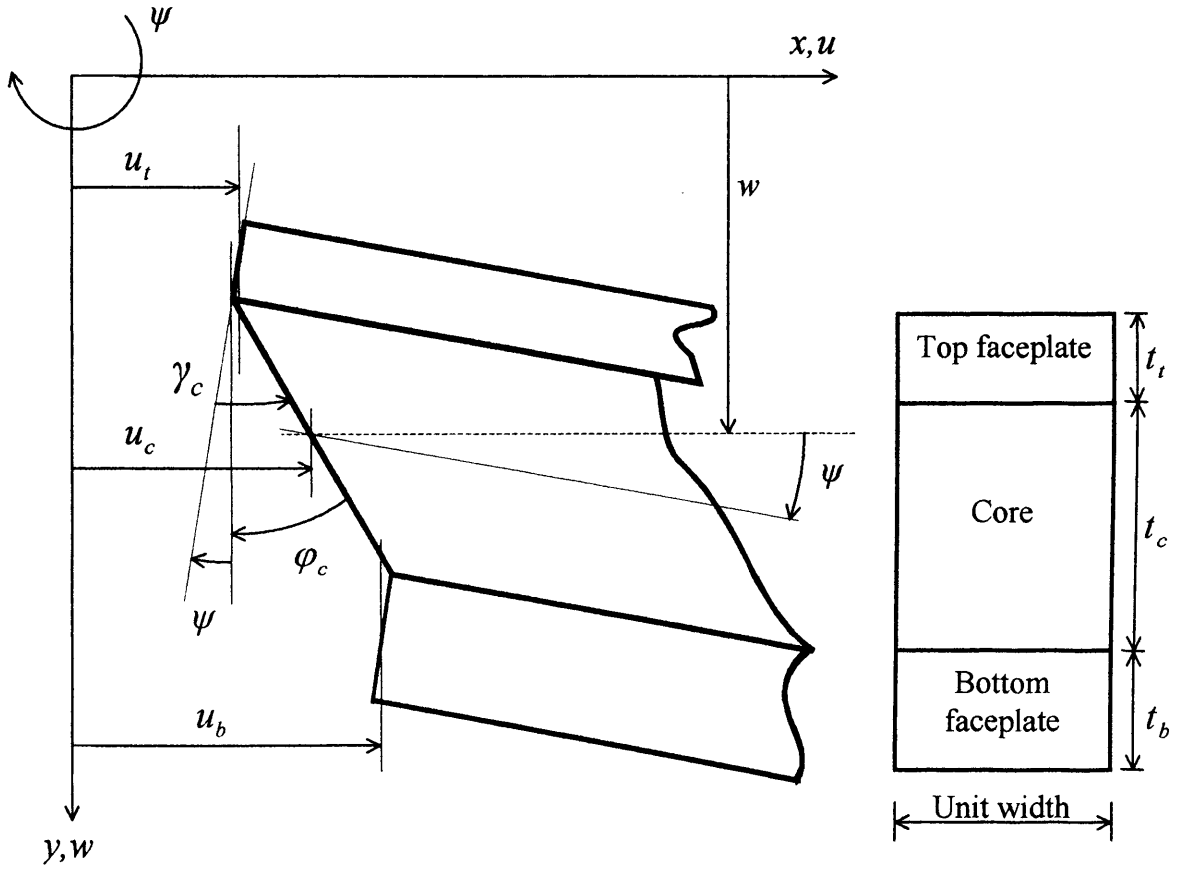

Figure 6.1: The displaced section, cross-section and co-ordinate system of a typical sandwich beam of unit width.

$$\gamma_c = \frac{d}{t_c}(\psi - \frac{u_t - u_b}{d}) \tag{6.3}$$

where $d = t_c + \frac{t_t + t_b}{2}$ is the distance between the centre lines of the faceplates. The force-displacement relationship for shearing deformation in the core is

$$q_c = t_c \tau_c = G_c t_c \gamma_c \tag{6.4}$$

where τ_c is the uniform shear stress through the core thickness and G_c is the effective shear modulus of the core material. Also from Figure 6.1 it is clear that u_c and φ_c, the average longitudinal displacement and rotation of the core, are given by

$$u_c = \frac{u_t + u_b}{2} + \psi\, e_1 \text{ and } \varphi_c = \frac{u_t - u_b - \psi\, e_2}{t_c}, \tag{6.5a,b}$$

respectively, where $e_1 = \frac{t_b - t_t}{4}$ and $e_2 = \frac{t_b + t_t}{2}$.

6.3 GENERAL VIBRATIONS OF A THREE-LAYER SANDWICH BEAM INCLUDING AXIAL INERTIA

6.3.2 Derivation of the governing differential equation of motion

The governing differential equations of motion can be derived in two ways: an Equilibrium approach and an Energy approach.

6.3.2.1 Equilibrium (Newtonian) approach

Consider Figure 6.2, which shows a typical elemental length of a member at some instant during the motion. The equation of horizontal equilibrium can then be written as

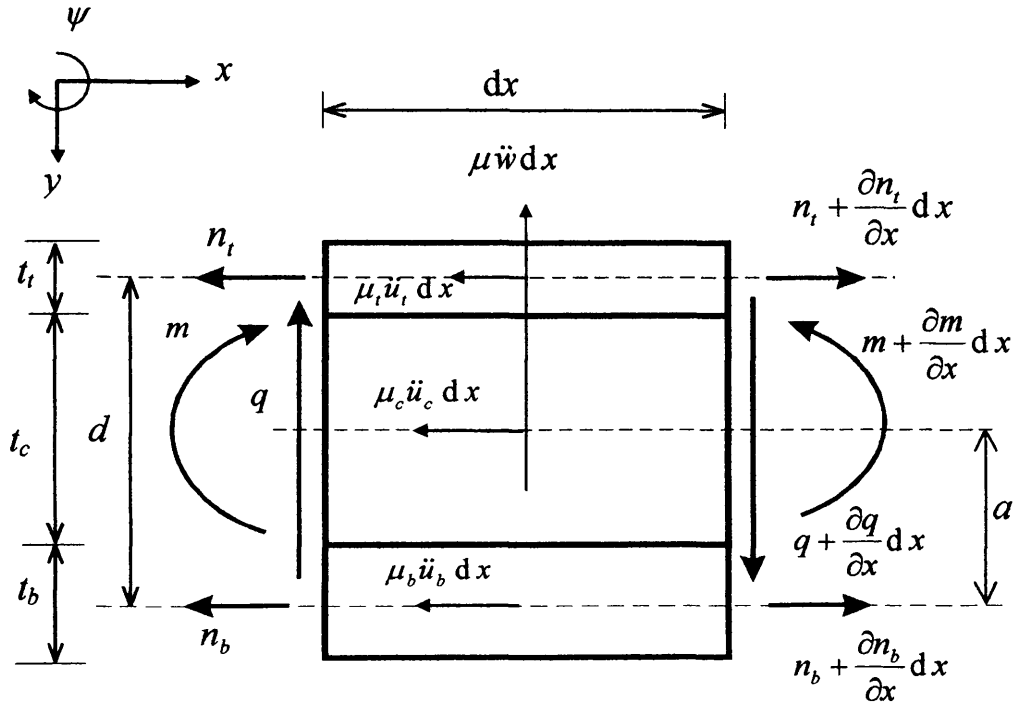

Figure 6.2: Positive resultant forces and moments and reversed linear inertias acting on a typical elemental length of a sandwich beam of unit width in local co-ordinates. The layer dimensions are also shown.

$$\frac{\partial n_t}{\partial x} + \frac{\partial n_b}{\partial x} = \mu_t \ddot{u}_t + \mu_c \ddot{u}_c + \mu_b \ddot{u}_b \tag{6.6}$$

where n_t and n_b are the axial forces in the top and bottom faceplates, respectively, μ_t, μ_b and μ_c are the mass/unit length of the top and bottom faces and core, respectively, and the dot notation refers to partial differentiation with respect to time in the usual way.

Substituting Eqs. (6.5a) and (6.1a) into Eq. (6.6) gives the first differential equation of motion as

$$K_t u_t'' + K_b u_b'' - (\mu_t + \frac{\mu_c}{2})\ddot{u}_t - (\mu_b + \frac{\mu_c}{2})\ddot{u}_b - \mu_c e_1 \ddot{\psi} = 0 \tag{6.7}$$

Since, in free vibration analysis, the only vertical force is the transverse flexural inertia, the equation of vertical equilibrium is

$$\frac{\partial q}{\partial x} = \mu \ddot{w} \tag{6.8}$$

From Figure 6.3 and Eq. (6.4), it is clear that $q = q_t + q_b + q_c$ is the resultant shear force at any normal section of the element, where q subscripted with t, b, or c relates to the shear force in the top faceplate, bottom faceplate and the core, respectively, and $\mu = \mu_t + \mu_b + \mu_c$ is the mass per unit length of the beam.

Taking moments about the centre line at the right hand side of the bottom faceplate in Figure 6.2 and ignoring terms of second order yields the moment equilibrium equation as

$$q\,\mathrm{d}x - \frac{\partial m}{\partial x}\mathrm{d}x + \frac{\partial n_t}{\partial x}\mathrm{d}x(d) - \mu_t \ddot{u}_t\,\mathrm{d}x(d) - \mu_c \ddot{u}_c\,\mathrm{d}x(a) = 0 \tag{6.9}$$

$a = \frac{t_c + t_b}{2}$ is the distance between the centre lines of the bottom faceplate and the core and m is the resultant bending moment at any section given by

$$m = m_t + m_b = -E_t I_t \psi' - E_b I_b \psi' = -\frac{\psi'}{\kappa} \tag{6.10}$$

where m_t and m_b (see Figure 6.3) are the bending moments in the top and bottom faceplates, respectively.

Substituting Eqs. (6.1a), (6.5a), (6.2) and (6.10) into Eq. (6.9) yields the resultant shear force as

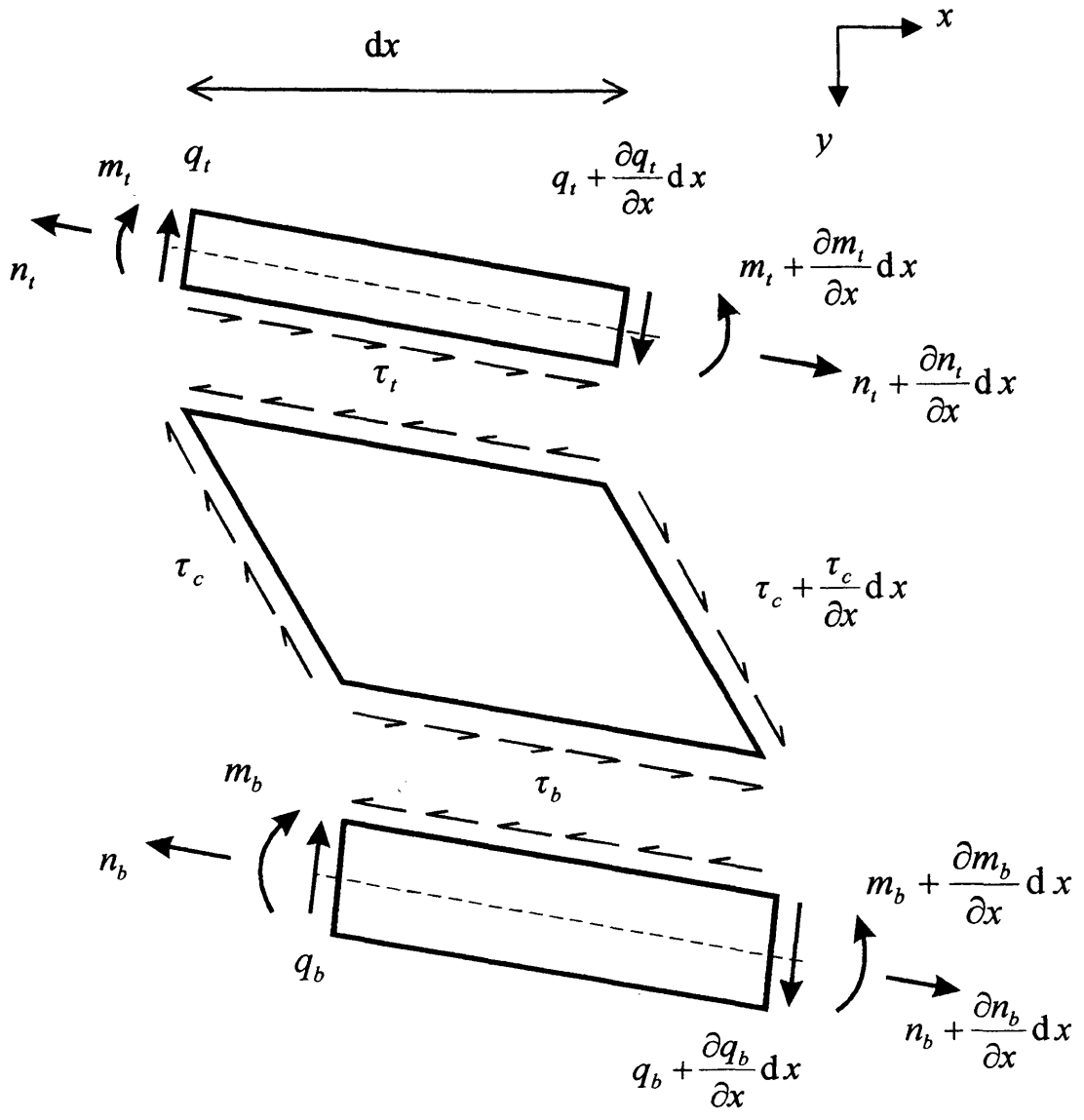

Figure 6.3: Component member forces and moments and inter member stresses on a typical elemental length of a sandwich beam.

$$q = -\frac{\psi''}{\kappa} - K_t d\, u_t'' + (d\mu_t + a\frac{\mu_c}{2})\ddot{u}_t + a\frac{\mu_c}{2}\ddot{u}_b + ae_1\mu_c\ddot{\psi} \tag{6.11}$$

Now, substituting Eqs. (6.11) into Eq. (6.8) gives the second differential equation of motion as

$$\mu\ddot{w} + \frac{\psi'''}{\kappa} + K_t d\, u_t''' - (d\mu_t + a\frac{\mu_c}{2})\ddot{u}_t' - a\frac{\mu_c}{2}\ddot{u}_b' - ae_1\mu_c\ddot{\psi}' = 0 \tag{6.12}$$

The equation of horizontal equilibrium for the top faceplate in Figure 6.3 may be written as

$$\frac{\partial n_t}{\partial x}\mathrm{d}x+\tau_t\,\mathrm{d}x=\mu_t\frac{\partial^2 u_t}{\partial t^2}\mathrm{d}x \tag{6.13}$$

where τ_t is the shear stress at the interface between the top faceplate and the core. It then follows that

$$\tau_t=-K_t u_t''+\mu_t\ddot{u}_t \tag{6.14}$$

In addition, the equation of horizontal equilibrium of the bottom faceplate in Figure 6.3 may be written as

$$\frac{\partial n_b}{\partial x}\mathrm{d}x-\tau_b\,\mathrm{d}x=\mu_b\frac{\partial^2 u_b}{\partial t^2}\mathrm{d}x \tag{6.15}$$

where τ_b is the shear stress at the interface between the bottom faceplate and the core and hence

$$\tau_b=K_b u_b''-\mu_b\ddot{u}_b \tag{6.16}$$

Since it was assumed that the shear stress through the core thickness has an average value of τ_c, the equation of moment equilibrium of the core about the centre line at the right hand side of the core in Figure 6.3 can be written as

$$-\tau_t\,\mathrm{d}x\frac{t_c}{2}-\tau_b\,\mathrm{d}x\frac{t_c}{2}+\tau_c t_c\,\mathrm{d}x=0 \tag{6.17}$$

Substituting from Eqs. (6.3), (6.4), (6.14) and (6.16) into Eq. (6.17) gives the final differential equation of motion as

$$K_t u_t'' - \mu_t \ddot{u}_t - K_b u_b'' + \mu_b \ddot{u}_b + \frac{2G_c d}{t_c}\psi - \frac{2G_c}{t_c}u_t + \frac{2G_c}{t_c}u_b = 0 \tag{6.18}$$

Attention is now confined to harmonic motion in which the time dependent terms are related to ω, the circular frequency, by

$$f(x,t) = F(x)\, e^{i\omega t} \tag{6.19}$$

and the upper case characters refer to the amplitude of the equivalent time dependent quantity. Hence, using Eq. (6.19) in the partial differential equations of Eqs. (6.12), (6.7) and (6.18) yields the following linear differential equations with constant coefficients

$$\left.\begin{aligned}
&-\mu\omega^2 W + \frac{W''''}{\kappa} + K_t d\, U_t''' + (d\mu_t + a\frac{\mu_c}{2})\omega^2 U_t' + a\frac{\mu_c}{2}\omega^2 U_b' + a e_1 \mu_c \omega^2 W'' = 0 \\
&K_t U_t'' + K_b U_b'' + (\mu_t + \frac{\mu_c}{2})\omega^2 U_t + (\mu_b + \frac{\mu_c}{2})\omega^2 U_b + \mu_c e_1 \omega^2 W' = 0 \\
&K_t U_t'' + \mu_t \omega^2 U_t - K_b U_b'' - \mu_b \omega^2 U_b + \frac{2G_c d}{t_c}W' - \frac{2G_c}{t_c}U_t + \frac{2G_c}{t_c}U_b = 0
\end{aligned}\right\} \tag{6.20}$$

Now using the operator $D = \mathrm{d}/\mathrm{d}x$, Eq. (6.20) can be written in matrix form as

$$\begin{bmatrix}
\frac{D^4}{\kappa} + a e_1 \mu_c \omega^2 D^2 - \mu\omega^2 & K_t d\, D^3 + (d\mu_t + a\frac{\mu_c}{2})\omega^2 D & a\frac{\mu_c}{2}\omega^2 D \\
\mu_c e_1 \omega^2 D & K_t D^2 + (\mu_t + \frac{\mu_c}{2})\omega^2 & K_b D^2 + (\mu_b + \frac{\mu_c}{2})\omega^2 \\
\frac{2G_c d}{t_c} D & K_t D^2 + \mu_t \omega^2 - \frac{2G_c}{t_c} & -K_b D^2 - \mu_b \omega^2 + \frac{2G_c}{t_c}
\end{bmatrix}
\begin{bmatrix} W \\ U_t \\ U_b \end{bmatrix} = 0 \tag{6.21}$$

Eq. (6.21) can be combined into one equation by eliminating either W, U_t or U_b to yield the linear eighth order differential equation as

$$[D^8 + c_1 D^6 + c_2 D^4 + c_3 D^2 + c_4]\, V = 0 \tag{6.22}$$

where $V = W$, U_t or U_b and

$$
\left.
\begin{aligned}
c_1 &= (\frac{1}{\hat{\varsigma}} + \frac{\mu_c}{4\varsigma} + \mu_c \kappa e_1^2)\omega^2 - \hat{S}_c(\frac{1}{d^2\varsigma} + \kappa) \\
c_2 &= (\frac{\mu_t \mu_b}{K_t K_b} + \frac{\mu_c(\mu_1+\mu_2)}{4K_t K_b} + \frac{\mu_c \kappa e_1^2}{\hat{\varsigma}})\omega^4 + \\
&\quad [\frac{\hat{S}_c \mu_c \kappa e_1}{\varsigma d}(\frac{K_t - K_b}{K_t + K_b} - \frac{e_1}{d}) - \hat{S}_c \kappa(\frac{1}{\hat{\varsigma}} + \frac{\mu_c}{4\varsigma}) - \mu(\kappa + \frac{\hat{S}_c}{d^2 K_t K_b})]\omega^2 \\
c_3 &= [\frac{\mu_c \mu_t \mu_b \kappa e_1^2}{K_t K_b}]\omega^6 \\
&\quad - \{\mu\kappa(\frac{1}{\hat{\varsigma}} + \frac{\mu_c}{4\varsigma}) + \frac{\hat{S}_c \kappa}{K_t K_b}[\mu_t \mu_b + \frac{\mu_c e_1}{d}(\mu_b - \mu_t) + \mu_c(\mu_t + \mu_b)(\frac{1}{4} + \frac{e_1^2}{d^2})]\}\omega^4 \\
&\quad + \frac{\hat{S}_c \mu \kappa}{\varsigma d^2}\omega^2 \\
c_4 &= -[\frac{\mu_t \mu_b}{K_t K_b} + \frac{\mu_c(\mu_t + \mu_b)}{4K_t K_b}]\mu\kappa\omega^6 + \frac{\hat{S}_c \mu^2 \kappa}{d^2 K_t K_b}\omega^4
\end{aligned}
\right\} \quad (6.23)
$$

where

$$
\varsigma = K_t K_b/(K_t + K_b); \quad \hat{\varsigma} = K_t K_b/(K_t \mu_t + K_b \mu_b); \quad \hat{S}_c = \frac{Gd^2}{t_c} \qquad (6.24)
$$

6.3.2.2 Energy approach

An alternative method for deriving the governing differential equations of motion is through an energy approach. In this way it is possible to avoid the vectorial equations of equilibrium by using scalar quantities associated with the variational form of Hamilton's principle. In this approach, variations of the potential and kinetic energy of the internal and inertial forces are utilised. The potential energy of the internal forces is strain energy, which is equal to the negative work of the internal forces, while the kinetic energy is calculated from the inertial forces.

6.3.2.2.1 Potential energy

The total strain energy for a beam of length L can now be written as

$$U=\int_0^L \begin{pmatrix} \frac{1}{2}q_c\gamma_c \\ +\frac{1}{2}n_t\varepsilon_t+\frac{1}{2}n_b\varepsilon_b \\ -\frac{1}{2}m\psi' \end{pmatrix} \mathrm{d}x \qquad \begin{matrix} \text{Strain energy of the core due to shear deformation} \\ \text{Strain energy of the faceplates due to axial deformation} \\ \text{Strain energy of the faceplates due to bending deformation.} \end{matrix} \qquad (6.25)$$

where $\varepsilon_i = u_i'$ is the average normal strain of faceplate i $(i = t, b)$. Now combining Eqs. (6.3) and (6.4) gives

$$\begin{aligned} q_c\gamma_c = Gt_c\gamma_c^2 &= Gt_c[\frac{d}{t_c}(\psi-\frac{u_t-u_b}{d})]^2 \\ &= \hat{S}_c(\psi^2+\frac{u_t^2}{d^2}+\frac{u_b^2}{d^2}-\frac{2\psi u_t}{d}+\frac{2\psi u_b}{d}-\frac{2u_tu_b}{d^2}) \end{aligned} \qquad (6.26)$$

where $\hat{S}_c=\dfrac{Gd^2}{t_c}$. Also from Eq. (6.1a) we have

$$n_i\varepsilon_i = E_it_iu_i'^2 = K_iu_i'^2 \qquad (6.27)$$

Substituting Eqs.(6.23), (6.24) and (6.10) into Eq. (6.25) gives the total strain energy as

$$U=\int_0^L [\frac{\hat{S}_c}{2}(\psi^2+\frac{u_t^2}{d^2}+\frac{u_b^2}{d^2}-\frac{2\psi u_t}{d}+\frac{2\psi u_b}{d}-\frac{2u_tu_b}{d^2})+\frac{K_t}{2}u_t'^2+\frac{K_b}{2}u_b'^2+\frac{\psi'^2}{2\kappa}]\,\mathrm{d}x \qquad (6.28)$$

6.3.2.2.2 Kinetic energy

In similar fashion, the kinetic energy of the sandwich beam including the axial and transverse inertia of the layers is given by

$$T=\int_0^L\left(\begin{array}{l}\frac{1}{2}\mu\dot{w}^2+\\ \frac{1}{2}\mu_t\dot{u}_t^2+\frac{1}{2}\mu_c\dot{u}_c^2+\frac{1}{2}\mu_b\dot{u}_b^2\end{array}\right)\mathrm{d}x \qquad \begin{array}{l}\text{Transverse inertia of full section}\\ \\ \text{Axial inertia of each layer}\end{array} \tag{6.29}$$

Substituting Eqs. (6.5a) into Eq. (6.29) enables the total kinetic energy to be written as

$$T=\int_0^L[\frac{1}{2}\mu\dot{w}^2+\frac{1}{2}\mu_t\dot{u}_t^2+\frac{1}{2}\mu_b\dot{u}_b^2+\frac{1}{2}\mu_c(\frac{\dot{u}_t^2}{4}+\frac{\dot{u}_b^2}{4}+\dot{\psi}^2e_1^2+\frac{\dot{u}_t\dot{u}_b}{2}+\dot{u}_t\dot{\psi}e_1+\dot{u}_b\dot{\psi}e_1)]\,\mathrm{d}x \tag{6.30a}$$

or

$$T=\int_0^L[\frac{1}{2}\mu\dot{w}^2+\frac{1}{2}\mu_ce_1^2\dot{\psi}^2+\frac{1}{2}\mu_ce_1\dot{\psi}(\dot{u}_t+\dot{u}_b)+\frac{1}{2}(\mu_t+\frac{\mu_c}{4})\dot{u}_t^2+\frac{\mu_c}{4}\dot{u}_t\dot{u}_b+\frac{1}{2}(\mu_b+\frac{\mu_c}{4})\dot{u}_b^2]\,\mathrm{d}x \tag{6.30b}$$

6.3.2.2.3 Application of Hamilton's principle

Applying Hamilton's principle in the form

$$\delta^{(1)}\phi=\delta^{(1)}\int_{t_1}^{t_2}L\mathrm{d}t=\delta^{(1)}\int_{t_1}^{t_2}(T-U)\mathrm{d}t=\delta^{(1)}\int_{t_1}^{t_2}\int_0^L F\,\mathrm{d}x\,\mathrm{d}t=0 \tag{6.31}$$

in which the Lagrangian, $L=T-U$, has bean replaced by the functional $\int_0^L Fdx$, where the function F can be identified from Eqs. (6.28) and (6.30b) as

$$\begin{aligned}F=&\frac{1}{2}\mu\dot{w}^2+\frac{1}{2}\mu_ce_1^2\dot{\psi}^2+\frac{1}{2}\mu_ce_1\dot{\psi}(\dot{u}_t+\dot{u}_b)+\frac{1}{2}(\mu_t+\frac{\mu_c}{4})\dot{u}_t^2+\frac{\mu_c}{4}\dot{u}_t\dot{u}_b\\&+\frac{1}{2}(\mu_b+\frac{\mu_c}{4})\dot{u}_b^2-\frac{\hat{S}_c}{2}(\psi^2+\frac{u_t^2}{d^2}+\frac{u_b^2}{d^2}-\frac{2\psi u_t}{d}+\frac{2\psi u_b}{d}-\frac{2u_tu_b}{d^2})\\&-\frac{K_t}{2}u_t'^2-\frac{K_b}{2}u_b'^2-\frac{\psi'^2}{2\kappa}\end{aligned} \tag{6.32}$$

generates the governing differential equations of the motion. This could be evaluated by solving Eq. (6.31) directly (Dym and Shames 1973), but use is made here of the Euler-

Lagrange equations for a functional involving higher-order derivatives with more than one independent variable that are given by

$$\left.\begin{aligned}
&\frac{\partial F}{\partial w}-\frac{\partial}{\partial x}\frac{\partial F}{\partial w'}-\frac{\partial}{\partial t}\frac{\partial F}{\partial \dot{w}}+\frac{\partial^2}{\partial x^2}\frac{\partial F}{\partial w''}+\frac{\partial^2}{\partial x\partial t}\frac{\partial F}{\partial \dot{w}'}=0\\
&\frac{\partial F}{\partial u_t}-\frac{\partial}{\partial x}\frac{\partial F}{\partial u_t'}-\frac{\partial}{\partial t}\frac{\partial F}{\partial \dot{u}_t}=0\\
&\frac{\partial F}{\partial u_b}-\frac{\partial}{\partial x}\frac{\partial F}{\partial u_b'}-\frac{\partial}{\partial t}\frac{\partial F}{\partial \dot{u}_b}=0
\end{aligned}\right\} \qquad (6.33)$$

Using Eq.(6.2) and imposing Eqs. (6.33) on Eq. (6.32) yields

$$\left.\begin{aligned}
&-\frac{\partial}{\partial x}(-\hat{S}_c w'+\frac{\hat{S}_c}{d}u_t-\frac{\hat{S}_c}{d}u_b)-\frac{\partial}{\partial t}(\mu\dot{w})+\frac{\partial^2}{\partial x^2}(-\frac{w''}{\kappa})+\frac{\partial^2}{\partial x\partial t}[\mu_c e_1^2\dot{\psi}+\frac{1}{2}\mu_c e_1(\dot{u}_t+\dot{u}_b)]=0\\
&(\frac{\hat{S}_c w'}{d}-\frac{\hat{S}_c}{d^2}u_t+\frac{\hat{S}_c}{d^2}u_b)-\frac{\partial}{\partial x}(-K_t u_t')-\frac{\partial}{\partial t}(\frac{\mu_c}{2}e_1\dot{w}'+(\mu_t+\frac{\mu_c}{4})\dot{u}_t+\frac{\mu_c}{4}\dot{u}_b=0\\
&(-\frac{\hat{S}_c w'}{d}+\frac{\hat{S}_c}{d^2}u_t-\frac{\hat{S}_c}{d^2}u_b)-\frac{\partial}{\partial x}(-K_b u_b')-\frac{\partial}{\partial t}(\frac{1}{2}\mu_c\dot{w}'e_1+\frac{1}{4}\mu_c\dot{u}_t+(\mu_t+\frac{\mu_c}{4})\dot{u}_b)=0
\end{aligned}\right\} \qquad (6.34)$$

The possible boundary conditions can also be deduced from Hamilton's principle as

$$\frac{\partial F}{\partial w''}=0 \quad \text{or} \quad w'=0 \qquad (6.35a,b)$$

$$\frac{\partial}{\partial x}\frac{\partial F}{\partial w''}+\frac{\partial}{\partial t}\frac{\partial F}{\partial \dot{w}'}-\frac{\partial F}{\partial w'}=0 \quad \text{or} \quad w=0 \qquad (6.36a,b)$$

$$\frac{\partial F}{\partial u_t'}=0 \quad \text{or} \quad u_t=0 \qquad (6.37a,b)$$

$$\frac{\partial F}{\partial u_b'}=0 \quad \text{or} \quad u_b=0 \qquad (6.38a,b)$$

Eqs. (35a-38a) are the natural boundary conditions at either end of the element, while Eqs. (35b-38b) are the kinematic boundary conditions. The natural boundary conditions state the requirements for bending moment, shear force and axial forces in the faceplates as

$$-\frac{w''}{\kappa} = m = 0 \tag{6.39}$$

$$\frac{\partial}{\partial x}(-\frac{w''}{\kappa}) + \frac{\partial}{\partial t}[\mu_c e_1^2 \dot{w}' + \mu_c e_1(\dot{u}_t + \dot{u}_b)] + \hat{S}_c(w' - \frac{u_t}{d} + \frac{u_b}{d}) = q = 0 \tag{6.40}$$

$$K_t u_t' = n_t = 0 \tag{6.41}$$

$$K_b u_b' = n_b = 0 \tag{6.42}$$

If attention is now confined to harmonic motion as defined by Eq. (6.19), Eq. (6.34) can be written as

$$\left.\begin{aligned}
&-\frac{W''''}{\kappa} + \hat{S}_c W'' - \mu_c e_1^2 \omega^2 W'' + \mu \omega^2 W - \frac{\hat{S}_c}{d}U_t' - \frac{\mu_c}{2}e_1\omega^2 U_t' + \frac{\hat{S}_c}{d}U_b' - \frac{\mu_c}{2}e_1\omega^2 U_b' = 0 \\
&\frac{\hat{S}_c W'}{d} + \frac{\mu_c}{2}\omega^2 e_1 W' - \frac{\hat{S}_c}{d^2}U_t + (\mu_t + \frac{\mu_c}{4})\omega^2 U_t + K_t U_t'' + \frac{\hat{S}_c}{d^2}U_b + \frac{\mu_c}{4}\omega^2 U_b = 0 \\
&-\frac{\hat{S}_c W'}{d} + \frac{\mu_c}{2}\omega^2 e_1 W' + \frac{\hat{S}_c}{d^2}U_t + \frac{\mu_c}{4}\omega^2 U_t - \frac{\hat{S}_c}{d^2}U_b + (\mu_b + \frac{\mu_c}{4})\omega^2 U_b + K_b U_b'' = 0
\end{aligned}\right\} \tag{6.43}$$

Multiplying the first equation of Eq. (6.43) by (–1) and using the operator $D = \mathrm{d}/\mathrm{d}x$, Eq. (6.43) can be written in matrix form as

$$\begin{bmatrix}
\frac{D^4}{\kappa} - \hat{S}_c D^2 + \underline{\underline{\mu_c e_1^2 \omega^2 D^2}} - \mu\omega^2 & \underline{\underline{\frac{\hat{S}_c}{d}D + \frac{\mu_c}{2}e_1\omega^2 D}} & \underline{\underline{-\frac{\hat{S}_c}{d}D + \frac{\mu_c}{2}e_1\omega^2 D}} \\
\underline{\underline{\frac{\hat{S}_c}{d}D + \frac{\mu_c}{2}\omega^2 e_1 D}} & \underline{\underline{-\frac{\hat{S}_c}{d^2} + (\mu_t + \frac{\mu_c}{4})\omega^2 + K_t D^2}} & \underline{\underline{\frac{\hat{S}_c}{d^2} + \frac{\mu_c}{4}\omega^2}} \\
\underline{\underline{-\frac{\hat{S}_c}{d}D + \frac{\mu_c}{2}\omega^2 e_1 D}} & \underline{\underline{\frac{\hat{S}_c}{d^2} + \frac{\mu_c}{4}\omega^2}} & \underline{\underline{-\frac{\hat{S}_c}{d^2} + (\mu_b + \frac{\mu_c}{4})\omega^2 + K_b D^2}}
\end{bmatrix}
\begin{bmatrix} W \\ U_t \\ U_b \end{bmatrix} = 0 \tag{6.44}$$

where the matrix operator is symmetric. The double underlined terms in Eq. (6.44) result from the inclusion of the longitudinal inertia. Combining Eq. (6.44) into one equation by eliminating either W, U_t or U_b yields a linear eighth order differential equation that is identical to Eq. (6.22). This can be seen from the fact that the matrix operator of

Eq.(6.21) can be determined from the matrix operator of Eq. (6.44) using matrix operations that don't change its determinant, as follows:

i) Differentiate the second row of Eq. (6.44) once, multiply by d and then add it to the first row of Eq. (6.44) to give the first row of Eq. (6.21),

ii) Add the last two rows of Eq. (6.44) to give the second row of Eq. (6.21), and finally

iii) Subtracting the second row from the third row of Eq. (6.44) yields the third row of Eq. (6.21).

For later use it is convenient to represent Eq. (6.44) in a more symbolic form as

$$\begin{bmatrix} A_1D^4 + A_2D^2 + A_3 & (A_4 + A_5)D & (-A_4 + A_5)D \\ (A_4 + A_5)D & A_6D^2 + A_7 & A_8 \\ (-A_4 + A_5)D & A_8 & A_9D^2 + A_{10} \end{bmatrix} \begin{bmatrix} W \\ U_t \\ U_b \end{bmatrix} = 0 \tag{6.45}$$

where

$$\left.\begin{aligned} &A_1 = 1/\kappa; \quad A_2 = -\hat{S}_c + \mu_c e_1^2 \omega^2; \quad A_3 = -\mu \omega^2; \quad A_4 = \hat{S}_c/d; \\ &A_5 = \frac{\mu_c}{2} e_1 \omega^2; \quad A_6 = K_t; \quad A_7 = (\mu_t + \mu_c/4)\,\omega^2 - \hat{S}_c/d^2; \\ &A_8 = \hat{S}_c/d^2 + \omega^2 \mu_c/4; \quad A_9 = K_b; \quad A_{10} = (\mu_b + \mu_c/4)\,\omega^2 - \hat{S}_c/d^2 \end{aligned}\right\} \tag{6.46}$$

6.3.3 Dynamic stiffness formulation

In the dynamic stiffness matrix method, the harmonically varying forces are related to the harmonically varying displacements. Expressions for the general displacements W, Ψ, U_t and U_b can be deduced from Eqs. (6.2), (6.19) and (6.22) and the expressions

for the corresponding forces can be obtained by substituting Eq. (6.19) into Eqs.(6.39)-(6.42) to yield

$$\left.\begin{aligned} Q &= -\frac{W'''}{\kappa} - (\mu_c e_1^2\omega^2 - \hat{S}_c)W' - (\mu_c\omega^2 e_1 + \frac{\hat{S}_c}{d})U_t - (\mu_c\omega^2 e_1 - \frac{\hat{S}_c}{d})U_b \\ M &= -\frac{W''}{\kappa} \\ N_t &= K_t U_t' \\ N_b &= K_b U_b' \end{aligned}\right\} \qquad (6.47)$$

Alternatively, Eq. (6.47) can be determined from the theory presented in the equilibrium approach by imposing Eq. (6.19) on Eq. (6.11), (6.10) and (6.1a). The only difference is that the expression for shear force is presented in an alternative, but numerically equal form as

$$Q = -\frac{W'''}{\kappa} - ae_1\mu_c\omega^2 W' - K_t d U_t'' - (\mu_t d + \mu_c\frac{a}{2})\omega^2 U_t - \mu_c\frac{a}{2}\omega^2 U_b \qquad (6.48)$$

6.3.3.1 Solution of the governing differential equation of motion

The next step is to solve the governing differential equations of motion, Eq. (6.22), for the harmonically varying displacement field. Eq. (6.22) is a linear differential equation with constant coefficients and its solution can be sought in the following form

$$V = \sum_{j=1}^{8} \overline{C}_{ij}\zeta_j \quad \text{where} \quad \zeta_j = e^{\eta_j x}; \quad 0 < x < L \qquad (6.49a,b)$$

η_j are the roots of the characteristic equation stemming from Eq. (6.22) and the $\overline{C}_{ij}$ are arbitrary constants where, for convenience in developing the work that follows, i is an assigned integer that defines a set of j arbitrary constants, e.g. $\overline{C}_{1j} = \overline{A}_j$, $\overline{C}_{2j} = \overline{B}_j$ etc., where $\overline{A}_j$, $\overline{B}_j$ are independent sets of arbitrary constants.

The η_j can now be determined as the roots of

$$\eta^8 + c_1\eta^6 + c_2\eta^4 + c_3\eta^2 + c_4 = 0 \tag{6.50}$$

The η_j define V (W, U_t or U_b), which may be substituted into Eq. (6.47) to yield the following results

$$\left.\begin{aligned} W &= \sum_{j=1}^{8} H_{1j}C_j\zeta_j \quad & Q &= \sum_{j=1}^{8} H_{5j}C_j\zeta_j \\ \Psi &= \sum_{j=1}^{8} H_{2j}C_j\zeta_j \quad & M &= \sum_{j=1}^{8} H_{6j}C_j\zeta_j \\ U_t &= \sum_{j=1}^{8} H_{3j}C_j\zeta_j \quad & N_t &= \sum_{j=1}^{8} H_{7j}C_j\zeta_j \\ U_b &= \sum_{j=1}^{8} H_{4j}C_j\zeta_j \quad & N_b &= \sum_{j=1}^{8} H_{8j}C_j\zeta_j \end{aligned}\right\} \tag{6.51}$$

where $H_{ij}C_j = \overline{C}_{ij}$, such that C_j is common to all the equations and H_{ij} is the relational constant. Noting that one of the H_{ij} is arbitrary, it is convenient to set $H_{1j} = 1$, which yields the following relationships between the H_{ij} of Eqs. (6.51)

$$\left.\begin{aligned} H_{1j} &= 1 \quad & H_{3j} &= \frac{A_8(A_1\eta_j^4 + A_2\eta_j^2 + A_3) - (A_5^2 - A_4^2)\eta_j^2}{[(A_6\eta_j^2 + A_7)(A_5 - A_4) - A_8(A_4 + A_5)]\eta_j} \\ H_{2j} &= \eta_j \quad & H_{4j} &= -\frac{(A_4 + A_5)\eta_j + (A_6\eta_j^2 + A_7)H_{3j}}{A_8} \\ H_{6j} &= -\eta_j^2/\kappa \quad & H_{5j} &= -[\frac{\eta_j^3}{\kappa} + (\mu_c e_1^2\omega^2 - \hat{S}_c)\eta_j + (\mu_c\omega^2 e_1 + \frac{\hat{S}_c}{d})H_{3j} \\ & & & \quad + (\mu_c\omega^2 e_1 - \frac{\hat{S}_c}{d})H_{4j}] \\ H_{7j} &= K_t\eta_j H_{3j} \quad & H_{8j} &= K_b\eta_j H_{4j} \end{aligned}\right\} \tag{6.52}$$

Alternatively, Eq. (6.48) yields H_{5j} as

$$H_{5j} = -\{\frac{\eta_j^3}{\kappa} + ae_1\mu_c\omega^2\eta_j + [K_t d\eta_j^2 + (\mu_t d + \mu_c\frac{a}{2})\omega^2]H_{3j} + \mu_c\frac{a}{2}\omega^2 H_{4j}\} \tag{6.53}$$

6.3.3.2 *Transformation between local and member co-ordinate systems*

All the equations developed so far have been based on the forces and displacements in the local co-ordinate system shown in Figure 6.4(a). The stiffness formulation requires all nodal forces and displacements to be represented in the member co-ordinate system shown in Figure 6.4(b). Hence, the nodal forces and displacements in the local co-ordinate system are now transformed to the member co-ordinate system.

The relationship between the forces and displacements in these two co-ordinate systems can be obtained by comparing Figures 6.4(a) and (b). This is equivalent to imposing the conditions of Eq. (6.54) onto Eq. (6.47).

$$
\left.\begin{array}{llll}
\text{At } x=0: & & & \\
W=W_1; & \Psi=\Psi_1; & U_t=U_{t1}; & U_b=U_{b1}; \\
Q=-Q_1; & M=M_1; & N_t=-N_{t1}; & N_b=-N_{b1} \\
 & & & \\
\text{At } x=L: & & & \\
W=W_2; & \Psi=\Psi_2, & U_t=U_{t2}, & U_b=U_{b1}, \\
Q=Q_2, & M=-M_2, & N_t=N_{t2}, & N_b=N_{b2}
\end{array}\right\} \qquad (6.54)
$$

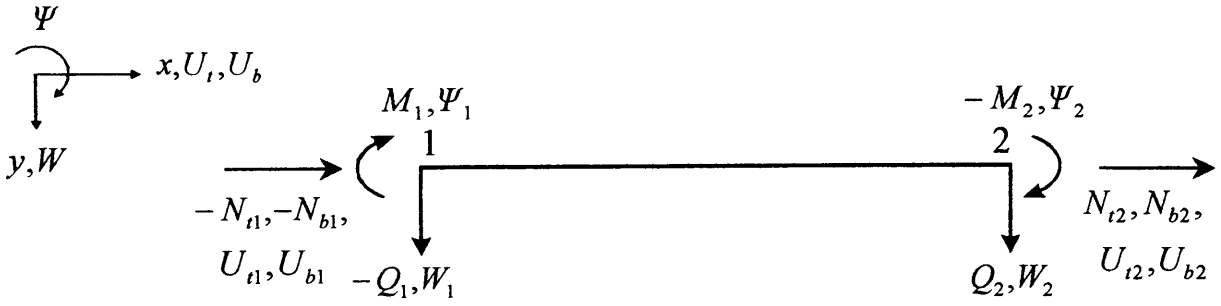

(a)

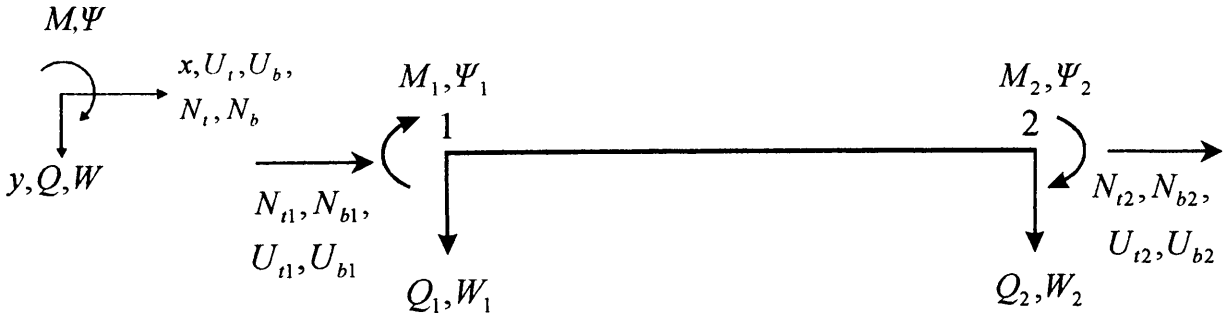

(b)

Figure 6.4: Nodal forces and displacements a) in local co-ordinates, b) in member co-ordinates.

6.3.3.3 Dynamic stiffness matrix

The dynamic stiffness matrix relates the forces to the displacements at the two end nodes of a member as

$$\mathbf{p} = \mathbf{k}\mathbf{d} \tag{6.55}$$

where

$$\mathbf{d} = \begin{bmatrix} W_1 \\ \Psi_1 \\ U_{t1} \\ U_{b1} \\ W_2 \\ \Psi_2 \\ U_{t2} \\ U_{b2} \end{bmatrix}; \qquad \mathbf{p} = \begin{bmatrix} Q_1 \\ M_1 \\ N_{t1} \\ N_{b1} \\ Q_2 \\ M_2 \\ N_{t2} \\ N_{b2} \end{bmatrix}; \tag{6.56}$$

and $\mathbf{k}$ is the eight by eight dynamic stiffness matrix. As a result of Eq. (6.51), all of the elements of $\mathbf{d}$ and $\mathbf{p}$ are related to the coefficient vector $\mathbf{C}$ through the matrices $\mathbf{S}$ and $\mathbf{S}^*$ by

$$\mathbf{d} = \mathbf{S}\mathbf{C} \qquad \text{and} \qquad \mathbf{p} = \mathbf{S}^*\mathbf{C} \tag{6.57a,b}$$

where

$$\mathbf{C} = \begin{bmatrix} C_1 \\ C_2 \\ C_3 \\ C_4 \\ C_5 \\ C_6 \\ C_7 \\ C_8 \end{bmatrix} \tag{6.58}$$

and s_{ij} and s_{ij}^*, the elements of $\mathbf{S}$ and $\mathbf{S}^*$, respectively, are as follows

$$\left.\begin{array}{llll} s_{1j}=H_{1j} \;; & s_{2j}=H_{2j} \;; & s_{3j}=H_{3j} \;; & s_{4j}=H_{4j} \\ s_{5j}=H_{1j}\chi_j \;; & s_{6j}=H_{2j}\chi_j \;; & s_{7j}=H_{3j}\chi_j \;; & s_{8j}=H_{4j}\chi_j \\ s^*_{1j}=-H_{5j} \;; & s^*_{2j}=H_{6j} \;; & s^*_{3j}=-H_{7j} \;; & s^*_{4j}=-H_{8j} \\ s^*_{5j}=H_{5j}\chi_j \;; & s^*_{6j}=-H_{6j}\chi_j \;; & s^*_{7j}=H_{7j}\chi_j \;; & s^*_{8j}=H_{8j}\chi_j \\ \chi_j=e^{\eta_j L} & (j=1,2,\ldots 8) & & \end{array}\right\} \quad (6.59)$$

where their subscripts correspond to row and column co-ordinates in the usual way.

The required dynamic stiffness matrix, **k**, follows through the following steps

$$\mathbf{C}=\mathbf{S}^{-1}\mathbf{d} \qquad \text{therefore} \qquad \mathbf{p}=\mathbf{S}^*\mathbf{S}^{-1}\mathbf{d} \qquad \text{and finally} \qquad \mathbf{k}=\mathbf{S}^*\mathbf{S}^{-1} \quad (6.60)$$

The dynamic stiffness matrix for the overall structure can now be assembled from the element matrices in the usual way. In the next section, the method for converging with certainty on the required natural frequencies is described. Once the required natural frequencies have been determined, the corresponding mode shapes can be retrieved by any reliable method, such as described in reference (Howson 1979).

6.3.4 Converging on the natural frequencies

The dynamic structure stiffness matrix, **K**, when assembled from the element matrices, yields the required natural frequencies as solutions of the equation

$$\mathbf{K}\,\mathbf{D}=\mathbf{0} \quad (6.61)$$

where **D** is the vector of amplitudes of the harmonically varying nodal displacements and **K** is a function of ω, the circular frequency. When **K** is developed from exact member theory the determinant is a highly irregular, transcendental function of ω and such a formulation necessitates the solution of a transcendental eigenvalue problem. This is accomplished using the Wittrick-Williams algorithm (Wittrick and Williams 1971a),

which determines how many natural frequencies lie below a specified trial frequency. The algorithm states that

$$J = J_0 + s\{\mathbf{K}\} \tag{6.62}$$

where J is the number of natural frequencies of the structure exceeded by some trial frequency, ω^*, J_0 is the number of natural frequencies which would still be exceeded if all the elements were clamped at their ends so as to make $\mathbf{D} = \mathbf{0}$, and $s\{\mathbf{K}\}$ is the sign count of the matrix $\mathbf{K}$. $s\{\mathbf{K}\}$ is defined in reference (Wittrick and Williams 1971a) and is equal to the number of negative elements on the leading diagonal of the upper triangular matrix obtained from $\mathbf{K}$, when $\omega = \omega^*$, by the standard form of Gauss elimination without row interchanges.

The knowledge of J corresponding to any trial frequency makes it possible to develop a method for converging upon any required natural frequency to any desired accuracy. However, while $s\{\mathbf{K}\}$ is easily computed, the value of J_0 is more difficult to determine and is dealt with below.

6.3.4.1 Determination of J_0

From the definition of J_0 it can be seen that

$$J_0 = \sum J_m \tag{6.63}$$

where J_m is the number of natural frequencies of a component element, with its ends clamped, which have been exceeded by ω^* and the summation extends over all such elements. In this case, the determination of J_m is achieved by an argument based on Eq. (6.62) which was originally put forward by Howson and Williams (Howson and Williams 1973).

Consider an element that has been isolated from the remainder of the structure by clamping its ends. Unfortunately, this structure cannot be solved easily. We therefore seek to establish a different set of boundary conditions that admit a simple symbolic solution and which enable solutions to the clamped ended case to be deduced. This is most easily achieved by imposing roller-roller supports which, in this case, permit rotation and longitudinal motion of the faceplates, i.e. Ψ, U_t and U_b respectively, but prevent lateral displacement W, (Figure 6.5).

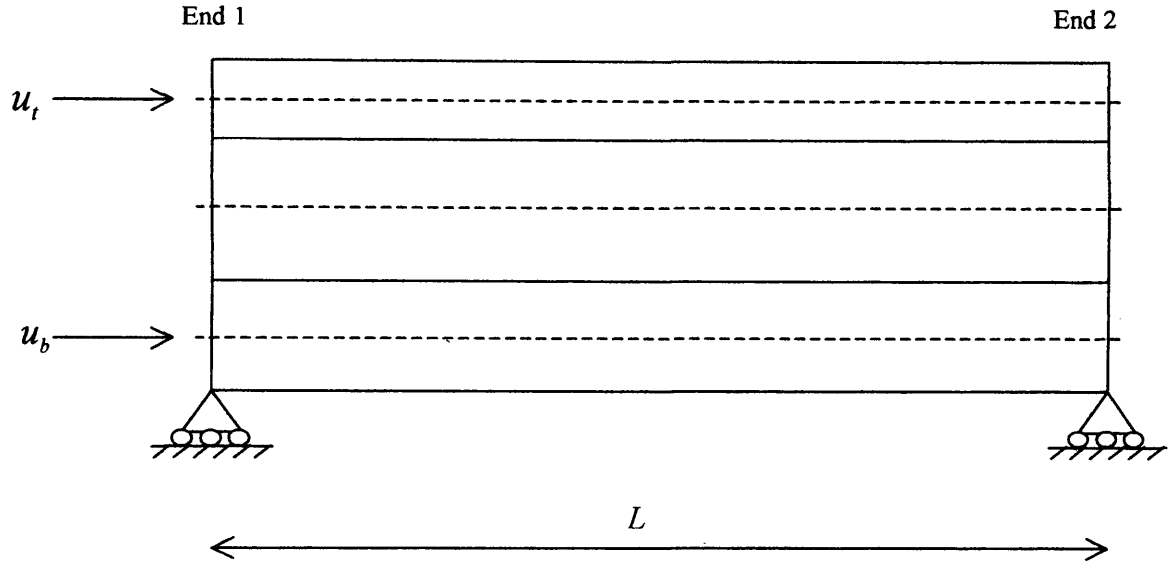

Figure 6.5: Roller-roller supported beam and the position of possible axial freedoms through the beam thickness.

Let the stiffness matrix for this structure is $\mathbf{k}^{rr}$, then the number of roots exceeded by ω^* is given by equation (6.62) and the arguments above as

$$J_{rr} = J_m + s\{\mathbf{k}^{rr}\} \tag{6.64}$$

where J_{rr} is the number of natural frequencies that lie below the trial frequency for the element with roller-roller supports. It then follows directly that

$$J_m = J_{rr} - s\{\mathbf{k}^{rr}\} \tag{6.65}$$

Once more $\mathbf{k}^{rr}$, and hence $s\{\mathbf{k}^{rr}\}$, is readily obtained, this time from Eq. (6.60). J_{rr} is slightly more difficult, but relates to the element with boundary conditions that yield a simple exact solution, as shown below.

For the roller-roller-supported case, the boundary conditions are defined by

$$M_1 = M_2 = W_1 = W_2 = 0 \tag{6.66}$$

These conditions are satisfied by assuming solutions of the form

$$\begin{aligned} W &= B_1 \sin \delta x \\ U_t &= B_2 \cos \delta x \\ U_b &= B_3 \cos \delta x \end{aligned} \tag{6.67}$$

where B_1, B_2 and B_3 are constants and $\delta = \frac{n\pi}{L}$, (n = 0,1,2,3,...). Since Eq. (6.22) is a combined equation which allows for the effects of W, U_t and U_b, substituting any part of Eq. (6.67) into Eq. (6.22) yields the frequency equation for a roller-roller supported beam as

$$\delta^8 - c_1\delta^6 + c_2\delta^4 - c_3\delta^2 + c_4 = 0 \tag{6.68}$$

Substituting Eqs.(6.23) into Eq. (6.68) leads to the following frequency equation

$$b_1\omega^6 + b_2\omega^4 + b_3\omega^2 + b_4 = 0 \tag{6.69}$$

where

$$
\left.
\begin{aligned}
b_1 &= -\frac{\kappa}{K_t K_b}[\mu_t \mu_b(\mu + \delta^2 \mu_c e_1^2) + \mu \mu_c(\mu_t + \mu_b)/4] \\
b_2 &= \frac{\hat{S}_c \mu^2 \kappa}{d^2 K_t K_b} + [\frac{\hat{S}_c \kappa}{K_t K_b}\{\mu_t \mu_b + \frac{\mu_c e_1}{d}(\mu_b - \mu_t) + \mu_c(\mu_t + \mu_b)(\frac{1}{4} + \frac{e_1^2}{d^2})\} \\
&\quad + \mu \kappa (\frac{1}{\hat{\varsigma}} + \frac{\mu_c}{4\varsigma})]\delta^2 + (\frac{\mu_t \mu_b}{K_t K_b} + \frac{\mu_c(\mu_t + \mu_b)}{4K_t K_b} + \frac{\mu_c \kappa e_1^2}{\hat{\varsigma}})\delta^4 \\
b_3 &= -\frac{\hat{S}_c \mu \kappa}{\varsigma d^2}\delta^2 + [\frac{\hat{S}_c \mu_c \kappa e_1}{\varsigma d}(\frac{K_t - K_b}{K_t + K_b} - \frac{e_1}{d}) - \hat{S}_c \kappa (\frac{1}{\hat{\varsigma}} + \frac{\mu_c}{4\varsigma}) - \mu(\kappa + \frac{\hat{S}_c}{d^2 K_t K_b})]\delta^4 \\
&\quad - (\frac{1}{\hat{\varsigma}} + \frac{\mu_c}{4\varsigma} + \mu_c \kappa e_1^2)\delta^6 \\
b_4 &= \hat{S}_c(\frac{1}{d^2 \varsigma} + \kappa)\delta^6 + \delta^8
\end{aligned}
\right\} \quad (6.70)
$$

Eq. (6.69) can be expressed as a cubic equation in ω^2 and consequently its real, positive roots are the square of its natural frequencies for each value of $n = 0, 1, 2, \ldots$. Hence J_{rr} is given by the number of positive values of ω_n that lie below the trial frequency, ω^*. Thus, substituting Eq. (6.65) into Eq. (6.63) gives

$$J_0 = \sum (J_{rr} - s\ \{\mathbf{k}^{rr}\}) \qquad (6.71)$$

The required value of J then follows from Eq. (6.62).

It is interesting to note that when $n = 0$, $\delta = 0$. The coefficients b_3 and b_4 are zero and it can be shown that b_1 is always negative and that b_2 is always positive. Eq. (6.69) then yields a single non-trivial real root. It is equally clear from Eq. (6.67) that

$$W = 0 \ ; \qquad U_t = B_2 \ ; \qquad U_b = B_3 \qquad (6.72)$$

Thus the mode corresponding to $n = 0$ has no lateral displacement and horizontal rigid body displacements of the faceplates. Furthermore, since there is no axial extension, the frequency corresponds to the fundamental shear thickness mode.

6.4 GENERAL VIBRATIONS OF A THREE-LAYER SANDWICH BEAM INCLUDING LONGITUDINAL AND ROTARY INERTIA

Although the inclusion of longitudinal inertia has a major influence on the theory of Chapter 5, the second order effects due to rotary inertia can be included to yield a more accurate version of the theory that is important when considering deep sandwich beams or when vibrations occur at high frequency. Hence, the only difference between this section and Section 6.3 is to modify the theory for the influence of rotary inertia. Hence only those equations that have to be modified are given.

6.4.2 Derivation of the governing differential equation of motion

6.4.2.1 Equilibrium approach

Consider a typical elemental length of a member at some instant during the motion, as shown in Figure 6.6. The only differences between this figure and Figure 6.2 are the reverse rotary inertia actions. Hence, Eqs. (6.6)-(6.8) still hold. Eq. (6.9) should be modified to include the rotary inertia effects as

$$q\,\mathrm{d}x-\frac{\partial m}{\partial x}\mathrm{d}x+\frac{\partial n_t}{\partial x}\mathrm{d}x(d)-\mu_t\ddot{u}_t\,\mathrm{d}x(d)-\mu_c\ddot{u}_c\,\mathrm{d}x(a) -(\mu_t\frac{t_t^2}{12}\mathrm{d}x+\mu_b\frac{t_b^2}{12}\mathrm{d}x)\ddot{w}'-\mu_c\frac{t_c^2}{12}\mathrm{d}x\ddot{\varphi}_c=0 \tag{6.73}$$

Now, substituting Eqs. (6.1a), (6.5), (6.2) and (6.10) into Eq. (6.73) yields the resultant shear force as

$$q=-\frac{\psi''}{\kappa}-K_t d\,u_t''+(\mu_t d+\mu_c\frac{a}{2}+\mu_c\frac{t_c}{12})\ddot{u}_t+(\mu_c\frac{a}{2}-\mu_c\frac{t_c}{12})\ddot{u}_b +(ae_1\mu_c+\mu_t\frac{t_t^2}{12}+\mu_b\frac{t_b^2}{12}-\mu_c\frac{t_c}{12}e_2)\ddot{\psi} \tag{6.74}$$

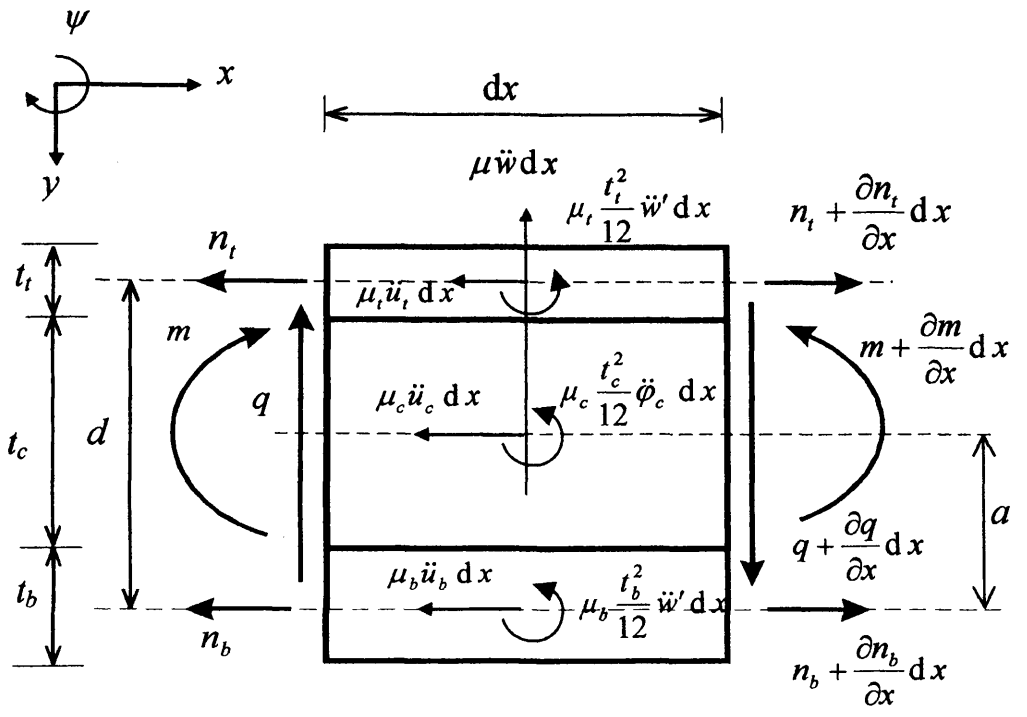

Figure 6.6: Positive resultant forces and moments and reversed linear and rotary inertias acting on a typical elemental length of a sandwich beam of unit width in local co-ordinates. The layer dimensions are also shown.

On substituting Eq. (6.74) into Eq. (6.8) the equivalent second differential equation of motion is given as

$$\mu\ddot{w} + \frac{\psi'''}{\kappa} + K_t d\, u_t''' - (d\mu_t + a\frac{\mu_c}{2} + \mu_c \frac{t_c}{12})\ddot{u}_t' - (a\frac{\mu_c}{2} - \mu_c \frac{t_c}{12})\ddot{u}_b' - (ae_1\mu_c + \mu_t \frac{t_t^2}{12} + \mu_b \frac{t_b^2}{12} - \mu_c \frac{t_c}{12}e_2)\ddot{\psi} = 0 \tag{6.75}$$

Eqs. (6.13)-(6.16) still hold, but Eq. (6.17), which is a moment equation, should be modified to include the rotary inertia of the core, as follows

$$-\tau_t\,dx\frac{t_c}{2} - \tau_b\,dx\frac{t_c}{2} + \tau_c t_c\,dx - \mu_c \frac{t_c^2}{12}dx\ddot{\varphi}_c = 0 \tag{6.76}$$

Substituting Eqs. (6.3), (6.4), (6.5b), (6.14) and (6.16) into Eq. (6.76) gives the equivalent final differential equation of motion as

$$K_t u_t'' - (\mu_t + \frac{\mu_c}{6})\ddot{u}_t - K_b u_b'' + (\mu_b + \frac{\mu_c}{6})\ddot{u}_b + \frac{2G_c d}{t_c}\psi - \frac{2G_c}{t_c}u_t + \frac{2G_c}{t_c}u_b + \frac{\mu_c}{6}e_2\ddot{\psi} = 0 \tag{6.77}$$

Substituting Eq. (6.19) into the partial differential equations of Eqs. (6.75), (6.7) and (6.77) yields the following linear differential equations with constant coefficients

$$\left.\begin{aligned} &-\mu\omega^2 W + \frac{W''''}{\kappa} + K_t d U_t''' + (d\mu_t + a\frac{\mu_c}{2} + \mu_c\frac{t_c}{12})\omega^2 U_t' + (a\frac{\mu_c}{2} - \mu_c\frac{t_c}{12})\omega^2 U_b' \\ &\qquad + (ae_1\mu_c + \mu_t\frac{t_t^2}{12} + \mu_b\frac{t_b^2}{12} - \mu_c\frac{t_c}{12}e_2)\omega^2 W'' = 0 \\ &K_t U_t'' + K_b U_b'' + (\mu_t + \frac{\mu_c}{2})\omega^2 U_t + (\mu_b + \frac{\mu_c}{2})\omega^2 U_b + \mu_c e_1\omega^2 W' = 0 \\ &K_t U_t'' + (\mu_t + \frac{\mu_c}{6})\omega^2 U_t - K_b U_b'' - (\mu_b + \frac{\mu_c}{6})\omega^2 U_b + \frac{2G_c d}{t_c}W' \\ &\qquad - \frac{2G_c}{t_c}U_t + \frac{2G_c}{t_c}U_b - \frac{\mu_c}{6}e_2\omega^2 W' = 0 \end{aligned}\right\} \tag{6.78}$$

Now using the operator $D = \mathrm{d}/\mathrm{d}x$, Eq. (6.78) can be written in matrix form as

$$\begin{bmatrix} \left\{\begin{matrix} \frac{D^4}{\kappa} - \mu\omega^2 + [\frac{\mu_t t_t^2 + \mu_b t_b^2}{12} \\ -\mu_c(ae_1 + \frac{t_c}{12}e_2)]\omega^2 D^2 \end{matrix}\right\} & \left\{\begin{matrix} K_t d D^3 + [d\mu_t \\ +\mu_c(\frac{a}{2} + \frac{t_c}{12})]\omega^2 D \end{matrix}\right\} & (a\frac{\mu_c}{2} - \mu_c\frac{t_c}{12})\omega^2 D \\ \mu_c e_1\omega^2 D & K_t D^2 + (\mu_t + \frac{\mu_c}{2})\omega^2 & K_b D^2 + (\mu_b + \frac{\mu_c}{2})\omega^2 \\ (\frac{2G_c d}{t_c} - \frac{\mu_c}{6}e_2\omega^2)D & \left\{\begin{matrix} K_t D^2 - \frac{2G_c}{t_c} \\ +(\mu_t + \frac{\mu_c}{6})\omega^2 \end{matrix}\right\} & \left\{\begin{matrix} -K_b D^2 + \frac{2G_c}{t_c} \\ -(\mu_b + \frac{\mu_c}{6})\omega^2 \end{matrix}\right\} \end{bmatrix} \begin{bmatrix} W \\ U_t \\ U_b \end{bmatrix} = 0 \tag{6.79}$$

Eq. (6.79) can be combined into one equation by eliminating either W, U_t or U_b to yield the corresponding linear eighth order differential equation. However this is postponed until application of the energy approach confirms Eq. (6.79).

6.4.2.2 Energy approach

Since inclusion of the rotary inertia terms does not affect the potential energy of the element, Eqs. (6.25-6.28) still hold.

6.4.2.2.1 Kinetic energy

The total kinetic energy of a sandwich beam of length L including the axial, rotary and transverse inertia of the layers is given by

$$T=\int_0^L\left(\begin{array}{ll}\frac{1}{2}\mu\dot{w}^2+ & \text{Transverse inertia of full section}\\ \frac{1}{2}\mu_t\dot{u}_t^2+\frac{1}{2}\mu_c\dot{u}_c^2+\frac{1}{2}\mu_b\dot{u}_b^2+ & \text{Axial inertia of each layer}\\ \frac{1}{2}\mu_t\frac{t_t^2}{12}\dot{w}'^2+\frac{1}{2}\mu_b\frac{t_b^2}{12}\dot{w}'^2+\frac{1}{2}\mu_c\frac{t_c^2}{12}\dot{\phi}_c^2 & \text{Rotary inertia of each layer}\end{array}\right)\mathrm{d}x \qquad (6.80)$$

Substituting Eqs. (6.5) into Eq. (6.80) enables the total kinetic energy to be written as

$$\begin{aligned}T=\int_0^L[&\frac{1}{2}\mu\dot{w}^2+\frac{1}{2}\mu_t\dot{u}_t^2+\frac{1}{2}\mu_b\dot{u}_b^2\\&+\frac{1}{2}\mu_c(\frac{\dot{u}_t^2}{4}+\frac{\dot{u}_b^2}{4}+\dot{w}'^2e_1^2+\frac{\dot{u}_t\dot{u}_b}{2}+\dot{u}_t\dot{w}'e_1+\dot{u}_b\dot{w}'e_1)+\frac{1}{2}(\mu_t\frac{t_t^2}{12}+\mu_b\frac{t_b^2}{12})\dot{w}'^2\\&+\frac{1}{2}\mu_c\frac{t_c^2}{12}(\frac{\dot{u}_t^2}{t_c^2}+\frac{\dot{u}_b^2}{t_c^2}+\frac{\dot{w}'^2e_2^2}{t_c^2}-\frac{2\dot{u}_t\dot{u}_b}{t_c^2}-\frac{2\dot{u}_t\dot{w}'e_2}{t_c^2}+\frac{2\dot{u}_b\dot{w}'e_2}{t_c^2})\,]\,\mathrm{d}x\end{aligned} \qquad (6.81)$$

or

$$\begin{aligned}T=\int_0^L[&\frac{1}{2}\mu\dot{w}^2+\frac{1}{2}r\dot{w}'^2+\mu_c\dot{w}'(\dot{u}_te_3+\dot{u}_be_4)\\&+\frac{\mu_c}{6}(\dot{u}_t^2+\dot{u}_b^2+\dot{u}_t\dot{u}_b)+\frac{1}{2}\mu_t\dot{u}_t^2+\frac{1}{2}\mu_b\dot{u}_b^2]\,\mathrm{d}x\end{aligned} \qquad (6.82)$$

where $e_3=\frac{e_1}{2}-\frac{e_2}{12}$; $e_4=\frac{e_1}{2}+\frac{e_2}{12}$ and $r=\frac{\mu_t t_t^2+\mu_b t_b^2}{12}+\mu_c e_1^2+\frac{\mu_c}{12}e_2^2$.

6.4.2.2.2 Application of Hamilton's principle

Considering the effects of rotary inertia in the kinetic energy Eq. (6.82) requires Eq. (6.32) to be modified as

$$F=\frac{1}{2}\mu\dot{w}^2+\frac{1}{2}r\dot{w}'^2+\mu_c\dot{w}'(\dot{u}_te_3+\dot{u}_be_4)+\frac{\mu_c}{6}(\dot{u}_t^2+\dot{u}_b^2+\dot{u}_t\dot{u}_b)+\frac{1}{2}\mu_t\dot{u}_t^2+\frac{1}{2}\mu_b\dot{u}_b^2$$
$$-\frac{\hat{S}_c}{2}(w'^2+\frac{u_t^2}{d^2}+\frac{u_b^2}{d^2}-\frac{2w'u_t}{d}+\frac{2w'u_b}{d}-\frac{2u_tu_b}{d^2})-\frac{K_t}{2}u_t'^2-\frac{K_b}{2}u_b'^2-\frac{w''^2}{2\kappa} \tag{6.83}$$

Imposing Eqs. (6.33) on Eq. (6.83) yields

$$\left.\begin{aligned}
&-\frac{\partial}{\partial x}(-\hat{S}_cw'+\frac{\hat{S}_c}{d}u_t-\frac{\hat{S}_c}{d}u_b)-\frac{\partial}{\partial t}(\mu\dot{w})+\frac{\partial^2}{\partial x^2}(-\frac{w''}{\kappa})+\frac{\partial^2}{\partial x\partial t}(r\dot{w}'+\mu_ce_3\dot{u}_t+\mu_ce_4\dot{u}_b)=0\\
&(\frac{\hat{S}_cw'}{d}-\frac{\hat{S}_c}{d^2}u_t+\frac{\hat{S}_c}{d^2}u_b)-\frac{\partial}{\partial x}(-K_tu_t')-\frac{\partial}{\partial t}(\mu_c\dot{w}'e_3+\frac{\mu_c}{3}\dot{u}_t+\frac{\mu_c}{6}\dot{u}_b+\mu_t\dot{u}_t)=0\\
&(-\frac{\hat{S}_cw'}{d}+\frac{\hat{S}_c}{d^2}u_t-\frac{\hat{S}_c}{d^2}u_b)-\frac{\partial}{\partial x}(-K_bu_b')-\frac{\partial}{\partial t}(\mu_c\dot{w}'e_4+\frac{1}{6}\mu_c\dot{u}_t+\frac{\mu_c}{3}\dot{u}_b+\mu_t\dot{u}_b)=0
\end{aligned}\right\} \tag{6.84}$$

The possible boundary conditions of Eqs. (6.35)-(6.39) and (6.41)-(6.42) have not been affected. However, the equivalent of Eq. (6.40), i.e the shear force, modified as follows.

$$\frac{\partial}{\partial x}(-\frac{w''}{\kappa})+\frac{\partial}{\partial t}[r\dot{w}'+\mu_c(\dot{u}_te_3+\dot{u}_be_4)]+\hat{S}_c(w'-\frac{u_t}{d}+\frac{u_b}{d})=q=0 \tag{6.85}$$

Once more attention is now confined to harmonic motion, as defined by Eq. (6.19), and Eq. (6.84) can be written as

$$\left.\begin{aligned}
&-\frac{W''''}{\kappa}+\hat{S}_cW''-r\omega^2W''+\mu\omega^2W-\frac{\hat{S}_c}{d}U_t'-\mu_ce_3\omega^2U_t'+\frac{\hat{S}_c}{d}U_b'-\mu_ce_4\omega^2U_b'=0\\
&\frac{\hat{S}_cW'}{d}+\mu_c\omega^2e_3W'-\frac{\hat{S}_c}{d^2}U_t+\bar{\mu}_t\omega^2U_t+K_tU_t''+\frac{\hat{S}_c}{d^2}U_b+\frac{\mu_c}{6}\omega^2U_b=0\\
&-\frac{\hat{S}_cW'}{d}+\mu_c\omega^2e_4W'+\frac{\hat{S}_c}{d^2}U_t+\frac{\mu_c}{6}\omega^2U_t-\frac{\hat{S}_c}{d^2}U_b+\bar{\mu}_b\omega^2U_b+K_bU_b''=0
\end{aligned}\right\} \tag{6.86}$$

Multiplying the first equation of Eq. (6.43) by (–1) and using the operator $D = \mathrm{d}/\mathrm{d}x$, Eq.(6.86) can be written in matrix form as

$$\begin{bmatrix} \frac{D^4}{\kappa} - \hat{S}_c D^2 + \underline{\underline{r\omega^2 D^2}} - \mu\omega^2 & \underline{\underline{\frac{\hat{S}_c}{d} D + \mu_c e_3 \omega^2 D}} & \underline{\underline{-\frac{\hat{S}_c}{d} D + \mu_c e_4 \omega^2 D}} \\ \underline{\underline{\frac{\hat{S}_c}{d} D + \mu_c \omega^2 e_3 D}} & \underline{\underline{-\frac{\hat{S}_c}{d^2} + (\mu_t + \frac{\mu_c}{3})\omega^2 + K_t D^2}} & \underline{\underline{\frac{\hat{S}_c}{d^2} + \frac{\mu_c}{6}\omega^2}} \\ \underline{\underline{-\frac{\hat{S}_c}{d} D + \mu_c \omega^2 e_4 D}} & \underline{\underline{\frac{\hat{S}_c}{d^2} + \frac{\mu_c}{6}\omega^2}} & \underline{\underline{-\frac{\hat{S}_c}{d^2} + (\mu_b + \frac{\mu_c}{3})\omega^2 + K_b D^2}} \end{bmatrix} \begin{bmatrix} W \\ U_t \\ U_b \end{bmatrix} = 0 \qquad (6.87)$$

The double underlined terms in Eq. (6.87) results from the inclusion of both longitudinal and rotary inertia terms. Furthermore, the matrix operators of Eqs. (6.79) and (6.87) are equivalent and the latter can be deduced from the former by utilising matrix operations which don't change its determinant, as follows:

i) Add the last two rows of Eq. (6.79), then divide the results by 2, to give the second row of Eq. (6.87);

ii) Subtract the third row from the second row of Eq. (6.79) and divide the results by 2 to yield the third row of Eq. (6.87); and finally

iii) Differentiate the resulting second row of Eq. (6.87) once, multiply by d and then subtract it from the first row of Eq. (6.79) to give the first row of Eq. (6.87).

For future use it is convenient to represent Eq. (6.44) in a more symbolic form as

$$\begin{bmatrix} A_1 D^4 + A_2 D^2 + A_3 & (A_4 + A_5)D & (-A_4 + A_6)D \\ (A_4 + A_5)D & A_7 D^2 + A_8 & A_9 \\ (-A_4 + A_6)D & A_9 & A_{10} D^2 + A_{11} \end{bmatrix} \begin{bmatrix} W \\ U_t \\ U_b \end{bmatrix} = 0 \qquad (6.88)$$

where

$$\left.\begin{aligned}
&A_1 = 1/\kappa;\quad A_2 = -\hat{S}_c + r\omega^2;\quad A_3 = -\mu\,\omega^2;\quad A_4 = \hat{S}_c/d;\\
&A_5 = \mu_c\omega^2 e_3;\quad A_6 = \mu_c\omega^2 e_4;\quad A_7 = K_t;\quad A_8 = (\mu_t + \frac{\mu_c}{3})\,\omega^2 - \hat{S}_c/d^2;\\
&A_9 = \hat{S}_c/d^2 + \omega^2\mu_c/6;\qquad A_{10} = K_b;\qquad A_{11} = (\mu_b + \frac{\mu_c}{3})\,\omega^2 - \hat{S}_c/d^2
\end{aligned}\right\} \tag{6.89}$$

Eq. (6.87) can be combined into one equation by eliminating either W, U_t or U_b to yield the corresponding linear eighth order differential equation as

$$[D^8 + c_1D^6 + c_2D^4 + c_3D^2 + c_4]\,V = 0 \tag{6.90}$$

where $V = W$, U_t or U_b and

$$\left.\begin{aligned}
c_1 &= (\frac{1}{\hat{\varsigma}} + \frac{\mu_c}{3\varsigma} + \kappa r\,)\omega^2 - \hat{S}_c(\frac{1}{d^2\varsigma} + \kappa\,)\\
c_2 &= [\frac{1}{K_tK_b}(\mu_t\mu_b + \frac{\mu\mu_c}{3} - \frac{\mu_c^2}{4}) + r\kappa(\frac{1}{\hat{\varsigma}} + \frac{\mu_c}{3\varsigma}) - \mu_c^2\kappa(\frac{e_3^2}{K_t} + \frac{e_4^2}{K_b})]\omega^4\\
&\quad -[\frac{\hat{S}_c r\kappa}{d^2\varsigma} + \frac{2\hat{S}_c\kappa\mu_c}{d}(\frac{e_3}{K_t} - \frac{e_4}{K_b}) + \hat{S}_c\kappa\,(\frac{1}{\hat{\varsigma}} + \frac{\mu_c}{3\varsigma}) + \mu(\kappa + \frac{\hat{S}_c}{d^2K_tK_b})]\omega^2\\
c_3 &= \{\frac{r\kappa}{K_tK_b}(\mu_t\mu_b + \frac{\mu\mu_c}{3} - \frac{\mu_c^2}{4}) - \frac{\mu_c^2\kappa}{K_tK_b}[\mu_be_3^2 + \mu_te_4^2 + \frac{\mu_c}{3}(e_3^2 + e_4^2 - e_3e_4)]\}\omega^6\\
&\quad -[\mu\kappa\,(\frac{1}{\hat{\varsigma}} + \frac{\mu_c}{3\varsigma}) + \frac{\hat{S}_c\kappa}{K_tK_b}\{\mu_t\mu_b + \mu(\frac{\mu_c}{3} + \frac{r}{d^2}) - \mu_c^2\,(\frac{1}{4} + \frac{e_1^2}{d^2}\,)\\
&\quad -2\frac{\mu_c}{d}[\mu\frac{e_2}{12} + \frac{e_1}{2}(\mu_t - \mu_b)]\}]\omega^4 + \frac{\hat{S}_c\mu\kappa}{d^2\varsigma}\,\omega^2\\
c_4 &= -\frac{\mu\kappa}{K_tK_b}(\mu_t\mu_b + \frac{\mu\mu_c}{3} - \frac{\mu_c^2}{4})\,\omega^6 + \frac{\hat{S}_c\mu^2\kappa}{d^2K_tK_b}\omega^4
\end{aligned}\right\} \tag{6.91}$$

where ς and $\hat{\varsigma}$ are defined in Eq. (6.24).

6.4.3 Dynamic stiffness formulation

Expressions for the general displacements W, Ψ, U_t and U_b can be deduced from Eqs. (6.2), (6.19) and (6.90) and the expressions for the corresponding forces can be obtained by substituting Eq. (6.19) into Eqs. (6.85), (6.39), (6.41) and (6.42) to yield

$$\left.\begin{aligned} Q &= -\frac{W'''}{\kappa} - (r\omega^2 - \hat{S}_c)W' - (\mu_c\omega^2 e_3 + \frac{\hat{S}_c}{d})U_t - (\mu_c\omega^2 e_4 - \frac{\hat{S}_c}{d})U_b \\ M &= -\frac{W''}{\kappa} \\ N_t &= K_t U_t' \\ N_b &= K_b U_b' \end{aligned}\right\} \tag{6.92}$$

An alternative form of Eq. (6.92) can be developed from the theory presented in the equilibrium approach by imposing Eq. (6.19) on Eq. (6.74), (6.10) and (6.2a). The only difference is that the expression for shear force can be presented in an alternative, but numerically equal form, as

$$\begin{aligned} Q = -\frac{W'''}{\kappa} &- (ae_1\mu_c + \mu_t\frac{t_t^2}{12} + \mu_b\frac{t_b^2}{12} - \mu_c\frac{t_c}{12}e_2)\omega^2 W' - K_t d U_t'' \\ &- (\mu_t d + \mu_c\frac{a}{2} + \mu_c\frac{t_c}{12})\omega^2 U_t - (\mu_c\frac{a}{2} - \mu_c\frac{t_c}{12})\omega^2 U_b \end{aligned} \tag{6.93}$$

6.4.3.1 Solution of the governing differential equation of motion

The solution of Eq. (6.90), which is a linear differential equation with constant coefficients, can be sought in the following form

$$V = \sum_{j=1}^{8} \overline{C}_{ij}\zeta_j \quad \text{where} \qquad \zeta_j = e^{\eta_j x}; \qquad 0 < x < L \tag{6.94a,b}$$

η_j are the roots of the characteristic equation stemming from Eq. (6.90) and the $\overline{C}_{ij}$ are arbitrary constants where, for convenience in developing the work that follows, i is an

assigned integer that defines a set of j arbitrary constants, e.g. $\overline{C}_{1j} = \overline{A}_j$, $\overline{C}_{2j} = \overline{B}_j$ etc., where $\overline{A}_j$, $\overline{B}_j$ are independent sets of arbitrary constants.

The η_j can now be determined as the roots of

$$\eta^8 + c_1\eta^6 + c_2\eta^4 + c_3\eta^2 + c_4 = 0 \tag{6.95}$$

The η_j define V (W, U_t or U_b), which may be substituted into Eq. (6.92) to yield the following results

$$\left.\begin{aligned} W &= \sum_{j=1}^{8} H_{1j}C_j\zeta_j \quad & Q &= \sum_{j=1}^{8} H_{5j}C_j\zeta_j \\ \Psi &= \sum_{j=1}^{8} H_{2j}C_j\zeta_j \quad & M &= \sum_{j=1}^{8} H_{6j}C_j\zeta_j \\ U_t &= \sum_{j=1}^{8} H_{3j}C_j\zeta_j \quad & N_t &= \sum_{j=1}^{8} H_{7j}C_j\zeta_j \\ U_b &= \sum_{j=1}^{8} H_{4j}C_j\zeta_j \quad & N_b &= \sum_{j=1}^{8} H_{8j}C_j\zeta_j \end{aligned}\right\} \tag{6.96}$$

where $H_{ij}C_j = \overline{C}_{ij}$, such that C_j is common to all the equations and H_{ij} is the relational constant. Noting that one of the H_{ij} is arbitrary, it is convenient to set $H_{1j} = 1$, which yields the following relationships between the H_{ij} of Eqs. (6.96)

$$\left.\begin{aligned} H_{1j} &= 1 \\ H_{2j} &= \eta_j \\ H_{6j} &= -\eta_j^2/\kappa \\ H_{7j} &= K_t\eta_j H_{3j} \end{aligned} \quad \begin{aligned} H_{3j} &= \frac{A_9(A_1\eta_j^4 + A_2\eta_j^2 + A_3) - (A_6 - A_4)(A_4 + A_5)\eta_j^2}{[(A_7\eta_j^2 + A_8)(A_6 - A_4) - A_9(A_4 + A_5)]\eta_j} \\ H_{4j} &= -\frac{(A_4 + A_5)\eta_j + (A_7\eta_j^2 + A_8)H_{3j}}{A_9} \\ H_{5j} &= -[\frac{\eta_j^3}{\kappa} + (r\omega^2 - \hat{S}_c)\eta_j + (\mu_c\omega^2 e_3 + \frac{\hat{S}_c}{d})H_{3j} \\ &\quad + (\mu_c\omega^2 e_4 - \frac{\hat{S}_c}{d})H_{4j}] \\ H_{8j} &= K_b\eta_j H_{4j} \end{aligned}\right\} \tag{6.97}$$

Alternatively, H_{5j} can be written based on Eq. (6.93) as

$$H_{5j} = -\{\frac{\eta_j^3}{\kappa} + (ae_1\mu_c + \mu_t\frac{t_t^2}{12} + \mu_b\frac{t_b^2}{12} - \mu_c\frac{t_c}{12}e_2)\omega^2\eta_j + [K_t d\eta_j^2 + (\mu_t d + \mu_c\frac{a}{2} + \mu_c\frac{t_c}{12})\omega^2]H_{3j} + \mu_c(\frac{a}{2} - \frac{t_c}{12})\omega^2 H_{4j}\} \quad (6.97a)$$

6.4.3.2 *Transformation between local and member co-ordinate systems*

The stiffness formulation requires all nodal forces and displacements to be represented in the member co-ordinate system. Since all the nodal forces and displacements developed so far refer to the local co-ordinate system shown in Figure 6.4(a), they should now be transformed to the member co-ordinate system of Figure 6.4(b). The necessary transformation can easily be achieved by imposing the conditions of Eq. (6.54) onto Eq. (6.92).

6.4.3.3 *Dynamic stiffness matrix*

The development of the required dynamic stiffness matrix, **k**, follows identically the steps described in Section 6.3.3.3.

6.4.4 *Converging on the natural frequencies*

Solutions of the equation

$$\mathbf{K}\,\mathbf{D} = \mathbf{0} \quad (6.98)$$

where **D** is the vector of amplitudes of the harmonically varying nodal displacements and **K** is the dynamic structure stiffness matrix yield the required natural frequencies. The solution procedure corresponds precisely to the one described in Section 6.3.4. Thus we seek to find J of Eq. (6.62) and this is achieved by substituting any part of Eq. (6.67) into

Eq. (6.90). This yields the frequency equation for a roller-roller supported beam that includes the effects of longitudinal and rotary inertia as

$$\delta^8 - c_1\delta^6 + c_2\delta^4 - c_3\delta^2 + c_4 = 0 \tag{6.99}$$

Substituting Eqs.(6.91) into Eq. (6.99) leads to the following frequency equation of degree six

$$b_1\omega^6 + b_2\omega^4 + b_3\omega^2 + b_4 = 0 \tag{6.100}$$

where

$$\left.\begin{aligned}
b_1 &= -\frac{\kappa}{K_t K_b}\{(\mu_t\mu_b + \frac{\mu\mu_c}{3} - \frac{\mu_c^2}{4})(\mu + r\delta^2) \\
&\qquad - \mu_c^2[(\mu_b + \frac{\mu_c}{3})e_3^2 + (\mu_t + \frac{\mu_c}{3})e_4^2 - \frac{\mu_c}{3}e_3 e_4]\} \\
b_2 &= \frac{\hat{S}_c\mu^2\kappa}{d^2K_tK_b} + [\frac{\hat{S}_c\kappa}{K_tK_b}\{\mu_t\mu_b + \mu(\frac{\mu_c}{3} + \frac{r}{d^2}) - \mu_c^2(\frac{1}{4} + \frac{e_1^2}{d^2}) \\
&\qquad - 2\frac{\mu_c}{d}[\mu\frac{e_2}{12} + \frac{e_1}{2}(\mu_t - \mu_b)]\} + \mu\kappa(\frac{1}{\hat{\varsigma}} + \frac{\mu_c}{3\varsigma})]\delta^2 \\
&\quad + [\frac{\mu_t\mu_b}{K_tK_b} + \frac{\mu\mu_c}{3K_tK_b} - \frac{\mu_c^2}{4K_tK_b} + r\kappa(\frac{1}{\hat{\varsigma}} + \frac{\mu_c}{3\varsigma}) - \mu_c^2\kappa(\frac{e_3^2}{K_t} + \frac{e_4^2}{K_b})]\delta^4 \\
b_3 &= -\frac{\hat{S}_c\mu\kappa}{d^2\varsigma}\delta^2 - [\frac{\hat{S}_c r\kappa}{d^2\varsigma} + \frac{2\hat{S}_c\kappa\mu_c}{d}(\frac{e_3}{K_t} - \frac{e_4}{K_b}) \\
&\qquad + S_c\kappa(\frac{1}{\hat{\varsigma}} + \frac{\mu_c}{3\varsigma}) + \mu(\kappa + \frac{\hat{S}_c}{d^2K_tK_b})]\delta^4 - (\frac{1}{\hat{\varsigma}} + \frac{\mu_c}{3\varsigma} + r\kappa)\delta^6 \\
b_4 &= \hat{S}_c(\frac{1}{d^2\varsigma} + \kappa)\delta^6 + \delta^8
\end{aligned}\right\} \tag{6.101}$$

Eq. (6.100) can be expressed as a cubic equation in ω^2 and consequently its real, positive roots are the square of its natural frequencies for each value of $n = 0,1,2, \ldots$. Hence J_{rr} is given by the number of positive values of ω_n that lie below the trial frequency, ω^*, and Eq. (6.71) gives the required value of J_0 to be used in the Wittrick-Williams algorithm Eq. (6.62).

It is necessary to note that when $n = 0$, $\delta = 0$ and similar to the case of Section 6.3 the coefficients b_3 and b_4 are zero and it can be shown that b_1 is always negative and that b_2 is always positive. Eq. (6.100) then yields a single non-trivial real root which corresponds to the fundamental shear thickness mode. As before, this mode does not involve either lateral displacement or axial extension.

6.5 TRANSFORMATION BETWEEN THE VARIOUS SETS OF BOUNDARY CONSTRAINTS THAT CAN BE IMPOSED ON A SANDWICH BEAM

Based on the configuration of Figure 6.1, the stiffness matrix formulation of the sandwich beam, including the effects of longitudinal and rotary inertia, leads to the set of boundary conditions stated in Eqs. (6.51) or (6.96). However, it is possible to use various sets of displacement field variables and consequently the stiffness formulation yields appropriate sets of boundary conditions. For example, rather than using the mid-layer displacement of the faceplates as being representative of the longitudinal displacement, u_t and u_b in Figure 6.7, the displacements at the interface of the core and the faceplates, u_2 and u_3, or the longitudinal displacements at the external fibres of the faceplates, u_1 and u_4, could also be used. In contrast with conventional homogeneous beams, these sets of axial displacements, which also correspond to possible locations of axial constraint, can play an important role when determining the natural frequencies of sandwich beams.

Alternatively, by proper transformation, the dynamic stiffness matrix of Section 6.3.3.3 or 6.4.3.3, can be made to be compatible with the desired field displacement.

One of the most practical sets of axial constraint is perhaps the one that comprises the longitudinal displacements at the external fibres of the faceplates, i.e. u_1 and u_4 of Figure 6.7. The necessary transformation between Eqs. (6.51) or (6.96) and the desired set of displacements and forces is

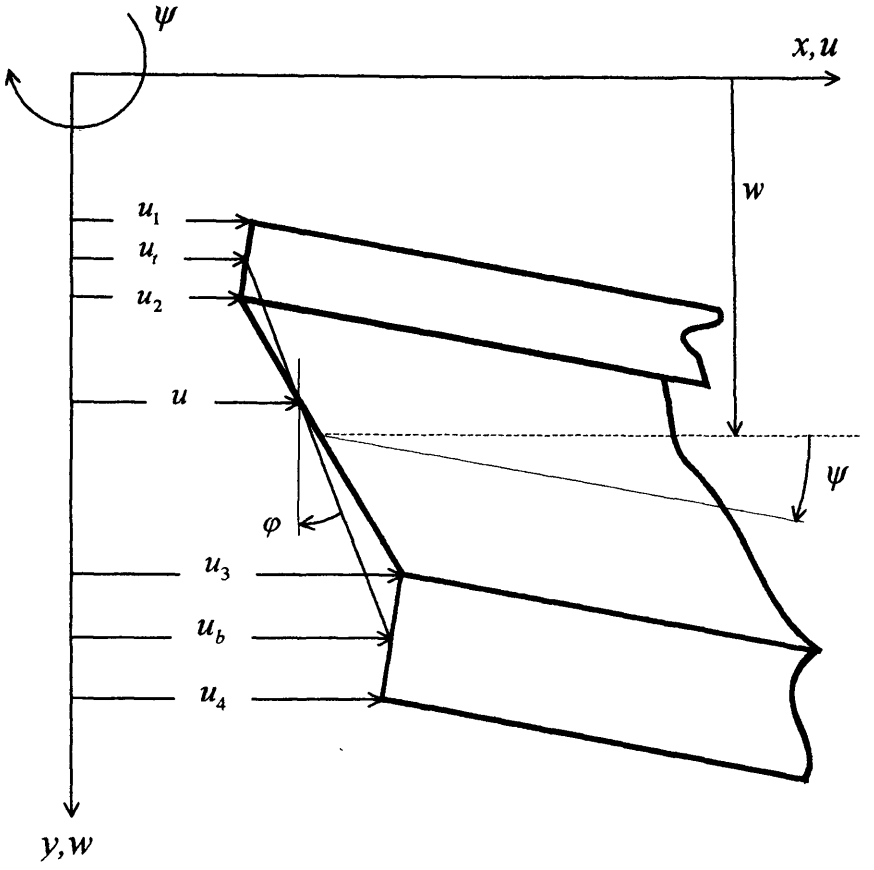

Figure 6.7: The displaced section showing the possible displacement field variables (u_i) of a typical sandwich beam section of unit width. Note that the vertical position of the longitudinal displacement u is not a geometric property of the section, but a function of u_t and u_b.

$$\mathbf{d} = \begin{bmatrix} W_1 \\ \Psi_1 \\ U_{t1} \\ U_{b1} \\ W_2 \\ \Psi_2 \\ U_{t2} \\ U_{b2} \end{bmatrix} = \mathbf{T}_1 \begin{bmatrix} W_1 \\ \Psi_1 \\ U_{11} \\ U_{41} \\ W_2 \\ \Psi_2 \\ U_{12} \\ U_{42} \end{bmatrix} = \mathbf{T}_1 \hat{\mathbf{d}}_1 \quad ; \quad \mathbf{p} = \begin{bmatrix} Q_1 \\ M_1 \\ N_{t1} \\ N_{b1} \\ Q_2 \\ M_2 \\ N_{t2} \\ N_{b2} \end{bmatrix} = \tilde{\mathbf{T}}_1 \begin{bmatrix} Q_1 \\ \tilde{M}_1 \\ N_{11} \\ N_{41} \\ Q_2 \\ \tilde{M}_2 \\ N_{12} \\ N_{42} \end{bmatrix} = \tilde{\mathbf{T}}_1 \hat{\mathbf{p}}_1 \tag{6.102}$$

where the transformation matrices are

$$\mathbf{T}_1 = \begin{bmatrix} 1 & 0 & 0 & 0 & 0 & 0 & 0 & 0 \\ 0 & 1 & 0 & 0 & 0 & 0 & 0 & 0 \\ 0 & -t_t/2 & 1 & 0 & 0 & 0 & 0 & 0 \\ 0 & t_b/2 & 0 & 1 & 0 & 0 & 0 & 0 \\ 0 & 0 & 0 & 0 & 1 & 0 & 0 & 0 \\ 0 & 0 & 0 & 0 & 0 & 1 & 0 & 0 \\ 0 & 0 & 0 & 0 & 0 & -t_t/2 & 1 & 0 \\ 0 & 0 & 0 & 0 & 0 & t_b/2 & 0 & 1 \end{bmatrix} \text{ and } \tilde{\mathbf{T}}_1 = \begin{bmatrix} 1 & 0 & 0 & 0 & 0 & 0 & 0 & 0 \\ 0 & 1 & t_t/2 & -t_b/2 & 0 & 0 & 0 & 0 \\ 0 & 0 & 1 & 0 & 0 & 0 & 0 & 0 \\ 0 & 0 & 0 & 1 & 0 & 0 & 0 & 0 \\ 0 & 0 & 0 & 0 & 1 & 0 & 0 & 0 \\ 0 & 0 & 0 & 0 & 0 & 1 & t_t/2 & -t_b/2 \\ 0 & 0 & 0 & 0 & 0 & 0 & 1 & 0 \\ 0 & 0 & 0 & 0 & 0 & 0 & 0 & 1 \end{bmatrix} \tag{6.103}$$

The transformed dynamic stiffness matrix, $\hat{\mathbf{k}}_1$, follows through the following steps

$$\tilde{\mathbf{T}}_1 \hat{\mathbf{p}}_1 = \mathbf{k}\mathbf{T}_1 \hat{\mathbf{d}}_1; \quad \hat{\mathbf{p}}_1 = \tilde{\mathbf{T}}_1^{-1}\mathbf{k}\mathbf{T}_1 \hat{\mathbf{d}}_1 \quad , \hat{\mathbf{p}}_1 = \hat{\mathbf{k}}_1 \hat{\mathbf{d}}_1; \quad \hat{\mathbf{k}}_1 = \tilde{\mathbf{T}}_1^{-1}\mathbf{k}\mathbf{T}_1 \tag{6.104}$$

From Eq. (6.103) it can be shown that $\tilde{\mathbf{T}}_1^{-1} = \mathbf{T}_1^{\mathrm{T}}$, where superscript T denotes the transpose of the matrix, and therefore

$$\hat{\mathbf{k}}_1 = \mathbf{T}_1^{\mathrm{T}}\mathbf{k}\mathbf{T}_1 \tag{6.105}$$

In the case where the core/faceplate interfaces are chosen as the axial freedoms, i.e. u_2 and u_3 in Figure 6.7, it is only necessary to change the sign of all of the non-diagonal elements of the transformation matrices of Eq. (6.103).

Another useful transformation enables the average axial displacement of the face layers, u, to be used, thus requiring only one axial displacement at each end of the beam. However, its vertical position through the beam thickness is not fixed and may vary due to changes in the values of u_t and u_b. The average rotation of the beam cross-section, φ, is the by-product of this transformation. From Figure 6.7, it is clear that

$$u = \frac{u_t + u_b}{2}; \qquad \varphi = \frac{u_t - u_b}{d} \tag{6.106a,b}$$

Consequently, the resultant axial force in the beam's cross-section, n, and the couple due to the axial forces developed in the top and bottom faceplates during bending, $\overline{m}$, become

$$n = n_t + n_b \; ; \qquad \overline{m} = n_t \frac{d}{2} - n_b \frac{d}{2} = (n_t - n_b)\frac{d}{2} \tag{6.107a,b}$$

With regard to Eq. (6.56), the necessary transformations between the displacements and forces can be written as

$$\mathbf{d} = \begin{bmatrix} W_1 \\ \Psi_1 \\ U_{t1} \\ U_{b1} \\ W_2 \\ \Psi_2 \\ U_{t2} \\ U_{b2} \end{bmatrix} = \mathbf{T}_2 \begin{bmatrix} W_1 \\ \Psi_1 \\ \Phi_1 \\ U_1 \\ W_2 \\ \Psi_2 \\ \Phi_2 \\ U_2 \end{bmatrix} = \mathbf{T}_2 \hat{\mathbf{d}}_2 \quad ; \quad \mathbf{p} = \begin{bmatrix} Q_1 \\ M_1 \\ N_{t1} \\ N_{b1} \\ Q_2 \\ M_2 \\ N_{t2} \\ N_{b2} \end{bmatrix} = \tilde{\mathbf{T}}_2 \begin{bmatrix} Q_1 \\ M_1 \\ \overline{M}_1 \\ N_1 \\ Q_2 \\ M_2 \\ \overline{M}_2 \\ N_2 \end{bmatrix} = \tilde{\mathbf{T}}_2 \hat{\mathbf{p}}_2 \tag{6.108}$$

where the transformation matrices are

$$\mathbf{T}_2 = \begin{bmatrix} 1 & 0 & 0 & 0 & 0 & 0 & 0 & 0 \\ 0 & 1 & 0 & 0 & 0 & 0 & 0 & 0 \\ 0 & 0 & d/2 & 1 & 0 & 0 & 0 & 0 \\ 0 & 0 & -d/2 & 1 & 0 & 0 & 0 & 0 \\ 0 & 0 & 0 & 0 & 1 & 0 & 0 & 0 \\ 0 & 0 & 0 & 0 & 0 & 1 & 0 & 0 \\ 0 & 0 & 0 & 0 & 0 & 0 & d/2 & 1 \\ 0 & 0 & 0 & 0 & 0 & 0 & -d/2 & 1 \end{bmatrix} \; ; \; \tilde{\mathbf{T}}_2 = \begin{bmatrix} 1 & 0 & 0 & 0 & 0 & 0 & 0 & 0 \\ 0 & 1 & 0 & 0 & 0 & 0 & 0 & 0 \\ 0 & 0 & 1/d & 1/2 & 0 & 0 & 0 & 0 \\ 0 & 0 & -1/d & 1/2 & 0 & 0 & 0 & 0 \\ 0 & 0 & 0 & 0 & 1 & 0 & 0 & 0 \\ 0 & 0 & 0 & 0 & 0 & 1 & 0 & 0 \\ 0 & 0 & 0 & 0 & 0 & 0 & 1/d & 1/2 \\ 0 & 0 & 0 & 0 & 0 & 0 & -1/d & 1/2 \end{bmatrix} \tag{6.109}$$

In similar fashion to Eq (6.104) the new transformed stiffness matrix is

$$\hat{\mathbf{k}}_2 = \mathbf{T}_2^{\mathrm{T}} \mathbf{k} \mathbf{T}_2 \tag{6.110}$$

Finally, to include a beam in a plane frame, it is necessary to transform the stiffness matrix from member co-ordinates to global co-ordinates (See Figure 6.8). During transformation, the axial and transverse displacements and forces are transformed, but the rotations and moments remain unchanged. From Figure 6.8 it is clear that

$$\begin{cases} X = W\sin\theta + U\cos\theta \\ Y = W\cos\theta - U\sin\theta \end{cases} \qquad \begin{cases} P_x = Q\sin\theta + N\cos\theta \\ P_y = Q\cos\theta - N\sin\theta \end{cases} \tag{6.111a,b}$$

The transformations can then be written in matrix notation as

$$\hat{\mathbf{d}}_2 = \begin{bmatrix} W_1 \\ \Psi_1 \\ \Phi_1 \\ U_1 \\ W_2 \\ \Psi_2 \\ \Phi_2 \\ U_2 \end{bmatrix} = \mathbf{T}_3 \begin{bmatrix} X_1 \\ Y_1 \\ \Psi_1 \\ \Phi_1 \\ X_2 \\ Y_2 \\ \Psi_2 \\ \Phi_2 \end{bmatrix} = \mathbf{T}_3\mathbf{d}_G \;; \qquad \hat{\mathbf{p}}_2 = \begin{bmatrix} Q_1 \\ M_1 \\ \overline{M}_1 \\ N_1 \\ Q_2 \\ M_2 \\ \overline{M}_2 \\ N_2 \end{bmatrix} = \mathbf{T}_3 \begin{bmatrix} P_{x1} \\ P_{y1} \\ M_1 \\ \overline{M}_1 \\ P_{x2} \\ P_{y2} \\ M_2 \\ \overline{M}_2 \end{bmatrix} = \mathbf{T}_3\mathbf{p}_G \tag{6.112}$$

where subscript G denotes quantities in global co-ordinates and the transformation matrix is

$$\mathbf{T}_3 = \begin{bmatrix} \sin\theta & \cos\theta & 0 & 0 & 0 & 0 & 0 & 0 \\ 0 & 0 & 1 & 0 & 0 & 0 & 0 & 0 \\ 0 & 0 & 0 & 1 & 0 & 0 & 0 & 0 \\ \cos\theta & -\sin\theta & 0 & 0 & 0 & 0 & 0 & 0 \\ 0 & 0 & 0 & 0 & \sin\theta & \cos\theta & 0 & 0 \\ 0 & 0 & 0 & 0 & 0 & 0 & 1 & 0 \\ 0 & 0 & 0 & 0 & 0 & 0 & 0 & 1 \\ 0 & 0 & 0 & 0 & \cos\theta & -\sin\theta & 0 & 0 \end{bmatrix} \tag{6.113}$$

Hence, the element stiffness matrix in global co-ordinates, $\mathbf{k}_G$, is

$$\mathbf{k}_G = \mathbf{T}_3^{\mathrm{T}}\hat{\mathbf{k}}_2\mathbf{T}_3 \tag{6.114}$$

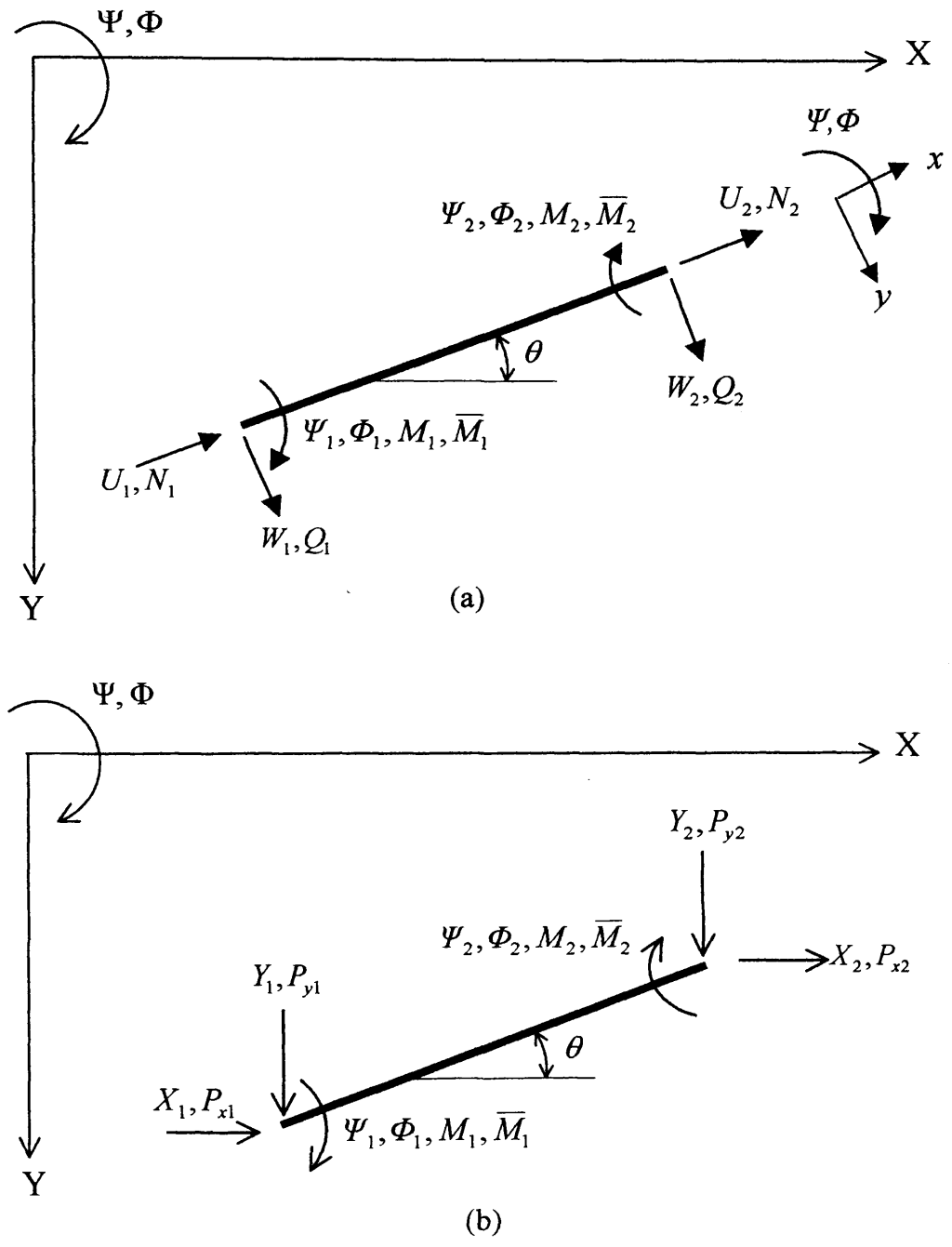

Figure 6.8: Nodal forces and displacements a) in member co-ordinates and b) in global co-ordinates.

6.6 NUMERICAL RESULTS

A number of examples are now given to validate the theory and indicate its range of application. The first two examples compare results obtained by a number of authors for a simply supported and cantilevered beam, respectively, which have been widely used as test examples. In these two examples, results from both the theories of Sections 6.3 and 6.4 are given, while for the other examples the more accurate theory of the latter is used. Examples 6.3 and 6.4 are used to validate the accuracy of the proposed theory in the analysis of frames formed from sandwich beams. Example 6.5 presents the crucial differences between ordinary and sandwich beams, while Example 6.6 shows the necessity of using the proposed theory for deep sandwich beams. The final example considers a simple frame for which the values of some of the natural frequencies can be argued through a self consistency check.

Example 6.1: The beam of Example 5.1 is now constrained by rollers at both ends. The results obtained by a number of authors are given in Table 6.1. In this table, 'Freq. No.' indicates the order of occurrence of the modes, while the second column gives the predominant component of the mode and its ordering number. For example, 'B1' indicates the first bending mode, 'A3', the third axial mode and 'S2', the second shear thickness mode etc.

It is necessary to note that except for the results of the current theory (Chapter 6), all comparable results correspond to what has been described as simply supported beam. However, as will be shown in Example 6.6, the term 'simply supported' needs to be clarified, since the position of the longitudinal constraint has a significant effect on the vibration of the beam. Furthermore, the theories behind the results in columns 5 and 6 clearly don't have the ability to consider any longitudinal constraint. On the other hand, the non exact field displacements used in those theories which give the results in the last two columns is the reason why they could not predict the importance of longitudinal constraint. Nevertheless, the first axial frequency in column 9 clearly refers to a roller-roller supported sandwich beam, rather than a beam that has been constrained at one end, i.e. a simply supported beam.

Table 6.1: Comparative results for the non-zero natural frequencies (Hz) of the roller-roller supported sandwich beam of Example 6.1.

Freq. No.	mode	Theory of Section 6.4	Theory of Section 6.3	Theory of Chapter 5	Sakiyama, 1996b	Ahmed, 1971	Rao, 2001	Marur, 1996
1	B1	57.12345	57.1241	57.1358	56.159	57.5	57.068	57.041
2	B2	219.423	219.431	219.585	215.82	-	218.569	218.361
3	B3	464.565	464.595	465.172	457.22	467	460.925	460.754
4	B4	766.850	766.915	768.177	755.05	-	757.642	758.692
5	B5	1104.52	1104.63	1106.68	1087.9	1111	1086.955	1097.055
6	B6	1462.17	1462.31	1465.10	1440.3	-	1433.920	1457.064
7	B7	1829.97	1830.14	1833.55	1802.7	1842	1789.345	1849.380
8	B8	2202.13	2202.32	2206.19	2169.8	-	2147.969	2275.916
9	A1	2563.22	2563.22	-	-	-	-	2562
10	B9	2575.41	2575.62	2579.79	2538.2	2594	-	-
11	B10	2948.08	2948.30	2952.65	2906.2	-	-	-
18	A2	5126.44	5126.44	-	-	-	-	-
27	A3	7689.67	7689.67	-	-	-	-	-
53	S1	15960.5	16406.4(54)*	-	-	-	-	-
55	S2	16190.3	16642.4(56)*	-	-	-	-	-

* Number in the brackets indicates the frequency number, if different from the first column.

Example 6.2: The proposed method of this chapter is now used to analyse the beam of Example 5.2. Results for the first eight natural frequencies are presented in Table 6.2.

Example 6.3: The free-free, rigid L-shaped frame of Figure 6.9 that is constructed from two sandwich beams of 0.175m and 0.4m length is now considered. The following material and cross-sectional geometric properties are used for both members.

$E_t = E_b = 69\,\text{GPa}$, $G_c = 440\,\text{MPa}$, $\rho_t = \rho_b = 3180\,\text{kg/m}^3$, $\rho_c = 83\,\text{kg/m}^3$,

$t_t = t_b = 0.56\,\text{mm}$, $t_c = 25.4\,\text{mm}$

Table 6.2: Comparative results for the natural frequencies (Hz) of the cantilevered sandwich beam of Example 6.2.

Freq. No.	Mode	Theory of Section 6.4	Theory of Section 6.3	Theory of Chapter 5	Ahmed, 1971	Sakiyama, 1996b	Banerjee, 2003	Marur, 1996	
								HOBT4b	HOBT5
1	B1	33.7456	33.7459	33.7513	33.97	33.146	31.46	33.7	33.7
2	B2	198.788	198.798	198.992	200.5	195.96	193.7	197.5	197.5
3	B3	511.373	511.420	512.307	517	503.43	529.2	505.5	505.5
4	B4	905.118	905.224	907.299	918	893.28	1006	890.5	890.5
5	B5	1346.06	1346.22	1349.65	1368	1328.5	-	1321	1321
6	A1	1647.79	1647.79	-	-	-	-	1648	1648
7	B6	1810.91	1811.20	1815.82	1844	1790.7	-	1786	1786
8	B7	2286.48	2286.79	2292.45	2331	2260.2	-	2271	2271
9	B8	2765.47	2765.81	2772.23	2824	2738.9	-	2792	2792
14	A2	4943.36	4943.39	-	-	-	-	4943*	4941*

*Refernce Marur, 1996) indicates that values correspond to second axial mode but 13th frequency number.

Reference (Petrone et al. 1999) considered a similar structure to that of Figure 6.9, except that the beams were replaced by equivalent sandwich plates of breadth 0.3m. A physical model was tested and the results verified using a finite element model. Clearly the plane model of Figure 6.9 can only identify in-plane modes and these are compared with the equivalent results of reference (Petrone et al. 1999) in Table 6.3. It should be noted that the mode corresponding to the higher frequency identified in reference (Petrone et al. 1999) contained a small, but distinct, torsional component.

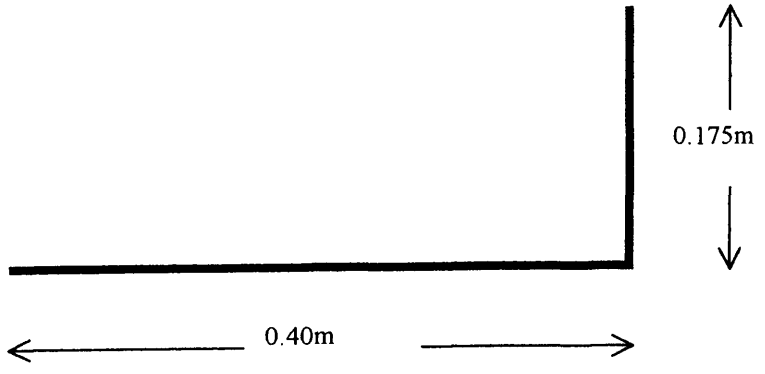

Figure 6.9: The free-free rigid frame of Example 6.3.

Table 6.3: Comparative results for the first five in-plane natural frequencies (Hz) of the free-free L-shape frame of Example 6.3.

Freq. No.	Theory of Section 6.4	Petrone, 1999	
		Experimental	FEM
1	482.78	479.24	478
2	1029.73	-	-
3	2278.39	-	-
4	3156.94	-	-
5	3947.3	-	-

***Example 6.4*:** A circularly curved sandwich beam that is fully clamped at both ends is now considered, see Figure 6.10. The material and cross-sectional properties are the same as those used in Example 6.1, while the length of the curve is 0.7112m and its radius is 4.2672m. The curved beam is modelled using 10 straight elements. Comparative results for the first five natural frequencies (Hz) of this beam are given in Table 6.4. In addition, Table 6.5 shows the results of modelling the beam with different numbers of straight elements. From Table 6.5 it is clear that modelling the curved beam with 4 straight element gives acceptable accuracy in the results.

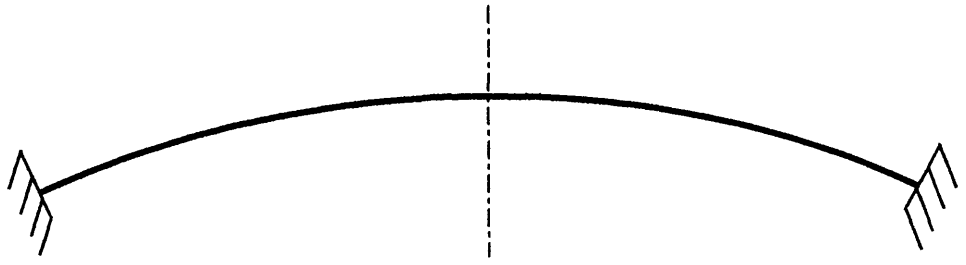

Figure 6.10: Clamped-clamped curved sandwich beam of Example 6.4. The length of the beam is 0.7112m and its radius is 4.2672m.

Table 6.4: Comparative results for the first five natural frequencies (Hz) of the clamped-clamped curved sandwich beam of Example 6.4. The results in column 2 were obtained by modelling the structure with 10 straight elements using the theory of Section 6.4. The results in the columns three and four were obtained using 10 curved sandwich beam, finite elements based on generalised mass matrices.

Freq. No.	Theory of Section 6.4	Ahmed, 1971	Ahmed, 1972	Sakiyama, 1997	Bozhevolnaya, 2004
1	244.164	264	240	244.6	237.8
2	484.363	522	474	485.6	504
3	855.966	889	843	859.8	866
4	1267.72	1312	1253	1276	1283
5	1710.28	1767	1697	1725	1728

Table 6.5: Adequacy of the idealisation when modelling the curved sandwich beam of Example 6.4 with straight elements for the first five natural frequencies (Hz).

Freq. No.	Number of straight elements to model the curve clamped-clamped sandwich beam							
	2	3	4	5	6	8	10	20
1	236.881	241.910	243.144	243.622	243.856	244.071	244.164	244.280
2	485.191	484.501	484.458	484.419	484.397	484.374	484.363	484.349
3	861.768	854.497	855.046	855.485	855.693	855.884	855.966	856.068
4	1268.78	1267.98	1268.34	1267.91	1267.85	1267.77	1267.72	1267.66
5	1714.11	1716.20	1710.10	1710.33	1710.15	1710.25	1710.28	1710.32

***Example 6.5*:** The roller-roller supported beam of Example 6.1 now has its axial freedom constrained in various ways so as to make the boundary conditions simply supported.

In case A, the axial freedom at the lower external edge of the beam is constrained by using a linear spring K_A, see Figure 6.11. In case B, spring K_B is imposed at the mid-thickness of the bottom faceplate, while the third case, case C, a spring K_C is attached at the interface of the core and bottom faceplate. Finally, in case D, the average displacement of the two faceplates is virtually constrained by spring K_D, although its vertical position is not a unique position.

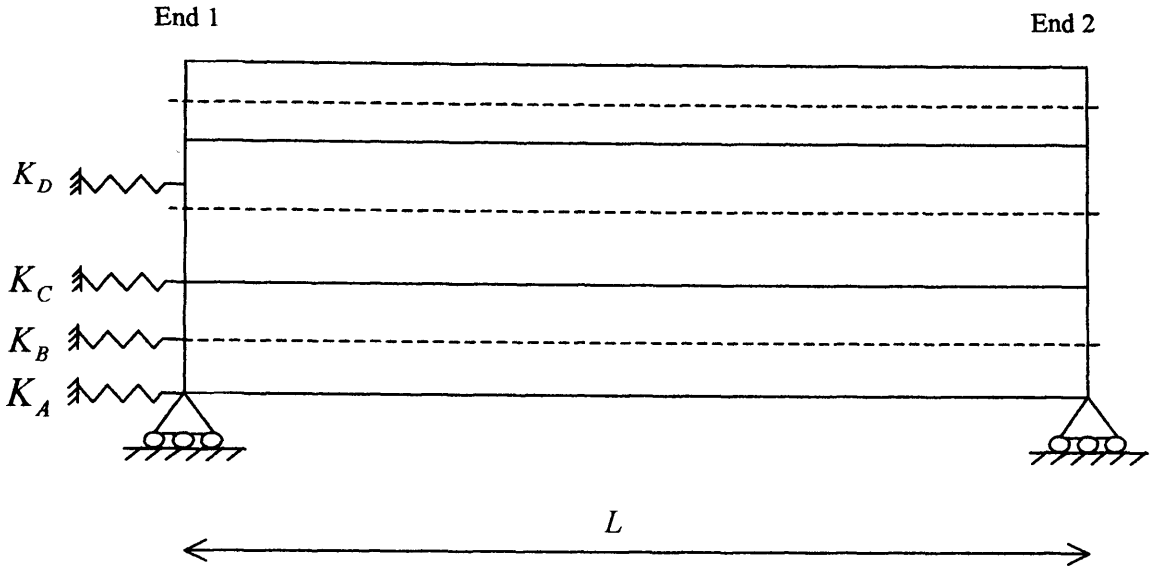

Figure 6.11: Simply supported three-layered sandwich beam constrained axially at various positions.

The results of the analysis of these different cases are shown in Tables 6.6 to 6.8. In Table 6.6, the differences between the frequencies of the various simply supported cases A-D are highlighted. The first six mode shapes of the roller-roller beam together with those of cases A-D of the simply supported beam are illustrated in Figures 6.12 to 6.16. Table 6.6 shows that in cases A-C all of the axial and shear thickness modes are coupled with bending. In the same way, Figures 6.13 to 6-15 illustrate the coupling between the axial and flexural components of the mode shapes of cases A-C. On the other hand, the mode shapes of the roller-roller supported beam (Figure 6.12) and case D of the simply supported beam (Figure 6.16) clearly show that the axial and flexural components of the mode shape are uncoupled. However, comparison between the second and the last columns clearly shows the obvious differences between the uncoupled axial frequencies in these two cases i.e. in the roller-roller case (column 2), the axial modes and frequencies are even multiples of the half-wave length $(1281.61\times 2,4,6,\ldots)$, while for the simply supported case (last column) the axial modes correspond to odd multiples of it $(1281.61\times 1,3,5,\ldots)$.

Tables 6.7 and 6.8 investigate the effect of increasing spring stiffness in cases C and D. The results show that imposing the spring introduces a predominantly axial mode whose

frequency increases with spring stiffness. See the first highlighted frequency. Also the frequency of the existing axial modes has been increased. At the same time, in case C the frequencies of the flexural modes with frequencies lower than the axial modes decrease noticeably while in case D they remain unchanged.

Table 6.6: Comparative natural frequencies (Hz) of the roller-roller supported beam of Example 6.1 and the four cases of the simply supported sandwich beam of Example 6.5.

Freq. No.	Roller-roller	Simply supported			
		Case A*	Case B	Case C	Case D
1	0	57.09382(B)	57.09583(B)	57.09777(B)	57.12345(B)
2	57.12345(B)†	219.022(B)	219.052(B)	219.080(B)	219.423(B)
3	219.423(B)	462.878(B)	463.019(B)	463.150(B)	464.565(B)
4	464.565(B)	761.778(B)	762.282(B)	762.721(B)	766.850(B)
5	766.850(B)	1081.84(B)	1084.61(B)	1086.43(B)	1104.52(B)
6	1104.52(B)	1227.12(BA)	1230.53(BA)	1228.08(BA)	1281.61(A)
7	1462.17(B)	1474.42(B)	1473.20(B)	1471.69(B)	1462.17(B)
8	1829.97(B)	1834.48(B)	1833.86(B)	1833.23(B)	1829.97(B)
9	2202.13(B)	2203.92(B)	2203.62(B)	2203.34(B)	2202.13(B)
10	2563.22(A)	2575.35(B)	2575.36(B)	2575.37(B)	2575.41(B)
11	2575.41(B)	2946.03(B)	2946.49(B)	2946.88(B)	2948.08(B)
12	2948.08(B)	3312.96(B)	3314.64(B)	3315.88(B)	3319.31(B)
13	3319.31(B)	3618.161BA)	3631.95(BA)	3632.17(BA)	3688.75(B)
14	3688.75(B)	3720.562B)	3717.96(B)	3708.83(B)	3844.83(A)
15	4056.32(B)	4061.86(B)	4060.31(B)	4058.82(B)	4056.32(B)
16	4422.08(B)	4424.56(B)	4423.76(B)	4423.07(B)	4422.08(B)
17	4786.17(B)	4787.22(B)	4786.85(B)	4786.54(B)	4786.17(B)
18	5126.44(A)	5148.67(B)	5148.70(B)	5148.72(B)	5148.74(B)
19	5148.74(B)	5508.38(B)	5509.06(B)	5509.53(B)	5509.96(B)
20	5509.96(B)	5863.40(B)	5866.55(B)	5868.44(B)	5869.99(B)
21	5869.99(B)	6067.26(BA)	6083.85(BA)	6071.05(BA)	6228.97(B)
22	6228.97(B)	6238.44(B)	6234.62(B)	6230.93(B)	6408.05(A)
23	6587.06(B)	6590.21(B)	6588.68(B)	6587.58(B)	6587.06(B)
26	6944.37(B)	7657.19(B)	7657.14(B)	7657.12(B)	7657.11(B)
52	7689.66(A)	15554.8(BA)	15556.0(BA)	15554.1(BA)	15828.1(B)
53	15828.12(B)	15828.5(B)	15828.2(B)	15828.2(B)	15960.5(S)
54	15960.5(S)	16024.2(BS)	16024.6(BS)	16024.2(BS)	16186.1(B)
55	16186.1(B)	16186.1(B)	16186.1(B)	16186.1(B)	16190.3(S)
56	16190.3(S)	16479.5(BS)	16483.9(BS)	16480.7(BS)	16544.5(B)
57	16544.5(B)	16546.4(B)	16544.7(B)	16544.8(B)	16660.9(A)
58	16859.9(S)	16903.3(B)	16903.4(B)	16903.4(B)	16859.8(S)
59	16903.4(B)	17231.4(B)	17242.5(B)	17236.2(B)	16903.4(B)

*In each case, the related spring is completely rigid while the stiffness of the other springs is zero.

†Brackets indicate the most dominant component(s) of the mode.

Table 6.7: Comparative results for natural frequencies (Hz) of the roller-roller supported sandwich beam of Example 6.1 ($K_C = 0$) and of the constrained beam of case C of Example 6.5. The highlighted frequencies correspond to axial modes.

Freq. No.	Stiffness of spring K_C									
	0	$1x10^3$	$1x10^5$	$5x10^5$	$1x10^6$	$1x10^7$	$1x10^8$	$1x10^9$	$1x10^{10}$	∞
1	0	3.10831	31.0668	57.0445	57.0846	57.0968	57.0976	57.0977	57.0977	57.0977
2	57.1234	57.1235	57.1342	69.4815	98.0208	218.723	219.061	219.078	219.079	219.079
3	219.422	219.422	219.429	219.459	219.505	302.423	462.670	463.113	463.146	463.150
4	464.564	464.564	464.570	464.593	464.622	465.465	740.390	762.299	762.682	762.721
5	766.849	766.849	766.853	766.871	766.893	767.337	804.337	1073.59	1085.56	1086.43
6	1104.52	1104.52	1104.52	1104.54	1104.55	1104.86	1108.48	1172.14	1221.67	1228.07
7	1462.16	1462.16	1462.16	1462.17	1462.19	1462.41	1464.19	1469.15	1471.35	1471.68
8	1829.96	1829.96	1829.96	1829.97	1829.98	1830.15	1831.18	1832.76	1833.18	1833.23
9	2202.13	2202.13	2202.13	2202.13	2202.14	2202.26	2202.79	2203.25	2203.33	2203.34
10	2563.22	2563.22	2563.59	2565.10	2566.97	2575.35	2575.37	2575.37	2575.37	2575.37
11	2575.41	2575.41	2575.41	2575.41	2575.42	2600.23	2860.62	2946.68	2946.86	2946.88
12	2948.08	2948.08	2948.08	2948.08	2948.09	2948.17	2950.97	3312.39	3315.7	3315.88
13	3319.31	3319.31	3319.31	3319.31	3319.32	3319.38	3320.12	3457.96	3615.39	3632.17
14	3688.75	3688.75	3688.75	3688.75	3688.75	3688.80	3689.25	3693.05	3704.05	3708.83
15	4056.32	4056.32	4056.32	4056.32	4056.32	4056.36	4056.66	4057.85	4058.67	4058.82
16	4422.08	4422.08	4422.08	4422.08	4422.08	4422.11	4422.31	4422.83	4423.04	4423.07
17	4786.17	4786.17	4786.17	4786.17	4786.17	4786.19	4786.31	4786.49	4786.53	4786.54
18	5126.44	5126.44	5126.63	5127.38	5128.32	5144.97	5148.71	5148.71	5148.71	5148.71
19	5148.74	5148.74	5148.74	5148.74	5148.74	5148.84	5292.73	5509.35	5509.52	5509.53
20	5509.95	5509.95	5509.95	5509.95	5509.96	5509.97	5510.17	5804.69	5868.19	5868.44
21	5869.98	5869.98	5869.98	5869.98	5869.98	5869.99	5870.10	5873.71	6039.44	6071.05
22	6228.97	6228.97	6228.97	6228.97	6228.97	6228.98	6229.05	6229.57	6230.56	6230.92
23	6587.06	6587.06	6587.06	6587.06	6587.06	6587.06	6587.11	6587.35	6587.53	6587.57
24	6944.37	6944.37	6944.37	6944.37	6944.37	6944.37	6944.41	6944.52	6944.58	6944.59
25	7301.02	7301.02	7301.02	7301.02	7301.02	7301.02	7301.04	7301.09	7301.11	7301.11
26	7657.11	7657.11	7657.11	7657.11	7657.11	7657.11	7657.11	7657.11	7657.11	7657.11
27	7689.66	7689.66	7689.79	7690.29	7690.92	7702.09	7802.4	8012.61	8012.65	8012.65
28	8012.73	8012.73	8012.73	8012.73	8012.73	8012.73	8012.75	8212.69	8367.43	8367.58
29	8367.96	8367.96	8367.96	8367.96	8367.96	8367.96	8367.98	8368.17	8449.80	8486.06
30	8722.89	8722.89	8722.89	8722.89	8722.89	8722.89	8722.90	8722.95	8723.03	8723.06

Table 6.8: Comparative results for natural frequencies (Hz) of the roller-roller supported sandwich beam of Example 6.1 ($K_D = 0$) and of the constrained beam of case D of Example 6.5. The highlighted frequencies correspond to axial modes.

Freq. No.	Stiffness of spring K_D									
	0	$1x10^3$	$1x10^5$	$5x10^5$	$1x10^6$	$1x10^7$	$1x10^8$	$1x10^9$	$1x10^{10}$	∞
1	0	3.108319	31.07575	57.12345	57.12345	57.12345	57.12345	57.12345	57.12345	57.12345
2	57.12345	57.12345	57.12345	69.42035	98.05678	219.4227	219.4227	219.4227	219.4227	219.4227
3	219.4227	219.4227	219.4227	219.4227	219.4227	303.5105	464.5649	464.5649	464.5649	464.5649
4	464.5649	464.5649	464.5649	464.5649	464.5649	464.5649	766.8495	766.8495	766.8495	766.8495
5	766.8495	766.8495	766.8495	766.8495	766.8495	766.8495	797.8619	1104.524	1104.524	1104.524
6	1104.524	1104.524	1104.524	1104.524	1104.524	1104.524	1104.524	1199.262	1272.841	1281.618
7	1462.165	1462.165	1462.165	1462.165	1462.165	1462.165	1462.165	1462.165	1462.165	1462.165
8	1829.966	1829.966	1829.966	1829.966	1829.966	1829.966	1829.966	1829.966	1829.966	1829.966
9	2202.13	2202.13	2202.13	2202.13	2202.13	2202.13	2202.13	2202.13	2202.13	2202.13
10	2563.222	2563.225	2563.598	2565.105	2566.985	2575.41	2575.41	2575.41	2575.41	2575.41
11	2575.41	2575.41	2575.41	2575.41	2575.41	2600.351	2881.368	2948.084	2948.084	2948.084
12	2948.084	2948.084	2948.084	2948.084	2948.084	2948.084	2948.084	3319.314	3319.314	3319.314
13	3319.314	3319.314	3319.314	3319.314	3319.314	3319.314	3319.314	3603.797	3688.753	3688.753
14	3688.753	3688.753	3688.753	3688.753	3688.753	3688.753	3688.753	3688.753	3818.532	3844.835
15	4056.322	4056.322	4056.322	4056.322	4056.322	4056.322	4056.322	4056.322	4056.322	4056.322
16	4422.085	4422.085	4422.085	4422.085	4422.085	4422.085	4422.085	4422.085	4422.085	4422.085
17	4786.171	4786.171	4786.171	4786.171	4786.171	4786.171	4786.171	4786.171	4786.171	4786.171
18	5126.443	5126.445	5126.632	5127.385	5128.327	5145.218	5148.741	5148.741	5148.741	5148.741
19	5148.741	5148.741	5148.741	5148.741	5148.741	5148.741	5305.61	5509.959	5509.959	5509.959
20	5509.959	5509.959	5509.959	5509.959	5509.959	5509.959	5509.959	5869.986	5869.986	5869.986
21	5869.986	5869.986	5869.986	5869.986	5869.986	5869.986	5869.986	6024.096	6228.974	6228.974
22	6228.974	6228.974	6228.974	6228.974	6228.974	6228.974	6228.974	6228.974	6364.246	6408.055
23	6587.061	6587.061	6587.061	6587.061	6587.061	6587.061	6587.061	6587.061	6587.061	6587.061
24	6944.372	6944.372	6944.372	6944.372	6944.372	6944.372	6944.372	6944.372	6944.372	6944.372
25	7301.022	7301.022	7301.022	7301.022	7301.022	7301.022	7301.022	7301.022	7301.022	7301.022
26	7657.111	7657.111	7657.111	7657.111	7657.111	7657.111	7657.111	7657.111	7657.111	7657.111
27	7689.665	7689.666	7689.79	7690.293	7690.921	7702.208	7812.402	8012.732	8012.732	8012.732
28	8012.732	8012.732	8012.732	8012.732	8012.732	8012.732	8012.732	8367.967	8367.967	8367.967
29	8367.967	8367.967	8367.967	8367.967	8367.967	8367.967	8367.967	8464.918	8722.89	8722.89
30	8722.89	8722.89	8722.89	8722.89	8722.89	8722.89	8722.89	8722.89	8910.001	8971.277

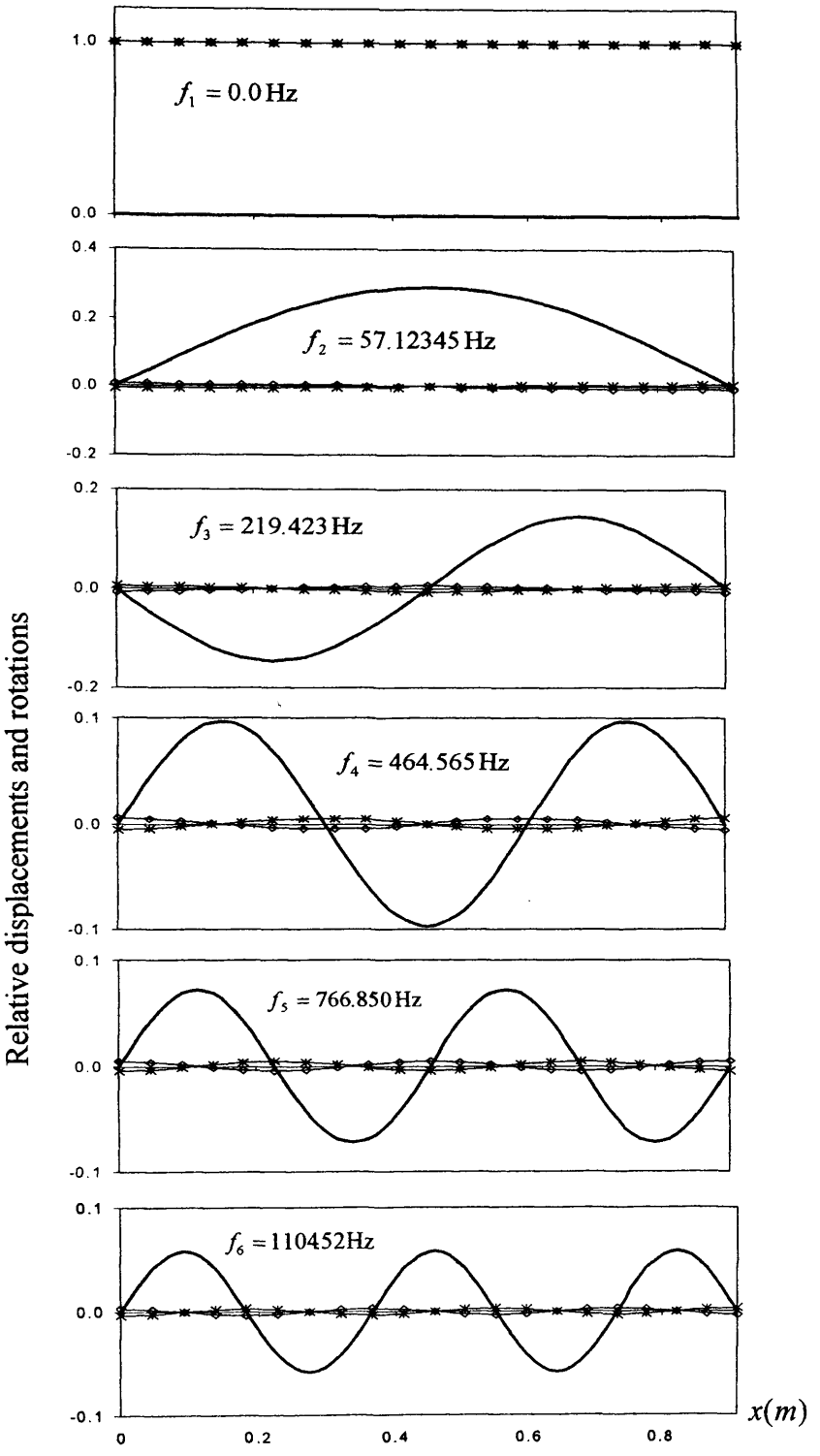

Figure 6.12: The first six natural frequencies and mode shapes of the roller-roller supported beam of Example 6.1 corresponding to column 2 of Table 6.6. The first mode is a rigid body mode and the next five modes are pure flexural modes. The graphs show (—) the modal transverse deflection W, (—◆—) longitudinal displacement u_t, and (—✱—) longitudinal displacement u_b.

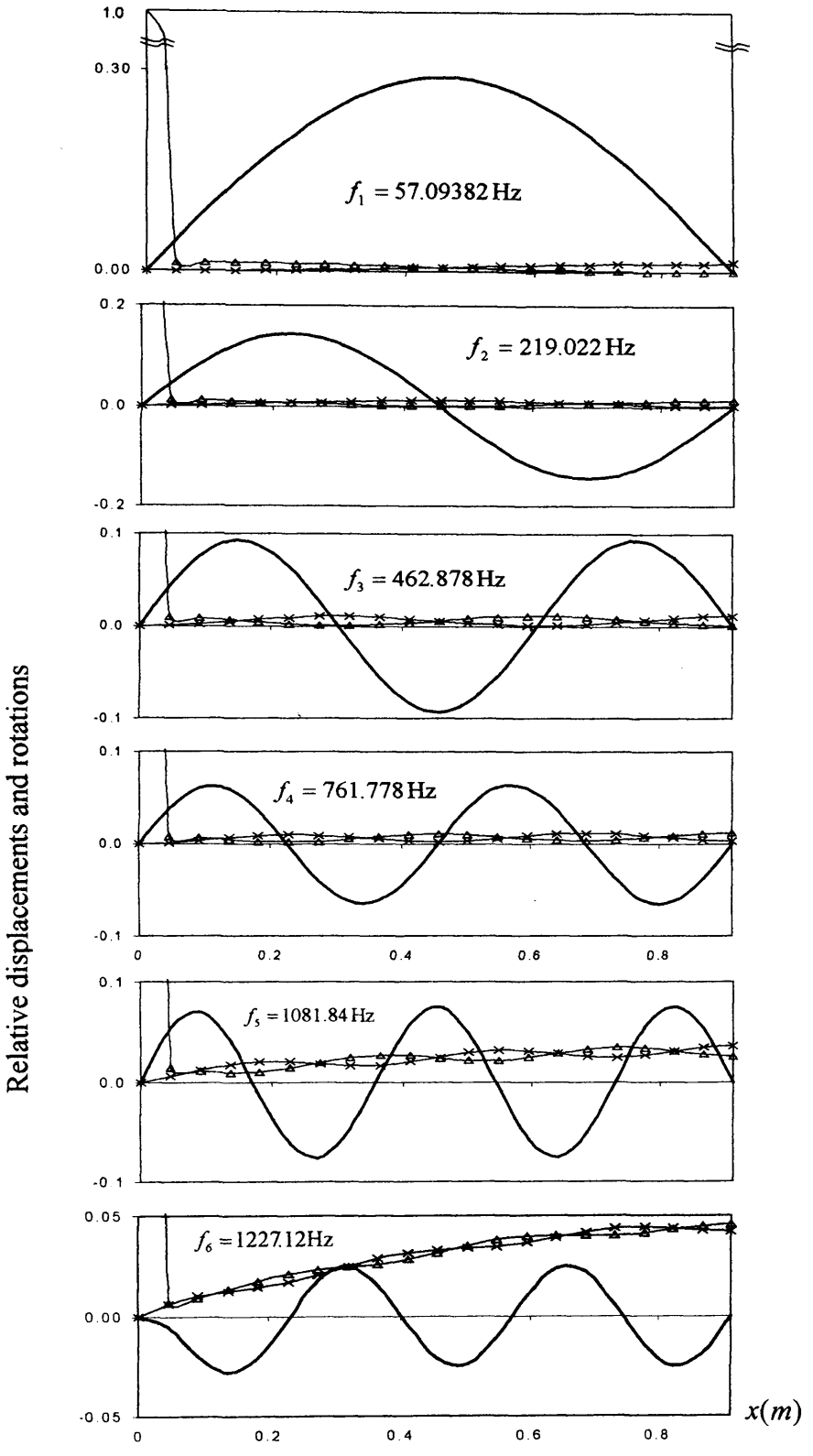

Figure 6.13: The first six natural frequencies and mode shapes of the simply supported beam (Case A) of Example 6.5 corresponding to column 3 of Table 6.6. All modes are coupled flexural and axial modes, but in the first five the flexural components of the modes are most dominant. The graphs show (—) the modal transverse deflection W, (—▵—) longitudinal displacement u_1 and (—✳—) longitudinal displacement u_4 in conjunction with Figure 6 .7.

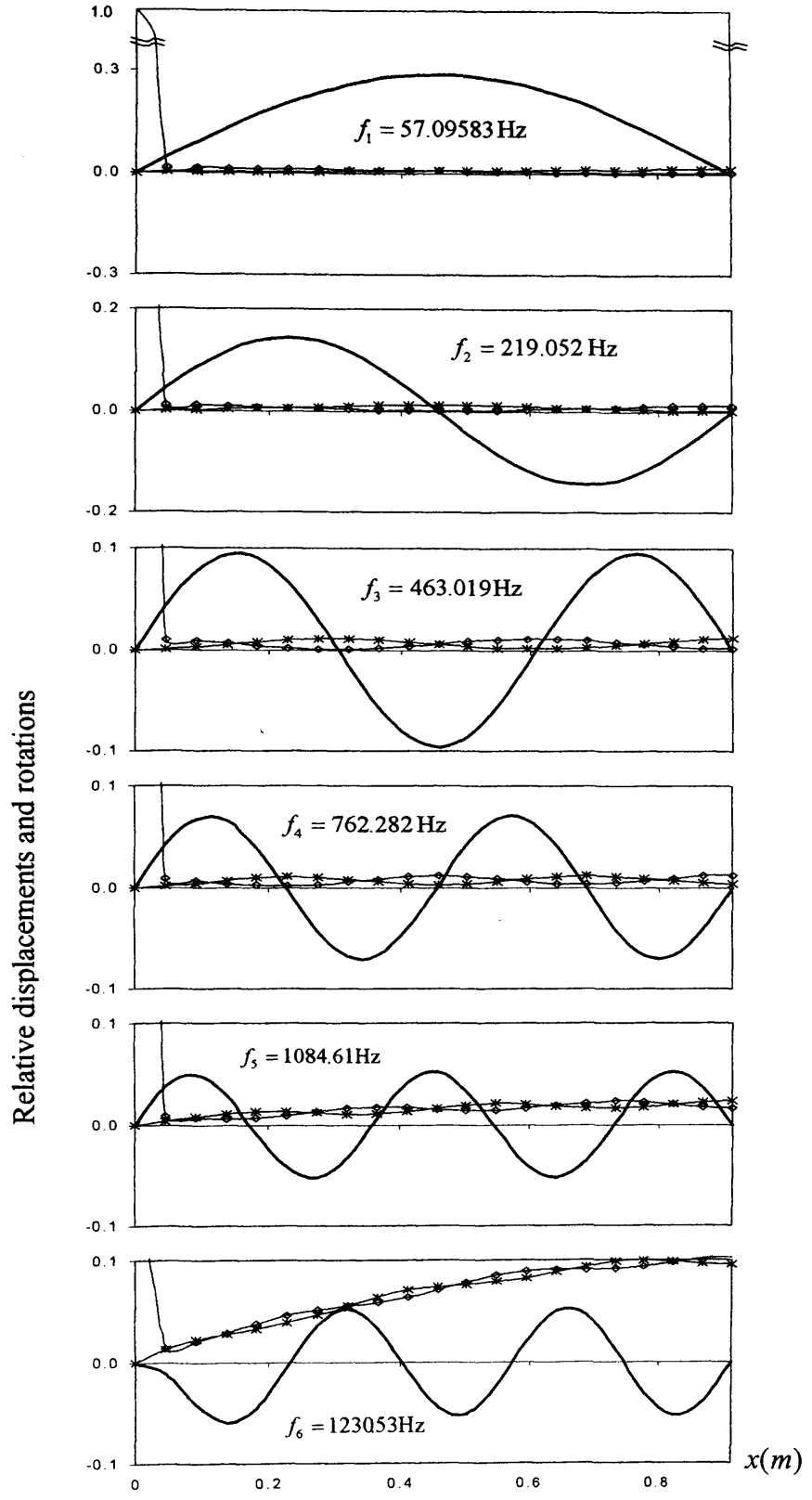

Figure 6.14: The first six natural frequencies and mode shapes of the simply supported beam (Case B) of Example 6.5 corresponding to column 4 of Table 6.6. All modes are coupled flexural and axial modes, but in the first five the flexural components of the modes are most dominant. The graphs show (—) the modal transverse deflection W, (-◇-) longitudinal displacement u_t, and (-✳-) longitudinal displacement u_b.

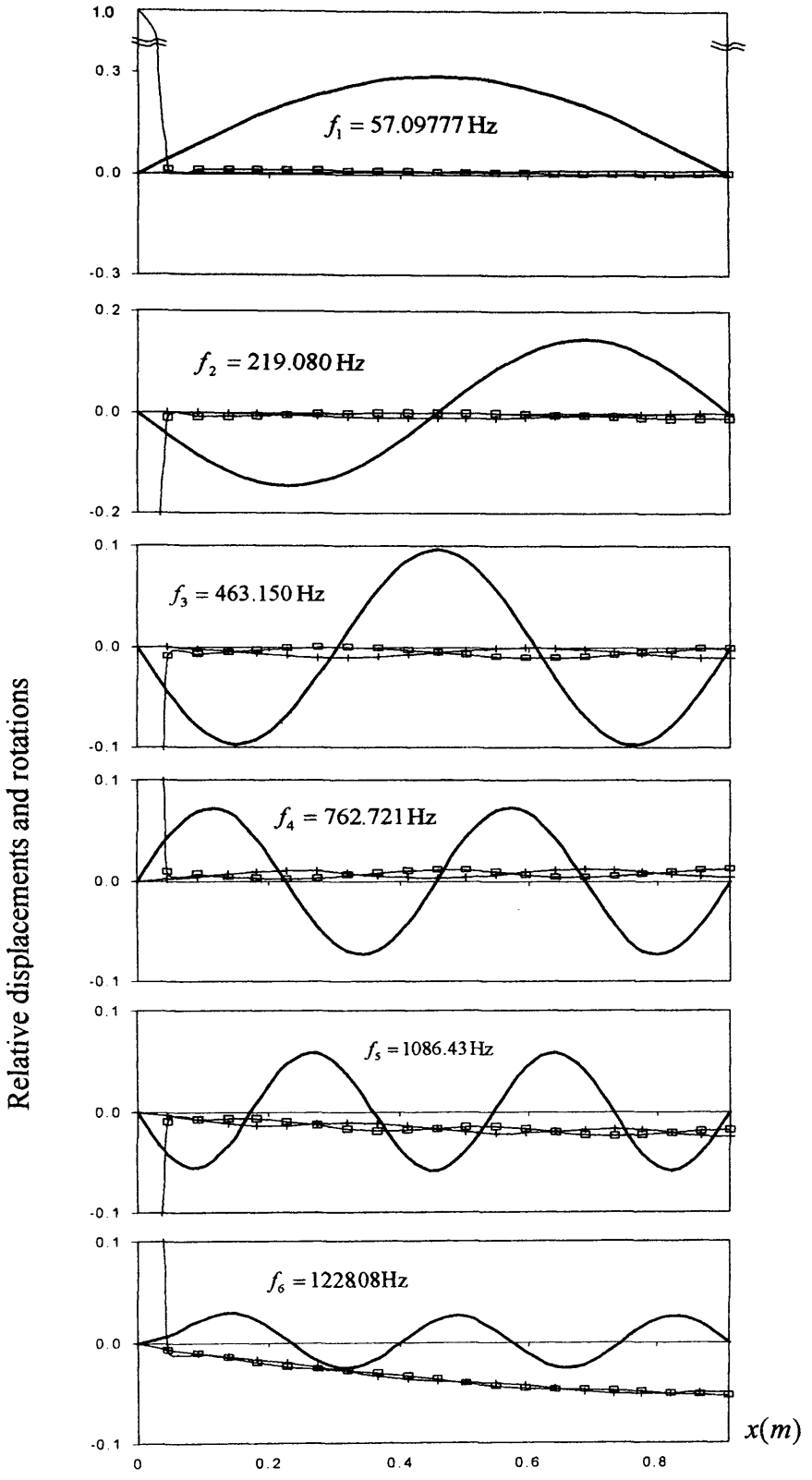

Figure 6.15: The first six natural frequencies and mode shapes of the simply supported beam (Case C) of Example 6.5 corresponding to column 5 of Table 6.6. All modes are coupled flexural and axial modes, but in the first five the flexural components of the modes are most dominant. The graphs show (—) the modal transverse deflection W, (-□-) longitudinal displacement u_2 and (-+-) longitudinal displacement u_3 in conjunction with Figure 6 .7.

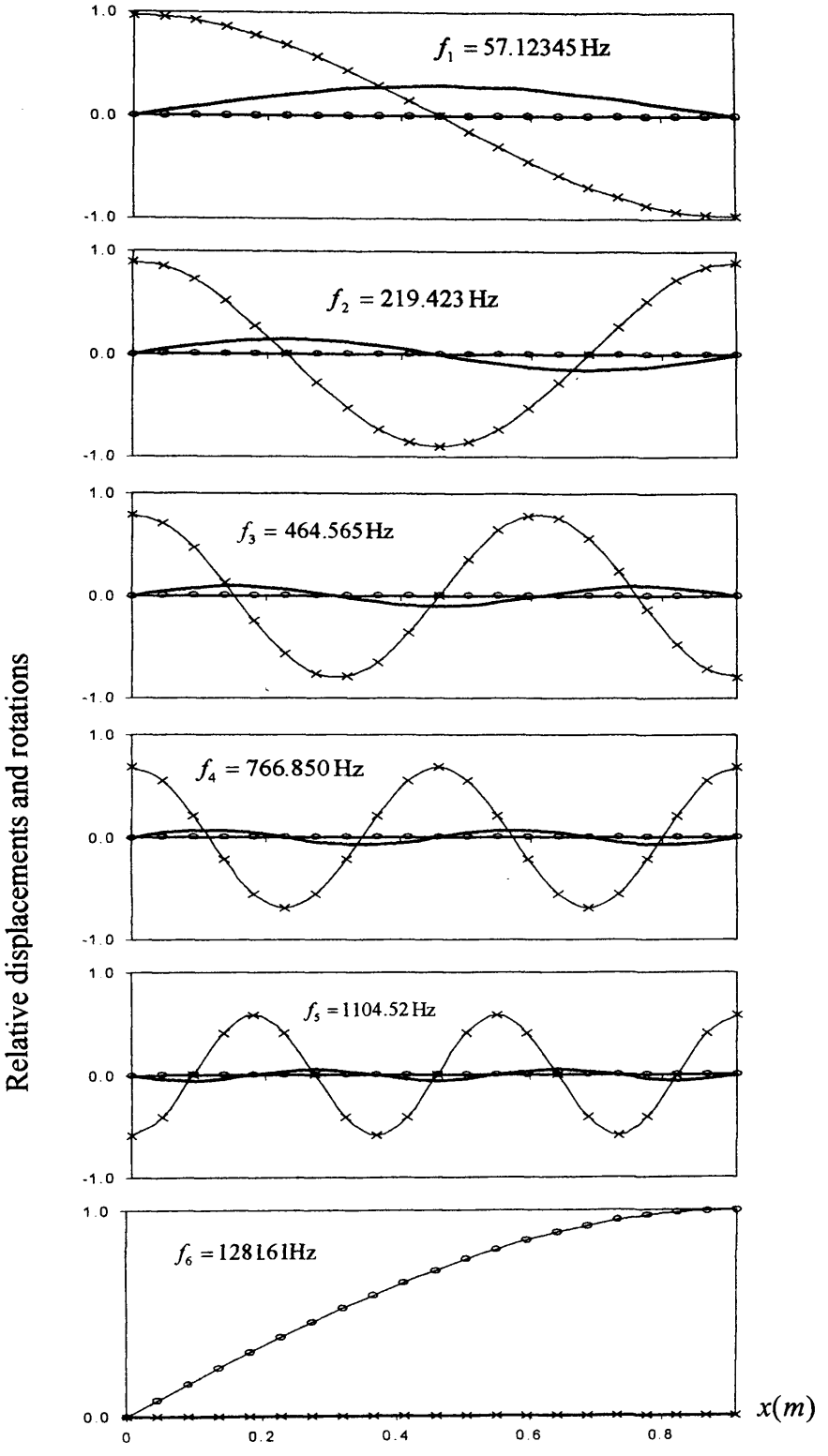

Figure 6.16: The first six natural frequencies and mode shapes of the simply supported beam (Case D) of Example 6.5 corresponding to column 6 of Table 6.6. The first five modes are pure flexural and the last mode is a pure axial mode. The graphs show (—) the modal transverse deflection W, (—o—) longitudinal displacement u and (—x—) average rotation of the beam's cross-section φ in conjunction with Figure 6 .7.

Example 6.6: The beam of Example 6.1 is now reanalysed, but the thickness of the layers is multiplied by 10. Various support conditions from roller-roller to simply supported are imposed (refer to Example 6.5 for an explanation of the abbreviations). The natural frequencies of the beam are given in Table 6.9. This shows that for deep beams the shear thickness mode may well be in the frequency range of interest.

Table 6.9: Comparative results for natural frequencies (Hz) of the deep sandwich beam of Example 6.6. Bracketed terms indicate predominant component of the mode.

Freq. No.	Roller-roller	Simply supported		
		Case A	Case B	Case D
1	294.808(B)	293.3143(B)	293.649(B)	294.808(B)
2	658.706(B)	653.6769(B)	656.326(B)	658.706(B)
3	1014.072(B)	798.6499(BA)	808.144(BA)	1014.072(B)
4	1368.797(B)	1017.041(B)	1014.942(B)	1281.61(A)
5	1596.045(S)	1369.641(B)	1368.925(B)	1368.797(B)
6	1726.274(B)	1725.17(B)	1726.184(B)	1596.045(S)
7	2088.462(B)	1871.087(SB)	1878.154(SB)	1726.274(B)
8	2456.815(B)	2090.327(B)	2088.557(B)	2088.462(B)
9	2563.221(A)	2457.229(B)	2456.828(B)	2456.815(B)
10	2832.561(B)	2818.611(B)	2831.836(B)	2832.561(B)
11	3138.852(S)	2846.612(B)	2837.661(B)	3138.852(S)
12	3216.797(B)	3216.38(B)	3216.791(B)	3216.797(B)
13	3610.531(B)	3607.184(B)	3610.504(B)	3610.531(B)
14	4014.702(B)	3988.061(B)	4014.565(B)	3844.832(A)
15	4430.183(B)	4098.532(SAB)	4118.046(SAB)	4014.702(B)
16	4857.791(B)	4437.404(B)	4430.219(B)	4430.183(B)
17	5126.451(A)	4860.223(B)	4857.799(B)	4857.791(B)
18	5298.285(B)	5293.185(B)	5298.272(B)	5298.285(B)
19	5628.741(S)	5365.328(SAB)	5365.453(SAB)	5628.741(S)
20	5752.372(B)	5750.872(B)	5752.370(B)	5752.372(B)

Example 6.7: Figure 6.17 shows a square, rigidly jointed plane frame constructed from four identical sandwich members. It is supported on pin-roller supports, where the axial constraint is imposed at the lower edge of the bottom faceplate i.e. case A. The length of each member is 0.40m and the remaining material and geometric properties are those used in Example 6.3. Since the author was unable to find any results in the literature for a

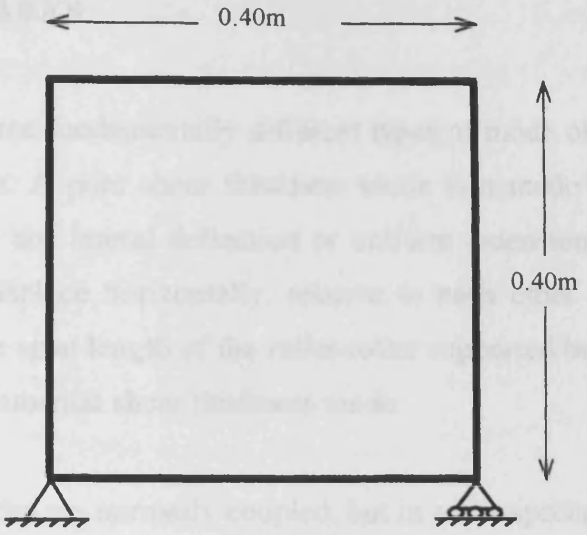

Figure 6.17: The pin-roller supported frame of Example 6.7.

comparable frame, the initial results for this frame were checked for consistency by increasing the axial rigidities by 10^3, a factor that is often used to make a structural element effectively in-extensible. On this assumption it is easy to argue that the fourth natural frequency of the frame will have a mode shape in which the moment contributed by each member at a joint balances to give zero rotation and must therefore correspond to the clamped ended natural frequency of an individual member. In this case the comparison will not be absolutely precise since the members are not completely in-extensible. The results are shown in Table 6.10.

Table 6.10: The first six natural frequencies (Hz) of the pin-roller supported frame of Example 6.7 for various axial rigidities of the faceplates. The clamped-ended frequency of a component member has been determined independently as 1794.926Hz and compares closely with the highlighted fourth frequency of the frame.

	Axial rigidity of each faceplate, $EA \times n$					
Freq. No	$n = 1$	5	10	50	100	1000
1	120.5509	236.2331	294.1437	393.201	414.1438	436.2441
2	449.098	898.7703	1137.255	1577.188	1676.598	1784.082
3	656.647	1158.188	1351.789	1632.714	1698.069	1784.597
4	750.296	1327.643	1551.083	1744.636	1770.457	1794.658
5	884.0354	1413.031	1573.057	1879.257	1954.636	2053.461
6	1546.225	2663.587	3035.215	3456.545	3522.757	3587.301

6.7 GENERAL REMARKS

Sandwich beams have three fundamentally different types of mode of vibration; flexural, axial and shear thickness. A pure shear thickness mode is a mode in which the beam remains straight, without any lateral deflection or uniform extension in the usual sense. Instead, the faceplates displace horizontally, relative to each other causing the core to deform in pure shear. The span length of the roller-roller supported beams does not effect the frequency of the fundamental shear thickness mode.

The three families of modes are normally coupled, but in some special cases it is possible to have uncoupled modes. For example, in a roller-roller supported sandwich beam with symmetric cross-section, the axial and flexural modes are uncoupled. Also the fundamental shear thickness mode is always a pure shear mode. Furthermore, the study of the mode shapes of the roller-roller beam shows that except for the fundamental shear thickness mode, the higher shear thickness modes always couple with flexural modes, with the results that two modes exist with the same number of half-waves in the transverse direction. The only difference between these two modes is an opposite sign associated with the average rotation of the cross-section and the general slope of the beam. Figure 6.18 shows a few of the lower modes of a roller-roller supported sandwich beam.

Figure 6.19 shows the influence of changing the beam's characteristics on the frequencies of the first flexural and axial modes and the fundamental coupled bending/shear mode for a roller-roller sandwich beam. The influence of increasing the axial rigidity of the faceplates is shown in Figure 6.19(a). From this figure it is clear that even for this completely symmetric beam, if the axial rigidity of the faceplates is increased, besides increasing the axial frequencies, the frequencies of the other families of modes are also increased. This means that the flexural and shear thickness modes are influenced by axial rigidity. Meanwhile, there are maximum and minimum values for the flexural frequency and only a minimum for the shear thickness mode, which is always greater than the frequency of the span independent, fundamental shear thickness mode. In Figure 6.19(b), the influence of changing the shear rigidity is examined and it is clear that this change does not affect the first axial frequency. A similar trend to the previous case may be

deduced for the other families of modes. Finally, Figure 6.19(c) shows that increasing the bending rigidity of the faces cause an increase in the frequency of the flexural mode, but it never exceeds the frequency of the first shear thickness mode. Although Figure 6.19 considers these influences for the lowest modes in each family, a similar trend can be discerned in the higher modes.

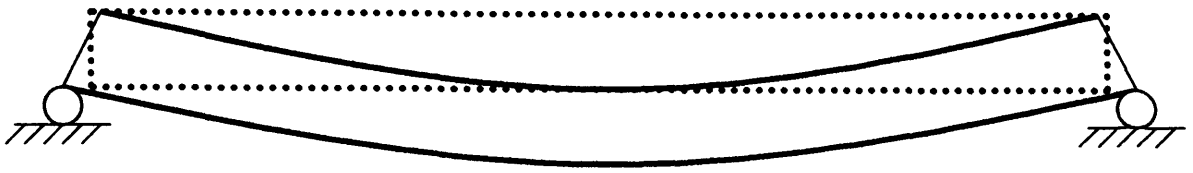

(a)

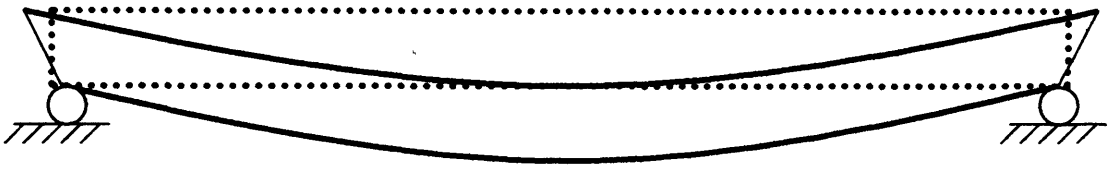

(b)

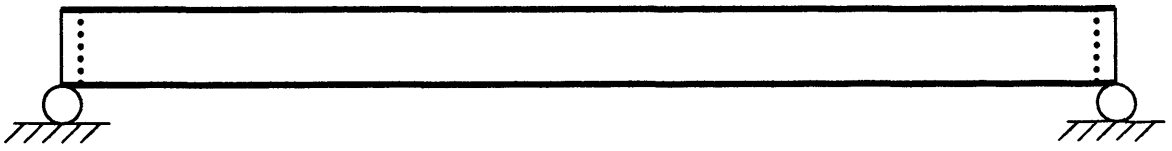

(c)

(d)

Figure 6.18: Examples of mode types of a roller-roller supported sandwich beam, a) fundamental bending mode, b) fundamental coupled bending/shear mode, c) fundamental axial mode and d) fundamental shear thickness mode. Dotted lines indicate undeformed shape.

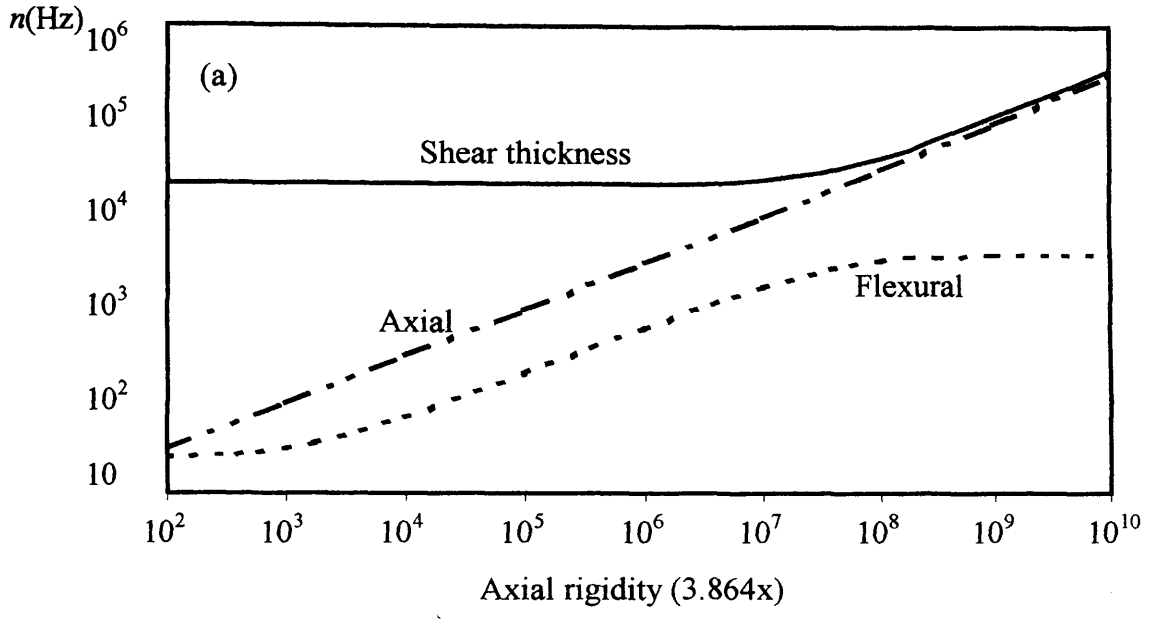
n(Hz)
10^6
10^5
10^4
10^3
10^2
10
(a)
Shear thickness
Axial
Flexural
10^2
10^3
10^4
10^5
10^6
10^7
10^8
10^9
10^10
Axial rigidity (3.864x)

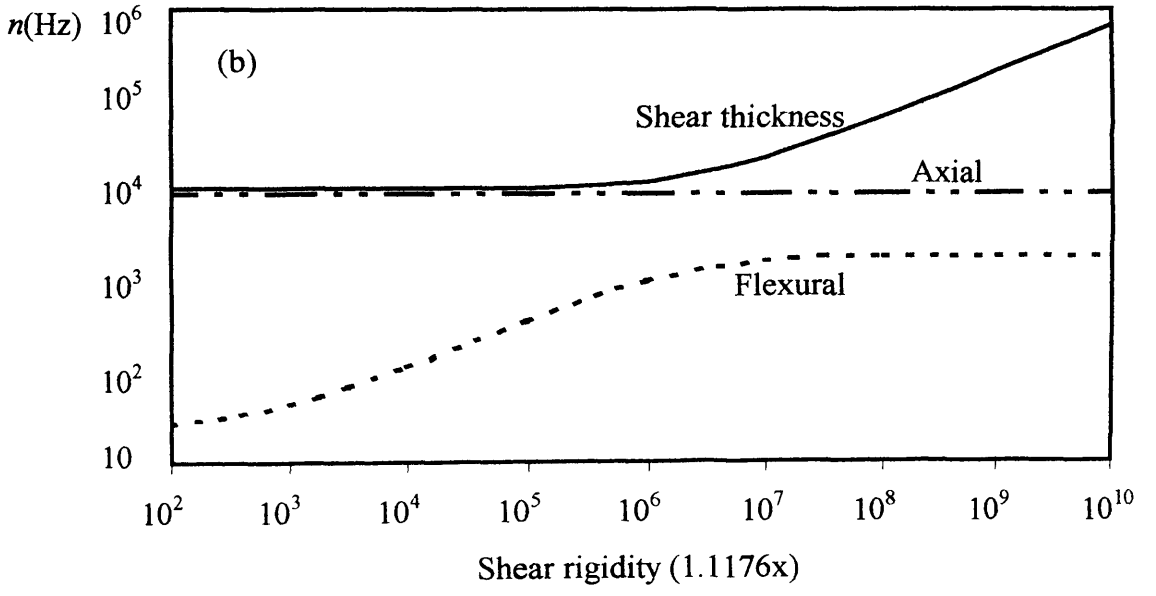
n(Hz)
10^6
10^5
10^4
10^3
10^2
10
(b)
Shear thickness
Axial
Flexural
10^2
10^3
10^4
10^5
10^6
10^7
10^8
10^9
10^10
Shear rigidity (1.1176x)

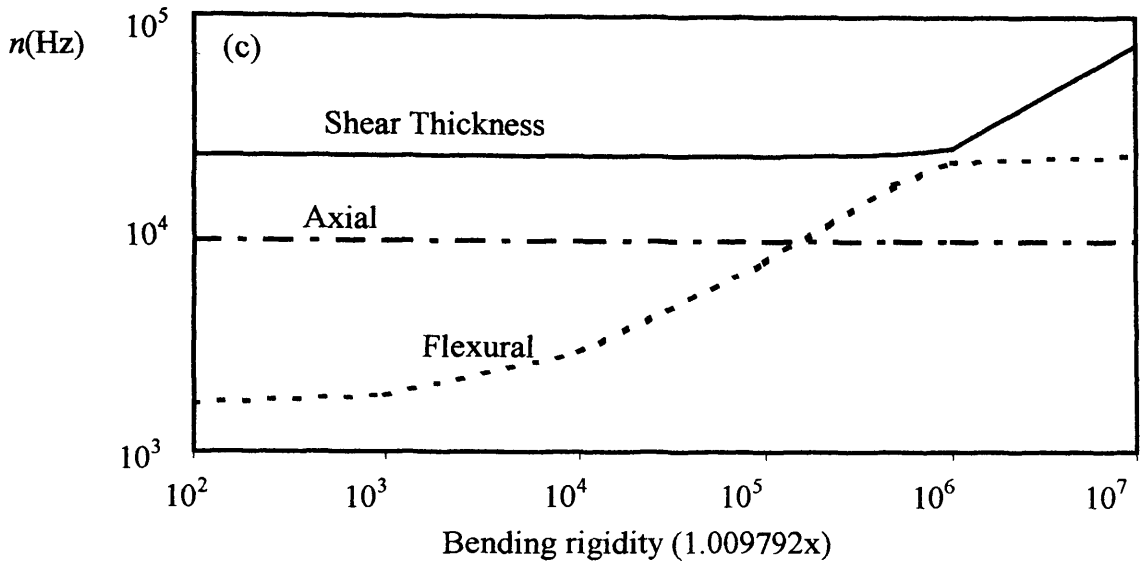

Figure 6.19: Variation of the frequency of single, half-wave modes due to increases in, a) axial, b) shear and c) bending rigidity of a roller-roller supported sandwich beam. Basic dimensions and material properties are the same as in Example 6.3.

Another crucial point is to distinguish fully between sandwich beams and homogeneous beams, since the thickness in the former plays an important role in the behaviour of the beam in the shear thickness mode of vibration and consequently on the coupling of the modes. Example 6.5 highlighted this issue. In contrast with homogeneous beams, the position of the axial constraint through the thickness of the beam is important. This leads to variations in coupling between the modes, as well as differences in corresponding frequencies.

The use of the stiffness method offers great flexibility to analyse frames, as well as to impose 'constraints' on any selected freedom of the structure. These will typically take the form of mass inertia, spring support stiffness or relationships that constrain one or more displacements to move in a predefined way relative to another set of displacements. Imposing such constraints follows the normal rules that would apply to a traditional beam element, except that more care is required to associate the constraint with the appropriate degree(s) of freedom. Also by using the appropriate transformations, as discussed in Section 6.5, the developed element can be used to model frames constructed from sandwich beams. Example 6.3 shows good correlation between the present author's

results for the L-shaped frame and the experimental and FEM results of reference (Petrone et al. 1999).

Furthermore, although the proposed element is straight, it can be used to model curved structures by using an appropriate number of straight elements to model the geometry of the curve. The results of Example 6.4 show that the number of straight elements needed is even less than the number of curved finite elements required to analyse a circularly curved arch. Reference (Ahmed 1972) compares the results of an FEM analysis with 6, 8 and 10 curved elements and shows that at least 10 elements are required for sufficient accuracy. However, Table 6.5 shows that the necessary convergence is achieved with only 4 of the proposed straight elements and the error with respect to the case with 10 such elements is less than 0.5 percent. Moreover, it is clear that the results from reference (Ahmed 1972) are always lower bounds, while those from (Ahmed 1971) are always upper bounds, due to the different assumptions in each reference.

The results of Examples 6.1 to 6.4 show good correlation between the current theory and a selection of comparable results available in the literature. The differences in the results are attributable to many factors that vary widely from their approximate solution techniques to differences in basic assumptions. Also, the results of Examples 6.5 to 6.7 provide a range of 'exact' solutions that may be helpful for future comparisons.

Finally, it is worth noting that while assembling the results it became apparent that it is relatively easy to generate an example in which the roots of the characteristic equation, Eq. (6.50), become sufficiently large that the value of ζ in Eq. (6.49b) overflows, even when using double precision arithmetic. However, because the combined effects of the roots and the length of the member are the source of this difficulty, reducing the length of the member (element) can help. Thus if difficulty is experienced a simple method is to subdivide the member into a greater number of elements until the problem is resolved.

CHAPTER 7

VIBRATIONS OF A THREE-LAYER, TIMOSHENKO SANDWICH BEAM INCLUDING COUPLED AXIAL INERTIA

7.1 INTRODUCTION

Mathematical models for the vibrational analysis of sandwich beams have been developed in various ways depending on the thickness of the faceplates. Thin faceplates can be assumed to act as flexible membranes that bend about the central axis of the section, with the total shear assumed to be carried solely by the shear-resisting core. Thick faces are assumed to behave as 'Bernoulli- Euler' beams having significant bending stiffness about their own centroidal axes and thus carry a part of the shear force acting across the section (Chapter 5). If the effect of rotary inertia is also considered, the faceplates can be treated as 'Rayleigh beams' (Section 6.4). In both cases it is assumed that the cross-sections of the faceplates remain plane and normal to the central axis and that the bending stiffness of the core is generally neglected.

However, the secondary effect of shear deformation can also be important for deeper beams. The combined effects of rotary inertia and transverse shear deformation on the dynamic behaviour of beams was first studied by Timoshenko (Timoshenko 1921) and the term 'Timoshenko beam' is used when both effects are considered. Timoshenko theory (Timoshenko 1921) retains the assumption of the elementary theory that cross-sections remain plane, but no longer assumes that they are normal to the central axis.

The theory developed in this chapter, is the most accurate so far and extends the theory of Chapter 6 to include the effects of shear deformation in the faceplates and the bending stiffness of the core. Hence, the faceplates and core are now governed by the same theory and it is no longer necessary to use the term 'core' for the central layer to distinguish it's behaviour from the top and bottom faceplates. The term 'core' or 'central layer' can thus be used interchangeably. The model can then be solved for any required frequency to any desired accuracy for both slender and deep beams using the Wittrick-Williams algorithm.

The dynamic stiffness matrix of a three-layer, Timoshenko sandwich beam is now developed from first principles. It accounts exactly for the uniform distribution of mass and stiffness in the member, subject only to the following assumptions:

(i) transverse direct strains in the faceplates and core are negligible so that small transverse displacements are the same for all points in a normal section;

(ii) there is perfect bonding at the core/faceplate interfaces.

7.2 FORCE-DISPLACEMENT RELATIONS

Figure 7.1 shows the positive displacement configuration for a typical section of the sandwich beam at some instant during the motion. Throughout this text the subscripts t, c, and b refer to the top faceplate, core and bottom faceplate or simply the top, central and bottom layers of the three-layered sandwich beam, respectively. The beam has unit width and t_t, t_c and t_b are the thickness of the top, central and bottom layers, respectively, u_j and u_{j+1} $(j = 1,2,3)$ are the longitudinal displacement of the top and bottom surfaces of the top, central and bottom layers, respectively. w is the transverse displacement

which, due to neglecting transverse direct strains in the layers, remains constant throughout the section at all layers and

$$\psi = w' \tag{7.1}$$

is the general slope of the beam, where the prime notation refers to partial differentiation with respect to x in the usual way.

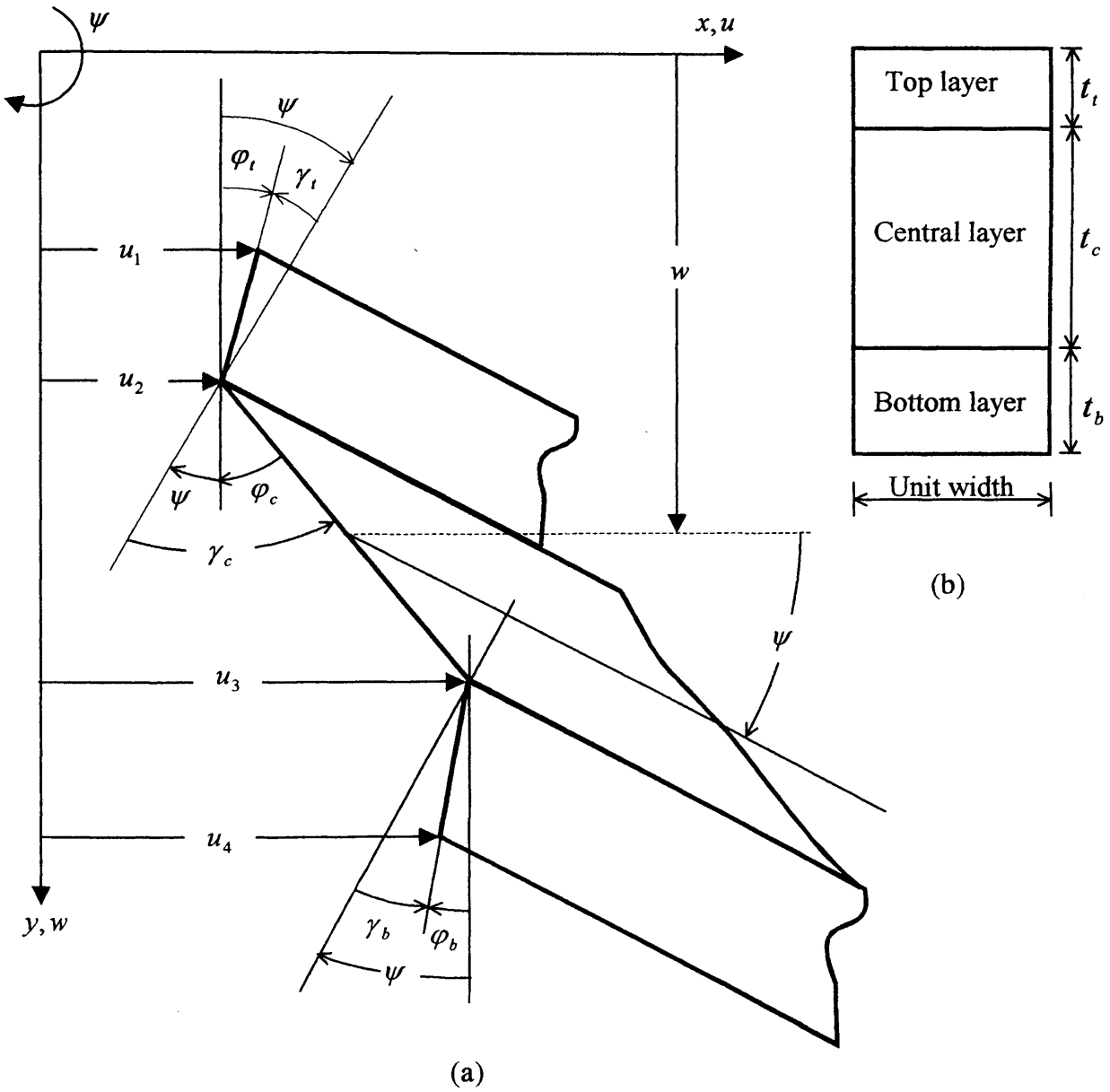

Figure 7.1: A typical sandwich beam section of unit width, a) the displaced section and co-ordinate system, b) the cross-section.

Since it is assumed that plane sections remain plane, the average rotation of the cross-section of the top, central and bottom layers (Figure 7.1), relative to their original configuration, can be written as

$$\varphi_t = \frac{u_1 - u_2}{t_t}; \qquad \varphi_c = \frac{u_2 - u_3}{t_c}; \qquad \varphi_b = \frac{u_3 - u_4}{t_b}; \tag{7.2a,b,c}$$

respectively. However, it is also assumed that due to shear deformation in the layers, the plane sections do not remain perpendicular to the beam axis, and therefore from Figure 7.1 it is clear that this deviation from perpendicular or the average shear strain in the layers, can be expressed as

$$\gamma_t = \psi - \varphi_t; \qquad \gamma_c = \psi - \varphi_c; \qquad \gamma_b = \psi - \varphi_b. \tag{7.3a,b,c}$$

The necessary force displacement relationships for axial extension and bending of the layers are

$$n_i = E_i t_i u_i' = K_i u_i' \quad \text{and} \quad m_i = -E_i I_i \varphi_i' \qquad (i = t,\ c \text{ and } b) \tag{7.4a,b}$$

respectively, where n_i and m_i are the axial force and bending moment in layer i, respectively, $K_i = E_i t_i$ and $E_i I_i$ are the axial and flexural rigidities per unit width, respectively, and u_i' is the average normal strain where

$$u_t = \frac{u_1 + u_2}{2}; \qquad u_c = \frac{u_2 + u_3}{2}; \qquad u_b = \frac{u_3 + u_4}{2}. \tag{7.5a,b,c}$$

The force-displacement relationships for shearing deformation in the layers are

$$q_i = t_i \tau_i = G_i t_i \gamma_i = S_i \gamma_i \qquad (i = t,\ c \text{ and } b) \tag{7.6}$$

where τ_i is the uniform average shear stress through the thickness of layer i, G_i is the effective shear modulus of the material and S_i is the shear rigidity.

7.3 DERIVATION OF THE GOVERNING DIFFERENTIAL EQUATION OF MOTION

The governing differential equations of motion can be derived via two different approaches; an Energy approach and an Equilibrium approach.

7.3.2 Energy approach

In complicated problems, where precision in establishing vectorial quantities requires great diligence, the energy approach can be used more easily. In this section, Hamilton's principle will be used to develop the governing differential equation of motion. The potential energy of the internal forces is called strain energy and is equal to the negative work of the internal forces. Kinetic energy is due to inertial forces.

7.3.2.1 Potential energy

The total strain energy for the beam of length L can now be written as

$$U = \int_0^L \begin{pmatrix} \frac{1}{2} q_t \gamma_t + \frac{1}{2} q_c \gamma_c + \frac{1}{2} q_b \gamma_b \\ + \frac{1}{2} n_t \varepsilon_t + \frac{1}{2} n_c \varepsilon_c + \frac{1}{2} n_b \varepsilon_b \\ - \frac{1}{2} m_t (\varphi_t')^2 - \frac{1}{2} m_c (\varphi_c')^2 \\ - \frac{1}{2} m_b (\varphi_b')^2 \end{pmatrix} \mathrm{d}x \qquad (7.7)$$

Strain energy of the three layers due to shear deformation

Strain energy of the three layers due to axial deformation

Strain energy of the three layers due to bending deformation.

where $\varepsilon_i = u'_i$ is the average normal strain of layer i ($i = t$, c and b). Using Eqs. (7.2a) and (7.3a) in Eq. (7.6) gives

$$\begin{aligned} q_t\gamma_t &= S_t\gamma_t^2 = S_t(\psi - \varphi_t)^2 = S_t(\psi^2 + \varphi_t^2 - 2\psi\varphi_t) \\ &= S_t\psi^2 + \frac{G_t}{t_t}u_1^2 + \frac{G_t}{t_t}u_2^2 - \frac{2G_t}{t_t}u_1u_2 - 2G_t\psi u_1 + 2G_t\psi u_2 \end{aligned} \tag{7.8}$$

and similarly

$$\begin{aligned} q_c\gamma_c &= S_c\gamma_c^2 = S_c(\psi - \varphi_c)^2 = S_c(\psi^2 + \varphi_c^2 - 2\psi\varphi_c) \\ &= S_c\psi^2 + \frac{G_c}{t_c}u_2^2 + \frac{G_c}{t_c}u_3^2 - \frac{2G_c}{t_c}u_2u_3 - 2G_c\psi u_2 + 2G_c\psi u_3 \end{aligned} \tag{7.9}$$

$$\begin{aligned} q_b\gamma_b &= S_b\gamma_b^2 = S_b(\psi - \varphi_b)^2 = S_b(\psi^2 + \varphi_b^2 - 2\psi\varphi_b) \\ &= S_b\psi^2 + \frac{G_b}{t_b}u_3^2 + \frac{G_b}{t_b}u_4^2 - \frac{2G_b}{t_b}u_3u_4 - 2G_b\psi u_3 + 2G_b\psi u_4 \end{aligned} \tag{7.10}$$

Also using Eq. (7.5) in Eq. (7.4a) yields

$$\left.\begin{aligned} n_t\varepsilon_t &= K_tu_t'^2 = \tfrac{1}{4}K_tu_1'^2 + \tfrac{1}{4}K_tu_2'^2 + \tfrac{1}{2}K_tu_1'u_2' \\ n_c\varepsilon_c &= K_cu_c'^2 = \tfrac{1}{4}K_cu_2'^2 + \tfrac{1}{4}K_cu_3'^2 + \tfrac{1}{2}K_cu_2'u_3' \\ n_b\varepsilon_b &= K_bu_b'^2 = \tfrac{1}{4}K_bu_3'^2 + \tfrac{1}{4}K_bu_4'^2 + \tfrac{1}{2}K_bu_3'u_4' \end{aligned}\right\} \tag{7.11}$$

Now substituting Eqs. (7.2) into Eq. (7.4b) where $I_i = t_i^3/12$ ($i = t$, c and b) gives

$$\left.\begin{aligned} m_t\varphi_t' &= -E_tI_t\varphi_t'^2 = -K_t(u_1'^2 + u_2'^2 - 2u_1'u_2')/12 \\ m_c\varphi_c' &= -E_cI_c\varphi_c'^2 = -K_c(u_2'^2 + u_3'^2 - 2u_3'u_3')/12 \\ m_b\varphi_b' &= -E_bI_b\varphi_b'^2 = -K_b(u_3'^2 + u_4'^2 - 2u_3'u_4')/12 \end{aligned}\right\} \tag{7.12}$$

Finally, substituting Eqs. (7.8) to (7.12) into Eq. (7.7) gives the total potential energy as

$$
\begin{aligned}
U = \int_0^L \{ & \tfrac{1}{2} S\psi^2 - [G_t u_1 - (G_t - G_c)u_2 - (G_c - G_b)u_3 - G_b u_4)]\psi \\
& + (\frac{1}{2}\frac{G_t}{t_t}u_1^2 - \frac{G_t}{t_t}u_1 u_2 + \frac{K_t}{6}u'^2_1 + \frac{K_t}{6}u'_1 u'_2) \\
& + (\frac{1}{2}(\frac{G_t}{t_t} + \frac{G_c}{t_c})u_2^2 - \frac{G_c}{t_c}u_2 u_3 + \frac{(K_t + K_c)}{6}u'^2_2 + \frac{K_c}{6}u'_2 u'_3) \\
& + (\frac{1}{2}(\frac{G_c}{t_c} + \frac{G_b}{t_b})u_3^2 - \frac{G_b}{t_b}u_3 u_4 + \frac{(K_c + K_b)}{6}u'^2_3 + \frac{K_b}{6}u'_3 u'_4) \\
& + (+\frac{1}{2}\frac{G_b}{t_b}u_4^2 + \frac{K_b}{6}u'^2_4)\} \mathrm{d}x
\end{aligned}
\tag{7.13}
$$

where $S = S_t + S_c + S_b$ is the total shear rigidity of the three-layer beam.

7.3.2.2 Kinetic energy

In similar fashion, the kinetic energy of the three-layer beam of length L including the axial, rotary and transverse inertia of all layers is given by

$$
T = \int_0^L \begin{pmatrix} \frac{1}{2}\mu\dot{w}^2 + & \text{Transverse inertia of full section} \\ \frac{1}{2}\mu_t\dot{u}_t^2 + \frac{1}{2}\mu_c\dot{u}_c^2 + \frac{1}{2}\mu_b\dot{u}_b^2 + & \text{Axial inertia of the three layers} \\ \frac{1}{2}\mu_t\frac{t_t^2}{12}\dot{\varphi}_t^2 + \frac{1}{2}\mu_c\frac{t_c^2}{12}\dot{\varphi}_c^2 + \frac{1}{2}\mu_b\frac{t_b^2}{12}\dot{\varphi}_b^2 & \text{Rotary inertia of the three layers} \end{pmatrix} \mathrm{d}x \tag{7.14}
$$

where μ_t, μ_c and μ_b are the mass/unit length of the top, central and bottom layers, respectively, and the dot notation refers to partial differentiation with respect to time in the usual way.

Substituting Eqs. (7.2) and (7.5) into Eq. (7.14) enables the total kinetic energy to be written as

$$T = \int_0^L (\frac{1}{2}\mu \dot{w}^2 + \frac{\mu_t}{6}\dot{u}_1^{\,2} + \frac{\mu_t}{6}\dot{u}_1\dot{u}_2 + \frac{(\mu_t+\mu_c)}{6}\dot{u}_2^{\,2} + \frac{\mu_c}{6}\dot{u}_2\dot{u}_3 + \frac{(\mu_c+\mu_b)}{6}\dot{u}_3^{\,2} + \frac{\mu_b}{6}\dot{u}_3\dot{u}_4 + \frac{\mu_b}{6}\dot{u}_4^{\,2})\,\mathrm{d}x \tag{7.15}$$

7.3.2.3 *Application of Hamilton's principle*

Applying Hamilton's principle in the form

$$\delta^{(1)}\phi = \delta^{(1)}\int_{t_1}^{t_2} L\,\mathrm{d}t = \delta^{(1)}\int_{t_1}^{t_2}(T-U)\,\mathrm{d}t = \delta^{(1)}\int_{t_1}^{t_2}\int_0^L F\,\mathrm{d}x\,\mathrm{d}t = 0 \tag{7.16}$$

in which the Lagrangian, $L = T - U$, has bean replaced by the functional $\int_0^L F\,\mathrm{d}x$, where the function F can be identified from Eqs. (7.13) and (7.15) as

$$\begin{aligned}
F =& \{\frac{1}{2}\mu\dot{w}^2 - \frac{1}{2}S\psi^2 + [G_t u_1 - (G_t - G_c)u_2 - (G_c - G_b)u_3 - G_b u_4)\psi\} \\
&+ \{\frac{\mu_t}{6}\dot{u}_1^{\,2} + \frac{\mu_t}{6}\dot{u}_1\dot{u}_2 - \frac{1}{2}\frac{G_t}{t_t}u_1^2 + \frac{G_t}{t_t}u_1u_2 - \frac{K_t}{6}u_1'^2 - \frac{K_t}{6}u_1'u_2'\} \\
&+ \{\frac{(\mu_t+\mu_c)}{6}\dot{u}_2^{\,2} + \frac{\mu_c}{6}\dot{u}_2\dot{u}_3 - \frac{1}{2}(\frac{G_t}{t_t}+\frac{G_c}{t_c})u_2^2 + \frac{G_c}{t_c}u_2u_3 - \frac{(K_t+K_c)}{6}u_2'^2 - \frac{K_c}{6}u_2'u_3'\} \\
&+ \{\frac{(\mu_c+\mu_b)}{6}\dot{u}_3^{\,2} + \frac{\mu_b}{6}\dot{u}_3\dot{u}_4 - \frac{1}{2}(\frac{G_c}{t_c}+\frac{G_b}{t_b})u_3^2 + \frac{G_b}{t_b}u_3u_4 - \frac{(K_c+K_b)}{6}u_3'^2 - \frac{K_b}{6}u_3'u_4'\} \\
&+ \{\frac{\mu_b}{6}\dot{u}_4^{\,2} - \frac{1}{2}\frac{G_b}{t_b}u_4^2 - \frac{K_b}{6}u_4'^2\}
\end{aligned} \tag{7.17}$$

generates the governing differential equations of motion. As before, Eq. (7.16) is solved by making use of the Euler-Lagrange equations for a functional involving higher-order derivatives with more than one independent variable given by

$$\left.\begin{aligned}
&\frac{\partial F}{\partial w}-\frac{\partial}{\partial x}\frac{\partial F}{\partial w'}-\frac{\partial}{\partial t}\frac{\partial F}{\partial \dot{w}}=0\\
&\frac{\partial F}{\partial u_1}-\frac{\partial}{\partial x}\frac{\partial F}{\partial u_1'}-\frac{\partial}{\partial t}\frac{\partial F}{\partial \dot{u}_1}=0\\
&\frac{\partial F}{\partial u_2}-\frac{\partial}{\partial x}\frac{\partial F}{\partial u_2'}-\frac{\partial}{\partial t}\frac{\partial F}{\partial \dot{u}_2}=0\\
&\frac{\partial F}{\partial u_3}-\frac{\partial}{\partial x}\frac{\partial F}{\partial u_3'}-\frac{\partial}{\partial t}\frac{\partial F}{\partial \dot{u}_3}=0\\
&\frac{\partial F}{\partial u_4}-\frac{\partial}{\partial x}\frac{\partial F}{\partial u_4'}-\frac{\partial}{\partial t}\frac{\partial F}{\partial \dot{u}_4}=0
\end{aligned}\right\} \qquad (7.18)$$

Using Eq.(7.1) and imposing Eqs. (7.18) on Eq. (7.17) yields

$$\left.\begin{aligned}
&-\frac{\partial}{\partial x}[-Sw'+G_tu_1-(G_t-G_c)u_2-(G_c-G_b)u_3-G_bu_4]-\frac{\partial}{\partial t}(\mu\dot{w})=0\\
&G_tw'+\frac{G_t}{t_t}u_2-\frac{G_t}{t_t}u_1-\frac{\partial}{\partial x}(-\frac{K_t}{3}u_1'-\frac{K_t}{6}u_2')-\frac{\partial}{\partial t}(\frac{\mu_t}{3}\dot{u}_1+\frac{\mu_t}{6}\dot{u}_2)=0\\
&-(G_t-G_c)w'+\frac{G_t}{t_t}u_1+\frac{G_c}{t_c}u_3-(\frac{G_t}{t_t}+\frac{G_c}{t_c})u_2\\
&-\frac{\partial}{\partial x}[-\frac{K_t}{6}u_1'-\frac{K_c}{6}u_3'-\frac{(K_t+K_c)}{3}u_2']-\frac{\partial}{\partial t}(\frac{\mu_t}{6}\dot{u}_1+\frac{\mu_c}{6}\dot{u}_3+\frac{(\mu_t+\mu_c)}{3}\dot{u}_2)=0\\
&-(G_c-G_b)w'+\frac{G_c}{t_c}u_2+\frac{G_b}{t_b}u_4-(\frac{G_c}{t_c}+\frac{G_b}{t_b})u_3\\
&-\frac{\partial}{\partial x}[-\frac{K_c}{6}u_2'-\frac{K_b}{6}u_4'-\frac{(K_c+K_b)}{3}u_3']-\frac{\partial}{\partial t}(\frac{\mu_c}{6}\dot{u}_2+\frac{\mu_b}{6}\dot{u}_4+\frac{(\mu_c+\mu_b)}{3}\dot{u}_3)=0\\
&-G_bw'+\frac{G_b}{t_b}u_3-\frac{G_b}{t_b}u_4-\frac{\partial}{\partial x}(-\frac{K_b}{6}u_3'-\frac{K_b}{3}u_4')-\frac{\partial}{\partial t}(\frac{\mu_b}{6}\dot{u}_3+\frac{\mu_b}{3}\dot{u}_4)=0
\end{aligned}\right\} \qquad (7.19)$$

The possible boundary conditions can also be deduced from Hamilton's principle as

$$-\frac{\partial F}{\partial w'}=0 \quad \text{or} \quad w=0 \qquad (7.20a,b)$$

$$-\frac{\partial F}{\partial u_1'}=0 \qquad \text{or} \qquad u_1=0 \tag{7.21a,b}$$

$$\frac{\partial F}{\partial u_2'}=0 \qquad \text{or} \qquad u_2=0 \tag{7.22a,b}$$

$$\frac{\partial F}{\partial u_3'}=0 \qquad \text{or} \qquad u_3=0 \tag{7.23a,b}$$

$$\frac{\partial F}{\partial u_4'}=0 \qquad \text{or} \qquad u_4=0 \tag{7.24a,b}$$

Eqs. (7.20a-7.24a) are the natural boundary conditions at either end of the element, while Eqs. (7.20b-7.24b) are the kinematic boundary conditions. The natural boundary conditions state the requirements for shear force on the beam and axial forces at the top and bottom surfaces of the top layer and the top and bottom surfaces of the bottom layer, as

$$S\psi+G_t u_1-(G_t-G_c)u_2-(G_c-G_b)u_3-G_b u_4=q=0 \tag{7.25}$$

$$\frac{K_t}{3}u_1'+\frac{K_t}{6}u_2'=n_1=0 \tag{7.26}$$

$$\frac{K_t}{6}u_1'+\frac{(K_t+K_c)}{3}u_2'+\frac{K_c}{6}u_3'=n_2=0 \tag{7.27}$$

$$\frac{K_c}{6}u_2'+\frac{(K_c+K_b)}{3}u_3'+\frac{K_b}{6}u_4'=n_3=0 \tag{7.28}$$

$$\frac{K_b}{6}u_3'+\frac{K_b}{3}u_4'=n_4=0 \tag{7.29}$$

Attention is now confined to harmonic motion in which the time dependent terms are related to ω, the circular frequency, by

$$f(x,t) = F(x)\, e^{i\omega t} \tag{7.30}$$

and the upper case characters refer to the amplitude of the equivalent time dependent quantity. Hence, using Eq. (7.30) in Eqs. (7.19) yields the following linear differential equations with constant coefficients

$$\left.\begin{aligned}
&-SW'' - \mu\omega^2 W + G_t U_1' - (G_t - G_c)U_2' - (G_c - G_b)U_3' - G_b U_4' = 0 \\
&G_t W' + \frac{G_t}{t_t}U_2 - \frac{G_t}{t_t}U_1 + \frac{K_t}{3}U_1'' + \frac{K_t}{6}U_2'' + \frac{\mu_t}{3}\omega^2 U_1 + \frac{\mu_t}{6}\omega^2 U_2 = 0 \\
&-(G_t - G_c)W' + \frac{G_t}{t_t}U_1 + \frac{G_c}{t_c}U_3 - (\frac{G_t}{t_t} + \frac{G_c}{t_c})U_2 \\
&+\frac{K_t}{6}U_1'' + \frac{K_c}{6}U_3'' + \frac{(K_t + K_c)}{3}U_2'' + \frac{\mu_t}{6}\omega^2 U_1 + \frac{\mu_c}{6}\omega^2 U_3 + \frac{(\mu_t + \mu_c)}{3}\omega^2 U_2 = 0 \\
&-(G_c - G_b)W' + \frac{G_c}{t_c}U_2 + \frac{G_b}{t_b}U_4 - (\frac{G_c}{t_c} + \frac{G_b}{t_b})U_3 \\
&+\frac{K_c}{6}U_2'' + \frac{K_b}{6}U_4'' + \frac{(K_c + K_b)}{3}U_3'' + \frac{\mu_c}{6}\omega^2 U_2 + \frac{\mu_b}{6}\omega^2 U_4 + \frac{(\mu_c + \mu_b)}{3}\omega^2 U_3 = 0 \\
&-G_b W' + \frac{G_b}{t_b}U_3 - \frac{G_b}{t_b}U_4 + \frac{K_b}{6}U_3'' - \frac{K_b}{3}U_4'' + \frac{\mu_b}{6}\omega^2 U_3 + \frac{\mu_b}{3}\omega^2 U_4 = 0
\end{aligned}\right\} \tag{7.31}$$

Using the operator $D = \mathrm{d}/\mathrm{d}x$, Eqs. (7.31) can be written in matrix form as

$$\begin{bmatrix}
A_1D^2 + A_2 & A_3D & A_4D & A_5D & A_6D \\
A_3D & A_7 + A_8D^2 & A_9 + A_{10}D^2 & 0 & 0 \\
A_4D & A_9 + A_{10}D^2 & A_{11} + A_{12}D^2 & A_{13} + A_{14}D^2 & 0 \\
A_5D & 0 & A_{13} + A_{14}D^2 & A_{15} + A_{16}D^2 & A_{17} + A_{18}D^2 \\
A_6D & 0 & 0 & A_{17} + A_{18}D^2 & A_{19} + A_{20}D^2
\end{bmatrix}
\begin{Bmatrix} W \\ U_1 \\ U_2 \\ U_3 \\ U_4 \end{Bmatrix} = \mathbf{0} \tag{7.32}$$

where

$$
\left.
\begin{aligned}
&A_1 = -S;\quad A_2 = -\mu\omega^2;\quad A_3 = G_t;\quad A_4 = -(G_t - G_c);\quad A_5 = -(G_c - G_b);\\
&A_6 = -G_b;\quad A_7 = -\frac{G_t}{t_t} + \frac{\mu_t}{3}\omega^2;\quad A_8 = \frac{K_t}{3};\quad A_9 = \frac{G_t}{t_t} + \frac{\mu_t}{6}\omega^2;\quad A_{10} = \frac{K_t}{6};\\
&A_{11} = -(\frac{G_t}{t_t} + \frac{G_c}{t_c}) + \frac{(\mu_t + \mu_c)}{3}\omega^2;\quad A_{12} = \frac{(K_t + K_c)}{3};\quad A_{13} = \frac{G_c}{t_c} + \frac{\mu_c}{6}\omega^2;\\
&A_{14} = \frac{K_c}{6};\quad A_{15} = -(\frac{G_c}{t_c} + \frac{G_b}{t_b}) + \frac{(\mu_c + \mu_b)}{3}\omega^2;\quad A_{16} = \frac{(K_c + K_b)}{3};\\
&A_{17} = \frac{G_b}{t_b} + \frac{\mu_b}{6}\omega^2;\quad A_{18} = \frac{K_b}{6};\quad A_{19} = -\frac{G_b}{t_b} + \frac{\mu_b}{3}\omega^2;\quad A_{20} = \frac{K_b}{3}
\end{aligned}
\right\} \qquad (7.33)
$$

Combining Eq. (7.32) into one equation by eliminating either W, U_1,U_2, U_3 or U_4 yields the following linear tenth order differential equation

$$[D^{10} + c_1 D^8 + c_2 D^6 + c_3 D^4 + c_4 D^2 + c_5]\, V = 0 \qquad (7.34)$$

where $V = W$, U_1,U_2, U_3 or U_4 and

$$
\left.
\begin{aligned}
c_1 &= (e_{18} + e_{28} + e_{38} + e_{48} + e_{58})/e_{110}\\
c_2 &= (e_{16} + e_{26} + e_{36} + e_{46} + e_{56})/e_{110}\\
c_3 &= (e_{14} + e_{24} + e_{34} + e_{44} + e_{54})/e_{110}\\
c_4 &= (e_{12} + e_{22} + e_{32} + e_{42} + e_{52})/e_{110}\\
c_5 &= e_{10}/e_{110}
\end{aligned}
\right\} \qquad (7.35)
$$

where

$$e_{110} = A_1 A_8 A_{12} A_{16} A_{20} - A_1 A_8 A_{12} A_{18}^2 - A_1 A_8 A_{14}^2 A_{20} - A_1 A_{10}^2 A_{16} A_{20} + A_1 A_{10}^2 A_{18}^2 \qquad (7.36)$$

$$
\begin{aligned}
e_{18} &= A_2 A_8 A_{12} A_{16} A_{20} - A_2 A_8 A_{12} A_{18}^2 - A_2 A_8 A_{14}^2 A_{20} - A_2 A_{10}^2 A_{16} A_{20} + A_2 A_{10}^2 A_{18}^2\\
&+ A_1 A_8 A_{12} A_{15} A_{20} + A_1 A_8 A_{12} A_{15} A_{19} - 2A_1 A_8 A_{12} A_{17} A_{18} + A_1 A_8 A_{11} A_{16} A_{20} - A_1 A_8 A_{11} A_{18}^2\\
&- A_1 A_8 A_{14}^2 A_{19} - 2A_1 A_8 A_{13} A_{14} A_{20} + A_1 A_7 A_{12} A_{16} A_{20} - A_1 A_7 A_{12} A_{18}^2 - A_1 A_7 A_{14}^2 A_{20}\\
&- 2A_1 A_9 A_{10} A_{16} A_{20} + 2A_1 A_9 A_{10} A_{18}^2 - A_1 A_{10}^2 A_{15} A_{20} - A_1 A_{10}^2 A_{16} A_{19} + 2A_1 A_{10}^2 A_{17} A_{18}
\end{aligned} \qquad (7.37)
$$

$$e_{16} = A_1A_7A_{12}A_{15}A_{20} + A_1A_7A_{12}A_{16}A_{19} - 2A_1A_7A_{12}A_{17}A_{18} + A_1A_7A_{11}A_{16}A_{20}$$
$$- A_1A_7A_{11}A_{18}^2 - A_1A_7A_{14}^2A_{19} - 2A_1A_7A_{13}A_{14}A_{20} + A_1A_8A_{11}A_{15}A_{20}$$
$$+ A_1A_8A_{11}A_{16}A_{19} - 2A_1A_8A_{11}A_{17}A_{18} + A_1A_8A_{12}A_{15}A_{19} - A_1A_8A_{12}A_{15}A_{17}^2$$
$$- 2A_1A_8A_{13}A_{14}A_{19} - A_1A_8A_{13}^2A_{20} - A_1A_{10}^2A_{15}A_{19} + A_1A_{10}^2A_{17}^2 - 2A_1A_9A_{10}A_{15}A_{20}$$
$$- 2A_1A_9A_{10}A_{16}A_{19} + 4A_1A_9A_{10}A_{17}A_{18} - A_1A_9^2A_{16}A_{20} + A_1A_9^2A_{18}^2 + A_2A_8A_{12}A_{15}A_{20} \quad (7.38)$$
$$+ A_2A_8A_{12}A_{16}A_{19} - 2A_2A_8A_{12}A_{17}A_{18} + A_2A_8A_{11}A_{16}A_{20} - A_2A_8A_{11}A_{18}^2$$
$$- A_2A_8A_{14}^2A_{19} - 2A_2A_8A_{13}A_{14}A_{20} + A_2A_7A_{12}A_{16}A_{20} - A_2A_7A_{12}A_{18}^2 - A_2A_7A_{14}^2A_{20}$$
$$- 2A_2A_9A_{10}A_{16}A_{20} + 2A_2A_9A_{10}A_{18}^2 - A_2A_{10}^2A_{15}A_{20} - A_2A_{10}^2A_{16}A_{19} + 2A_2A_{10}^2A_{17}A_{18}$$

$$e_{14} = A_1A_7A_{11}A_{15}A_{20} + A_1A_7A_{11}A_{16}A_{19} - 2A_1A_7A_{11}A_{17}A_{18} + A_1A_7A_{12}A_{15}A_{19}$$
$$- A_1A_7A_{12}A_{17}^2 - 2A_1A_7A_{13}A_{14}A_{19} - A_1A_7A_{13}^2A_{20} + A_1A_8A_{11}A_{15}A_{19}$$
$$- A_1A_8A_{11}A_{17}^2 - A_1A_8A_{13}^2A_{19} - A_1A_9^2A_{15}A_{20} - A_1A_9^2A_{16}A_{19} + 2A_1A_9^2A_{17}A_{18}$$
$$- 2A_1A_9A_{10}A_{15}A_{19} + 2A_1A_9A_{10}A_{17}^2 + A_2A_7A_{12}A_{15}A_{20} + A_2A_7A_{12}A_{16}A_{19}$$
$$- 2A_2A_7A_{12}A_{17}A_{18} + A_2A_7A_{11}A_{16}A_{20} - A_2A_7A_{11}A_{18}^2 - A_2A_7A_{14}^2A_{19} \quad (7.39)$$
$$- 2A_2A_7A_{13}A_{14}A_{20} + A_2A_8A_{11}A_{15}A_{20} + A_2A_8A_{11}A_{15}A_{19} - 2A_2A_8A_{11}A_{17}A_{18}$$
$$+ A_2A_8A_{12}A_{15}A_{19} - A_2A_8A_{12}A_{17}^2 - 2A_2A_8A_{13}A_{14}A_{19} - A_2A_8A_{13}^2A_{20} - A_2A_{10}^2A_{15}A_{19}$$
$$+ A_2A_{10}^2A_{17}^2 - 2A_2A_9A_{10}A_{15}A_{20} - 2A_2A_9A_{10}A_{16}A_{19} + 4A_2A_9A_{10}A_{17}A_{18}$$
$$- A_2A_9^2A_{16}A_{20} + A_2A_9^2A_{18}^2$$

$$e_{12} = A_1A_7A_{11}A_{15}A_{19} - A_1A_7A_{11}A_{17}^2 - A_1A_7A_{13}^2A_{19} - A_1A_9^2A_{15}A_{19} + A_1A_9^2A_{17}^2$$
$$+ A_2A_7A_{11}A_{15}A_{20} + A_2A_7A_{11}A_{16}A_{19} - 2A_2A_7A_{11}A_{17}A_{18} + A_2A_7A_{12}A_{15}A_{19}$$
$$- A_2A_7A_{12}A_{17}^2 - 2A_2A_7A_{13}A_{14}A_{19} - A_2A_7A_{13}^2A_{20} + A_2A_8A_{11}A_{15}A_{19} \quad (7.40)$$
$$- A_2A_8A_{11}A_{17}^2 - A_2A_8A_{13}^2A_{19} - A_2A_9^2A_{15}A_{20} - A_2A_9^2A_{16}A_{19} + 2A_2A_9^2A_{17}A_{18}$$
$$- 2A_2A_9A_{10}A_{15}A_{19} + 2A_2A_9A_{10}A_{17}^2$$

$$e_{10} = A_2A_7A_{11}A_{15}A_{19} - A_2A_7A_{11}A_{17}^2 - A_2A_7A_{13}^2A_{19} - A_2A_9^2A_{15}A_{19} + A_2A_9^2A_{17}^2 \quad (7.41)$$

$$e_{28} = A_3A_4A_{10}A_{16}A_{20} - A_3A_4A_{10}A_{18}^2 - A_3A_5A_{10}A_{14}A_{20} + A_3A_6A_{10}A_{14}A_{18} \quad (7.42)$$
$$- A_3^2A_{12}A_{16}A_{20} + A_3^2A_{12}A_{18}^2 + A_3^2A_{14}^2A_{20}$$

$$e_{26} = A_3A_4A_9A_{16}A_{20} - A_3A_4A_9A_{18}^2 - A_3A_5A_9A_{14}A_{20} + A_3A_6A_9A_{14}A_{18}$$
$$+ A_3A_4A_{10}A_{15}A_{20} + A_3A_4A_{10}A_{16}A_{19} - 2A_3A_4A_{10}A_{17}A_{18} - A_3A_5A_{10}A_{13}A_{20}$$
$$+ A_3A_6A_{10}A_{13}A_{18} - A_3A_6A_{10}A_{14}A_{19} + A_3A_6A_{10}A_{14}A_{17} - A_3^2A_{12}A_{15}A_{20} \quad (7.43)$$
$$- A_3^2A_{12}A_{16}A_{19} + 2A_3^2A_{12}A_{17}A_{18} - A_3^2A_{11}A_{16}A_{20} + A_3^2A_{11}A_{18}^2 + A_3^2A_{14}^2A_{19}$$
$$+ 2A_3^2A_{13}A_{14}A_{20}$$

$$e_{24} = A_3A_4A_9A_{15}A_{20} + A_3A_4A_9A_{16}A_{19} - 2A_3A_4A_9A_{17}A_{18} - A_3A_5A_9A_{13}A_{20} + A_3A_6A_9A_{13}A_{18} - A_3A_5A_9A_{14}A_{19} + A_3A_6A_9A_{14}A_{17} + A_3A_4A_{10}A_{15}A_{19} - A_3A_4A_{10}A_{17}^2 - A_3A_5A_{10}A_{13}A_{19} + A_3A_6A_{10}A_{13}A_{17} - A_3^2A_{11}A_{15}A_{20} - A_3^2A_{11}A_{16}A_{19} + 2A_3^2A_{11}A_{17}A_{18} - A_3^2A_{12}A_{15}A_{19} + A_3^2A_{12}A_{17}^2 + 2A_3^2A_{13}A_{14}A_{19} + A_3^2A_{13}^2A_{20} \quad (7.44)$$

$$e_{22} = A_3A_4A_9A_{15}A_{19} - A_3A_4A_9A_{17}^2 - A_3A_5A_9A_{13}A_{19} + A_3A_6A_9A_{13}A_{17} - A_3^2A_{11}A_{15}A_{19} + A_3^2A_{11}A_{17}^2 + A_3^2A_{13}^2A_{19} \quad (7.45)$$

$$e_{38} = A_3A_4A_{10}A_{16}A_{20} - A_3A_4A_{10}A_{18}^2 - A_4^2A_8A_{16}A_{20} + A_4^2A_8A_{18}^2 + A_4A_5A_8A_{14}A_{20} - A_4A_6A_8A_{14}A_{19} \quad (7.46)$$

$$e_{36} = A_3A_4A_9A_{16}A_{20} - A_3A_4A_9A_{18}^2 + A_3A_4A_{10}A_{15}A_{20} + A_3A_4A_{10}A_{16}A_{19} - 2A_3A_4A_{10}A_{17}A_{18} - A_4^2A_7A_{16}A_{20} + A_4^2A_7A_{18}^2 + A_4A_5A_7A_{14}A_{20} - A_4A_6A_7A_{14}A_{18} - A_4^2A_8A_{15}A_{20} - A_4^2A_8A_{16}A_{19} + 2A_4^2A_8A_{17}A_{18} + A_4A_5A_8A_{13}A_{20} - A_4A_6A_8A_{13}A_{19} + A_4A_5A_8A_{14}A_{19} - A_4A_6A_8A_{14}A_{17} \quad (7.47)$$

$$e_{34} = A_3A_4A_9A_{15}A_{20} + A_3A_4A_9A_{16}A_{19} - 2A_3A_4A_9A_{17}A_{18} + A_3A_4A_{10}A_{15}A_{19} - A_3A_4A_{10}A_{17}^2 - A_4^2A_7A_{15}A_{20} - A_4^2A_7A_{16}A_{19} + 2A_4^2A_7A_{17}A_{18} + A_4A_5A_7A_{13}A_{20} - A_4A_6A_7A_{13}A_{18} + A_4A_5A_7A_{14}A_{19} - A_4A_6A_7A_{14}A_{17} - A_4^2A_8A_{15}A_{19} + A_4^2A_8A_{17}^2 + A_4A_5A_8A_{13}A_{19} - A_4A_6A_8A_{13}A_{17} \quad (7.48)$$

$$e_{32} = A_3A_4A_9A_{15}A_{19} - A_3A_4A_9A_{17}^2 - A_4^2A_7A_{15}A_{19} + A_4A_5A_7A_{13}A_{19} - A_4A_6A_7A_{13}A_{17} + A_4^2A_7A_{17}^2 \quad (7.49)$$

$$e_{48} = A_5A_6A_8A_{12}A_{18} - A_5A_6A_{10}^2A_{18} - A_3A_5A_{10}A_{14}A_{20} + A_4A_5A_8A_{14}A_{20} - A_5^2A_8A_{12}A_{20} + A_5^2A_{10}^2A_{20} \quad (7.50)$$

$$e_{46} = A_5A_6A_8A_{12}A_{17} - A_5A_6A_{10}^2A_{17} + A_5A_6A_7A_{12}A_{18} + A_5A_6A_8A_{11}A_{18} - 2A_5A_6A_9A_{10}A_{18} - A_3A_5A_{10}A_{14}A_{19} + A_4A_5A_8A_{14}A_{19} - A_3A_5A_9A_{14}A_{20} - A_3A_5A_{10}A_{13}A_{20} + A_4A_5A_7A_{14}A_{20} + A_4A_5A_8A_{13}A_{20} - A_5^2A_7A_{12}A_{20} - A_5^2A_8A_{11}A_{20} + 2A_5^2A_9A_{10}A_{20} - A_5^2A_8A_{12}A_{19} + A_5^2A_{10}^2A_{19} \quad (7.51)$$

$$e_{44} = A_5A_6A_7A_{12}A_{17} + A_5A_6A_8A_{11}A_{17} - 2A_5A_6A_9A_{10}A_{17} + A_5A_6A_7A_{11}A_{18} - A_5A_6A_9^2A_{18} - A_3A_5A_9A_{14}A_{19} - A_3A_5A_{10}A_{13}A_{19} + A_4A_5A_7A_{14}A_{19} - A_3A_5A_9A_{13}A_{20} + A_4A_5A_7A_{13}A_{20} + A_4A_5A_8A_{13}A_{19} - A_5^2A_7A_{12}A_{19} - A_5^2A_8A_{11}A_{19} + 2A_5^2A_9A_{10}A_{19} - A_5^2A_7A_{11}A_{20} + A_5^2A_9^2A_{20} \quad (7.52)$$

$$e_{42} = A_5A_6A_7A_{11}A_{17} - A_5A_6A_9^2A_{17} - A_3A_5A_9A_{13}A_{19} + A_4A_5A_7A_{13}A_{19} - A_5^2A_7A_{11}A_{19} + A_5^2A_9^2A_{19} \tag{7.53}$$

$$e_{58} = A_3A_6A_{10}A_{14}A_{18} - A_5A_6A_{10}^2A_{18} + A_6^2A_{10}^2A_{16} - A_4A_6A_8A_{14}A_{18} + A_5A_6A_8A_{12}A_{18} - A_6^2A_8A_{12}A_{16} + A_6^2A_8A_{14}^2 \tag{7.54}$$

$$\begin{aligned} e_{56} = {} & A_3A_6A_9A_{14}A_{18} - A_5A_6A_9A_{10}A_{18} + A_6^2A_9A_{10}A_{16} + A_3A_6A_{10}A_{13}A_{18} \\ & + A_3A_6A_{10}A_{14}A_{17} - A_5A_6A_9A_{10}A_{18} - A_5A_6A_{10}^2A_{17} + A_6^2A_9A_{10}A_{16} \\ & + A_6^2A_{10}^2A_{15} - A_4A_6A_7A_{14}A_{18} + A_5A_6A_7A_{12}A_{18} - A_4A_6A_8A_{13}A_{18} \\ & - A_4A_6A_8A_{14}A_{17} + A_5A_6A_8A_{11}A_{18} + A_5A_6A_8A_{12}A_{17} - A_6^2A_7A_{12}A_{16} \\ & + A_6^2A_7A_{14}^2 - A_6^2A_8A_{11}A_{16} - A_6^2A_8A_{12}A_{15} + 2A_6^2A_8A_{13}A_{14} \end{aligned} \tag{7.55}$$

$$\begin{aligned} e_{54} = {} & A_3A_6A_9A_{13}A_{18} + A_3A_6A_9A_{14}A_{17} - A_5A_6A_9^2A_{18} - A_5A_6A_9A_{10}A_{17} \\ & + A_6^2A_9^2A_{16} + A_6^2A_9A_{10}A_{15} + A_3A_6A_{10}A_{13}A_{17} - A_5A_6A_9A_{10}A_{17} + \\ & A_6^2A_9A_{10}A_{15} - A_4A_6A_7A_{13}A_{18} - A_4A_6A_7A_{14}A_{17} + A_5A_6A_7A_{11}A_{18} \\ & + A_5A_6A_7A_{12}A_{17} - A_4A_6A_8A_{13}A_{17} + A_5A_6A_8A_{11}A_{17} - A_6^2A_7A_{11}A_{16} \\ & - A_6^2A_7A_{12}A_{15} + 2A_6^2A_7A_{13}A_{14} - A_6^2A_8A_{11}A_{15} + A_6^2A_8A_{13}^2 \end{aligned} \tag{7.56}$$

$$\begin{aligned} e_{52} = {} & A_3A_6A_9A_{13}A_{17} - A_5A_6A_9^2A_{17} + A_6^2A_9^2A_{15} - A_4A_6A_7A_{13}A_{17} \\ & + A_5A_6A_7A_{11}A_{17} - A_6^2A_7A_{11}A_{17} + A_6^2A_7A_{13}^2 \end{aligned} \tag{7.57}$$

7.3.3 Equilibrium approach

Consider a typical elemental length of a member at some instant during the motion, Figure 7.2. The equation of horizontal equilibrium can then be written as

$$\frac{\partial n_t}{\partial x} + \frac{\partial n_c}{\partial x} + \frac{\partial n_b}{\partial x} = \mu_t\ddot{u}_t + \mu_c\ddot{u}_c + \mu_b\ddot{u}_b \tag{7.58}$$

Substituting from Eqs. (7.4a) and (7.5) into Eq. (7.58) gives the first differential equation of motion as

$$\begin{aligned} & K_tu_1'' - \mu_t\ddot{u}_1 + (K_t + K_c)u_2'' - (\mu_t + \mu_c)\ddot{u}_2 + \\ & \qquad (K_c + K_b)u_3'' - (\mu_c + \mu_b)\ddot{u}_3 + K_bu_4'' - \mu_b\ddot{u}_4 = 0 \end{aligned} \tag{7.59}$$

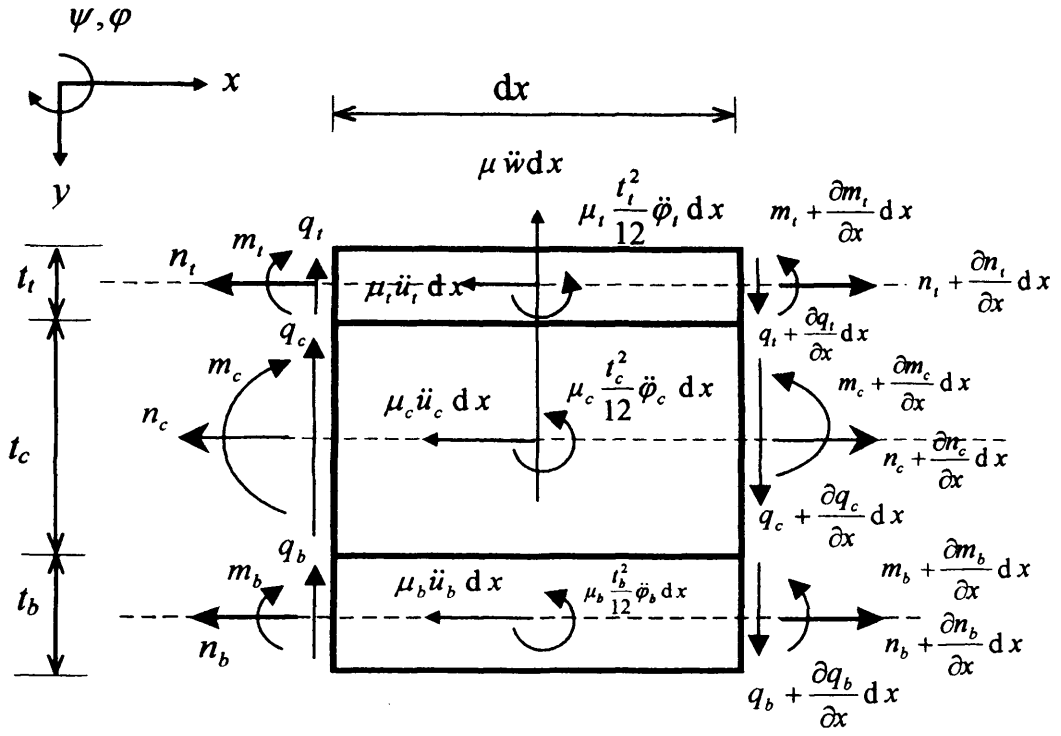

Figure 7.2: Positive resultant forces and moments and reverse linear and rotary inertias acting on a typical elemental length of a three-layer sandwich beam of unit width in local co-ordinates.

Since in free vibration analysis, the only external vertical force is the transverse inertia, the equation of vertical equilibrium is

$$\frac{\partial q}{\partial x} = \mu \ddot{w} \tag{7.60}$$

where, from Figure 7.2, it is clear that $q = q_t + q_b + q_c$ is the resultant shear force at any normal section of the element in which q, subscripted with t, c, or b, relates to the shear force of the top, central and bottom layers, respectively, and $\mu = \mu_t + \mu_b + \mu_c$ is the mass per unit length of the beam.

Taking moments about the bottom right hand corner of the element in Figure 7.2 and ignoring terms of second order yields the moment equilibrium as

$$
\begin{aligned}
q\,\mathrm{d}x-\frac{\partial m}{\partial x}\mathrm{d}x+\frac{\partial n_t}{\partial x}\mathrm{d}x(\frac{t_t}{2}+t_c+t_b)-\mu_t\ddot{u}_t\,\mathrm{d}x(\frac{t_t}{2}+t_c+t_b)+ \\
\frac{\partial n_c}{\partial x}\mathrm{d}x(\frac{t_c}{2}+t_b)-\mu_c\ddot{u}_c\,\mathrm{d}x(\frac{t_c}{2}+t_b)+ \\
\frac{\partial n_b}{\partial x}\mathrm{d}x(\frac{t_b}{2})-\mu_b\ddot{u}_b\,\mathrm{d}x(\frac{t_b}{2}) \\
=\mu_t\frac{t_t^2}{12}\mathrm{d}x\ddot{\varphi}_t+\mu_c\frac{t_c^2}{12}\mathrm{d}x\ddot{\varphi}_c+\mu_b\frac{t_b^2}{12}\mathrm{d}x\ddot{\varphi}_b
\end{aligned}
\tag{7.61}
$$

where m is the resultant bending moment at any section given by

$$
m=m_t+m_c+m_b \tag{7.62}
$$

Using Eqs. (7.4b) and (7.2) in Eq. (7.62) yields the resultant bending moment as

$$
\begin{aligned}
m&=-E_tI_t\varphi_t'-E_cI_c\varphi_c'-E_bI_b\varphi_b' \\
&=-\frac{K_tt_t}{12}(u_1'-u_2')-\frac{K_ct_c}{12}(u_2'-u_3')-\frac{K_bt_b}{12}(u_3'-u_4')
\end{aligned}
\tag{7.63}
$$

Now, substituting Eqs. (7.63), (7.4a), (7.5) and (7.2) into Eq. (7.61) yields the resultant shear force as

$$
\begin{aligned}
q=&-\frac{K_tt_t}{12}u_1''+\frac{K_tt_t}{12}u_2''-\frac{K_ct_c}{12}u_2''+\frac{K_ct_c}{12}u_3''-\frac{K_bt_b}{12}u_3''+\frac{K_bt_b}{12}u_4'' \\
&-\frac{K_t}{2}(\frac{t_t}{2}+t_c+t_b)u_1''-\frac{K_t}{2}(\frac{t_t}{2}+t_c+t_b)u_2''+\frac{\mu_t}{2}(\frac{t_t}{2}+t_c+t_b)\ddot{u}_1+\frac{\mu_t}{2}(\frac{t_t}{2}+t_c+t_b)\ddot{u}_2 \\
&-\frac{K_c}{2}(\frac{t_c}{2}+t_b)u_2''-\frac{K_c}{2}(\frac{t_c}{2}+t_b)u_3''+\frac{\mu_c}{2}(\frac{t_c}{2}+t_b)\ddot{u}_2+\frac{\mu_c}{2}(\frac{t_c}{2}+t_b)\ddot{u}_3 \\
&-\frac{K_b}{2}(\frac{t_b}{2})u_3''-\frac{K_b}{2}(\frac{t_b}{2})u_4''+\frac{\mu_b}{2}(\frac{t_b}{2})\ddot{u}_3+\frac{\mu_b}{2}(\frac{t_b}{2})\ddot{u}_4 \\
&+\mu_t\frac{t_t}{12}\ddot{u}_1-\mu_t\frac{t_t}{12}\ddot{u}_2+\mu_c\frac{t_c}{12}\ddot{u}_2-\mu_c\frac{t_c}{12}\ddot{u}_3+\mu_b\frac{t_b}{12}\ddot{u}_3-\mu_b\frac{t_b}{12}\ddot{u}_4
\end{aligned}
\tag{7.64}
$$

or in a more compact form as

$$
\begin{aligned}
q = &-\frac{K_t}{2}(\frac{2t_t}{3}+t_c+t_b)u_1''+\frac{\mu_t}{2}(\frac{2t_t}{3}+t_c+t_b)\ddot{u}_1 \\
&-[\frac{K_t}{2}(\frac{t_t}{3}+t_c+t_b)+\frac{K_c}{2}(\frac{2t_c}{3}+t_b)]u_2''+[\frac{\mu_t}{2}(\frac{t_t}{3}+t_c+t_b)+\frac{\mu_c}{2}(\frac{2t_c}{3}+t_b)]\ddot{u}_2 \\
&-[\frac{K_c}{2}(\frac{t_c}{3}+t_b)+\frac{K_b}{2}(\frac{2t_b}{3})]u_3''+[\frac{\mu_c}{2}(\frac{t_c}{3}+t_b)+\frac{\mu_b}{2}(\frac{2t_b}{3})]\ddot{u}_3 \\
&-\frac{K_b}{2}(\frac{t_b}{3})u_4''+\frac{\mu_b}{2}(\frac{t_b}{3})\ddot{u}_4
\end{aligned}
\tag{7.65}
$$

Now, substituting Eq. (7.65) into Eq. (7.60) yields a further differential equation of motion as

$$
\begin{aligned}
&\mu\ddot{w}+\frac{K_t}{2}(\frac{2t_t}{3}+t_c+t_b)u_1'''-\frac{\mu_t}{2}(\frac{2t_t}{3}+t_c+t_b)\ddot{u}_1' \\
&+[\frac{K_t}{2}(\frac{t_t}{3}+t_c+t_b)+\frac{K_c}{2}(\frac{2t_c}{3}+t_b)]u_2'''-[\frac{\mu_t}{2}(\frac{t_t}{3}+t_c+t_b)+\frac{\mu_c}{2}(\frac{2t_c}{3}+t_b)]\ddot{u}_2' \\
&+[\frac{K_c}{2}(\frac{t_c}{3}+t_b)+\frac{K_b}{2}(\frac{2t_b}{3})]u_3'''-[\frac{\mu_c}{2}(\frac{t_c}{3}+t_b)+\frac{\mu_b}{2}(\frac{2t_b}{3})]\ddot{u}_3' \\
&+\frac{K_b}{2}(\frac{t_b}{3})u_4'''-\frac{\mu_b}{2}(\frac{t_b}{3})\ddot{u}_4'=0
\end{aligned}
\tag{7.66}
$$

Before proceeding it should be noted that around Eqs. (7.3) and (7.6) it was assumed that the shear stress or strain through the thickness of each layer has a uniform average value, whereas in fact they vary. However, the exact relationship for the shear stress at the interfaces of the layers can be determined using the differential equation of equilibrium of each layer. For instance, consider Figure 7.3 which shows the shearing stress $\tau_t(z)$ at any distance $0<z<t_t$ from the top surface of the top layer. The equation of horizontal equilibrium for Figure 7.3 can be written as

$$
\tau_t(z)\,\mathrm{d}x+\int_0^z\frac{\partial\sigma(\zeta)}{\partial x}\,\mathrm{d}x\,d\zeta=\int_0^z\rho_t\,\mathrm{d}x\,\ddot{u}(\zeta)\,\mathrm{d}\zeta \tag{7.67}
$$

where σ is the normal stress at any point $0<\zeta<z$ through the thickness of the layer, ρ_t is the mass density of the top layer and $\mathrm{d}\zeta$ is the elemental thickness. The longitudinal

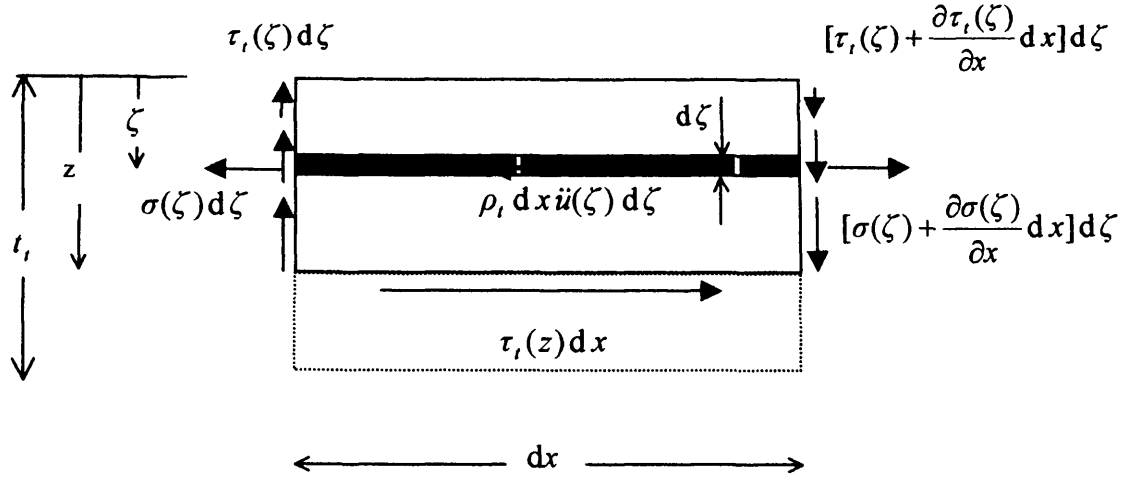

Figure 7.3: Shear stress through the thickness of the top layer.

displacement at any point with $0 < \zeta < z$ can be determined by interpolation between the longitudinal displacements at the top and bottom of the layer as

$$u(\zeta) = u_1 - \zeta\varphi_t = u_1 - \zeta\frac{u_1 - u_2}{t_t} = u_1(1-\frac{\zeta}{t_t}) + u_2\frac{\zeta}{t_t} \tag{7.68}$$

Now, by using Eq. (7.68) the normal stress and the mass acceleration through the thickness of the top layer can be given as

$$\sigma(\zeta) = E_t\varepsilon(\zeta) = E_t u'(\zeta) = E_t[u_1'(1-\frac{\zeta}{t_t}) + u_2'\frac{\zeta}{t_t}] \tag{7.69}$$

and

$$\ddot{u}(\zeta) = [\ddot{u}_1(1-\frac{\zeta}{t_t}) + \ddot{u}_2\frac{\zeta}{t_t}] \tag{7.70}$$

Substituting Eqs. (7.69) and (7.70) into Eq. (7.67) and performing the necessary integration yields the shear stress at any point through the thickness of the top layer as

$$\tau_t(z) = -E_t[(z - \frac{z^2}{2t_t})u_1'' + (\frac{z^2}{2t_t})u_2''] + \rho_t[(z - \frac{z^2}{2t_t})\ddot{u}_1 + (\frac{z^2}{2t_t})\ddot{u}_2] \tag{7.71}$$

which is a parabolic distribution of shear stress. Eq. (7.71) gives the shear stress at the top and bottom fibre of the top layer as

$$\tau_t(z=0) = 0\,; \qquad \tau_t(z=t_t) = \tau_t = -K_t(\frac{u_1'' + u_2''}{2}) + \mu_t(\frac{\ddot{u}_1 + \ddot{u}_2}{2}) \tag{7.71a,b}$$

and using Eq. (7.71), the shear force q_t can be written as

$$q_t = \int_0^{t_t} \tau_t(z)\,\mathrm{d}z = -E_t t_t^2(\frac{u_1''}{3} + \frac{u_2''}{6}) + \rho_t t_t^2(\frac{\ddot{u}_1}{3} + \frac{\ddot{u}_2}{6}) \tag{7.72}$$

Hence, substituting Eqs. (7.72) and (7.3a) into Eq. (7.6) gives the next differential equation of motion as

$$G_t\psi - \frac{G_t}{t_t}u_1 + \frac{K_t}{3}u_1'' - \frac{\mu_t}{3}\ddot{u}_1 + \frac{G_t}{t_t}u_2 + \frac{K_t}{6}u_2'' - \frac{\mu_t}{6}\ddot{u}_2 = 0 \tag{7.73}$$

Now consider Figure 7.4 which shows the shearing stress $\tau_b(z)$ at any distance $0 < z < t_b$ from the top surface of the bottom layer. The equation of horizontal equilibrium for Figure 7.4 can then be written as

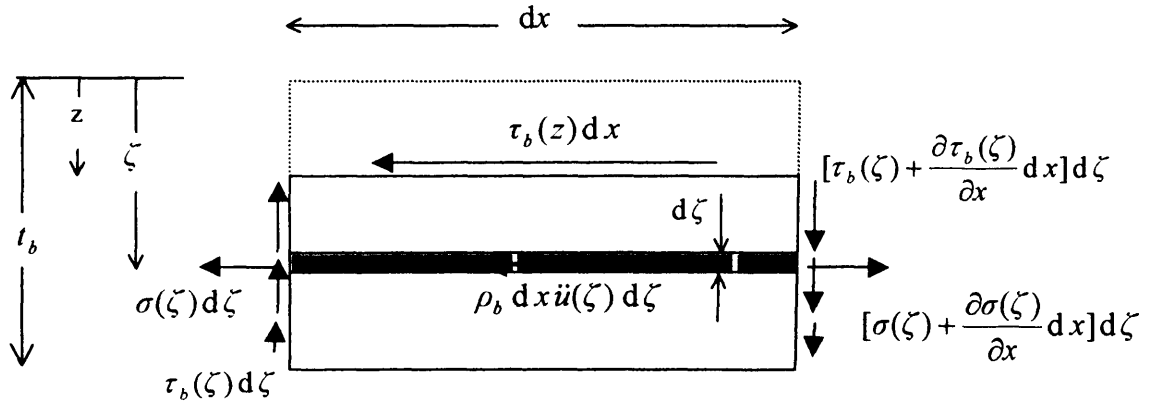

Figure 7.4 Shear stress through the thickness of the bottom layer.

$$-\tau_b(z)\,\mathrm{d}x+\int_z^{t_b}\frac{\partial\sigma(\zeta)}{\partial x}\,\mathrm{d}x\,\mathrm{d}\zeta=\int_z^{t_b}\rho_b\,\mathrm{d}x\,\ddot{u}(\zeta)\,\mathrm{d}\zeta \tag{7.74}$$

where σ is the normal stress at any point $z<\zeta<t_b$ through the thickness of the layer, ρ_b is the mass density of the bottom layer and $\mathrm{d}\zeta$ is the elemental thickness. Similar to the case of the top layer, the longitudinal displacement at any point with $z<\zeta<t_b$ can be determined by interpolation between the longitudinal displacements at the top and bottom of the bottom layer as

$$u(\zeta)=u_3-\zeta\varphi_b=u_3-\zeta\frac{u_3-u_4}{t_b}=u_3(1-\frac{\zeta}{t_b})+u_4\frac{\zeta}{t_b} \tag{7.75}$$

The normal stress and the mass acceleration through the thickness of the bottom layer can be obtained by using Eq. (7.75) as

$$\sigma(\zeta)=E_b\varepsilon(\zeta)=E_bu'(\zeta)=E_b[u_3'(1-\frac{\zeta}{t_b})+u_4'\frac{\zeta}{t_b}] \tag{7.76}$$

and

$$\ddot{u}(\zeta)=[\ddot{u}_3(1-\frac{\zeta}{t_b})+\ddot{u}_4\frac{\zeta}{t_b}] \tag{7.77}$$

Substituting Eqs. (7.76) and (7.77) into Eq. (7.74) and then performing the necessary integration yields a parabolic distribution of shear stress through the thickness of the bottom layer as

$$\tau_b(z)=E_b\{[\frac{(t_b-z)^2}{2t_b}]u_3''+[\frac{t_b^{\,2}-z^2}{2t_b}]u_4''\}-\rho_b\{[\frac{t_b^{\,2}-z^2}{2t_b}]\ddot{u}_4+[\frac{(t_b-z)^2}{2t_b}]\ddot{u}_3\} \tag{7.78}$$

The shear stress at the top and bottom fibre of the bottom layer can be determined from Eq. (7.78) as

$$\tau_b(z=0)=\tau_b=K_b(\frac{u_3''+u_4''}{2})-\mu_b(\frac{\ddot{u}_3+\ddot{u}_4}{2});\qquad \tau_b(z=t_b)=0; \tag{7.78a,b}$$

and using Eq. (7.78), the shear force q_b can be written as

$$q_b=\int_0^{t_b}\tau_b(z)\,\mathrm{d}z=E_b t_b^2(\frac{u_4''}{3}+\frac{u_3''}{6})-\rho_b t_b^2(\frac{\ddot{u}_4}{3}+\frac{\ddot{u}_3}{6}) \tag{7.79}$$

Thus, substituting Eqs. (7.79) and (7.3c) into Eq. (7.6) gives another differential equation of motion as

$$G_b\psi-\frac{G_b}{t_b}u_3-\frac{K_b}{6}u_3''+\frac{\mu_b}{6}\ddot{u}_3+\frac{G_b}{t_b}u_4-\frac{K_b}{3}u_4''+\frac{\mu_b}{3}\ddot{u}_4=0 \tag{7.80}$$

Finally, taking moments about the point O in Figure 7.5 and ignoring terms of second order yields the moment equilibrium of the central layer as

$$-\tau_b\,\mathrm{d}x\,t_c+q_c\,\mathrm{d}x-\int_0^{t_c}z\frac{\partial\sigma(z)}{\partial x}\mathrm{d}x\,\mathrm{d}z+\int_0^{t_c}z\rho_c\,\mathrm{d}x\,\ddot{u}(z)\,\mathrm{d}z=0 \tag{7.81}$$

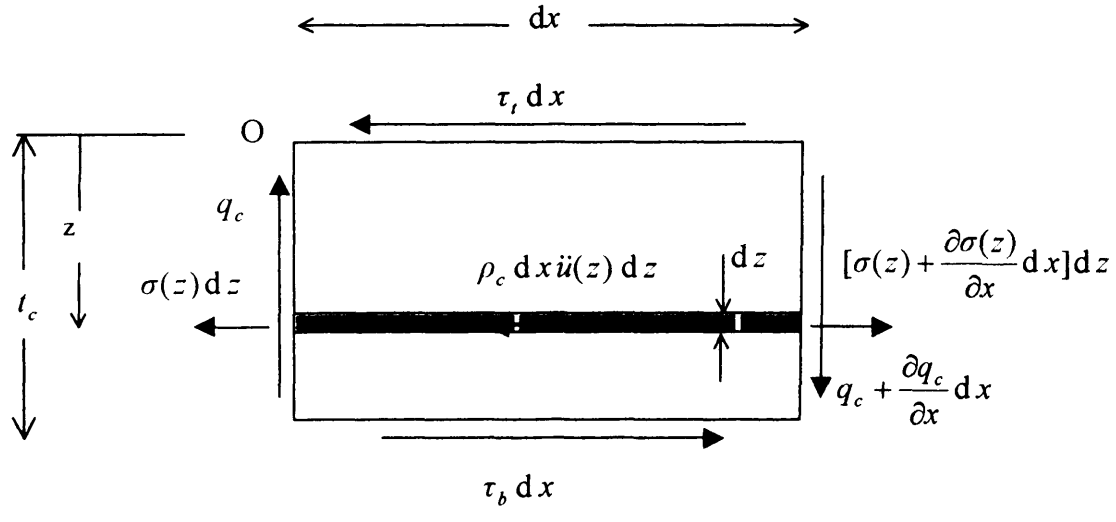

Figure 7.5: State of shear through the central layer.

where σ is the normal stress at any point $0 < z < t_c$ through the thickness of the central layer, ρ_c is the mass density of the central layer and dz is the elemental thickness. Now, the longitudinal displacement at any point with $0 < z < t_c$ can be determined by interpolation between the longitudinal displacements at top and bottom of the central layer as

$$u(z) = u_2 - z\varphi_c = u_2 - z\frac{u_2 - u_3}{t_c} = u_2(1 - \frac{z}{t_c}) + u_3\frac{z}{t_c} \tag{7.82}$$

The normal stress and the mass acceleration through the thickness of the bottom layer can be obtain by using Eq. (7.82) as

$$\sigma(z) = E_c\varepsilon(z) = E_c u'(z) = E_c[u_2'(1 - \frac{z}{t_c}) + u_3'\frac{z}{t_c}] \tag{7.83}$$

and

$$\ddot{u}(z) = [\ddot{u}_2(1 - \frac{z}{t_c}) + \ddot{u}_3\frac{z}{t_c}] \tag{7.84}$$

Now substituting Eqs. (7.78a) (7.83) and (7.84) into Eq. (7.81) and performing the necessary integration yields the shear force through the thickness of the central layer as

$$q_c = E_b t_c(\frac{t_b}{2}u_3'' + \frac{t_b}{2}u_4'') - \rho_b t_c(\frac{t_b}{2}\ddot{u}_4 + \frac{t_b}{2}\ddot{u}_3) + \frac{K_c}{6}t_c(u_2'' + 2u_3'') - \frac{\mu_c}{6}t_c(\ddot{u}_2 + 2\ddot{u}_3) \tag{7.85}$$

It can be shown that the exact shear variation through the thickness of the central layer is also quadratic and the continuity of transverse shear stress at the interface of the layers holds exactly.

Finally, substituting Eqs. (7.85) and (7.3b) into Eq. (7.6) gives the final differential equation of motion as

$$G_c\psi+(-\frac{G_c}{t_c}u_2-\frac{K_c}{6}u_2''+\frac{\mu_c}{6}\ddot{u}_2)+(\frac{G_c}{t_c}u_3-\frac{K_c}{3}u_3''-\frac{K_b}{2}u_3''+\frac{\mu_c}{3}\ddot{u}_3+\frac{\mu_b}{2}\ddot{u}_3)$$
$$+(-\frac{K_b}{2}u_4''+\frac{\mu_b}{2}\ddot{u}_4)=0 \qquad (7.86)$$

Hence, if attention is now confined to harmonic motion as defined by Eq. (7.30), the partial differential Eqs. (7.59), (7.66), (7.73), (7.80) and (7.86) yield the following linear differential equations with constant coefficients

$$\left.\begin{aligned}
&-\mu\omega^2W+\frac{K_t}{2}(\frac{2t_t}{3}+t_c+t_b)U_1'''+\frac{\mu_t}{2}(\frac{2t_t}{3}+t_c+t_b)\omega^2U_1'\\
&+[\frac{K_t}{2}(\frac{t_t}{3}+t_c+t_b)+\frac{K_c}{2}(\frac{2t_c}{3}+t_b)]U_2'''+[\frac{\mu_t}{2}(\frac{t_t}{3}+t_c+t_b)+\frac{\mu_c}{2}(\frac{2t_c}{3}+t_b)]\omega^2U_2'\\
&+[\frac{K_c}{2}(\frac{t_c}{3}+t_b)+\frac{K_b}{2}(\frac{2t_b}{3})]U_3'''+[\frac{\mu_c}{2}(\frac{t_c}{3}+t_b)+\frac{\mu_b}{2}(\frac{2t_b}{3})]\omega^2U_3'\\
&+\frac{K_b}{2}(\frac{t_b}{3})U_4'''-\frac{\mu_b}{2}(\frac{t_b}{3})\omega^2U_4'=0\\
&K_tU_1''+\mu_t\omega^2U_1+(K_t+K_c)U_2''+(\mu_t+\mu_c)\omega^2U_2+(K_c+K_b)U_3''\\
&+(\mu_c+\mu_b)\omega^2U_3+K_bU_4''+\mu_b\omega^2U_4=0\\
&G_tW'-\frac{G_t}{t_t}U_1+\frac{K_t}{3}U_1''+\frac{\mu_t}{3}\omega^2U_1+\frac{G_t}{t_t}U_2+\frac{K_t}{6}U_2''+\frac{\mu_t}{6}\omega^2U_2=0\\
&G_bW'-\frac{G_b}{t_b}U_3-\frac{K_b}{6}U_3''-\frac{\mu_b}{6}\omega^2U_3+\frac{G_b}{t_b}U_4-\frac{K_b}{3}U_4''-\frac{\mu_b}{3}\omega^2U_4=0\\
&G_cW'-(\frac{G_c}{t_c}U_2+\frac{K_c}{6}U_2''+\frac{\mu_c}{6}\omega^2U_2)\\
&+(\frac{G_c}{t_c}U_3-\frac{K_c}{3}U_3''-\frac{K_b}{2}U_3''-\frac{\mu_c}{3}\omega^2U_3-\frac{\mu_b}{2}\omega^2U_3)-(\frac{K_b}{2}U_4''+\frac{\mu_b}{2}\omega^2U_4)=0
\end{aligned}\right\} \qquad (7.87)$$

Now using the operator $D = \mathrm{d}/\mathrm{d}x$, Eq. (7.87) can be written in matrix form as

$$
\begin{bmatrix}
\left[-\mu\omega^2\right] & \begin{Bmatrix}(\frac{t_t}{3}+\frac{t_c}{2}+\frac{t_b}{2}) \\ (K_t D^3+\mu_t\omega^2 D)\end{Bmatrix} & \begin{Bmatrix}(\frac{t_t}{6}+\frac{t_c}{2}+\frac{t_b}{2})(K_t D^3+\mu_t\omega^2 D) \\ +(\frac{t_c}{3}+\frac{t_b}{2})(K_c D^3+\mu_c\omega^2 D)\end{Bmatrix} & \begin{Bmatrix}(\frac{t_c}{6}+\frac{t_b}{2})(K_c D^3+\mu_c\omega^2 D) \\ +(\frac{t_b}{3})(K_b D^3+\mu_b\omega^2 D)\end{Bmatrix} & \begin{Bmatrix}(\frac{t_b}{6})(K_b D^3+\mu_b\omega^2 D)\end{Bmatrix} \\
0 & (K_t D^2+\mu_t\omega^2) & [(K_t+K_c)D^2+(\mu_t+\mu_c)\omega^2] & [(K_c+K_b)D^2+(\mu_c+\mu_b)\omega^2] & (K_b D^2+\mu_b\omega^2) \\
G_t D & (-\frac{G_t}{t_t}+\frac{K_t}{3}D^2+\frac{\mu_t}{3}\omega^2) & (\frac{G_t}{t_t}+\frac{K_t}{6}D^2+\frac{\mu_t}{6}\omega^2) & 0 & 0 \\
G_b D & 0 & 0 & -(\frac{G_b}{t_b}+\frac{K_b}{6}D^2+\frac{\mu_b}{6}\omega^2) & (\frac{G_b}{t_b}-\frac{K_b}{3}D^2-\frac{\mu_b}{3}\omega^2) \\
G_c D & 0 & -(\frac{G_c}{t_c}+\frac{K_c}{6}D^2+\frac{\mu_c}{6}\omega^2) & \begin{Bmatrix}-[-\frac{G_c}{t_c}+(\frac{K_c}{3}+\frac{K_b}{2})D^2] \\ +(\frac{\mu_c}{3}+\frac{\mu_b}{2})\omega^2]\end{Bmatrix} & -(\frac{K_b}{2}D^2+\frac{\mu_b}{2}\omega^2)
\end{bmatrix}
\begin{Bmatrix} W \\ U_1 \\ U_2 \\ U_3 \\ U_4 \end{Bmatrix} = 0 \qquad (7.88)
$$

Although the matrix operator in Eqs. (7.32) and (7.88) seem to be different, the latter can be deduced from the former by utilising matrix operations which don't change its determinant, as follows

i) Differentiate the third, fourth and fifth rows of Eq. (7.88) once and then multiply the results by t_t, t_b and t_c, respectively, and add them together. Now multiply the second row by $[\frac{1}{2}(t_c + t_b)]$ and add it to the previous summation. Finally, subtract the results from the first row of Eq. (7.88) to give the first row of Eq. (7.32);

ii) The Third row of Eq. (7.88) is the same as the second row of Eq. (7.32);

iii) Adding half of the second row of Eq. (7.88) to its fifth row and then subtracting the third row of Eq. (7.88) from the result yields the third row of Eq. (7.32);

iv) Subtracting the fifth row from the fourth row of Eq. (7.88) gives the fourth row of Eq. (7.32).

v) Multiplying the fourth row of Eq. (7.88) by (-1) yields the fifth row of Eq. (7.32).

Therefore, combining Eq. (7.88) into one equation by eliminating either W, U_1, U_2, U_3 or U_4 yields an identical tenth order linear differential equation to that of Eq. (7.34).

7.3.4 Dynamic stiffness formulation

The dynamic stiffness matrix method relates the harmonically varying forces to the harmonically varying displacements. Expressions for the general displacements W, U_1, U_2, U_3 and U_4 can be deduced from Eq. (7.34) and the expressions for the corresponding forces can be obtained by substituting Eq. (7.30) into Eqs.(7.25)-(7.29) to yield

$$\left.\begin{aligned} Q &= SW' + G_t U_1 - (G_t - G_c)U_2 - (G_c - G_b)U_3 - G_b U_4 \\ N_1 &= \frac{K_t}{3}U_1' + \frac{K_t}{6}U_2' \\ N_2 &= \frac{K_t}{6}U_1' + \frac{(K_t + K_c)}{3}U_2' + \frac{K_c}{6}U_3' \\ N_3 &= \frac{K_c}{6}U_2' + \frac{(K_c + K_b)}{3}U_3' + \frac{K_b}{6}U_4' \\ N_4 &= \frac{K_b}{6}U_3' + \frac{K_b}{3}U_4' \end{aligned}\right\} \qquad (7.89)$$

Eqs. (7.89) are functions of W, U_1, U_2, U_3 and U_4. Hence, the next step is to solve the governing differential equations of motion, Eq. (7.34), for the harmonically varying displacement field.

7.3.4.1 Solution of the governing differential equation of motion

Eq. (7.34) is a linear tenth order differential equation with constant coefficients and its solution can be sought in the following form

$$V = \sum_{j=1}^{10} \overline{C}_{ij}\zeta_j \quad \text{where} \qquad \zeta_j = e^{\eta_j x}; \qquad 0 \le x \le L \qquad (7.90a,b)$$

η_j are the roots of the characteristic equation stemming from Eq. (7.34) and the $\overline{C}_{ij}$ are arbitrary constants where, for convenience in developing the work that follows, i is an assigned integer that defines a set of j arbitrary constants, e.g. $\overline{C}_{1j} = \overline{A}_j$, $\overline{C}_{2j} = \overline{B}_j$ etc., where $\overline{A}_j$, $\overline{B}_j$ are independent sets of arbitrary constants.

The η_j can now be determined as the roots of

$$\eta^{10} + c_1\eta^8 + c_2\eta^6 + c_3\eta^4 + c_4\eta^2 + c_5 = 0 \qquad (7.91)$$

Eq. (7.91) is a quintic polynomial equation in $z = \eta^2$, i.e.

$$z^5 + c_1 z^4 + c_2 z^3 + c_3 z^2 + c_4 z + c_5 = 0 \qquad (7.92)$$

Eq. (7.92) can be solved by any appropriate method such that described in Appendix C, where its five roots could be real, imaginary or complex. The ten roots of Eq. (7.91) then follow automatically. These ten roots, η_j $(j=1,2,...,10)$, which can also be real, imaginary or complex, define V $(W, U_1, U_2, U_3 \text{ or } U_4)$ and the other necessary quantities for the stiffness formulation of the problem, i.e. Eq. (7.89), to yield the following results

$$\left.\begin{aligned} W &= \sum_{j=1}^{10} H_{1j} C_j \zeta_j \qquad Q = \sum_{j=1}^{10} H_{6j} C_j \zeta_j \\ U_1 &= \sum_{j=1}^{10} H_{2j} C_j \zeta_j \qquad N_1 = \sum_{j=1}^{10} H_{7j} C_j \zeta_j \\ U_2 &= \sum_{j=1}^{10} H_{3j} C_j \zeta_j \qquad N_2 = \sum_{j=1}^{10} H_{8j} C_j \zeta_j \\ U_3 &= \sum_{j=1}^{10} H_{4j} C_j \zeta_j \qquad N_3 = \sum_{j=1}^{10} H_{9j} C_j \zeta_j \\ U_4 &= \sum_{j=1}^{10} H_{5j} C_j \zeta_j \qquad N_4 = \sum_{j=1}^{10} H_{10j} C_j \zeta_j \end{aligned}\right\} \tag{7.93}$$

where $H_{ij} C_j = \overline{C}_{ij}$, such that C_j is common to all the equations and H_{ij} is the relational constant. Noting that one of the H_{ij} is arbitrary, it is usually convenient to set $H_{1j} = 1$, but since the order of magnitude of the values of U_1, U_2, U_3 and U_4 are almost the same, a numerical instability could occur. Therefore, in the current problem. it is safer for the value of H_{2j} to be specified as unity. Now, substituting Eqs (7.93) into the first, third, fourth and fifth equation of Eq. (7.31) yields a system of linear algebraic equations given by

$$\begin{bmatrix} A_1\eta_j^2 + A_2 & A_4\eta_j & A_5\eta_j & A_6\eta_j \\ A_3\eta_j & A_9 + A_{10}\eta_j^2 & 0 & 0 \\ A_4\eta_j & A_{11} + A_{12}\eta_j^2 & A_{13} + A_{14}\eta_j^2 & 0 \\ A_5\eta_j & A_{13} + A_{14}\eta_j^2 & A_{15} + A_{16}\eta_j^2 & A_{17} + A_{18}\eta_j^2 \end{bmatrix} \begin{Bmatrix} H_{1j} \\ H_{3j} \\ H_{4j} \\ H_{5j} \end{Bmatrix} = \begin{Bmatrix} -A_3\eta_j \\ -(A_7 + A_8\eta_j^2) \\ -(A_9 + A_{10}\eta_j^2) \\ 0 \end{Bmatrix} \quad (j = 1, 2, ...,10) \tag{7.94}$$

Eq.(7.94) can be solved by Gauss elimination to yield H_{1j}, H_{3j}, H_{4j} and H_{5j}. Furthermore, using Eqs (7.93) in Eqs. (7.89) gives $H_{6j}, H_{7j}, H_{8j}, H_{9j}$ and H_{10j} as

$$\left.\begin{aligned}
H_{6j} &= S\eta_j H_{1j} + G_t H_{2j} - (G_t - G_c)H_{3j} - (G_c - G_b)H_{4j} - G_b H_{5j} \\
H_{7j} &= \frac{K_t}{3}\eta_j H_{2j} + \frac{K_t}{6}\eta_j H_{3j} \\
H_{8j} &= \frac{K_t}{6}\eta_j H_{2j} + \frac{(K_t + K_c)}{3}\eta_j H_{3j} + \frac{K_c}{6}\eta_j H_{4j} \\
H_{9j} &= \frac{K_c}{6}\eta_j H_{3j} + \frac{(K_c + K_b)}{3}\eta_j H_{4j} + \frac{K_b}{6}\eta_j H_{5j} \\
H_{10j} &= \frac{K_b}{6}\eta_j H_{4j} + \frac{K_b}{3}\eta_j H_{5j}
\end{aligned}\right\} (j = 1, 2, \ldots, 10) \quad (7.95)$$

7.3.4.2 Transformation between local and member co-ordinate systems

All the equations developed so far have been based on the forces and displacements in the local co-ordinate system shown in Figure 7.6(a). The stiffness formulation requires all nodal forces and displacements to be represented in the member co-ordinate system of Figure 7.6(b). Hence, the nodal forces and displacements in the local co-ordinate system are now transformed to the member co-ordinate system which, by comparing Figures 7.6(a) and (b), the necessary relationship can be obtained. This is equivalent to imposing the conditions of Eq. (7.96) onto Eq. (7.89).

$$\left.\begin{aligned}
&\text{At } x = 0: \\
&W = W_1; \quad U_1 = U_{11}; \quad U_2 = U_{21}; \quad U_3 = U_{31}; \quad U_4 = U_{41}; \\
&Q = -Q_1; \quad N_1 = -N_{11}; \quad N_2 = -N_{21}; \quad N_3 = -N_{31}; \quad N_4 = -N_{41} \\
&\text{At } x = L: \\
&W = W_2; \quad U_1 = U_{12}; \quad U_2 = U_{22}; \quad U_3 = U_{32}; \quad U_4 = U_{42}; \\
&Q = Q_2; \quad N_1 = N_{12}; \quad N_2 = N_{22}; \quad N_3 = N_{32}; \quad N_4 = N_{42}
\end{aligned}\right\} \quad (7.96)$$

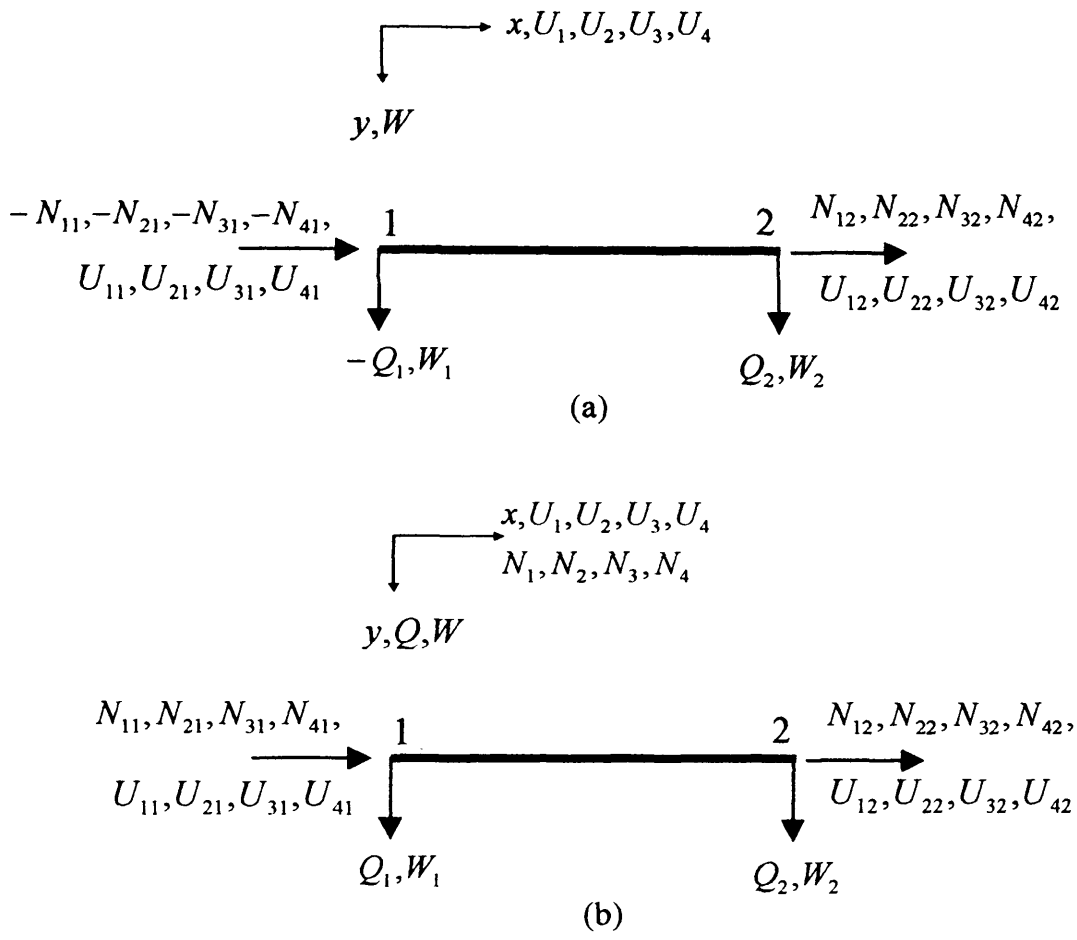

Figure 7.6: Nodal forces and displacements a) in local co-ordinates, b) in member co-ordinates.

7.3.4.3 Dynamic stiffness matrix

The dynamic stiffness matrix relates the forces to the displacements at the two end nodes of a member as

$$\mathbf{p} = \mathbf{k}\mathbf{d} \qquad \text{where} \qquad \mathbf{d} = \mathbf{S}\mathbf{C} \qquad \text{and} \qquad \mathbf{p} = \mathbf{S}^{*}\mathbf{C} \tag{7.97}$$

where **k** is the ten by ten dynamic stiffness matrix,

$$\mathbf{d}=\begin{bmatrix} W_1 \\ U_{11} \\ U_{21} \\ U_{31} \\ U_{41} \\ W_2 \\ U_{12} \\ U_{22} \\ U_{32} \\ U_{42} \end{bmatrix}; \qquad \mathbf{p}=\begin{bmatrix} Q_1 \\ N_{11} \\ N_{21} \\ N_{31} \\ N_{41} \\ Q_2 \\ N_{12} \\ N_{22} \\ N_{32} \\ N_{42} \end{bmatrix}; \qquad \mathbf{C}=\begin{bmatrix} C_1 \\ C_2 \\ C_3 \\ C_4 \\ C_5 \\ C_6 \\ C_7 \\ C_8 \\ C_9 \\ C_{10} \end{bmatrix} \tag{7.98}$$

and the matrices **S** and $\mathbf{S}^*$ relate the elements of **d** and **p**, respectively, to the coefficient vector **C** through Eq. (7.93). s_{ij} and s^*_{ij}, the elements of **S** and $\mathbf{S}^*$, respectively, are as follows

$$\left.\begin{array}{l} s_{1j}=H_{1j} \;;\; s_{2j}=H_{2j} \;;\; s_{3j}=H_{3j} \;;\; s_{4j}=H_{4j} \;;\; s_{5j}=H_{5j} \\ s_{6j}=H_{1j}\chi_j \;;\; s_{7j}=H_{2j}\chi_j \;;\; s_{8j}=H_{3j}\chi_j \;;\; s_{9j}=H_{4j}\chi_j \;;\; s_{10j}=H_{5j}\chi_j \\ s^*_{1j}=-H_{6j} \;;\; s^*_{2j}=-H_{7j} \;;\; s^*_{3j}=-H_{8j} \;;\; s^*_{4j}=-H_{9j} \;;\; s^*_{5j}=-H_{10j} \\ s^*_{6j}=H_{6j}\chi_j \;;\; s^*_{7j}=H_{7j}\chi_j \;;\; s^*_{8j}=H_{8j}\chi_j \;;\; s^*_{9j}=H_{9j}\chi_j \;;\; s^*_{10j}=H_{10j}\chi_j \\ \\ \chi_j=e^{\eta_j L} \qquad (j=1,2,\ldots 10) \end{array}\right\} \tag{7.99}$$

where their subscripts correspond to row and column co-ordinates in the usual way.

The required dynamic stiffness matrix, **k**, follows through the following steps

$$\mathbf{C}=\mathbf{S}^{-1}\mathbf{d} \qquad \text{therefore} \qquad \mathbf{p}=\mathbf{S}^*\mathbf{S}^{-1}\mathbf{d} \qquad \text{and finally} \qquad \mathbf{k}=\mathbf{S}^*\mathbf{S}^{-1} \tag{7.100}$$

The dynamic stiffness matrix for the overall structure can now be assembled from the element matrices in the usual way. In the next section, the method for converging with

certainty on the required natural frequencies is described. Once the required natural frequencies have been determined, the corresponding mode shapes can be retrieved by any reliable method, such as described in reference (Howson 1979).

7.3.5 Converging on the natural frequencies

Solutions of the equation

$$\mathbf{K}\,\mathbf{D} = \mathbf{0} \tag{7.101}$$

where **D** is the vector of amplitudes of the harmonically varying nodal displacements and **K** is the dynamic structure stiffness matrix yield the required natural frequencies. The solution procedure corresponds precisely to the one described in Section 6.3.4. Thus we seek to find J_0 of Eq. (6.62) by considering a roller-roller supported Timoshenko sandwich beam in which the longitudinal and rotational motions are permitted at the supports, but lateral displacement W, is prevented (Figure 7.7). For the roller-roller-supported case, the boundary conditions are defined by

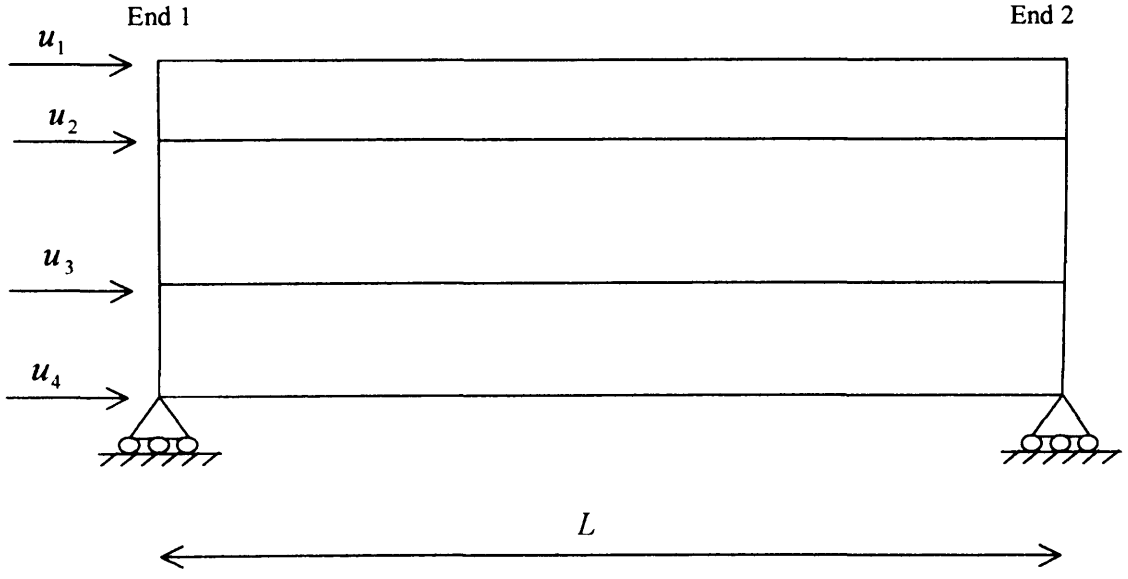

Figure 7.7: Roller-roller supported three-layer beam and the position of longitudinal freedoms through the beam thickness.

$$M_1 = M_2 = W_1 = W_2 = 0 \tag{7.102}$$

These conditions are satisfied by assuming solutions of the form

$$\begin{aligned} W &= Z_1 \sin \delta x \\ U_1 &= Z_2 \cos \delta x \\ U_2 &= Z_3 \cos \delta x \\ U_3 &= Z_4 \cos \delta x \\ U_4 &= Z_5 \cos \delta x \end{aligned} \tag{7.103}$$

where Z_1, Z_2, Z_3, Z_4 and Z_5 are constants and $\delta = \frac{n\pi}{L}$, ($n = 0, 1, 2, 3, \ldots$). To yield the frequency equation, Eq. (7.31) has been written in different matrix form as

$$\begin{bmatrix} B_1\omega^2 + B_2 & B_3 & B_4 & B_5 & B_6 \\ B_3 & B_7 + B_8\omega^2 & B_9 + B_{10}\omega^2 & 0 & 0 \\ B_4 & B_9 + B_{10}\omega^2 & B_{11} + B_{12}\omega^2 & B_{13} + B_{14}\omega^2 & 0 \\ B_5 & 0 & B_{13} + B_{14}\omega^2 & B_{15} + B_{16}\omega^2 & B_{17} + B_{18}\omega^2 \\ B_6 & 0 & 0 & B_{17} + B_{18}\omega^2 & B_{19} + B_{20}\omega^2 \end{bmatrix} \begin{Bmatrix} W \\ U_1 \\ U_2 \\ U_3 \\ U_4 \end{Bmatrix} = \mathbf{0} \tag{7.104}$$

where

$$\left.\begin{aligned} &B_1 = -\mu; \quad B_2 = -SD^2; \quad B_3 = G_t D; \quad B_4 = -(G_t - G_c)D; \quad B_5 = -(G_c - G_b)D; \\ &B_6 = -G_b D; \quad B_7 = -\frac{G_t}{t_t} + \frac{K_t}{3}D^2; \quad B_8 = \frac{\mu_t}{3}; \quad B_9 = \frac{G_t}{t_t} + \frac{K_t}{6}D^2; \quad B_{10} = \frac{\mu_t}{6}; \\ &B_{11} = -(\frac{G_t}{t_t} + \frac{G_c}{t_c}) + \frac{(K_t + K_c)}{3}D^2; \quad B_{12} = \frac{(\mu_t + \mu_c)}{3}; \quad B_{13} = \frac{G_c}{t_c} + \frac{K_c}{6}D^2; \\ &B_{14} = \frac{\mu_c}{6}; \quad B_{15} = -(\frac{G_c}{t_c} + \frac{G_b}{t_b}) + \frac{(K_c + K_b)}{3}D^2; \quad B_{16} = \frac{(\mu_c + \mu_b)}{3}; \\ &B_{17} = \frac{G_b}{t_b} + \frac{K_b}{6}D^2; \quad B_{18} = \frac{\mu_b}{6}; \quad B_{19} = -\frac{G_b}{t_b} + \frac{K_b}{3}D^2; \quad B_{20} = \frac{\mu_b}{3} \end{aligned}\right\} \tag{7.105}$$

where $D = \mathrm{d}/\mathrm{d}x$. Reducing Eq. (7.104) to one equation by eliminating W, U_1, U_2, U_3 or U_4 yields the following differential equation

$$[g_0\omega^{10} + g_1\omega^8 + g_2\omega^6 + g_3\omega^4 + g_4\omega^2 + g_5]V = 0 \tag{7.106}$$

where $V = W, U_1, U_2, U_3$ or U_4 and g_0, g_1, g_2, g_3, g_4 and g_5 contain only the even orders of the differential operator $D = \mathrm{d}/\mathrm{d}x$. Noting that the form of Eqs. (7.104) and (7.32) are similar, makes it easy to determine the coefficients in Eq. (7.106) by recalling Eqs. (7.36) to (7.57) and substituting B_i (Eq. (7.105)) in place of A_i (Eq. (7.33)). This yields

$$\left.\begin{aligned} g_0 &= e_{110} \\ g_1 &= e_{18} \\ g_2 &= e_{16} + e_{28} + e_{38} + e_{48} + e_{58} \\ g_3 &= e_{14} + e_{26} + e_{36} + e_{46} + e_{56} \\ g_4 &= e_{12} + e_{24} + e_{34} + e_{44} + e_{54} \\ g_5 &= e_{10} + e_{22} + e_{32} + e_{42} + e_{52} \end{aligned}\right\} \tag{7.107}$$

Furthermore, since Eq. (7.107) is a combined equation which allows for the effects of W, U_1, U_2, U_3 and U_4, substituting any part of Eq. (7.103) into Eq. (7.107) yields the frequency equation for a roller-roller supported beam as

$$\omega^{10} + b_1\omega^8 + b_2\omega^6 + b_3\omega^4 + b_4\omega^2 + b_5 = 0 \tag{7.108}$$

where b_1, b_2, b_3, b_4 and b_5 can be obtained from Eq. (7.107). On the other hand, for any part of Eq. (7.103) the following hold

$$D^2(.) = -\delta^2(.);\ D^4(.) = \delta^4(.);\ D^6(.) = -\delta^6(.);\ D^8(.) = \delta^8(.);\ D^{10}(.) = -\delta^{10}(.) \tag{7.109}$$

Hence, for the determination of the coefficients in Eq. (7.108), it is more practical if all (D^2) and (D) in Eq. (7.105) are replaced by ($-\delta^2$) and (δ), respectively. Then using these modified B_i (Eq. (7.105)) instead of the A_i (Eq. (7.33)) in Eqs. (7.36) to (7.57), the coefficients of Eq. (7.108) can be written as

$$\left.\begin{aligned} b_1 &= e_{18}/e_{110} \\ b_2 &= (e_{16} - e_{28} - e_{38} - e_{48} - e_{58})/e_{110} \\ b_3 &= (e_{14} - e_{26} - e_{36} - e_{46} - e_{56})/e_{110} \\ b_4 &= (e_{12} - e_{24} - e_{34} - e_{44} - e_{54})/e_{110} \\ b_5 &= (e_{10} - e_{22} - e_{32} - e_{42} - e_{52})/e_{110} \end{aligned}\right\} \qquad (7.110)$$

Note that the minus signs in Eq. (7.110) are due to the first order differential operator $D(.)$ in Eq. (7.105), while all of the related terms in Eq. (7.107) contain only even powers of the operator and therefore they are treated in the same way as $D^2(.) = -\delta^2(.)$.

Now, Eq. (7.108) can be expressed as a quintic equation in ω^2 and consequently its real, positive roots are the square of its natural frequencies for each value of $n = 0,1,2,\ldots$. Hence J_{rr} is given by the number of positive values of ω_n that lie below the trial frequency, ω^*. Thus, substituting Eq. (6.65) in to Eq. (6.63) gives

$$J_0 = \sum (J_{rr} - s\ \{\mathbf{k}^{rr}\}) \qquad (7.111)$$

The required value of J then follows from Eq. (6.62).

It is interesting to note that when $n = 0$, $\delta = 0$. The coefficients b_4 and b_5 are then zero and it can be shown that b_1 is always negative, b_2 is always positive and b_3 is always negative. Eq. (7.108) then yields three non-trivial real roots. It is equally clear from Eq. (7.102) that

$$V = 0 \ ; \qquad U_1 = Z_2 \ ; \qquad U_2 = Z_3 ; \qquad U_3 = Z_4 \ ; \qquad U_4 = Z_5 \qquad (7.112)$$

Thus the mode corresponding to $n = 0$ has no lateral displacement and rigid body displacements horizontally. Also there is no axial extension and therefore the frequencies correspond to the fundamental shear thickness mode, designated 'S' and two other pure shear thickness modes designated 'SA' and 'SB' as shown in Figure 7.8.

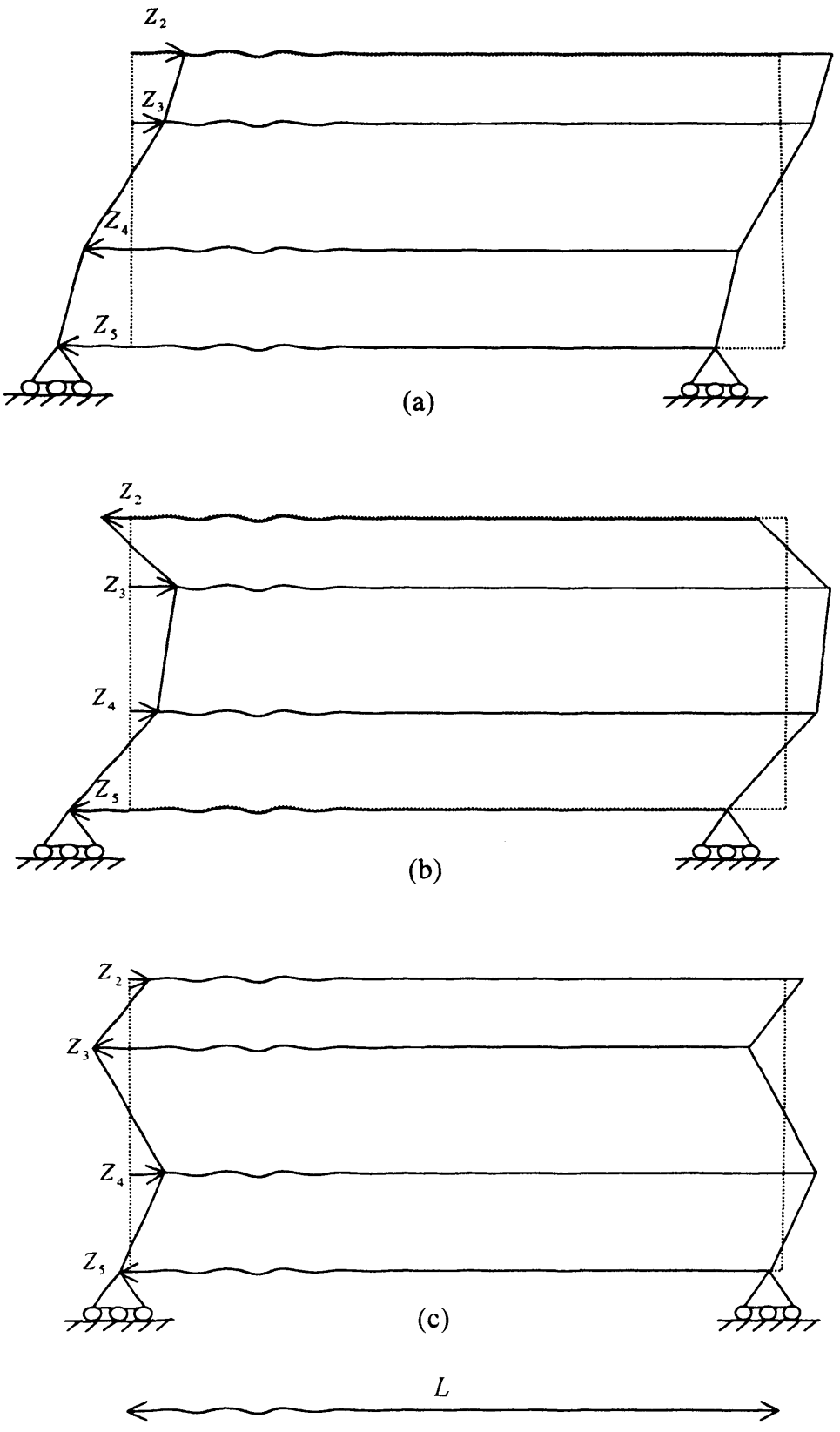

Figure 7.8: Three possible pure shear thickness modes of a roller-roller supported three-layer Timoshenko beam, a) S mode, b) SA mode, and c) SB mode.

7.4 NUMERICAL RESULTS

A number of examples are now given to validate the theory and indicate its range of application. The current theory assumes that all three layers of the beam have axial, flexural and shear rigidities. However, in the comparative results where some of these rigidities are notionally zero, a very small rigidity is eventually considered to assure numerical stability. The first six examples compare results obtained by various authors for a variety of sandwich beams that have been used as test examples in the literature. In these examples, where appropriate, the results from previous chapters are also included. Example 7.7 considers a one-layer deep beam which highlights the occurrence of three different classes of shear thickness modes.

***Example 7.1*:** The roller-roller supported beam of Example 6.1 is now reanalysed for the case in which the core has bending and axial rigidity and the faceplates allow for shear deformation. The results obtained by a number of authors and using a variety of methods are given in Table 7.1. The geometric and material properties of the beam are exactly the same as those in Example 6.1 and the additional elastic properties of the layers for use with the current theory are as follows

$$G_t = G_b = 8.268\,\text{GPa}\,; \quad E_c = 0.689\,\text{GPa}$$

In Table 7.1, 'Freq. No.' indicates the order of occurrence of the modes while the second column gives the predominant component of the mode and its ordering number. For example, 'B1' indicates the first bending mode, 'A1', the first axial mode, 'S2', the second shear thickness mode and so on.

It is necessary to note that except for the results stemming from the theories of Chapters 6 and 7, all other results have been given as the results for a simply supported beam. However, it was shown in Example 6.6 that the use of the term 'simply supported' must be used more carefully in the case of a sandwich beam, since the position of the longitudinal constraint plays a significant role on the vibration of the beam. Furthermore,

Table 7.1: Comparative results for the non-zero natural frequencies (Hz) of the roller-roller supported sandwich beam of Example 7.1.

Freq. No.	mode	Theory of Chapter 7	Theory of Section 6.4	Theory of Section 6.3	Theory of Chapter 5	Sakiyama, 1996b	Rao, 2001	Marur, 1996
1	B1	57.2431	57.12345	57.1241	57.1358	56.159	57.068	57.041
2	B2	219.843	219.423	219.431	219.585	215.82	218.569	218.361
3	B3	465.346	464.565	464.595	465.172	457.22	460.925	460.754
4	B4	767.946	766.850	766.915	768.177	755.05	757.642	758.692
5	B5	1105.84	1104.52	1104.63	1106.68	1087.9	1086.955	1097.055
6	B6	1463.61	1462.17	1462.31	1465.10	1440.3	1433.920	1457.064
7	B7	1831.45	1829.97	1830.14	1833.55	1802.7	1789.345	1849.380
8	B8	2203.60	2202.13	2202.32	2206.19	2169.8	2147.969	2275.916
9	A1	2580.96	2563.22	2563.22	-	-	-	2562
10	B9	2576.82	2575.41	2575.62	2579.79	2538.2	-	-
11	B10	2949.41	2948.08	2948.30	2952.65	2906.2	-	-
18	A2	5161.92	5126.44	5126.44	-	-	-	-
27	A3	7742.88	7689.67	7689.67	-	-	-	-
53	S1	15960.33	15960.5	16406.4(54)*	-	-	-	-
55	S2	16191.17	16190.3	16642.4(56)*	-	-	-	-

* Number in the brackets indicates the frequency number, if different from the first column.

due to the capability of considering more realistic material for the individual layers of the beam, the current results are the most precise ones yet available.

Comparison of the results for the flexural frequencies with those from Chapter 6 is not so simple. This is due to the fact that including the bending and axial rigidities of the core increases the stiffness of the beam, while on the other hand, due to considering the shear deformation of the faceplates, the stiffness of the beam is decreased. Therefore, the influence of this combination is not clear. However, it is clear that the current theory should evaluate the frequency of the axial modes as being higher than the comparable results from the theories of Chapter 6.

Finally, it should be noted that for use in the current theory the beam has been modelled using 18 elements, where the number of elements required to model the beam using the theories of Chapters 5 and 6 was only two. This is not for the purposes of accuracy, since all theories are exact and the accuracy is independent of the number of elements. It is due

to the fact that using a smaller number of elements, which implies that the length of the each element increases, leads to the situation that the value of χ_j in Eq. (7.99) overflows. (In both cases double precision variables are used.) Therefore, by using a sufficiently large number of elements, the difficulty can be overcome.

Example 7.2: Using the current theory, the beam of Example 6.2 is now reanalysed using the material properties of Example 7.1. Results for the frequencies of the first eight flexural modes and the first two axial modes are presented in Table 7.2 and compared with those from other references. It is worth noting that here the beam has been modelled using 14 elements, whereas the beam can be modelled with only two elements when using the theories of Chapters 5 and 6.

Table 7.2: Comparative results for the natural frequencies (Hz) of the cantilevered sandwich beam of Example 7.2.

Freq. No.	Mode	Theory of Chapter 7	Theory of Section 6.4	Theory of Section 6.3	Theory of Chapter 5	Ahmed, 1971	Banerjee, 2003	Marur , 1996	
								HOBT4b	HOBT5
1	B1	33.7796	33.7456	33.7459	33.7513	33.97	31.46	33.7	33.7
2	B2	199.154	198.788	198.798	198.992	200.5	193.7	197.5	197.5
3	B3	512.160	511.373	511.420	512.307	517	529.2	505.5	505.5
4	B4	906.241	905.118	905.224	907.299	918	1006	890.5	890.5
5	B5	1347.39	1346.06	1346.22	1349.65	1368	-	1321	1321
6	A1	1659.19	1647.79	1647.79	-	-	-	1648	1648
7	B6	1812.33	1810.91	1811.20	1815.82	1844	-	1786	1786
8	B7	2287.91	2286.48	2286.79	2292.45	2331	-	2271	2271
9	B8	2766.84	2765.47	2765.81	2772.23	2824	-	2792	2792
14	A2	4977.57	4943.36	4943.39	-	-	-	4943*	4941*

*Values correspond to the second axial mode, but the 13^{th} frequency.

Example 7.3: The influence of more realistic core material and the allowance for shear deformation in the faceplates are now investigated for the beam of Example 6.6, where the only differences in data are those used in Example 7.1. Roller-roller and simply

supported boundary conditions are imposed, but refer to Example 6.5 for further clarification. Results for the natural frequencies of the beam are given in Table 7.3, which give good agreement with the results of theory of Chapter 6. It should be noted that here the necessary number of elements to model the beam is 2, where as the necessary number of elements to use with the theories of Chapter 6 was only one.

Table 7.3: Comparative results for natural frequencies (Hz) of the thick sandwich beam of Example 7.3.

Freq. No.	Roller-roller		Simply supported*	
	Theory of Chapter 7	Theory of Section 6.4	Theory of Chapter 7	Theory of Section 6.4
1	0	0	293.4543(B)	293.3143(B)
2	294.9411(B)	294.808(B)	653.7430(B)	653.6769(B)
3	658.7402(B)	658.706(B)	799.2592(BA)	798.6499(BA)
4	1014.058(B)	1014.072(B)	1017.039(B)	1017.041(B)
5	1368.794(B)	1368.797(B)	1369.641(B)	1369.641(B)
6	1596.033(S)	1596.045(S)	1725.246(B)	1725.17(B)
7	1726.345(B)	1726.274(B)	1874.164(SB)	1871.087(SB)
8	2088.676(B)	2088.462(B)	2090.620(B)	2090.327(B)
9	2457.246(B)	2456.815(B)	2457.720(B)	2457.229(B)
10	2580.959(A)	2563.221(A)	2823.933(B)	2818.611(B)
11	2833.287(B)	2832.561(B)	2853.328(B)	2846.612(B)
12	3144.195(S)	3138.852(S)	3217.501(B)	3216.38(B)
13	3217.897(B)	3216.797(B)	3608.775(B)	3607.184(B)
14	3612.081(B)	3610.531(B)	3991.592(B)	3988.061(B)
15	4016.77(B)	4014.702(B)	4106.674(SAB)	4098.532(SAB)
16	4432.83(B)	4430.183(B)	4440.401(B)	4437.404(B)
17	4861.062(B)	4857.791(B)	4863.724(B)	4860.223(B)
18	5161.911(A)	5126.451(A)	5298.846(B)	5293.185(B)
19	5302.211(B)	5298.285(B)	5387.452(SAB)	5365.328(SAB)
20	5640.703(S)	5628.741(S)	5755.551(B)	5750.872(B)

* Longitudinal freedom u_4 at Figure 7.7 is constrained.

Example 7.4: Another deep symmetric sandwich beam is now analysed to show the good agreement obtained between the results of the current theory and those of other theories in reference (Marur and Kant 1996). In reference (Marur and Kant 1996) a simply

supported beam of length 0.762m, which consists of six orthotropic layers of thickness 0.0254m is considered. The top two and bottom two layers have their strong axis parallel to the beam's longitudinal axis and act as stiff faceplates, while the other two layers, with a 90 degrees rotation of their lay-up, form a soft core. The material properties in the current notation are as follows

$$E_t = E_b = 525\text{GPa}\ ;\ E_c = 21\text{GPa}\ ;\ G_t = G_c = G_b = 10.5\text{GPa}\ ;\ \rho_t = \rho_c = \rho_b = 775\text{Kg/m}^3 .$$

The comparative results are given in Table 7.4. The natural frequencies are non-dimensionalized by using the expression $\overline{\omega} = \omega L^2[\rho_t/(E_t h^2)]^{1/2}$ where ω is the circular frequency and h is the beam's total thickness. The difference in results are due to various assumed shear distributions across the cross-section, from constant transverse shear strain in first order beam theory (FOBT) to parabolic transverse shear strain distribution in higher order beam theories (HOBT) and the current theory, which are not only problem dependent but also mode dependent (Marur and Kant 1996).

Table 7.4: Comparative results for non-zero frequencies of the thick beam of Example 7.4.

Freq. No	Mode	Current Theory	Marur, 1996			
			FOBT	HOBT4a	HOBT4b	HOBT5
1	B1	1.702	1.639	1.736	1.656	1.656
2	B2	4.039	3.81	4.125	3.923	3.923
3	B3	6.336	5.912	6.439	6.191	6.191
4	B4	8.611	7.988	8.722	8.47	8.47
5	B5	10.872	10.1	11.042	10.803	10.803
6	S1	11.619	11.181	12.248	11.111	11.111
7	A1	12.596	12.188	12.636	12.953	12.636
8	B6	13.125	12.953	13.333	13.117	13.117
9	B7	15.370	14.392	15.751	15.561	15.561
10	B8	17.611	16.732	18.313	18.151	18.151
11	S2	19.141	19.088	19.747	18.927	18.927
12	B9	19.849	19.205	21.021	20.889	20.889
13	B10	22.083	20.874	22.865	22.763	22.763
14	A2	23.375	25.91	23.597	25.91	25.597

Example 7.5: As another example, a cantilevered sandwich beam with three identical layers and various lengths is used (Deng and Vu-Quoc 1998). The non-dimensional geometric and material properties for each layer are as follows

$$t_t = t_c = t_b = 0.02; \quad \rho = 50.0; \quad E = 3\times10^6; \quad G = 1.2\times10^6$$

The comparative results are given in Table 7.5. Although reference (Deng and Vu-Quoc 1998) modelled the beam with 20 linear elements the results are an overestimate. Only one element was required for the current theory.

Table 7.5: Comparative results for the non-dimensional natural frequencies of the cantilever beam of Example 7.5.

Freq. No	L=3.0		L=0.3	
	Current theory	Deng, 1998	Current theory	Deng, 1998
1	1.656983	1.658292	161.1896	162.615
2	10.36621	10.46547	878.8707	926.5694
3	28.94521	29.70036	1282.55	1276.478
4	56.49338	59.43545	2112.978	2329.802

Example 7.6: A symmetric simply supported sandwich beam with overhangs is now considered which has the following non-dimensional geometric and material properties. (Deng and Vu-Quoc 1998)

$$t_t = t_b = 0.05; \qquad \rho_t = \rho_b = 20.0; \qquad E_t = E_b = 400{,}000; \quad G_t = G_b = 160{,}000;$$

$$t_c = 1.0; \qquad \rho_c = 1.0; \qquad E_c = 1000$$

The total non-dimensional beam length is 40, while the length of each overhang is considered to be 10. Comparative results for two different shear modulli of the core layer are given in Table 7.6. The results in columns 2 and 3 of this table represent the frequencies of a sandwich beam with a relatively soft core, while results in the fourth and fifth columns refer to the frequencies of a sandwich beam with relatively stiff core. Here also the FEM results shown an overestimate of the frequencies.

Table 7.6: Comparative results for the non-dimensional natural frequencies of the simply supported beam with overhangs of Example 7.6.

Freq. No	G_c= 400		G_c= 8000	
	Current theory	Deng, 1998	Current theory	Deng, 1998
1	0.763137	0.767121	0.827483	0.833069
2	0.994415	1.002488	1.344796	1.358937
3	1.608263	1.630904	2.713123	2.781141
4	3.338055	3.490406	6.505164	6.965818

***Example 7.7*:** A roller-roller supported homogeneous beam is now analysed that has a sufficiently deep section that it would usually be analysed as a Timoshenko beam. The geometric and material properties of the beam are as follows

$E = 1.0\,\text{GPa}$; $G = 0.333\,\text{GPa}$; $\rho = 7500\,\text{Kg/m}^3$; $t = 2.0\,\text{m}$. $L = 4.0\,\text{m}$

In order to model the beam for use in the current theory, it is necessary to model the beam as a three-layer beam and therefore various layers thicknesses are considered and the results are reported in Table 7.7. To distinguish between different modes B, A, S, SA, SB are used to indicate bending, axial and first, second and third classes of shear thickness modes, respectively. Also where a number follows them, it indicates the number of half wave-lengths in the mode.

The second and third columns of Table 7.7 gives the results of 'CHNFIN', a program for the analysis of plane frames with axially loaded Timoshenko members (Howson 1979), which is based on the theory given in reference (Howson and Williams 1973). In this reference, first order shear theory has been used to model the shear deformation of members, which assumes a constant transverse shear strain across the cross-section together with a shear correction factor. In this example, although the same assumption of constant transverse shear strain through the cross-section of each layer of the beam has been made, modelling the beam with three Timoshenko beam layers imposes less constraint on the system and also makes it possible to consider different classes of shear

modes. Hence, for comparison, the beam is modelled using three Timoshenko beam layers with various combinations of symmetric thickness varying from two very thin outer layers and a thick central layer to two rather thick outer layers and a very thin central layer. The results are presented in columns 3 to 24 of Table 7.7.

It can be seen from Table 7.7 that considering the beam as a three-layer beam allows the beam to have two more classes of shear modes. Also for every combination of layer thickness, the corresponding frequency is less than that of the beam with only one layer, since it is equivalent to providing additional flexibility to the system.

Finally, the proposed results of columns 25 and 26 contain the minimum calculated frequencies for each of the various vibration modes whose vibration frequencies are less than 319.5Hz, the frequency of the 7^{th} axial mode. In the other words, these columns list any possible vibration modes and their frequency that lies below the 7^{th} axial mode, despite the different thickness combination used in modelling the beam. Perhaps, these frequencies would be generated if at least a third order shear deformation theory were used in analysing the deep beam.

It is worth noting that the fundamental mode of each class of shear thickness mode is always a pure shear mode, while the higher modes are always coupled with either bending or axial behaviour. Study of the resulting modes for this roller-roller supported beam shows that the class SA of shear thickness modes is mostly coupled with axial effects, where the class SB is largely coupled with bending effects (See Figure 7.9). The mode shapes of the class S of shear thickness modes are similar to the shear modes in Chapter 6.

Table 7.7: Results of the roller-roller supported beam of Example 7.7.

Freq. No	CHNFIN (Howson,1979)		Current theory with various layer thickness combinations through the cross-section i.e. top layer-middle layer- bottom layer																											
			0.01-1.98-0.01		0.1-1.8-0.1		0.2-1.6-0.2		0.3-1.4-0.3		0.4-1.2-0.4		0.5-1.0-0.5		0.6-0.8-0.6		0.7-0.6-0.7		0.8-0.4-0.8		0.9-0.2-0.9		0.99-0.02-0.99		Proposed	
1	15.646	B	15.620	B	15.444	B	15.330	B	15.283	B	15.284	B	15.318	B	15.372	B	15.438	B	15.508	B	15.579	B	15.639	B	15.283	B1
2	42.760	B	42.634	B	41.764	B	41.259	B	41.098	B	41.154	B	41.336	B	41.584	B	41.862	B	42.153	B	42.450	B	42.727	B	41.098	B2
3	45.644	A	45.644	A	45.644	A	45.644	A	45.644	A	45.644	A	45.644	A	45.644	A	45.644	A	45.644	A	45.644	A	45.644	A	45.644	A1
4	58.113	S	57.830	S	55.870	S	54.591	S	53.962	S	53.819	S	54.065	S	54.623	S	55.415	S	56.344	S	57.288	S	58.039	S	53.819	S1
5	70.826	B	70.565	B	68.824	B	67.940	B	67.775	B	67.991	B	68.380	B	68.833	B	69.301	B	69.770	B	70.255	B	70.759	B	67.775	B3
6	76.877	S	76.624	S	74.886	S	73.758	S	73.199	S	73.064	S	73.269	S	73.753	S	74.453	S	75.285	S	76.135	S	76.810	S	73.064	S2
7	91.287	A	91.287	A	91.287	A	91.287	A	91.287	A	91.287	A	91.287	A	91.287	A	91.287	A	91.287	A	91.287	A	91.287	A	91.287	A2
8	98.592	B	98.190	B	95.586	B	94.480	B	94.462	B	94.905	B	95.496	B	96.104	B	96.686	B	97.245	B	97.823	B	98.491	B	94.462	B4
9	112.515	S	112.297	S	110.811	S	109.859	S	109.387	S	109.266	S	109.428	S	109.827	S	110.417	S	111.132	S	111.870	S	112.458	S	109.266	S3
10	126.013	B	125.469	B	122.074	B	120.929	B	121.162	B	121.842	B	122.593	B	123.298	B	120.455	SA	114.854	SA	113.262	SA	115.676	SA	113.262	SA1
11	136.931	A	136.931	A	136.931	A	136.931	A	136.931	A	136.931	A	136.931	A	130.598	SA	123.933	B	123.592	SA	122.113	SA	124.356	SA	120.929	B5
12	152.842	S	152.488	B	148.396	B	147.372	B	147.903	B	148.788	B	147.014	SA	136.931	A	128.812	SA	124.517	B	125.116	B	125.879	B	122.113	SA2
13	153.172	B	152.655	S	151.400	S	150.606	S	150.213	S	150.110	S	149.650	B	138.344	SA	136.931	A	136.931	A	136.931	A	136.931	A	136.931	A3
14	180.146	B	179.323	B	174.634	B	173.854	B	174.680	B	173.644	SA	150.239	S	150.404	B	151.052	B	146.714	SA	145.470	SA	147.358	SA	145.470	SA3
15	182.574	A	182.574	A	182.574	A	182.574	A	182.574	A	175.724	B	153.936	SA	150.567	S	151.058	S	151.627	B	152.207	B	152.792	S	147.372	B6
16	195.194	S	195.034	S	193.972	S	193.306	S	192.977	S	179.542	SA	173.050	SA	159.340	SA	151.138	SA	151.661	S	152.290	S	153.009	B	150.110	S4
17	206.987	B	206.029	B	200.840	B	200.386	B	201.478	B	182.574	A	176.652	B	176.715	SB	174.994	SB	178.611	B	177.703	SA	179.251	SA	173.854	B7
18	228.218	A	228.218	A	227.045	B	226.964	B	220.037	SA	192.890	S	182.574	A	177.422	B	178.060	B	178.722	SA	179.153	B	179.957	B	174.994	SB1
19	233.733	B	232.640	B	228.218	A	228.218	A	224.721	SA	196.177	SA	188.870	SB	182.574	A	181.034	SB	182.574	A	182.574	A	182.574	A	177.703	SA4
20	238.624	S	238.490	S	237.577	S	237.011	S	228.218	A	202.634	B	192.996	S	182.749	SB	182.371	SA	187.299	SB	194.723	S	195.152	S	181.034	SB2
21	260.407	S	259.181	B	253.269	B	253.577	B	228.279	B	213.472	SB	194.558	SB	189.224	SA	182.574	A	192.894	SB	205.995	B	206.775	B	182.574	A4
22	273.861	A	273.861	A	273.861	A	273.861	A	236.732	S	218.531	SB	200.906	SA	193.268	S	193.679	S	194.188	S	214.853	SA	216.135	SA	192.890	S5
23	282.692	S	282.572	B	279.521	B	280.215	B	238.222	S	221.138	SA	203.594	B	199.662	SB	197.974	SB	205.495	B	228.218	A	228.218	A	197.974	SB3
24	287.028	B	285.669	S	281.782	S	281.292	S	255.071	B	228.218	A	210.608	S	204.359	B	204.976	B	208.740	SB	232.758	B	233.500	B	200.386	B8
25	313.606	B	312.117	B	305.805	B	306.867	B	259.165	SA	229.508	B	228.218	A	224.475	SA	218.730	SA	215.696	SA	235.278	SB	238.588	S	214.853	SA5
26	319.505	A	319.505	A	319.505	A	315.158	SA	259.244	SB	232.977	SB	230.475	B	224.840	SB	223.208	SB	228.218	A	238.219	S	255.860	SA	223.208	SB
27							318.446	SA	263.418	SB	236.657	S	234.406	SA	228.218	A	228.218	A	232.300	B	239.707	SB	260.157	B	226.964	B9
28							319.505	A	273.861	A	251.963	SA	234.726	S	231.223	B	231.813	B	232.672	SB	252.517	SB	273.861	A	228.218	A5
29									275.516	SB	255.069	SB	236.746	S	236.976	S	237.326	S	237.760	S	254.778	SA	282.660	S	236.657	S6
30									281.051	S	256.341	B	257.300	B	255.734	SB	254.186	SB	255.490	SA	259.460	B	286.763	B	253.269	B10
31									281.845	B	273.861	A	264.584	S	258.023	B	258.056	SA	259.039	B	272.505	SB	297.289	SA	254.186	SB4
32									285.919	SA	280.986	S	271.471	SA	262.943	SA	258.584	B	262.425	SB	273.861	A	313.329	B	254.778	SA6
33									294.468	SB	282.896	SB	273.861	A	273.861	A	273.861	A	273.861	A	282.338	S	319.505	A	273.861	A6
34									308.597	B	283.132	B	281.062	S	281.261	S	281.562	S	281.939	S	286.112	B			279.521	B11
35									317.017	SA	286.767	SA	284.072	B	284.768	B	285.300	B	285.726	B	296.358	SA			280.986	S7
36									318.956	SB	309.884	B	298.401	S	290.479	SB	289.028	SB	296.222	SB	298.208	SB			289.028	SB5
37									319.505	A	314.866	SB	310.799	B	303.407	SA	299.181	SA	296.971	SA	312.725	B			296.358	SA7
38											319.505	A	310.826	SA	311.466	B	311.970	B	312.370	B	319.505	A			305.805	B12
39													319.505	A	319.505	A	319.505	A	319.505	A					319.505	A7

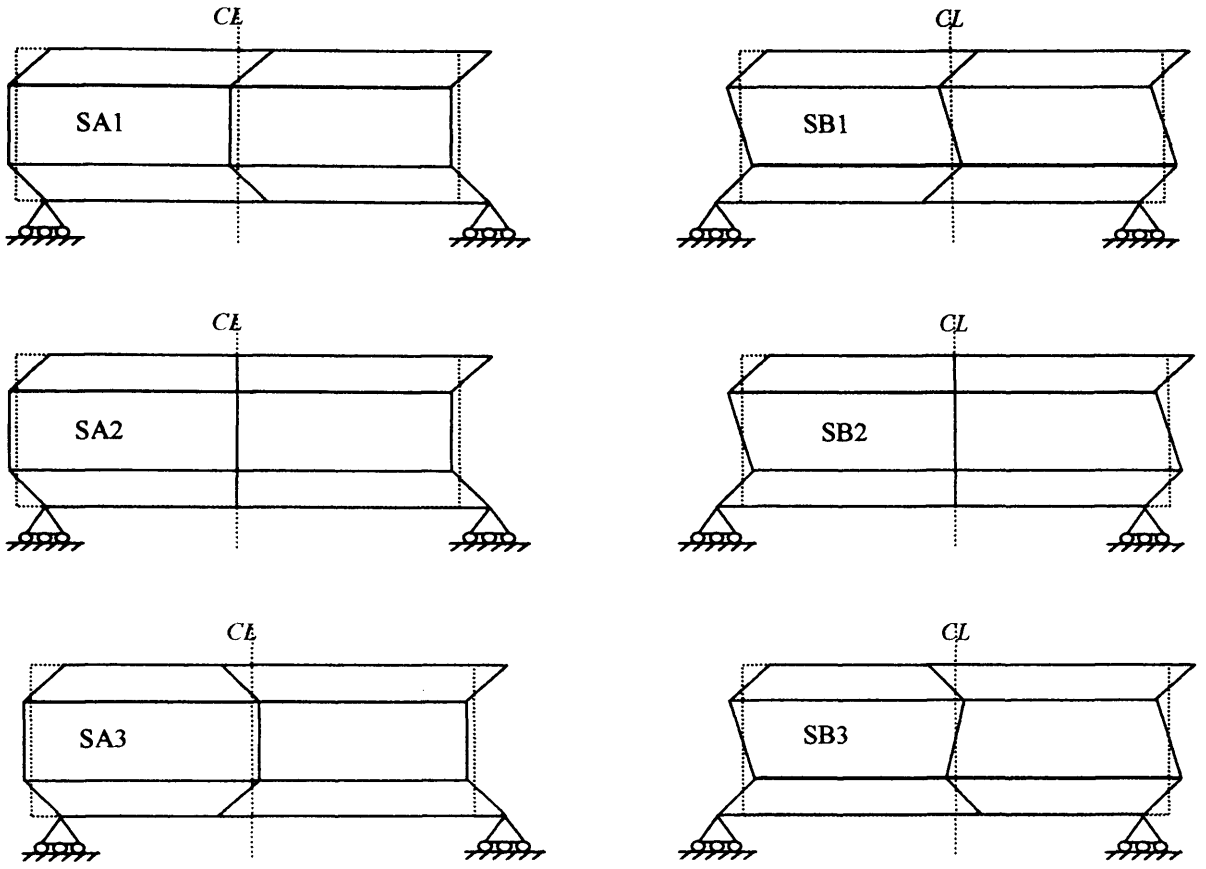

Figure 7.9: Schematic shapes of the 1st, 2nd and 3rd modes of the SA and SB classes of shear thickness modes of the roller-roller beam of Example 7.7. For simplicity the coupled bending component has been ignored.

7.5 GENERAL REMARKS

Due to the importance of the secondary effect of shear deformation for deeper beams, a dynamic stiffness matrix method has been developed to include this effect for all layers of a three-layer beam. Hence, the proposed model can be used for analysing any deep beam for which Timoshenko beam theory is normally needed. However, it is equally applicable to modelling slender beams. The Wittrick-Williams algorithm can then be used to solve the model for any required frequency to any desired accuracy.

The theory presented in this chapter corresponds to second order shear theory and clearly meets all the requirements of shear and displacement compatibility at the interface of the layers. It assumes a linear and quadratic variation for the normal strain and transverse shear, respectively, across the thickness of the cross-section of each layer. Therefore, all possible secondary effects are included and there is no need for a shear correction coefficient.

Since, in the present theory, the governing differential equation is of tenth order, its characteristic equation leads to a quintic algebraic equation in ω^2, which usually takes more time to solve in comparison to the quartic or cubic equations in Chapters 6 and 5, respectively. Therefore, unless very precise results are required or shearing deformation of the layers is important or the bending and axial rigidities of the central layer have almost the same order of magnitude as the other layers, it is recommended that the theory of Section 6.4 is used.

Considering a beam as a three-layer beam allows the beam to have two more classes of shear modes, SA and SB, besides the flexural, axial and usual shear thickness modes. Also for every combination of layer thickness, the corresponding frequencies of latter modes are less than that of the beam with only one layer, since it is equivalent to providing additional flexibility to the system. However, a suitable combination of layer thickness for any mode may be found that yields a minimum value for the corresponding frequency. Perhaps, these frequencies would be generated for a single layer homogeneous beam if at least a third order shear deformation theory were used in analysing the deep beam.

It is worth noting that the SA and SB classes of shear thickness modes are in the frequency range of interest if the thickness of the layers have almost the same order of magnitude. However, it is clear that even the S class of shear mode can only occur in beams that are sufficiently deep.

The results of Examples 7.1 to 7.6 show good correlation between the current theory and a selection of comparable results available in the literature. Also, the results of Example 7.7 provide a range of 'exact' solutions that may be helpful for future comparisons.

Finally, it is worth emphasising that it is relatively easy to generate examples in which the roots of the characteristic equation, Eq. (7.91), become sufficiently large that the value of ζ in Eq. (7.90b) overflows, even when using double precision arithmetic. However, because the combined effects of the value of the root and the length of the member are the source of this difficulty, it is only necessary to reduce the length of the member (element) and this incurs no approximation. Thus if difficulty is experienced a simple method is to subdivide the member into a greater number of elements until the problem is resolved.

CHAPTER 8

SUMMARY, CONCLUSION AND FUTURE WORK

8.1 SUMMARY

Transcendental stiffness matrices for vibration (or buckling) have long been available for a range of structural members. Such stiffness matrices are exact in the sense that they are obtained from the analytical solution of the governing differential equations of the member. Hence, assembly of the member stiffnesses to obtain the overall stiffness matrix of the structure results in a transcendental eigenproblem that yields exact solutions and which can be solved with certainty using the Wittrick-Williams algorithm.

When such an exact solution exists, the member has a recently discovered property that can also be expressed analytically and is called its member stiffness determinant. The member stiffness determinant is a property of the member when fully clamped boundary conditions are imposed upon it. It is then defined as the determinant of the member stiffness matrix when the member is sub-divided into an infinite number of identical sub-members. Each sub-member is therefore of infinitely small length so that its clamped-

ended natural frequencies are infinitely large. Hence the contribution from the member stiffness matrix to the J_0 count of the W-W algorithm will be zero. In general, the member stiffness determinant is normalised by dividing by its value when the eigenparameter (i.e. the frequency or buckling load factor) is zero, as otherwise it would become infinite.

Part A of this thesis developed the first two applications of member stiffness determinants to the calculation of natural frequencies or elastic buckling loads of prismatic plate assemblies comprising either isotropic or orthotropic plates subject to in-plane axial and transverse loads.

Part B presented the development of exact dynamic stiffness matrices for three models of sandwich beams. The simplest one is only able to model the flexural vibration of asymmetric sandwich beams. The first model was then extended to include axial and rotary inertia, which made it possible to predict the axial and shear thickness modes of vibration in addition to those corresponding to flexure. This culminated in the development of a unique model for a three layer Timoshenko beam.

Also, by using the appropriate transformations, Section 6.5, the developed element of Chapters 6 and 7 can be used to model frames constructed from sandwich elements.

Numerous examples have been given to validate the theories and to indicate their range of application. The results presented in these examples are identical to those developed from alternative exact techniques, and otherwise show good correlation with a selection of comparable results that are available in the literature. In the latter case, the differences in the results are attributable to many factors that vary widely from approximate solution techniques to differences in basic assumptions.

8.2 CONCLUSIONS

In the exact method for deriving the member dynamic stiffness matrix, the partial differential equation of motion is solved analytically in such a way that the closed form

solution satisfies inter-element compatibility as well as the boundary conditions. In contrast with the finite element approximation, the dynamic member stiffness matrix is a single matrix in which the exact and continuous mass distribution is automatically accounted for and the model therefore has an infinite number of degrees of freedom. The dynamic stiffness matrix in this case contains terms that are transcendental functions of frequency and therefore a suitable eigenvalue problem solver is needed.

8.2.2 Conclusion for Part A

Transcendental structural eigenproblems based on exact stiffness formulations are now routinely solved by use of the Wittrick-Williams algorithm, which guarantees convergence on any required eigenvalue to any required accuracy with absolute certainity that none have been missed. The eigenvalues are natural frequencies in vibration problems or critical load factors for buckling problems. Convergence is commonly achieved by bisection, despite the fact that the method is known to be relatively slow. Quicker methods are available, but their implementation is hampered by the highly volatile nature of the determinant of the structure's transcendental stiffness matrix, particularly in the vicinity of the poles, which may or may not correspond to eigenvalues.

A major advantage of the member stiffness determinant is that, when its values for all members of a structure are multiplied together and are also multiplied by the determinant of the transcendental overall stiffness matrix of the structure, the result is a determinant which has no poles and is substantially less volatile when plotted against the eigenparameter. Such plots provide a significantly better platform for the development of efficient, computer-based routines for convergence on eigenvalues by curve prediction techniques.

8.2.3 Conclusion for Part B

The use of the stiffness method offers great flexibility to analyse frames, as well as to impose 'constraints' on any selected freedom of the structure. These will typically take

the form of mass inertia, spring support stiffness or relationships that constrain one or more displacements to move in a predefined way relative to another set of displacements. Imposing such constraints follows the normal rules that would apply to a traditional beam element, except that more care is required to associate the constraint with the appropriate degree(s) of freedom.

The crucial difference of the inclusion of axial inertia in the second model enables the resulting member dynamic stiffness matrix (exact finite element) to be included in general two dimensional structures for the first time. Furthermore, although the developed element is straight, it can be used to model curved structures by using an appropriate number of straight elements to model the geometry of the curve.

A number of issues arising from the difference between sandwich beams and homogeneous beams, such as co-ordinate transformations, modal coupling and the application of boundary conditions are considered. In the case of single beams, it is confirmed that the modes of vibration are largely coupled at frequencies of practical interest, especially for unsymmetrical boundary conditions. However, the predominant component of the mode can be classified into one of the three families of modes; flexural, extensional and thickness shear.

Another crucial point is to distinguish between sandwich beams and homogeneous beams, since the thickness in the former plays an important role in the behaviour of the beam in the shear thickness mode of vibration and consequently on the coupling of the modes. In contrast with ordinary beams, the position of the axial constraint through the thickness of the beam is important. It always leads to coupling between the modes, but the value of the corresponding natural frequency depends on the location of the constraint.

Furthermore, despite the fact that the developed models are for straight elements, they can be used to model curved structures by using an appropriate number of straight elements to model the geometry of the curve. The results of Example 6.4 show that the number of straight elements needed to achieve comparable accuracy is even less than the number needed when using curved finite elements.

Finally, it has been understood that considering a beam as a three-layer beam allows the beam to have additional shear modes, besides the flexural, axial and usual shear thickness modes. Also for every combination of layer thickness, the corresponding frequencies of latter modes are less than that of the beam with only one layer, since it is equivalent to providing additional flexibility to the system. However, a suitable combination of layer thickness for any mode may be found that yields a minimum value for the corresponding frequency. Perhaps, these frequencies would be generated for a single layer homogeneous beam if at least a third order shear deformation theory were used in analysing the deep beam.

8.3 SUGGESTIONS FOR FUTURE WORK

The following suggestions are made as to how the current research study may be extended.

1. Derivation of member stiffness determinants for curved Euler-Bernoulli and Timoshenko beams with the knowledge that in-plane and out-of-plane behaviour are uncoupled.
2. Developing a model for a sandwich beam on an elastic foundation.
3. Developing a sandwich model that considers the compressibility of the core.
4. Developing an exact curved sandwich model for use in a generally curved structure.
5. Developing a model for tapered sandwich beams.
6. Developing a sandwich model that utilizes a higher order shear theory for the layers.
7. A study of the out-of-plane and torsional behaviour of sandwich beams using the exact dynamic stiffness method.
8. Developing a model for considering the global and local buckling of sandwich beams.

Appendices

APPENDIX A

CONSTITUTIVE RELATIONS FOR PRISMATIC PLATES

The uncoupled out-of-plane and in-plane elastic properties of a prismatic plate are defined by the following two sets of equations (Wittrick and Williams 1974)

$$\begin{Bmatrix} m_x \\ m_y \\ m_{xy} \end{Bmatrix} = -\begin{bmatrix} D_{11} & D_{12} & 0 \\ D_{21} & D_{22} & 0 \\ 0 & 0 & D_{33} \end{bmatrix} \begin{Bmatrix} \kappa_x \\ \kappa_y \\ 2\kappa_{xy} \end{Bmatrix} = -D_{22} \begin{bmatrix} \alpha_{11} & \alpha_{12} & 0 \\ \alpha_{12} & 1 & 0 \\ 0 & 0 & \alpha_{33} \end{bmatrix} \begin{Bmatrix} \kappa_x \\ \kappa_y \\ 2\kappa_{xy} \end{Bmatrix} \tag{A.1}$$

$$\begin{Bmatrix} n_x \\ n_y \\ n_{xy} \end{Bmatrix} = \begin{bmatrix} A_{11} & A_{12} & 0 \\ A_{21} & A_{22} & 0 \\ 0 & 0 & A_{33} \end{bmatrix} \begin{Bmatrix} \varepsilon_x \\ \varepsilon_y \\ \gamma_{xy} \end{Bmatrix} = A_{22} \begin{bmatrix} \alpha_{11} & \alpha_{12} & 0 \\ \alpha_{12} & 1 & 0 \\ 0 & 0 & \alpha_{33} \end{bmatrix} \begin{Bmatrix} \varepsilon_x \\ \varepsilon_y \\ \gamma_{xy} \end{Bmatrix} \tag{A.2}$$

where m_x, m_y and m_{xy} are the perturbation bending and twisting moments per unit length, n_x, n_y and n_{xy} are the perturbation membrane forces per unit length, κ_x, κ_y and κ_{xy} are the perturbation curvature and twist, and ε_x, ε_y and γ_{xy} are the

perturbation membrane strain. The sign convention for the bending moments and membrane forces is shown in Figure A.1.

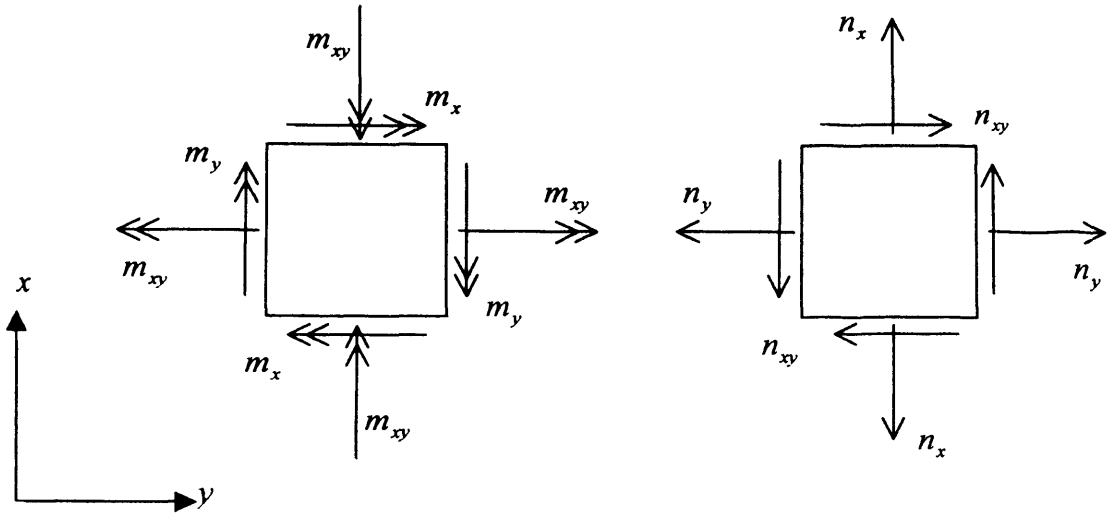

Figure A.1: Positive resultant forces acting on a typical element of an orthotropic plate.

Also

$$\kappa_x = \frac{\partial^2 w}{\partial x^2} \qquad \kappa_y = \frac{\partial^2 w}{\partial y^2} \qquad \kappa_{xy} = \frac{\partial^2 w}{\partial x \partial y}$$
$$\varepsilon_x = \frac{\partial u}{\partial x} \qquad \varepsilon_y = \frac{\partial v}{\partial y} \qquad \gamma_{xy} = \frac{\partial u}{\partial x} + \frac{\partial v}{\partial y} \tag{A.3}$$

and

$$D_{22} = \frac{E_2 h^3}{12(1-\nu_1\nu_2)}; \qquad A_{22} = \frac{E_2 h}{(1-\nu_1\nu_2)}$$
$$\alpha_{11} = \frac{E_1}{E_2}; \qquad \alpha_{12} = \nu_1; \qquad \alpha_{33} = \frac{G(1-\nu_1\nu_2)}{E_2} \tag{A.4}$$

where u, v and w are the perturbation displacements at a point (x, y) on the middle plane of the plate.

To use Eqs. (A.1) and (A.2) it is required that the principal elastic axis of orthotropic properties are parallel to the x and y axes of the plate and therefore, E_1, ν_1 and E_2, ν_2 are Young's modulus and Poisson's ratio in the x and y directions, respectively.

Now, based on Eqs. (A.1) to (A.4), the uncoupled out-of-plane and in-plane elastic properties for an isotropic plate may be defined by the following two sets of equations

$$\begin{Bmatrix} m_x \\ m_y \\ m_{xy} \end{Bmatrix} = -D \begin{bmatrix} 1 & \nu & 0 \\ \nu & 1 & 0 \\ 0 & 0 & \dfrac{(1-\nu)}{2} \end{bmatrix} \begin{Bmatrix} \kappa_x \\ \kappa_y \\ 2\kappa_{xy} \end{Bmatrix} \tag{A.5}$$

$$\begin{Bmatrix} n_x \\ n_y \\ n_{xy} \end{Bmatrix} = A \begin{bmatrix} 1 & \nu & 0 \\ \nu & 1 & 0 \\ 0 & 0 & \dfrac{(1-\nu)}{2} \end{bmatrix} \begin{Bmatrix} \varepsilon_x \\ \varepsilon_y \\ \gamma_{xy} \end{Bmatrix} \tag{A.6}$$

where

$$D = \frac{E h^3}{12(1-\nu^2)}; \qquad A = \frac{E h}{(1-\nu^2)} \tag{A.7}$$

APPENDIX B

SOME USEFUL IDENTITIES

B.1. GENERAL IDENTITIES

Various trigonometric manipulations have been made to revise the coefficients of the stiffness matrices for prismatic plates. The principal identities are given below. It should be noted that the definitions of Eqs. (2.10) or (2.24), which define p_χ and q_χ for the case of isotropic and orthotropic plates, respectively, are equally valid in the identities below and hold for both definitions, irrespective of whether $\hat{\chi}$ or χ is real.

B.1.1. Single argument identities

$$q_\chi^2 - \chi^2 p_\chi^2 = 1 \tag{B.1}$$

$$q_\chi^2 + \chi^2 p_\chi^2 = q_{2\chi} \tag{B.2}$$

$$p_\chi q_\chi = p_{2\chi} \tag{B.3}$$

B.1.2. Double arguments identities

The following identities hold even if one of the arguments is real and the other is imaginary. Alternatively α and γ can be replaced by τ and ζ and the identities still hold.

$$q_{(\alpha+\gamma)} = q_\alpha q_\gamma + \alpha\gamma\, p_\alpha p_\gamma \tag{B.4}$$

$$q_{(\alpha-\gamma)} = q_\alpha q_\gamma - \alpha\gamma\, p_\alpha p_\gamma \tag{B.5}$$

$$(\alpha+\gamma)p_{(\alpha+\gamma)} = \alpha\, p_\alpha q_\gamma + \gamma\, q_\alpha p_\gamma \tag{B.6}$$

$$(\alpha-\gamma)p_{(\alpha-\gamma)} = \alpha\, p_\alpha q_\gamma - \gamma\, q_\alpha p_\gamma \tag{B.7}$$

$$q_\alpha q_\gamma = \tfrac{1}{2}\left(q_{(\alpha+\gamma)} + q_{(\alpha-\gamma)} \right) \tag{B.8}$$

$$\alpha\gamma\ p_\alpha p_\gamma = \tfrac{1}{2}\left(q_{(\alpha+\gamma)} - q_{(\alpha-\gamma)}\right) \tag{B.9}$$

$$\alpha\ \ p_\alpha q_\gamma = \tfrac{1}{2}\left[(\alpha+\gamma)p_{(\alpha+\gamma)} + (\alpha-\gamma)p_{(\alpha-\gamma)}\right] \tag{B.10}$$

$$\gamma\ \ q_\alpha p_\gamma = \tfrac{1}{2}\left[(\alpha+\gamma)p_{(\alpha+\gamma)} - (\alpha-\gamma)p_{(\alpha-\gamma)}\right] \tag{B.11}$$

$$\alpha^2 p_\alpha^2 q_\gamma^2 + \gamma^2 p_\gamma^2 q_\alpha^2 = \tfrac{1}{2}\left(q_{2\alpha} q_{2\gamma} - 1\right) = \tfrac{1}{4}\left(q_{2(\alpha+\gamma)} + q_{2(\alpha-\gamma)} - 2\right) \tag{B.12}$$

$$\alpha^2 p_\alpha^2 q_\gamma^2 - \gamma^2 p_\gamma^2 q_\alpha^2 = \tfrac{1}{2}\left(q_{2\alpha} - q_{2\gamma}\right) = (\alpha^2 - \gamma^2)\, p_{(\alpha+\gamma)}\, p_{(\alpha-\gamma)} \tag{B.13}$$

$$q_\alpha^2 q_\gamma^2 - \alpha^2 \gamma^2 p_\gamma^2 p_\alpha^2 = \tfrac{1}{2}(q_{2\alpha} + q_{2\gamma}) = q_{(\alpha+\gamma)} q_{(\alpha-\gamma)} \tag{B.14}$$

B.2. SPECIAL IDENTITIES

Some combinations of p and q may have different equivalent forms depending on the definitions of α , γ, τ and ζ, as follows:

B.2.1. Out-of-plane isotropic plate

$$p_{(\alpha+\gamma)}^2 - p_{(\alpha-\gamma)}^2 = \frac{\alpha\gamma}{2\eta^2}(4p_{2\alpha}p_{2\gamma} - q_{2\alpha}q_{2\gamma} + 1) \tag{B.15}$$

B.2.2. Out-of-plane orthotropic plate

$$p_{(\alpha+\gamma)}^2 - p_{(\alpha-\gamma)}^2 = \frac{\alpha\gamma}{2L}(4Tp_{2\alpha}p_{2\gamma} - q_{2\alpha}q_{2\gamma} + 1) \tag{B.16}$$

B.2.3. In-plane orthotropic plate

$$p_{(\tau+\zeta)}^2 - p_{(\tau-\zeta)}^2 = \frac{\tau\zeta}{2(B^2 - C)}(4Bp_{2\tau}p_{2\zeta} - q_{2\tau}q_{2\zeta} + 1) \tag{B.17}$$

$$p_{(\alpha+\gamma)}^2 + p_{(\alpha-\gamma)}^2 = \frac{1}{2(B^2 - C)}[-4Cp_{2\alpha}p_{2\gamma} + B(q_{2\alpha}q_{2\gamma} - 1)] \tag{B.18}$$

B.3. IDENTITIES FOR SUB-STRUCTURING

In the derivation of the stiffness coefficients for the sub-structure at level i, the following hold

$$p_{i,2\chi} = \tfrac{1}{2} p_{i-1,\chi} \tag{B.19}$$

$$q_{i,2\chi} = q_{i-1,\chi} \tag{B.20}$$

where

$$\varphi_i = \frac{\varphi}{2^i} \tag{B.21}$$

for either

$$p_{i,\chi} = (1/\chi)\sinh\frac{\varphi_i\chi}{2} = (1/\hat{\chi})\ \sin\frac{\varphi_i\hat{\chi}}{2}\ ; \quad q_{i,\chi} = \cosh\frac{\varphi_i\chi}{2} = \cos\frac{\varphi_i\hat{\chi}}{2} \tag{B.22a,b}$$

or

$$\begin{aligned} p_{i,\chi} &= (1/\chi)\sinh\varphi_i\chi = (1/\hat{\chi})\ \sin\varphi_i\hat{\chi}\ ; \quad q_{i,\chi} = \cosh\varphi_i\chi = \cos\varphi_i\hat{\chi} \\ \hat{p}_{i,\chi} &= (1/\chi)\sin\varphi_i\chi\ ; \quad \hat{q}_{i,\chi} = \cos\varphi_i\chi \end{aligned} \tag{B.23a,b,c,d}$$

and for constants

$$p_4 = p_2 q_2\,; \qquad p_{i,4} = p_{i,2} q_{i,2}\,; \qquad p_{i,4} = \tfrac{1}{2} p_{i-1,2} \tag{B.24a,b,c}$$

APPENDIX C

SOLUTION OF ALGEBRAIC EQUATIONS

C.1. INTRODUCTION

Solution of the governing differential equations can be achieved in on of two different ways. The most popular approach is to classify the domain of interest into sub-domain, such that in each sub-domain the required solution can be presented using real analytic expressions. Alternatively, by using the theory of complex variables, a single solution procedure can be adopted, but requires the use of complex arithmetic. Therefore, in Part B of the thesis, the theory of functions of a complex variable plays a central role in numerical computations. This role commences with the solution of the characteristic equation of the ordinary differential equation resulting from the governing partial differential equations of the problem. Although in problems with real material properties, the coefficients of the characteristic equation and any final results are real, such as a stiffness matrix and vibration frequencies etc., whereas in general the roots of the characteristic equation may be complex. Consequently, all computations stemming from the roots of the characteristic equation must be carried out using complex arithmetic.

However, the imaginary parts of the elements of the resulting dynamic stiffness matrix are zero and therefore from this point on the computations can be carried out using real arithmetic.

The following sections give a brief overview of complex variables and the solutions of cubic, quartic and quintic algebraic equations. It is clear that most parts of the methods of solving equations require complex variables and it is normal to seek all possible roots, be they real or complex. For further details the reader can refer to reference (Grove and Ladas 1974).

C.2. BACKGROUND

A complex number is defined as $z = (x + \mathrm{i}\, y)$ where $\mathrm{i} = \sqrt{-1}$ and x and y are real. Such a number has a complex conjugate $\bar{z} = (x - \mathrm{i}\, y)$. x and y are called the real and imaginary parts of z, respectively. Its geometric representation is $z = |z|(\cos\theta + i\sin\theta)$, where $|z| = +\sqrt{x^2 + y^2}$ is called the absolute value of z, and $\cos\theta = \frac{x}{|z|}$ and $\sin\theta = \frac{y}{|z|}$. The co-ordinate θ is real and called the argument of z. The nth roots of z are

$$\sqrt[n]{z} = \sqrt[n]{|z|}(\cos\frac{\theta + 2\pi k}{n} + i\sin\frac{\theta + 2\pi k}{n}) \text{ where } k = 0,1,2,\ldots,n-1 \qquad \text{(C.1)}$$

Eq. (C.1) implies that any number, real or complex, has n distinctive roots which may be real or complex.

C.3. CUBIC EQUATIONS

Consider the cubic equation with real coefficients

$$z^3 + az^2 + bz + c = 0 \tag{C.2}$$

The transformation

$$z = w - a/3 \tag{C.3}$$

reduces Eq. (C.2) to an equation in w of the form

$$w^3 + pz + q = 0 \tag{C.4}$$

where

$$p = b - \frac{a^2}{3} \text{ and } q = c - \frac{ab}{3} + \frac{2a^3}{27} \tag{C.5}$$

are both real. Now introduce two unknowns u and v with the property that

$$u + v = w \qquad \text{and} \qquad uv = -\frac{p}{3} \tag{C.6a,b}$$

Then $u^3 + v^3 = (u+v)^3 - 3uv(u+v) = w^3 + pw = -q$, and $u^3 v^3 = -\frac{p^3}{27}$. It follows that u^3 and v^3 are roots of the quadratic equation

$$t^2 + qt - \frac{p^3}{27} = 0 \tag{C.7}$$

Let t_1 and t_2 denote, in general, the two complex roots of Eq. (C.7)

$$t_1 = -\frac{q}{2} + \sqrt{\frac{q^2}{4} + \frac{p^3}{27}} \qquad \text{and} \qquad t_2 = -\frac{q}{2} - \sqrt{\frac{q^2}{4} + \frac{p^3}{27}} \tag{C.8}$$

If $\sqrt[3]{t_1}$ denotes one of the three cubic roots of t_1, then the three possible values of u are (Grove and Ladas 1974)

$$u = \sqrt[3]{t_1}\,; \qquad u = s\sqrt[3]{t_1} \qquad \text{and} \qquad u = s^2\sqrt[3]{t_1} \tag{C.9}$$

where $s = \cos\frac{2\pi}{3} + i\sin\frac{2\pi}{3}$ and $s^2 = \bar{s}$. Only $\sqrt[3]{t_2}$, which satisfies Eq. (C.6b) through the relation

$$\sqrt[3]{t_2} = -\frac{p}{3\sqrt[3]{t_1}} \tag{C.10}$$

can be used (except when $\sqrt[3]{t_1}$ equals zero) in the following relations for the roots of Eq. (C.4) as

$$w_1 = \sqrt[3]{t_1} + \sqrt[3]{t_2}\,; \qquad w_2 = s\sqrt[3]{t_1} + \bar{s}\sqrt[3]{t_2} \qquad \text{and} \qquad w_3 = \bar{s}\sqrt[3]{t_1} + s\sqrt[3]{t_2} \tag{C.11}$$

and then the roots of Eq. (C.1) can be extracted through the transformation of Eq. (C.3).

C.4. QUARTIC EQUATIONS

Consider the quartic equation with real coefficients

$$z^4 + az^3 + bz^2 + cz + d = 0 \tag{C.12}$$

Rearranging and introducing the variable w, we obtain (Grove and Ladas 1974)

$$(z^2 + \frac{a}{2}z + w)^2 = (\frac{a^2}{4} - b + 2w)z^2 + (aw - c)z + (w^2 - d) \tag{C.13}$$

Now to solve Eq. (C.12) it is necessary to solve its resolvent equation given by

$$(aw-c)^2-4(\frac{a^2}{4}-b+2w)(w^2-d)=0 \tag{C.14}$$

which is a cubic equation in w in the form of

$$w^3+(\frac{-b}{2})w^2+(\frac{ac}{4}-d)w+(\frac{4bd-a^2d-c^2}{8})=0 \tag{C.15}$$

It is clear that by using any non-zero root of Eq. (C.15), the right-hand side of Eq. (C.13) is a perfect square and extracting square roots of both sides of Eq. (C.13) yields two quadratic equations that give the four roots of Eq. (C.12) through the following equations

$$z_{1,2}=\tfrac{1}{2}\left[\left(\frac{a}{2}-\sqrt{\frac{a^2}{4}-b+2w}\right)\pm\sqrt{\left(\frac{a}{2}-\sqrt{\frac{a^2}{4}-b+2w}\right)^2-4\left(w+(-1)^k\sqrt{w^2-d}\right)}\right] \tag{C.16}$$

$$z_{3,4}=\tfrac{1}{2}\left[\left(\frac{a}{2}-\sqrt{\frac{a^2}{4}-b+2w}\right)\pm\sqrt{\left(\frac{a}{2}-\sqrt{\frac{a^2}{4}-b+2w}\right)^2-4\left(w-(-1)^k\sqrt{w^2-d}\right)}\right] \tag{C.17}$$

where $k=1$ when $(aw-c)$ is real and negative, otherwise $k=2$.

C.5. QUINTIC EQUATIONS

Consider the quintic equation with real coefficients

$$z^5+az^4+bz^3+cz^2+dz+e=0 \tag{C.18}$$

The fundamental theorem of algebra states that every polynomial equation of degree n has n roots in the complex plane. However, the solution of the general quintic cannot be written as a finite formula involving only the four arithmetic operations and the extraction

of roots. Therefore, there is no analytical or closed form solution for quintic equations. Inspection of Figure C.1 gives some idea of the possible form of the quintic equation and the number of its real root(s).

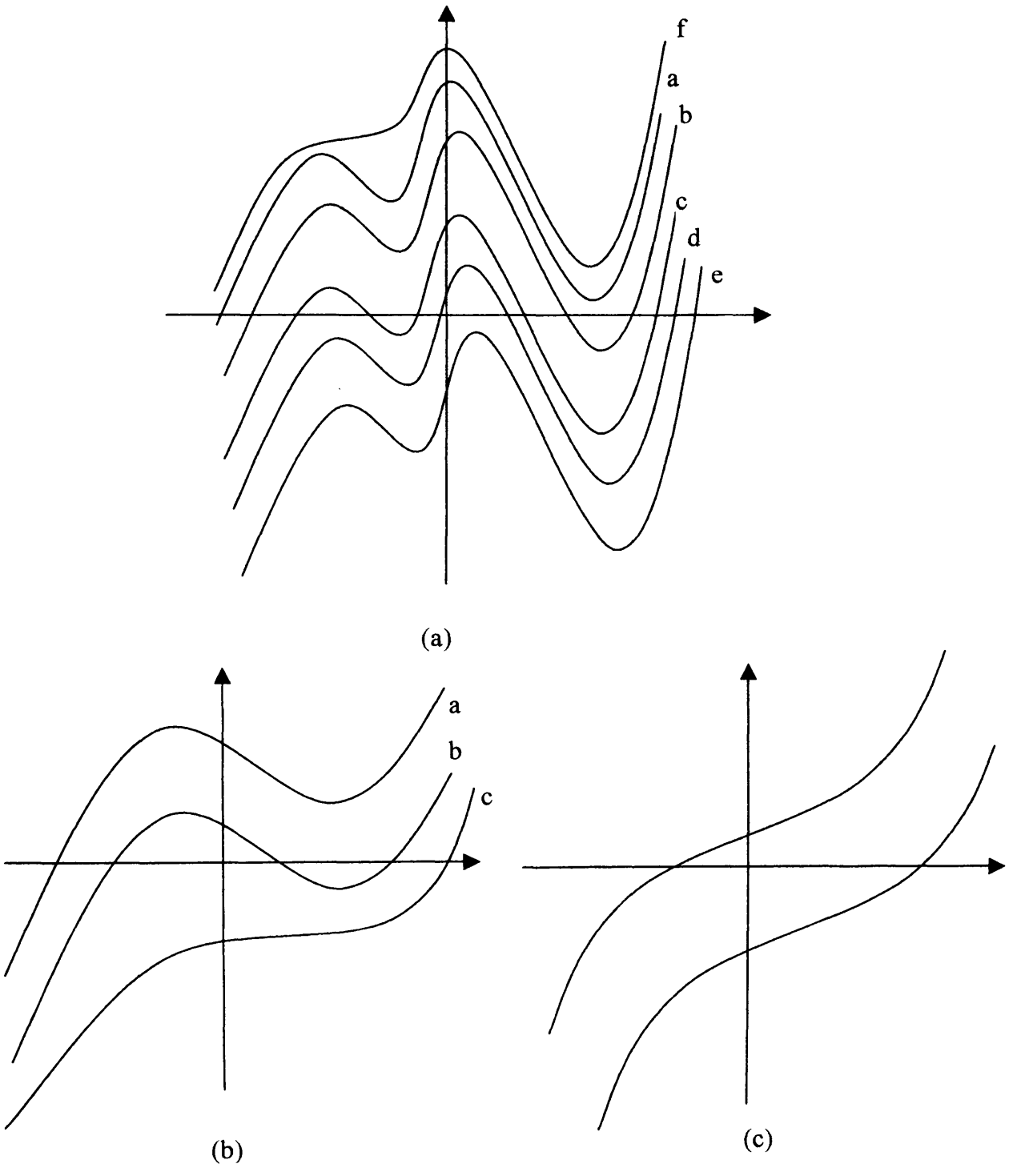

Figure C.1: Graphs of quintic polynomials, (a) with four real extremum, (b) with two real extremum and (c) without any real extremum.

Figure C.1(a) shows a series of quintic polynomials having four real extremum points (graphs a-e). In graph f of figure 1(a) two of those extremum are coincident at the point at which the slope and curvature are zero. For these sets of quintic polynomials, the number of possible real roots can vary from one to five. Figure C.1(b) shows the quintic polynomials with two real extremum, which may be coincident as in graph c. In this case the number of real roots can vary from one to three. Finally Figure C.1(c) shows quintic polynomials with no real extremum at all.

Hence, it is clear that a quintic equation has, at least, one real root and this real root can be found by using any numerical method. Consequently, the other four roots of quintic equation (C.18) can be found from the quartic equation obtains by extracting the real root from Eq. (C.18).

To find a real root of Eq. (C.18) the procedure is as follows. Using the following quartic equation

$$5z^4 + 4az^3 + 3bz^2 + 2cz + d = 0 \qquad \text{(C.19)}$$

which is the first derivative of Eq. (C.18), four possible extreme points of Eq. (C.18) are determined. These points are sorted into ascending order. To increase the accuracy of the extraction method, attention is confined to the largest real root of Eq. (C.18) which, when used, generates the most favourable conditions for providing stable results.

The nature of Eq. (C.18) indicates that the values of the equation in the second and fourth extreme point are minima. Hence, if one of these values is negative, the largest real root of Eq. (C.18) is on the right-hand side of that extreme point. Otherwise, the only real root is either on the left-hand side of the first extreme point, if the value of Eq. (C.18) is positive, or somewhere else without restriction.

After deciding about the position of the real root of Eq. (C.18), the Newton-Raphson method can be applied to find it (say z_1) to any desired accuracy. To choose a suitable starting point for the iterations, the appropriate root of Eq. (C.19) is multiplied by α, which is chosen to be 1.1 if the expected root is on the right side of the extreme point,

otherwise 0.9. In the case where there is no restriction for the position of the real root, $z = 0$ is used as the starting point for the iteration.

In the next step, by dividing Eq. (C.18) by $(z - z_1)$, a quartic equation containing the other four roots of Eq. (C.18) is given by

$$z^4 + (a + z_1)z^3 + (b + a z_1 + z_1^2)z^2 + (c + b z_1 + a z_1^2 + z_1^3)z + (d + c z_1 + b z_1^2 + a z_1^3 + z_1^4) = 0 \qquad \text{(C.20)}$$

Now, by using the method described in Section C.4, Eq. (C.20) can be solved for the remaining real or complex roots.

C.6. ILL CONDITIONING AND NUMERICAL STABILITY

Increasing the degree of a polynomial that also has large coefficients (like the ones dealt with in Chapter 7) can cause numerical instability in the results. The reason is that in such polynomials, the slope of the tangent at the roots is so big that it only requires small changes in the trial value to cause the value of the polynomial to change from a large negative value to a large positive value. In such cases the machine accuracy is often insufficient to enable the value of the polynomial to converge sufficiently close to zero. To overcome this ill-conditioning, it is necessary to use double precision or even quadruple precision when programming. However, as this accuracy is machine dependent and is sometimes insufficient, it is better to use a proper transformation that makes the coefficients as small as possible. The easiest transformation is

$$y = z / a; \qquad (a \neq 0) \qquad \text{(C.21)}$$

Transformation using Eq. (C.21) can be used for any standard form of polynomial of degree n and usually makes the coefficients small enough to give good accuracy in the results. For instance, by using Eq. (C.21), Eq. (C.18) can be reformed to

$$y^5 + y^4 + \frac{b}{a^2} y^3 + \frac{c}{a^3} y^2 + \frac{d}{a^4} y + \frac{e}{a^5} = 0 \qquad \text{(C.22)}$$

which is most effective if the order of magnitude of b, c, d and e are almost the same as the order of magnitude of a^2, a^3, a^4 and a^5. This was the case for the characteristic equation of Chapter 7.

REFERENCES

Åkesson, B. A. (1976). "PFVIBAT- a computer program for plane frame vibration analysis by an exact method." *International Journal for Numerical Methods in Engineering*, 10, 1221-1231.

Abramovich, H., Eisenberger, M., and Shulepov, O. (1995). "Vibrations of multispan nonsymmetrical composite beams." *Composites Engineering*, 5(4), 397-404.

Ahmed, K. M. (1971). "Free vibration of curved sandwich beams by the method of finite element." *Journal of Sound and vibration*, 18, 61-74.

Ahmed, K. M. (1972). "Dynamic analysis of sandwich beams." *Journal of Sound and vibration*, 21(3), 263-276.

Allen, H. G. (1969). *Analysis and design of structural sandwich panels*, Pergamon press, Oxford.

Ammar, S., Dhatt, G., and Fafard, M. (1996). "Exact stability model of space frames." *Computers & Structures*, 60(1), 59-71.

Anderson, M. S., and Williams, F. W. (1986). "BUNVIS-RG: An exact buckling and vibration program for latice structures, with repetitive geometry and substructuring options." *27th AIAA/ASME/ASCE/AHS Structures, Structural Dynamics and Materials Conference*, San Antonio, Texas, 211-220.

Armstrong, I. D. (1969). "The natural frequencies of multi-story frames." *Structural Engineering*, 47, 299-308.

Baber, T. T., Maddox, R. A., and Orozco, C. E. (1998). "A finite element model for harmonically excited viscoelastic sandwich beams." *Computers & Structures*, 66(1), 105-113.

Banerjee, J. R. (1989). "Coupled bending-torsional dynamic stiffness matrix for beam elements." *International Journal for Numerical Methods in Engineering*, 28(6), 1283-98.

Banerjee, J. R. (1997). "Dynamic stiffness formulation for structural elements: A general approach." *Computers & Structures*, 63(1), 101-103.

Banerjee, J. R. (1998). "Free vibration of axially loaded composite Timoshenko beams using the dynamic stiffness matrix method." *Computers & Structures*, 69(2), 197-208.

Banerjee, J. R. (2001). "Free vibration analysis of a twisted beam using the dynamic stiffness method." *International Journal of Solids and Structures*, 38(38-39), 6703-6722.

Banerjee, J. R. (2003). "Free vibration of sandwich beams using the dynamic stiffness method." *Computers & Structures*, 81(18-19), 1915-1922.

Banerjee, J. R. (2004). "Development of an exact dynamic stiffness matrix for free vibration analysis of a twisted Timoshenko beam." *Journal of Sound and Vibration*, 270(1-2), 379-401.

Banerjee, J. R., Guo, S., and Howson, W. P. (1996). "Exact dynamic stiffness matrix of a bending-torsion coupled beam including warping." *Computers & Structures*, 59(4), 613-621.

Banerjee, J. R., and Williams, F. W. (1985). "Exact Bernoulli-Euler Dynamic Stiffness Matrix for a Range of Tapered Beams." *International Journal for Numerical Methods in Engineering*, 21(12), 2289-2302.

Banerjee, J. R., and Williams, F. W. (1992). "Coupled Bending-Torsional Dynamic Stiffness Matrix for Timoshenko Beam Elements." *Computers & Structures*, 42(3), 301-310.

Banerjee, J. R., and Williams, F. W. (1994a). "Coupled Bending-Torsional Dynamic Stiffness Matrix of an Axially Loaded Timoshenko Beam Element." *International Journal of Solids and Structures*, 31(6), 749-762.

Banerjee, J. R., and Williams, F. W. (1994b). "An Exact Dynamic Stiffness Matrix for Coupled Extensional Torsional Vibration of Structural Members." *Computers & Structures*, 50(2), 161-166.

Banerjee, J. R., and Williams, F. W. (1995). "Free-Vibration of Composite Beams - an Exact Method Using Symbolic Computation." *Journal of Aircraft*, 32(3), 636-642.

Banerjee, J. R., and Williams, F. W. (1996). "Exact dynamic stiffness matrix for composite Timoshenko beams with applications." *Journal of Sound and Vibration*, 194(4), 573-585.

Bateson, L. E., Kelmanson, M. A., and Knudsen, C. (1999). "Solution of a transcendental eigenvalue problem via interval analysis." *Computers & Mathematics with Applications*, 38(7-8), 133-142.

Bercin, A. N. (1995). "Analysis of orthotropic plate structures by the direct-dynamic stiffness method." *Mechanics Research Communications*, 22(5), 461-466.

Bercin, A. N. (1997). "Eigenfrequencies of rectangular plate assemblies." *Computers & Structures*, 65(5), 703-711.

Bercin, A. N., and Langley, R. S. (1996). "Application of the dynamic stiffness technique to the in-plane vibrations of plate structures." *Computers & Structures*, 59(5), 869-875.

Bitzer, T. N. (1992). "Honeycomb material and application." *Sandwich construction 2*, UK, 681-691.

Bozhevolnaya, E., and Sun, J. Q. (2004). "Free vibration analysis of curved sandwich beams." *Journal of Sandwich Structures & Materials*, 6(1), 47-73.

Busool, W., and Eisenberger, M. (2002). "Free vibration of helicoidal beams of arbitrary shape and variable cross section." *Journal of Vibration and Acoustics-Transactions of the ASME*, 124(3), 397-409.

Cabanska-Placzkiewicz, K. (2000). "Dynamic analysis of viscoelastic sandwich beams." *International Applied Mechanics*, 36(5), 673-681.

Capron, M. D., and Williams, F. W. (1988). "Exact dynamic stiffnesses for an axially loaded uniform Timoshenko member embedded in an elastic medium.." *Journal of Sound and Vibration*, 124(3), 453-66.

Cheng, F. Y. (1970). "Vibrations of Timoshenko beams and frameworks." *Journal of Structural Engineering-ASCE*, 96(ST3), 551-571.

Chonan, S. (1982). "Vibration and stability of sandwich beams with elastic bonding." *Journal of Sound and Vibration*, 85(4), 525-537.

Davies, J. M. (2001). *Lightweight Sandwich Construction*, Blackwell Pub.

Deng, H., and Vu-Quoc, L. (1998). "Dynamics of geometrically exact sandwich structures." *International Journal of Mechanical Sciences*, 40(5), 421-441.

Desai, Y. M., Ramtekkar, G. S., and Shah, A. H. (2003). "Dynamic analysis of laminated composite plates using a layer- wise mixed finite element model." *Composite Structures*, 59(2), 237-249.

Dewa, H. (1990). "Numerical analysis for torsional stress and rigidity of nonsymmetrical three-layered beams subjected to torsion." *Journal of the Society of Materials Science*, 39(442), 852-858.

DiTaranto, R. A. (1965). "Theory of vibratory bending for elastic and viscoelastic layered finite-length beams." *Journal of Applied Mechanics-Transactions of the ASME*, 32, 881-886.

Dugundji, J. (2002). "Cantilever boundary condition, deflections, and stresses of sandwich beams." *AIAA Journal*, 40(5), 987-995.

Dym, C. L., and Shames, I. H. (1973). *Solid mechanics : A variational approach*, McGraw-Hill, New York.

Eisenberger, M. (1990). "Exact static and dynamic stiffness matrices for general variable cross-section members." *AIAA Journal*, 28(6), 1105-1109.

Eisenberger, M. (1991). "Exact longitudinal vibration frequencies of a variable cross-section rod." *Applied Acoustics*, 34(2), 123-130.

Eisenberger, M. (1994). "Vibration frequencies for beams on variable one-parameter and two-parameter elastic foundations." *Journal of Sound and Vibration*, 176(5), 577-584.

Eisenberger, M. (1995). "Dynamic stiffness matrix for variable cross-section Timoshenko beams." *Communications in Numerical Methods in Engineering*, 11(6), 507-513.

Eisenberger, M. (1997). "Torsional vibrations of open and variable cross-section bars." *Thin-Walled Structures*, 28(3-4), 269-278.

Eisenberger, M. (2003). "Dynamic stiffness vibration analysis using a high-order beam model." *International Journal for Numerical Methods in Engineering*, 57(11), 1603-1614.

Eisenberger, M., Abramovich, H., and Shulepov, O. (1995). "Dynamic stiffness analysis of laminated beams using a first- order shear deformation theory." *Composite Structures*, 31(4), 265-271.

Eisenberger, M., and Efraim, E. (2001). "In-plane vibrations of shear deformable curved beams." *International Journal for Numerical Methods in Engineering*, 52(11), 1221-1234.

Farghaly, S. H., and Shebl, M. G. (1992). "Vibration characteristics of end mass loaded undamped sandwich beams with elastically constrained ends." *Journal of Sound and Vibration*, 159(2), 237-249.

Fasana, A., and Marchesiello, S. (2001). "Rayleigh-Ritz analysis of sandwich beams." *Journal of Sound and Vibration*, 241(4), 643-652.

Fontgalland, G., Baudrand, H., and Guglielmi, M. (1998). "Application of a monotonous function to the analysis of ridged waveguides." *Journal of Microwaves and Optoelectronics*, 1(3), 25-34.

Fotiu, P. (1987). "Dynamic analysis of viscoplastic sandwich beams using Green functions." *Zeitschrift Fur Angewandte Mathematik Und Mechanik*, 67(4), T75-T77.

Friberg, P. O. (1983). "Coupled Vibrations of Beams - an Exact Dynamic Element Stiffness Matrix." *International Journal for Numerical Methods in Engineering*, 19(4), 479-493.

Frid, A. (1989). "Fluid vibration in piping systems-a structural mechanics approach, I. Theory." *Journal of Sound and Vibration*, 133(3), 423-38.

Frid, A. (1990). "A modified Wittrick-Williams algorithm for eigenvalue analysis of fluid vibration in piping systems." *Journal of Sound and Vibration*, 141(2), 355-358.

Frostig, Y. (1992). "Behaviour of delaminated sandwich beam with transversely flexible core - High-order theory." *Composite Structures*, 20(1), 1-16.

Frostig, Y. (1993). "High-order behaviour of sandwich beams with flexible core and transverse diaphragms." *Journal of Engineering Mechanics-ASCE*, 119(5), 955-972.

Frostig, Y., and Baruch, M. (1994). "Free vibrations of sandwich beams with a transversely flexible core: A high order approach." *Journal of Sound and Vibration*, 176(2), 195-208.

Frostig, Y., and Thomsen, O. T. (2004). "High-order free vibration of sandwich panels with a flexible core." *International Journal of Solids and Structures*, 41(5-6), 1697-1724.

Ganapathi, M., Patel, B. P., and Kumar, T. S. (1999a). "Torsional vibration and damping analysis of sandwich beams." *Journal of Reinforced Plastics and Composites*, 18(2), 96-117.

Ganapathi, M., Patel, B. P., Polit, O., and Touratier, M. (1999b). "A C-1 finite element including transverse shear and torsion warping for rectangular sandwich beams." *International Journal for Numerical Methods in Engineering*, 45(1), 47-75.

Gorman, D. J. (1982). *Free vibration analysis of rectangular plates*, Elsevier, New York.

Grove, E. A., and Ladas, G. (1974). *Introduction to complex variables*, Houghton Mifflin, Boston.

Hallauer, W. L. J., and Liu, R. Y. L. (1982). "Beam bending-torsion dynamic stiffness method for calculation of exact vibration modes." *Journal of Sound and Vibration*, 85(1), 105-13.

Hashemi, S. M., and Richard, M. J. (2000a). "A Dynamic Finite Element (DFE) method for free vibrations of bending-torsion coupled beams." *Aerospace Science and Technology*, 4(1), 41-55.

Hashemi, S. M., and Richard, M. J. (2000b). "Free vibrational analysis of axially loaded bending-torsion coupled beams: a dynamic finite element." *Computers & Structures*, 77(6), 711-724.

Hashemi, S. M., and Richard, M. J. (2001). "Natural frequencies of rotating uniform beams with Coriolis effects." *Journal of Vibration and Acoustics-Transactions of the ASME*, 123(4), 444-455.

He, S., and Rao, M. D. (1993). "Vibration and damping analysis of multi-span sandwich beams with arbitrary boundary conditions." *Journal of Sound and Vibration*, 164(1), 125-142.

Heinisuo, M. (1988). "An exact finite element technique for layered beams." *Computers & Structures*, 30(3), 615-22.

Henshell, and Warburton. (1969). "Transmission of vibration in beam systems." *International Journal for Numerical Methods in Engineering*, 1, 47-66.

Hjelmgren, J. P., Lunden, R., and Åkesson, B. (1993). "Some comments on damped 2nd-order Rayleigh Timoshenko beam vibration in space - An exact complex dynamic member stiffness matrix." *International Journal for Numerical Methods in Engineering*, 36(24), 4267-4268.

Howson, W. P. (1979). "A compact method for computing the eigenvalues and eigenvectors of plane frames." *Advances in Engineering Software*, 1(4), 181-190.

Howson, W. P., and Jemah, A. K. (1999a). "Exact dynamic stiffness method for planar natural frequencies of curved Timoshenko beams." *Proceedings of the Institution of Mechanical Engineers Part C- Journal of Mechanical Engineering Science*, 213(7), 687-696.

Howson, W. P., and Jemah, A. K. (1999b). "Exact out-of-plane natural frequencies of curved Timoshenko beams." *Journal of Engineering Mechanics-ASCE*, 125(1), 19-25.

Howson, W. P., and Williams, F. W. (1973). "Natural frequencies of frames with axially loaded Timoshenko members." *Journal of Sound and Vibration*, 26(4), 503-515.

Howson, W. P., Williams, F. W., and Watson, A. (2001). "A methodology for finding inter-disciplinary applications of the Wittrick-Williams algorithm." *7th EPMESC Conference*, Shanghai, China, 143-55.

Howson, W. P., and Zare, A. (2004). "Exact dynamic stiffness matrix for flexural vibration of three-layered sandwich beams." *Journal of Sound and vibration*, In Press, Corrected Proof, Available online 5 November 2004.

Huang, C. S., Tseng, Y. P., Chang, S. H., and Hung, C. L. (2000). "Out-of-plane dynamic analysis of beams with arbitrarily varying curvature and cross-section by dynamic stiffness matrix method." *International Journal of Solids and Structures*, 37(3), 495-513.

Huang, C. S., Tseng, Y. P., Leissa, A. W., and Nieh, K. Y. (1998). "An exact solution for in-plane vibrations of an arch having variable curvature and cross section." *International Journal of Mechanical Sciences*, 40(11), 1159-1173.

Jabareen, M., and Eisenberger, M. (2001). "Free vibrations of non-homogeneous circular and annular membranes." *Journal of Sound and Vibration*, 240(3), 409-29.

Kant, T., and Gupta, A. (1988). "A finite element model for a higher order shear deformable beam theory." *Journal of Sound and Vibration*, 125(1), 193-202.

Kant, T., Marur, S. R., and Rao, G. S. (1998). "Analytical solution to the dynamic analysis of laminated beams using higher order refined theory." *Composite Structures*, 40(1), 1-9.

Kennedy, D., Watkins, W. J., and Williams, F. W. (1995). "Hybrid Parallel Computation of Transcendental Structural Eigenvalues." *AIAA Journal*, 33(11), 2194-2198.

Kennedy, D., and Williams, F. W. (1991). "More efficient use of determinants to solve transcendental structural eigenvalue problems reliably." *Computers & Structures*, 41(5), 973-979.

Kennedy, D., and Williams, F. W. (1997). "Parallel computation for transcendental structural eigenproblems." *Structural Engineering and Mechanics*, 5(5), 635-644.

Kerwin, E. M. (1959). "Damping of flexural waves by a constrained visco-elastic layer." *Journal of the Acoustical Society of America*, 31, 952-962.

Kim, M. Y., Yun, H. T., and Kim, N. I. (2003). "Exact dynamic and static element stiffness matrices of nonsymmetric thin-walled beam-columns." *Computers & Structures*, 81(14), 1425-1448.

Kolousek, V. (1941). "Anwendung des Gesetzes der virtuellen Verschiebungen und des Reziprozitatssatzes in der Stabwerksdynamic." *Ing.-Archiv*, 12, 363-370.

Kolousek, V. (1943). "Berechnung der schwingenden Stockwerahmen nach der Deformationmethode." *Der Stahlbau*, 16, 5-6 and 11-13.

Kolousek, V. (1973). *Dynamics in Engineering Structures*, Butterworths, London.

Kumpinsky, E. (1992). "The solution of transcendental trigonometric characteristic equations." *Industrial & Engineering Chemistry Research*, 31(1), 440-445.

Laursen, H. I., Shubinski, R. P., and Clough, R. W. (1962). "Dynamic matrix analysis of framed structures." *The fourth U.S. National Congress on Applied Mechanics*.

Lee, J., and Thompson, D. J. (2001). "Dynamic stiffness formulation, free vibration and wave motion of helical springs." *Journal of Sound and Vibration*, 239(2), 297-320.

Lekhnitskii, S. J. (1968). *Anisotropic plates*, Gordon and Breach, New York.

Leung, A. Y. T. (1992). "Dynamic stiffness analysis of thin-walled structures." *Thin-Walled Structures*, 14(3), 209-222.

Leung, A. Y. T. (1993). *Dynamic stiffness and substructures*, Springer, London.

Leung, A. Y. T., and Zhou, W. E. (1995a). "Dynamic stiffness analysis of axially loaded nonuniform timoshenko columns." *Computers & Structures*, 56(4), 577-588.

Leung, A. Y. T., and Zhou, W. E. (1995b). "Dynamic stiffness analysis of nonuniform Timoshenko beams." *Journal of Sound and Vibration*, 181(3), 447-456.

Leung, A. Y. T., and Zhou, W. E. (1996). "Dynamic stiffness analysis of laminated composite plates." *Thin-Walled Structures*, 25(2), 109-133.

Li, J., Shen, R., and Hua, H. (2003). "Coupling bending-torsional vibration of Bernoulli-Euler thin-walled beam including warping effect." *Journal of Mechanical Strength*, 25(5), 486-9.

Lunden, R., and Åkesson, B. (1983). "Damped 2nd-order Rayleigh-Timoshenko beam vibration in space - An exact complex dynamic member stiffness matrix." *International Journal for Numerical Methods in Engineering*, 19(3), 431-449.

Mace, M. (1994). "Damping of beam vibrations by means of a thin constrained viscoelastic layer - Evaluation of a new theory." *Journal of Sound and Vibration*, 172(5), 577-591.

Maheri, M. R., and Adams, R. D. (1998). "On the flexural vibration of Timoshenko beams, and the applicability of the analysis to a sandwich configuration." *Journal of Sound and Vibration*, 209(3), 419-442.

Marguerre, K. (1944). "The optimum buckling load of a flexibly supported plate composed of two sheets joined by a light weight filler when under longitudinal compression." *Deutsche viertaljahrsschrift fur literaturwissenschaft und giests geschichte, DVL (ZWB UM 1360/2), Oct 28.*

Marur, S. R., and Kant, T. (1996). "Free vibration analysis of fibre reinforced composite beams using higher order theories and finite element modelling." *Journal of Sound and Vibration*, 194(3), 337-351.

Marur, S. R., and Kant, T. (1998). "Transient dynamics of laminated beams: an evaluation with a higher-order refined theory." *Composite Structures*, 41(1), 1-11.

Matsui, Y., and Hayashikawa, T. (2001). "Dynamic stiffness analysis for torsional vibration of continuous beams with thin-walled cross-section." *Journal of Sound and Vibration*, 243(2), 301-316.

Mead, D., and Markus, S. (1969). "The forced vibration of a three-layer, damped sandwich beam with arbitrary boundary conditions." *Journal of Sound and Vibration*, 10(2), 163-175.

Mead, D., and Markus, S. (1970a). "Loss factors and resonant frequencies of encastre damped sandwich beams." *Journal of Sound and Vibration*, 12(1), 99-112.

Mead, D. J. (1971). "The vibration characteristics of damped sandwich plates with stiffeners and various boundary conditions." *Strojnicky Casopis*, 22, 53-67.

Mead, D. J. (1982). "Comparison of some equations for the flexural vibration of damped sandwich beams." *Journal of Sound and Vibration*, 83(3), 363-377.

Mead, D. J., and Markus, S. (1970b). "On the problem of bending vibration of sandwich cantilevers with various boundary conditions applied at the free end." *strojnicky casopis*, 21, 3-14.

Mead, D. J., and Markus, S. (1985). "Coupled flexural, longitudinal and shear wave motion in two- and three-layered damped beams." *Journal of Sound and Vibration*, 99(4), 501-519.

Mead, D. J., and Sivakumuran, S. (1966). "The stodolla method applied to sandwich beam vibration." *Proceedings of the symposium on numerical methods for vibration problems, University of Southampton*, 66-80.

Mikhailov, M. D., and Ozisik, M. N. (1984). *Unified analysis and solutions of heat and mass diffusion*, John Wiley, New York.

Mikhailov, M. D., Ozisik, M. N., and Vulchanov, N. L. (1983). "Diffusion in composite layers with automatic solution of the eigenvalue problem." *International Journal of heat amd mass transfer*, 26, 1131-1141.

Mikhailov, M. D., and Vulchanov, N. L. (1983). "Computational procedure for Sturm-Liouville problems." *Journal of Computational Physics*, 50(3), 323-36.

Moon-Young, K., Hee-Taek, Y., and Nam, K. (2003a). "Exact dynamic and static element stiffness matrices of nonsymmetric thin-walled beam-columns." *Computers & Structures*, 81(14), 1425-48.

Moon-Young, K., Nam, K., and Hee-Taek, Y. (2003b). "Exact dynamic and static stiffness matrices of shear deformable thin-walled beam-columns." *Journal of Sound and Vibration*, 267(1), 29-55.

Mou, Y. H., Han, R. P. S., and Shah, A. H. (1997). "Exact dynamic stiffness matrix for beams of arbitrarily varying cross sections." *International Journal for Numerical Methods in Engineering*, 40(2), 233-250.

Nashif, A. D., Jones, D. I. G., and Henderson, J. P. (1985). *Vibration damping*, John Wiley & Sons, Inc, New Yory.

Nilsson, E., and Nilsson, A. C. (2002). "Prediction and measurement of some dynamic properties of sandwich structures with honeycomb and foam cores." *Journal of Sound and Vibration*, 251(3), 409-430.

Patel, B. P., and Ganapathi, M. (2001). "Non-linear torsional vibration and damping analysis of sandwich beams." *Journal of Sound and Vibration*, 240(2), 385-393.

Paz, M. (1973). "Mathematical observations in structural dynamics." *Computers & Structures*, 3(2), 385-96.

Pearson, D., and Wittrick, W. H. (1986). "An exact solution for the vibration of helical springs using a Bernoulli-Euler model." *International Journal of Mechanical Sciences*, 28(2), 83-96.

Petrone, F., Garesci, F., Lacagnina, M., and Sinatra, R. (1999). "Dynamical joints influence of sandwich plates." *The 3rd European Nonlinear Oscillations Conference*, Copenhagen, Denmark.

Plantema, F. J. (1966). *Sandwich construction: the bending and buckling of sandwich beams, plates and shells*, Wiley, New York.

Qi, Z. H., Kennedy, D., and Williams, F. W. (2004). "An accurate method for transcendental eigenproblems with a new criterion for eigenfrequencies." *International Journal of Solids and Structures*, 41(11-12), 3225-3242.

Raffa, F. A., and Vatta, F. (1996). "The dynamic stiffness method for linear rotor-bearing systems." *Journal of Vibration and Acoustics-Transactions of the ASME*, 118(3), 332-339.

Raffa, F. A., and Vatta, F. (2002). "A new finding on the dynamic stiffness matrices of asymmetric and axisymmetric shafts." *Journal of Vibration and Acoustics-Transactions of the ASME*, 124(4), 649-653.

Ramtekkar, G. S., Desai, Y. M., and Shah, A. H. (2002). "Natural vibrations of laminated composite beams by using mixed finite element modelling." *Journal of Sound and Vibration*, 257(4), 635-651.

Rao, D. K. (1977). "Vibration of short sandwich beams." *Journal of Sound and Vibration*, 52(2), 253-263.

Rao, D. K. (1978). "Frequencies and loss factors of sandwich beams under various boundary conditions." *Journal of Mechanical Engineering Science*, 20(5), 271.

Rao, M. K., and Desai, Y. M. (2004). "Analytical solutions for vibrations of laminated and sandwich plates using mixed theory." *Composite Structures*, 63(3-4), 361-373.

Rao, M. K., Desai, Y. M., and Chitnis, M. R. (2001). "Free vibrations of laminated beams using mixed theory." *Composite Structures*, 52(2), 149-160.

Rao, Y. V. K. S., and Nakra, B. C. (1970). "Influence of rotary and translatory inertia on the vibrations of unsymmetrical sandwich beams." *ISTAM 1970*, 301-314.

Rao, Y. V. K. S., and Nakra, B. C. (1973). "Theory of vibratory bending of unsymmetrical sandwich plates." *Archives of Mechanics*, 25(2), 213-225.

Raville, M. E., Ueng, E.-S., and Lei, M.-M. (1961). "Natural frequencies of vibration of fixed-fixed sandwich beams." *Journal of Applied Mechanics Transaction of ASME*, 83, 367-371.

Romeiras, F. J., and Rowlands, G. (1986). "Exact solution of a nonlinear eigenvalue problem." *Physical Review A*, 33(5), 3499-3501.

Sainsbury, M., and Zhang, Q. (1999). "The Galerkin element method applied to the vibration of damped sandwich beams." *Computers & Structures*, 71(3), 239-56.

Sakiyama, T., Matsuda, H., and Morita, C. (1996a). "Free vibration analysis of continuous sandwich beams with elastic or viscoelastic cores by applying the discrete Green function." *Journal of Sound and Vibration*, 198(4), 439-454.

Sakiyama, T., Matsuda, H., and Morita, C. (1996b). "Free vibration analysis of sandwich beam with elastic or viscoelastic core by applying the discrete green function." *Journal of Sound and Vibration*, 191(2), 189-206.

Sakiyama, T., Matsuda, H., and Morita, C. (1997). "Free vibration analysis of sandwich arches with elastic or viscoelastic core and various kinds of axis-shape and boundary conditions." *Journal of Sound and Vibration*, 203(3), 505-522.

Schill, M. (1988). "Damped 2nd-order Rayleigh-Timoshenko semi-infinite beam vibration - An exact complex dynamic member stiffness matrix." *International Journal for Numerical Methods in Engineering*, 26(8), 1893-1905.

Shastry, B. S. (1983). "Exact solution of a non-linear eigenvalue problem in one dimension." *Physical Review Letters*, 50(9), 633-636.

Silverman, I. K. (1995). "Natural frequencies of sandwich beams including shear and rotary effects." *Journal of Sound and Vibration*, 183(3), 547-561.

Silverman, I. K. (1997). "Oscillations of Timoshenko sandwich cantilever beam." *Journal of Sound and Vibration*, 202(1), 139-144.

Simpson, A. (1974). "Scanning Kron's determinant." *Quarterly Journal of Mechanics and Applied Mathematics*, 27(1), 27-43.

Simpson, A. (1984). "A Newtonian procedure for the solution of Sx=0." *Journal of Sound and Vibration*, 97, 153-164.

Simpson, A., and Tabarrok, B. (1968). "On Kron's eigenvalue procedure and related methods of frequency analysis." *Quarterly Journal of Mechanics and Applied Mathematics*, 21.

Singh, K. V., and Ram, Y. M. (2002). "Transcendental eigenvalue problem and its applications." *AIAA Journal*, 40(7), 1402-1407.

Sokolinsky, V. S., Frostig, Y., and Nutt, S. R. (2001). "Special behavior of soft-core sandwich beams." *46th International SAMPE symposium and exhibition*, Long Beach, California,, 1185-1197.

Sokolinsky, V. S., Von Bremen, H. F., Lavoie, J. A., and Nutt, S. R. (2004). "Analytical and experimental study of free vibration response of soft-core sandwich beams." *Journal of Sandwich Structures & Materials*, 6(3), 239-261.

Sotiropoulos, G. H. (1982). "The transcendental eigenvalue problem of the exact dynamic stiffness matrix of linearly elastic plane frames." *Zeitschrift Fur Angewandte Mathematik Und Mechanik*, 62(7), 313-319.

Sun, C. T., and Lu, Y. P. (1995). *Vibration damping in structural elements*, Printice-Hall, Inc, New Jersey.

Szilard, R. (1974). *Theory and analysis of plates*, Printice-Hall, New Jersy.

Tanghe-Carrier, F., and Gay, D. (2000). "Nonuniform warping torsion of orthotropic composite beams." *Archive of Applied Mechanics*, 70(8-9), 635-648.

Timoshenko, S. P. (1921). "On the correction for shear of the differential equation for transverse vibration of prismatic bars." *Philosophical Magazine*, 41.

Veletsos, A. S., and Newmark, N. M. (1956). "Determination of natural frequencies of continous plates hinged along two opposite edges." *Journal of Applied Mechanics-Transactions of the ASME*, 23, 97-102.

Vinson, J. R. (1999). *The behaviour of sandwich structures of isotropic and composite materials*, Technomic, Lancaster PA,.

Vinson, J. R. (2001). "Sandwich structures." *Applied Mechanics Review*, 54(3), 201-214.

Vuo-Quoc, L., and Ebcioglu, I. K. (1995). "Dynamic formulation for geometrically exact sandwich beams and one-dimensional plates." *Journal of Applied Mechanics-Transactions of the ASME*, 62(3), 756-763.

Vu-Quoc, L., and Deng, H. (1995). "Dynamics of geometrically exact sandwich beams/1-D plates: computational aspects." *American Society of Mechanical Engineers, Design Engineering Division (Publication) DE*, 84(3), 703-713.

VuQuoc, L., Deng, H., and Ebcioglu, I. K. (1996). "Multilayer beams: A geometrically exact formulation." *Journal of Nonlinear Science*, 6(3), 239-270.

Wang, T. M., and Kinsman, T. A. (1971). "Vibration of frame structures according to the Timoshenko theory." *Journal of Sound and Vibration*, 14, 215-227.

Williams, F. W., Howson, W. P., and Watson, A. (2004a). "Application of the Wittrick-Williams algorithm to the Sturm- Liouville problem on homogeneous trees: A structural mechanics analogy." *Proceedings of the Royal Society of London Series A- Mathematical Physical and Engineering Sciences*, 460(2045), 1243-1268.

Williams, F. W., and Kennedy, D. (1988). "Reliable use of determinant to solve non-linear structural eigenvalue analysis." *International Journal of Numerical Methods for Engineering*, 26, 1825-41.

Williams, F. W., and Kennedy, D. (1996). "Accelerated solutions for transcendental stiffness matrix eigenproblems." *Shock and Vibration*, 3(4), 287-292.

Williams, F. W., and Kennedy, D. (2003). "Derivation of new transcendental member stiffness determinant for vibrating frames." *International Journal of Structural Stability and Dynamics*, 3(2), 299-305.

Williams, F. W., Kennedy, D., and Djoudi, M. S. (2002a). "The member stiffness determinant and its uses for the transcendental eigenproblems of structural engineering and other disciplines." *Proceedings of the Royal Society of London Series A- Mathematical Physical and Engineering Sciences*, 459(2032), 1001-1019.

Williams, F. W., Kennedy, D., and Djoudi, M. S. (2004b). "Exact determinant for infinite order FEM representation of a Timoshenko beam-column via improved transcendental member stiffness matrices." *International Journal for Numerical Methods in Engineering*, 59(10), 1355-1371.

Williams, F. W., and Wittrick, W. H. (1970). "An automatic computational procedure for calculating natural frequencies of skeleton structures." *International Journal of Mechanical Sciences*, 12(9), 781-791.

Williams, F. W., Yuan, S., Ye, K., Kennedy, D., and Djoudi, M. S. (2002b). "Towards deep and simple understanding of the transcendental eigenproblem of structural vibrations." *Journal of Sound and Vibration*, 256(4), 681-693.

Wittrick, W. H. (1968a). "General sinusoidal stiffness matrix for buckling and vibration analysis of thin flat-walled structures." *International Journal of Mechanical Sciences*, 10, 949-966.

Wittrick, W. H. (1968b). "A unified approach to the initial buckling of stiffened panels in compression." *The Aeronautical Quarterly*, 19, 265-83.

Wittrick, W. H., and Williams, F. W. (1971a). "A general algorithm for computing natural frequencies of elastic structures." *Quarterly Journal of Mechanics and Applied Mathematics*, 24(3), 263-284.

Wittrick, W. H., and Williams, F. W. (1971b). "Natural vibrations of thin, prismatic flat-walled structures." *International Union of Theoretical and Applied Mechanics Symposium on High Speed Computing of Elastic Structures*, University of Liege, Belgium, 563-588.

Wittrick, W. H., and Williams, F. W. (1973a). "An algorithm for computing critical buckling loads of elastic structures." *Journal of Structural Mechanics*, 1, 497-518.

Wittrick, W. H., and Williams, F. W. (1973b). "New procedures for structural eigenvalue calculations." *4th Australasian Conference on the Mechanics of Structures and Materials*, Brisbane, Australia, 299-308.

Wittrick, W. H., and Williams, F. W. (1974). "Buckling and vibration of anisotropic or isotropic plate assemblies under combined loadings." *International Journal of Mechanical Sciences*, 16(4), 209-239.

Wittrick, W. H., and Wright, C. J. (1978). "A compact computer program for calculating buckling stresses and natural frequencies of vibration of prismatic plate assemblies." *International Journal for Numerical Methods in Engineering*, 12, 1429-1456.

Yan, M., and Dowell, E. (1974). "Elastic sandwich beam or plate equations equivalent to classical theory." *Journal of Applied Mechanics-Transactions of the ASME*, 41(2), 526-527.

Yanghu, M., Han, R. P. S., and Shah, A. H. (1997). "Exact dynamic stiffness matrix for beams of arbitrarily varying cross sections." *International Journal for Numerical Methods in Engineering*, 40(2), 233-50.

Zare, A., Howson, W. P., and Kennedy, D. (2003a). "An overview of member stiffness determinants for prismatic plate assemblies." *ICCES'03: International Conference on Computational and Experimental Engineering and Sciences*, Corfu, Greece, 1-6.

Zare, A., Howson, W. P., Kennedy, D., and Williams, F. W. (2003b). "The exact member stiffness determinant of orthotropic prismatic plates and a proposed approximation for anisotropic plates." *International Journal of Mechanical Sciences*, Submitted for publication.

Zare, A., Howson, W. P., Kennedy, D., and Williams, F. W. (2003c). "Member stiffness determinants for use with axially loaded isotropic prismatic plate assemblies." *Journal of Sound and Vibration*, Submitted for publication.

Zenkert, D. (1997). *The handbook of sandwich construction*, Chameleon press, London.

Zhang, Q. J., and Sainsbury, M. G. (2000). "The Galerkin element method applied to the vibration of rectangular damped sandwich plates." *Computers & Structures*, 74(6), 717-730.